ISSN 1948-0210 (online)

World Journal of *Stem Cells*

World J Stem Cells 2015 July 26; 7(6): 894-991

Published by Baishideng Publishing Group Inc

WJSC World Journal of Stem Cells

A peer-reviewed, online, open-access journal of stem cells

Editorial Board

2010-2015

The *World Journal of Stem Cells* Editorial Board consists of 719 members, representing a team of worldwide experts in infectious diseases. They are from 44 countries, including Argentina (2), Australia (10), Austria (6), Belgium (3), Brazil (10), Canada (16), China (74), Cyprus (1), Czech Republic (5), Denmark (7), Egypt (2), Finland (3), France (19), Germany (36), Greece (1), Hungary (3), India (10), Iran (9), Ireland (4), Israel (10), Italy (52), Japan (55), Jordan (1), Malaysia (1), Mexico (1), Morocco (1), Netherlands (8), Norway (3), Portugal (1), Romania (1), Russia (3), Singapore (19), Slovakia (1), South Korea (45), Spain (17), Sweden (4), Switzerland (4), Thailand (1), Tunisia (1), Turkey (5), United Arab Emirates (1), United Kingdom (29), United States (233), and Venezuela (1).

Li Deng, *Chengdu*
Jian Dong, *Shanghai*
Jun Dou, *Nanjing*
Jian-Xin Gao, *Shanghai*
Zhi-Liang Gao, *Guangzhou*
Zi-Kuan Guo, *Beijing*
Zhong-Chao Han, *Tianjin*
Ling-Ling Hou, *Beijing*
Jian-Guo Hu, *Bengbu*
Yi-Ping Hu, *Shanghai*
Dong-Sheng Huang, *Guangzhou*
Jian-Hua Huang, *Yinchuan*
Jiu-Hong Kang, *Shanghai*
Dong-Mei Lai, *Shanghai*
Anskar YH Leung, *Hong Kong*
Gang Li, *Hong Kong*
Gui-Rong Li, *Hong Kong*
Jin-Jun Li, *Shanghai*
Xiang-Yun Li, *Baoding*
Xiao-Rong Li, *Tianjin*
Zong-Jin Li, *Tianjin*
Qi-Zhou Lian, *Hong Kong*
Hong Liao, *Nanjing*
Kai-Yan Liu, *Beijing*
Lei Liu, *Chengdu*
Yi-Jia Lou, *Hangzhou*
Pauline Po Yee Lui, *Hong Kong*
Xue-Tao Pei, *Beijing*
Cai-Ping Ren, *Changsha*
Chun-Meng Shi, *Chongqing*
Guan-Bin Song, *Chongqing*
Jing-He Tan, *Tanan*
Kent Kam Sze Tsang, *Hong Kong*
Jin-Fu Wang, *Hangzhou*
Tie-Qiao Wen, *Shanghai*
Ji Wu, *Shanghai*
Ren-Hua Wu, *Shantou*
Rui-An Xu, *Xiamen*
Chuan Ye, *Guiyang*
Xi-Yong Yu, *Guangzhou*
Hao Zhang, *Beijing*
Shu-Ren Zhang, *Beijing*
Yun-Hai Zhang, *Hefei*
Lei Zhao, *Wuhan*
Xiao-Gang Zhong, *Nanning*
Bo Zhu, *Chongqing*
Zhong-Min Zou, *Chongqing*

Cyprus

Pantelis Georgiades, *Nicosia*

Czech Republic

Eva Bártová, *Brno*
Petr Dvorak, *Brno*
Vladimir Holan, *Prague*
Jaroslav Mokry, *Hradec Kralove*
Jakub Suchánek, *Hradec Kralove*

Denmark

Basem M Abdallah, *Odense*
Poul Hyttel, *Frederiksberg*
Lin Lin, *Tjele*
Morten Meyer, *Blommenslyst*
Nedime Serakinci, *Vejle*
Soren Paludan Sheikh, *Odense*
Vladimir Zachar, *Aalborg*

Egypt

Mohamed Ahmed Ghoneim, *Mansora*
Alaa Eldin Ismail, *Cairo*

Finland

Jukka Partanen, *Helsinki*
Petri Salven, *Helsinki*
Heli Teija Kristiina Skottman, *Tampere*

France

Ez-Zoubir Amri, *Nice*
Bernard Binetruy, *Marseille*
Alain Chapel, *Far*
Yong Chen, *Paris*
Dario Coleti, *Paris*
Christelle Coraux, *Reims*
Anne Claude Fernandez, *Montpellier*
Loïc Fouillard, *Cergy-Pontoise*
Norbert-Claude Gorin, *Paris*
Enzo Lalli, *Valbonne*
Gwendal Lazennec, *Montpellier*
Nathalie Lefort, *Evry*
Laurent Lescaudron, *Nantes*
David Magne, *Villeurbanne*
Muriel Perron, *Orsay*
Xavier Thomas, *Lyon*
Ali G Turhan, *Villejuif*
Didier Wion, *Grenoble*

Germany

Nasreddin Abolmaali, *Dresden*
James Adjaye, *Berlin*
Halvard Bonig, *Frankfurt*
Sven Brandau, *Essen*
Christian Buske, *Ulm*
Federico Calegari, *Dresden*
Denis Corbeil, *Dresden*
Hassan Dihazi, *Goettingen*
Juergen Dittmer, *Halle/Saale*
Thomas Dittmar, *Witten*
Frank Edenhofer, *Bonn*
José Tomás Egaña Erazo, *Munich*
Ursula Margarethe Gehling, *Langen*
Alexander Ghanem, *Bonn*
Eric Gottwald, *Eggenstein-Leopoldshafen*
Gerhard Gross, *Braunschweig*
Kaomei Guan, *Goettingen*
Christel Herold-Mende, *Heidelberg*
Jorg Kleeff, *Munich*
Gesine Kögler, *Düsseldorf*
Steffen Koschmieder, *Muenster*
Nan Ma, *Rostock*
Ulrich R Mahlknecht, *Homburg/Saar*
Ulrich Martin, *Hannover*
Glenn Mcgee, *Berlin*
Kurt Paul Pfannkuche, *Cologne*
Michael Platten, *Heidelberg*
Arjang Ruhparwar, *Heidelberg*
Heinrich Sauer, *Giessen*
Richard Schäfer, *Tübingen*
Nils Ole Schmidt, *Hamburg*
Sonja Schrepfer, *Hamburg*
Dimitry Spitkovsky, *Cologne*
Bodo-Eckehard Strauer, *Düsseldorf*
Sergey V Tokalov, *Dresden*
Wolfgang Wagner, *Aachen*

Greece

Nicholas P Anagnou, *Athens*

Hungary

Ferenc Uher, *Dioszegiut*

India

Anirban Basu, *Haryana*
Chiranjib Chakraborty, *Vellore*
Gugdutta U Gangenahalli, *New Delhi*
Minal Garg, *Lucknow*
Devendra K Gupta, *New Delhi*
Asok Mukhopadhyay, *New Delhi*
Riaz Ahmad Shah, *Kashmir*
Prathibha Harish Shetty, *Navi Mumbai*
Anjali Suhas Shiras, *Maharashtra*
Malancha Ta, *Bangalore*

Iran

Hossein Baharvand, *Tehran*
Mohamadreza B Eslaminejad, *Tehran*
Iraj Ragerdi Kashani, *Tehran*
Mansoureh Movahedin, *Tehran*
Seyed Javad Mowla, *Tehran*
Ghasem Hosseini Salekdeh, *Tehran*
Masoud Soleimani, *Tehran*
M Mehdi Yaghoobi, *Ostandari St. Kerman*
Arash Zaminy, *Tehran*

Ireland

Frank P Barry, *Galway*
Leo Quinlan, *Galway*
Philippe Taupin, *Dublin*
Ralf Michael Zwacka, *Galway*

Israel

Nadir Askenasy, *Petach Tikva*
Zeev Blumenfeld, *Haifa*
Benayahu Dafna, *Tel Aviv*
Benjamin Dekel, *Tel-Hashomer*
Dan Gazit, *Jerusalem*
Gal Goldstein, *Tel-Hashomer*
Eran Meshorer, *Jerusalem*
Rachel Sarig, *Rehovot*
Avichai Shimoni, *Tel-Hashomer*
Shimon Slavin, *Tel Aviv*

Italy

Andrea Barbuti, *Milan*

Carlo Alberto Beltrami, *Udine*
Bruno Bonetti, *Verona*
Paola Bruni, *Florence*
Laura Calzà, *Ozzano Emilia*
Giovanni Camussi, *Turin*
Domenico Capone, *Naples*
Francesco Carinci, *Ferrara*
Carmelo Carlo-Stella, *Milan*
Clotilde Castaldo, *Naples*
Angela Chambery, *Caserta*
Massimo De Felici, *Rome*
Enzo Di Iorio, *Zelarino*
Francesco Dieli, *Palermo*
Massimo Dominici, *Modena*
Stefania Filosa, *Naples*
Guido Frosina, *Genova*
Pompilio Giulio, *Milan*
Antonio Graziano, *Naples*
Brunella Grigolo, *Bologna*
Annalisa Grimaldi, *Varese*
Angela Gritti, *Milan*
Alessandro Isidori, *Pesaro*
Caterina AM La Porta, *Milan*
Giampiero La Rocca, *Palermo*
Giampiero Leanza, *Trieste*
Enrico Lucarelli, *Bologna*
Margherita Maioli, *Sassari*
Ferdinando Mannello, *Urbino*
Tullia Maraldi, *Modena*
Gianvito Martino, *Milan*
Monica Mattioli-Belmonte, *Ancona*
Fabrizio Michetti, *Rome*
Gabriella Minchiotti, *Naples*
Roberta Morosetti, *Rome*
Gianpaolo Papaccio, *Naples*
Felicita Pedata, *Florence*
Maurizio Pesce, *Milan*
Anna Chiara Piscaglia, *Rome*
Vito Pistoia, *Genova*
Francesca Pistollato, *Ispra*
Alessandro Poggi, *Genova*
Domenico Ribatti, *Bari*
Sergio Rutella, *Rome*
Sonia Scarfi', *Genova*
Arianna Scuteri, *Monza*
Luca Steardo, *Rome*
Gianluca Vadalà, *Rome*
Maria Teresa Valenti, *Verona*
Carlo Ventura, *Bologna*
Stefania Violini, *Lodi*

Japan

Manabu Akahane, *Nara*
Yasuto Akiyama, *Shizuoka*
Tomoki Aoyama, *Kyoto*
Sachiko Ezoe, *Osaka*
Yusuke Furukawa, *Tochigi*
Masayuki Hara, *Osaka*
Eiso Hiyama, *Hiroshima*
Kanya Honoki, *Kashihara*
Yuichi Hori, *Kobe*
Susumu Ikehara, *Osaka*
Ken-ichi Isobe, *Aichi*
Masamichi Kamihira, *Fukuoka*
Yonehiro Kanemura, *Osaka*
Hiroshi Kanno, *Yokohama*
Masaru Katoh, *Tokyo*
Eihachiro Kawase, *Kyoto*
Toru Kondo, *Sapporo*
Toshihiro Kushibiki, *Osaka*
Tao-Sheng Li, *Yamaguchi*
Yasuhisa Matsui, *Sendai*
Taro Matsumoto, *Tokyo*
Yuko Miyagoe-Suzuki, *Tokyo*
Hiroyuki Miyoshi, *Ibaraki*
Hiroyuki Mizuguchi, *Osaka*
Hiroshi Mizuno, *Sendai*
Takashi Nagasawa, *Kyoto*
Kohzo Nakayama, *Nagano*
Tetsuhiro Niidome, *Kyoto*
Toshio Nikaido, *Toyama*
Shoko Nishihara, *Tokyo*
Hirofumi Noguchi, *Okayama*
Tsukasa Ohmori, *Tochigi*
Katsutoshi Ozaki, *Tochigi*
Kumiko Saeki, *Tokyo*
Masanori Sasaki, *Hokkaido*
Kazunobu Sawamoto, *Aichi*
Goshi Shiota, *Yonago*
Mikiko C Siomi, *Tokyo*
Yoshiaki Sonoda, *Osaka*
Takashi Tada, *Kyoto*
Miyako Takaki, *Nara*
Kenzaburo Tani, *Fukuoka*
Shihori Tanabe, *Tokyo*
Shuji Toda, *Saga*
Atsunori Tsuchiya, *Niigata*
Kohichiro Tsuji, *Tokyo*
Shingo Tsuji, *Osaka*
Akihiro Umezawa, *Tokyo*
Hiroshi Wakao, *Sapporo*
Yoichi Yamada, *Nagoya*
Takashi Yokota, *Kanazawa*
Yukio Yoneda, *Ishikawa*
Kotaro Yoshimura, *Tokyo*
Katsutoshi Yoshizato, *Hiroshima*
Louis Yuge, *Hiroshima*

Jordan

Khitam Salem Odeh Alrefu, *Karak*

Malaysia

Rajesh Ramasamy, *Selangor*

Mexico

Marco A Velasco-Velazquez, *Mexico City*

Morocco

Radouane Yafia, *Ouarzazate*

Netherlands

Robert Paul Coppes, *Groningen*
Dirk Gijsbert de Rooij, *Amsterdam*
Christine Mummery, *Leiden*
Vered Raz, *Leiden*
Bernardus A Johannes Roelen, *Utrecht*
Marten Piet Smidt, *Utrecht*
Frank JT Staal, *Leiden*
Ruurd Torensma, *Nijmegen*

Norway

Brynjar Foss, *Stavanger*
Zhenhe Suo, *Oslo*
Berit Bølge Tysnes, *Bergen*

Portugal

Inês M Araújo, *Coimbra*

Romania

Mihaela Chivu Economescu, *Bucharest*

Russia

Igor A Grivennikov, *Moscow*
Sergey L Kiselev, *Moscow*
Serov Oleg, *Novosibirsk*

Singapore

Yu Cai, *Singapore*
Tong Cao, *Singapore*
Jerry Chan, *Singapore*
Ken Kwok-Keung Chan, *Singapore*
Woon Khiong Chan, *Singapore*
Gavin Stewart Dawe, *Singapore*
Peter Dröge, *Singapore*
Seet Li Fong, *Singapore*
Boon Chin Heng, *Singapore*
Yunhan Hong, *Singapore*
Yuin-Han Loh, *Singapore*
Koon Gee Neoh, *Singapore*
Steve Kah Weng Oh, *Singapore*
Kian Keong Poh, *Singapore*
Seeram Ramakrishna, *Singapore*
Herbert Schwarz, *Singapore*
Winston Shim, *Singapore*
Vivek M Tanavde, *Singapore*
Shu Wang, *Singapore*

Slovakia

Lubos Danisovic, *Bratislava*

South Korea

Kwang-Hee Bae, *Daejeon*
Hyuk-Jin Cha, *Seoul*
Jong Wook Chang, *Seoul*
Kyu-Tae Chang, *Chungcheongbuk-do*
Chong-Su Cho, *Seoul*
Myung Soo Cho, *Seoul*
Ssang-Goo Cho, *Seoul*
Kang-Yell Choi, *Seoul*
Ho Jae Han, *Gwangju*
Myung-Kwan Han, *Jeonju*
Chan Yeong Heo, *Gyeonggido*

Dong-Youn Hwang, *Seongnam*
Ki-Chul Hwang, *Seoul*
Sin-Soo Jeun, *Seoul*
Youngjoon Jun, *Gyeonggi-do*
Ji-Won Jung, *Chungbuk*
Jin Sup Jung, *Gyeongsangnam-do*
Kyung-Sun Kang, *Seoul*
Gilson Khang, *Jeonju*
Byung Soo Kim, *Seoul*
Haekwon Kim, *Seoul*
Hoeon Kim, *Daejeon*
Hyo-Soo Kim, *Seoul*
Jong-Hoon Kim, *Seoul*
Mee Kum Kim, *Seoul*
Moon Suk Kim, *Suwon*
Sang Gyung Kim, *Daegu*
Song Cheol Kim, *Seoul*
Yoon Jun Kim, *Seoul*
Dong Ryul Lee, *Seoul*
Jong Eun Lee, *Seoul*
Kwang-Bok Lee, *Chonbuk*
Soo-Hong Lee, *Gyunggi-do*
Younghee Lee, *Chungbuk*
Dae-Sik Lim, *Daejeon*
Kyu Lim, *Daejeon*
Do Sik Min, *Busan*
Byung Soon Park, *Seoul*
Jong-Beom Park, *Seoul*
Gyu-Jin Rho, *Jinju*
Chun Jeih Ryu, *Seoul*
Sun U Song, *Incheon*
Jong-Hyuk Sung, *Seoul*
Jong-Ho Won, *Seoul*
Seung Kwon You, *Seoul*

Spain

Luis M Antón Aparicio, *Coruña*
Angel Ayuso-Sacido, *Valencia*
Fernando Cobo, *Granada*
Maria P De Miguel, *Madrid*
Sabrina C Desbordes, *Barcelona*
Ramon Farre, *Barcelona*
Damian Garcia-Olmo, *Madrid*
Boulaiz Houria, *Granada*
Juan M Hurle, *Santander*
Antonia Aránega Jiménez, *Granada*
Marta Muñoz Llamosas, *España*
Juan Antonio Marchal, *Granada*
Pablo Menendez, *Granada*
María Dolores Miñana, *Valencia*
Eduardo Moreno, *Madrid*
Felipe Prosper, *Navarra*
Manuel Ramírez, *Madrid*

Sweden

M Quamrul Islam, *Linkoping*
Stefan Karlsson, *Lund*
Stephen C Strom, *Stockholm*
Rachael Victoria Sugars, *Huddinge*

Switzerland

Thomas Daikeler, *Basel*
Anis Feki, *Geneva*
Sabrina Mattoli, *Basel*
Arnaud Scherberich, *Basel*

Thailand

Rangsun Parnpai, *Nakhon Ratchasima*

Tunisia

Faouzi Jenhani, *Monastir*

Turkey

Kamil C Akcali, *Ankara*
Berna Arda, *Ankara*
Alp Can, *Ankara*
Y Murat Elcin, *Ankara*
Erdal Karaoz, *Kocaeli*

United Arab Emirates

Sherif M Karam, *Al-Ain*

United Kingdom

Malcolm Ronald Alison, *London*
Charles Archer, *Cardiff*
Dominique Bonnet, *London*
Kristin Mary Braun, *London*
Wei Cui, *London*
Nicholas R Forsyth, *Stoke-on-Trent*
Rasmus Freter, *Oxford*
Hassan T Hassan, *Paisley*
David C Hay, *Edinburgh*
Wael Kafienah, *Bristol*
Francis L Martin, *Lancaster*
Stuart McDonald, *London*
Pankaj Kumar Mishra, *Wolverhampton*
Ali Mobasheri, *Leicestershire*
Mike Modo, *London*
Donald Palmer, *London*
Stefano Pluchino, *Cambridge*
Julia Margaret Polak, *London*
Stefan Alexander Przyborski, *Durham*
James Alexander Ross, *Edinburgh*
Susan Gaynor Shawcross, *Manchester*
Alastair James Sloan, *Cardiff*
Virginie Sottile, *Nottingham*
Petros V Vlastarakos, *Stevenage*
Hong Wan, *London*
Christopher M Ward, *Manchester*
Heping Xu, *Foresterhill*
Lingfang Zeng, *London*
Rike Zietlow, *Cardiff*

United States

Gregor Barr Adams, *Los Angeles*
Arshak R Alexanian, *Milwaukee*
Ali Syed Arbab, *Charlestown*
Kinji Asahina, *Los Angeles*
Atsushi Asakura, *Minneapolis*
Prashanth Asuri, *Santa Clara*
Craig S Atwood, *Madison*
Debabrata Banerjee, *New Brunswick*
David W Barnes, *Lawrenceville*
Surinder Kumar Batra, *Omaha*
Aline M Betancourt, *New Orleans*
John J Bright, *Indianapolis*
Bruce Alan Bunnell, *New Orleans*
Matthew E Burow, *New Orleans*
Anthony Wing Sang Chan, *Atlanta*
Rebecca J Chan, *Indianapolis*
Joe Y Chang, *Houston*
G Rasul Chaudhry, *Rochester*
Caifu Chen, *Foster City*
Ke Cheng, *Los Angeles*
Jonathan Donald Chesnut, *Carlsbad*
Herman S Cheung, *Coral Gables*
Kent W Christopherson II, *Chicago*
David Wade Clapp, *Indianapolis*
Claudius Conrad, *Boston*
Charles Samuel Cox Jr, *Houston*
Ronald G Crystal, *New York*
Hiranmoy Das, *Columbus*
Ivana de la Serna, *Toledo*
Marcos de Lima, *Houston*
Douglas C Dean, *Lousiville*
Bridget M Deasy, *Pittsburgh*
Weiwen Deng, *Grand Rapids*
Goberdhan Dimri, *Evanston*
David Dingli, *Rochester*
Juan Domínguez-Bendala, *Miami*
Sergey V Doronin, *Stony Brook*
Fu-Liang Du, *Vernon*
Gary L Dunbar, *Mt. Pleasant*
Todd Evans, *New York*
Toshihiko Ezashi, *Columbia*
Vincent Falanga, *Providence*
Zhongling Fen, *Oceanside*
Markus Frank, *Boston*
Mohamed A Gaballa, *Sun City*
G Ian Gallicano, *Washington*
Yair Gazitt, *San Antonio*
Sanga Gehmert, *Houston*
Yong-Jian Geng, *Houston*
Jorge A Genovese, *Salt Lake City*
Mehrnaz Gharaee-Kermani, *Ann Arbor*
Ali Gholamrezanezhad, *Baltimore*
Joseph C Glorioso, *Pittsburgh*
W Scott Goebel, *Indianapolis*
Brigitte N Gomperts, *Los Angeles*
Joel S Greenberger, *Pittsburgh*
Kristbjorn Orri Gudmundsson, *Frederick*
Preethi H Gunaratne, *Houston*
Yan-Lin Guo, *Hattiesburg*
Robert G Hawley, *Washington*
Tong-Chuan He, *Chicago*
Mary JC Hendrix, *Chicago*
Charles C Hong, *Nashville*
Yiling Hong, *Dayton*
Courtney W Houchen, *Oklahoma City*
George TJ Huang, *Boston*
Jing Huang, *Bethesda*
Johnny Huard, *Pittsburgh*
Jaclyn Y Hung, *San Antonio*
Lorraine Iacovitti, *Philadelphia*
Tony Ip, *Worcester*
D Joseph Jerry, *Springfield*
Kun-Lin Jin, *Novato*
Lixin Kan, *Chicago*
Winston Whei-Yang Kao, *Cincinnati*
Sunil Kapila, *Ann Arbor*
Partow Kebriaei, *Houston*
Mary J Kelley, *Portland*
Sophia K Khaldoyanidi, *San Diego*

Mahesh Khatri, *Wooster*
Jaspal S Khillan, *Pittsburgh*
Michael R King, *Ithaca*
Katsuhiro Kita, *Galveston*
Prasanna Krishnamurthy, *Chicago*
Marlene Anastassova Kristeva, *Van Nuys*
John S Kuo, *Madison*
Mark A LaBarge, *Berkeley*
Uma Lakshmipathy, *Carlsbad*
Hillard Michael Lazarus, *Shaker Heights*
Techung Lee, *Buffalo*
Jianxue Li, *Boston*
Joshua Li, *Charlottesville*
Shaoguang Li, *Worcester*
Shengwen Calvin Li, *Orange*
Xiao-Nan Li, *Houston*
Ching-Shwun Lin, *San Francisco*
P Charles Lin, *Nashville*
Shuo Lin, *Los Angeles*
Ning Liu, *Madison*
Suling Liu, *Ann Arbor*
Zhenguo Liu, *Columbus*
Aurelio Lorico, *Las Vegas*
Jean-Pierre Louboutin, *Philadelphia*
Bingwei Lu, *Stanford*
Qing Richard Lu, *Dallas*
Nadya L Lumelsky, *Bethesda*
Hong-Bo R Luo, *Boston*
Hinh Ly, *Atlanta*
Teng Ma, *Tallahassee*
Kenneth Maiese, *Newark*
Zubin Master, *Albany*
Debra JH Mathews, *Baltimore*
Robert L Mauck, *Philadelphia*
Lucio Miele, *Jackson*
Robert H Miller, *Cleveland*
David K Mills, *Ruston*
Murielle Mimeault, *Omaha*
Prasun J Mishra, *Bethesda*
Kalpana Mujoo, *Houston*
Masato Nakafuku, *Cincinnati*
Mary B Newman, *Chicago*
Wenze Niu, *Dallas*
Christopher Niyibizi, *Hershey*
Jon M Oatley, *Pullman*
Seh-Hoon Oh, *Gainesville*
Shu-ichi Okamoto, *La Jolla*
Frank Pajonk, *Los Angeles*
Nishit Pancholi, *Chicago*
Deric M Park, *Charlottesville*
Gregory M Pastores, *New York*
Ming Pei, *Morgantown*
Derek A Persons, *Memphis*
Donald G Phinney, *Jupiter*
John S Pixley, *Reno*
Dimitris G Placantonakis, *New York*
George E Plopper, *Troy*
Mark EP Prince, *Ann Arbor*
April Pyle, *Los Angeles*
Derek Radisky, *Jacksonville*
Murugan Ramalingam, *Gaithersburg*
Pranela Rameshwar, *Newark*
Guangwen Ren, *Piscataway*
Brent A Reynolds, *Gainesville*
Jeremy N Rich, *Cleveland*
Angie Rizzino, *Omaha*
Fred Jerrold Roisen, *Louisville*
Rouel S Roque, *Henderson*
Carl Barth Rountree Jr, *Lititz*
Clinton T Rubin, *Stony Brook*
Donald Sakaguchi, *Ames*
Paul Ronald Sanberg, *Tampa*
Gerald Phillip Schatten, *Pittsburgh*
Stewart Sell, *Albany*
Arun Sharma, *Chicago*
Jinsong Shen, *Dallas*
Ashok Kumar Shetty, *Durham*
Songtao Shi, *Los Angeles*
Yanhong Shi, *Duarte*
Vassilios I Sikavitsas, *Norman*
Igor I Slukvin, *Madison*
Shay Soker, *Winston-Salem*
Hongjun Song, *Baltimore*
Edward F Srour, *Indianapolis*
Hua Su, *Francisco*
Jun Sun, *Rochester*
Tao Sun, *New York*
Siamak Tabibzadeh, *Stony Brook*
Kenichi Tamama, *Columbus*
Masaaki Tamura, *Manhattan*
Tetsuya S Tanaka, *Notre Dame*
Dean G Tang, *Smithville*
Hugh S Taylor, *New Haven*
Jonathan L Tilly, *Boston*
Jakub Tolar, *Minneapolis*
Deryl Troyer, *Manhattan*
Scheffer Chuei-Goong Tseng, *Miami*
Cho-Lea Tso, *Los Angeles*
Andre Van Wijnen, *Worcester*
Lyuba Varticovski, *Bethesda*
Tandis Vazin, *Berkeley*
Kent E Vrana, *Hershey*
Qi Wan, *Reno*
Charles Wang, *Los Angeles*
Guo-Shun Wang, *New Orleans*
Lianchun Wang, *Athens*
Limin Wang, *Ann Arbor*
Shu-Zhen Wang, *Birmingham*
Yigang Wang, *Cincinnati*
Zack Z Wang, *Scarborough*
Zhiqiang Wang, *Duarte*
David Warburton, *Los Angeles*
Li-Na Wei, *Minneapolis*
Christof Westenfelder, *Salt Lake City*
Marc Adrian Williams, *Rochester*
J Mario Wolosin, *New York*
Raymond Ching-Bong Wong, *Irvine*
Joseph C Wu, *Stanford*
Lizi Wu, *Gainesville*
Ping Wu, *Galveston*
Sean M Wu, *Boston*
Wen-Shu Wu, *Scarborough*
Meifeng Xu, *Cincinnati*
Xiaowei Xu, *Philadelphia*
Yan Xu, *Pittsburgh*
Dean Takao Yamaguchi, *Los Angeles*
Jun Yan, *Louisville*
Feng-Chun Yang, *Indianapolis*
Jing Yang, *Orange*
Phillip Chung-Ming Yang, *Stanford*
Shang-Tian Yang, *Columbus*
Xiaoming Yang, *Seattle*
Youxin Yang, *Boston*
Kaiming Ye, *Fayetteville*
Pampee Paul Young, *Nashville*
Hui Yu, *Pittsburgh*
John S Yu, *Los Angeles*
P Hong Yu, *Miami*
Seong-Woon Yu, *East Lansing*
Xian-Min Zeng, *Novato*
Ming Zhan, *Baltimore*
Baohong Zhang, *Greenville*
Chengcheng Zhang, *Dallas*
Qunzhou Zhang, *Los Angeles*
Yan Zhang, *Houston*
Ying Zhang, *Baltimore*
Pan Zheng, *Ann Arbor*
X Long Zheng, *Philadelphia*
Xuesheng Zheng, *Charlestown*
John F Zhong, *Los Angeles*
Bin Zhou, *Boston*
Feng C Zhou, *Indianapolis*
Xianzheng Zhou, *Minneapolis*

Venezuela

Pedro M Aponte, *Estado Aragua*

WJSC

World Journal of Stem Cells

Contents

Monthly Volume 7 Number 6 July 26, 2015

World Journal of Stem Cells
Volume 7 Number 6 July 26, 2015

Contents

NAME OF JOURNAL
World Journal of Stem Cells

ISSN
ISSN 1948-0210 (online)

LAUNCH DATE
December 31, 2009

FREQUENCY
Monthly

Room 903, Building D, Ocean International Center,
No. 62 Dongsihuan Zhonglu, Chaoyang District,
Beijing 100025, China
Telephone: +86-10-85381891
Fax: +86-10-85381893
E-mail: editorialoffice@wjgnet.com
Help Desk: http://www.wjgnet.com/esps/helpdesk.aspx
http://www.wjgnet.com

PUBLISHER
Baishideng Publishing Group Inc
8226 Regency Drive,
Pleasanton, CA 94588, USA
Telephone: +1-925-223-8242
Fax: +1-925-223-8243
E-mail: bpgoffice@wjgnet.com
Help Desk: http://www.wjgnet.com/esps/helpdesk.aspx
http://www.wjgnet.com

PUBLICATION DATE
July 26, 2015

INSTRUCTIONS TO AUTHORS
Full instructions are available online at http://www.wjgnet.com/1948-0210/g_info_20100313165700.htm

ONLINE SUBMISSION
http://www.wjgnet.com/esps/

World Journal of Stem Cells

Submit a Manuscript: http://www.wjgnet.com/esps/
Help Desk: http://www.wjgnet.com/esps/helpdesk.aspx
DOI: 10.4252/wjsc.v7.i6.894

World J Stem Cells 2015 July 26; 7(6): 894-898
ISSN 1948-0210 (online)

EDITORIAL

Enhancing endothelial progenitor cell for clinical use

Lei Ye, Kian-Keong Poh

Lei Ye, National Heart Research Institute Singapore, National Heart Centre Singapore, Singapore 169609, Singapore

Kian-Keong Poh, Department of Medicine, Yong Loo Lin School of Medicine, National University of Singapore, Singapore 119077, Singapore

Kian-Keong Poh, Department of Cardiology, National University Heart Center, National University Health System, Singapore 119228, Singapore

Author contributions: Both authors contributed to this manuscript.

Conflict-of-interest statement: None.

Correspondence to: Kian-Keong Poh, MBBChir, FRCP, FACC, Associate Professor, Department of Cardiology, National University Heart Centre, National University Health System, 1E, Kent Ridge Road, NUHS Tower Block, Level 9, Singapore 119228, Singapore. kian_keong_poh@nuhs.edu.sg
Telephone: +65-92373289
Fax: +65-68722998

Received: February 2, 2015
Peer-review started: February 4, 2015
First decision: March 20, 2015
Revised: April 3, 2015
Accepted: May 16, 2015
Article in press: May 18, 2015
Published online: July 26, 2015

Abstract

Circulating endothelial progenitor cells (EPCs) have been demonstrated to correlate negatively with vascular endothelial dysfunction and cardiovascular risk factors. However, translation of basic research into the clinical practice has been limited by the lack of unambiguous and consistent definitions of EPCs and reduced EPC cell number and function in subjects requiring them for clinical use. This article critically reviews the definition of EPCs based on commonly used protocols, their value as a biomarker of cardiovascular risk factor in subjects with cardiovascular disease, and strategies to enhance EPCs for treatment of ischemic diseases.

Key words: Endothelial progenitor cells; Cell therapy; Enhancing function and number; CD34; Clinical trials

Core tip: Circulating endothelial progenitor cells (EPCs) have important potential for use in the treatment of ischemic diseases. However, their clinical application is limited by the lack of unambiguous and consistent definitions. This article reviews the definition of EPCs, their status in subjects with cardiovascular disease and discusses strategies to enhance EPCs for treatment of ischemic diseases. In patients with cardiovascular conditions who may require EPC administration, EPC numbers are low and EPCs are dysfunctional. Augmenting these cells may eventually improve their clinical efficacy.

Ye L, Poh KK. Enhancing endothelial progenitor cell for clinical use. *World J Stem Cells* 2015; 7(6): 894-898 Available from: URL: http://www.wjgnet.com/1948-0210/full/v7/i6/894.htm DOI: http://dx.doi.org/10.4252/wjsc.v7.i6.894

INTRODUCTION

Circulating endothelial progenitor cells (EPCs) are bone marrow - derived mononuclear cells that have the capacity to migrate, proliferate, and differentiate into mature endothelial cells (ECs)[1]. Asahara *et al*[2],

reported that $CD34^+$ hematopoietic progenitor cells from adults can differentiate *ex vivo* to an endothelial phenotype, expressing EC markers and incorporating into neovessels. Since then, many publications have demonstrated the phenotype and function of these cells and use them in animal models and clinical studies[3-7].

HETEROGENEITY OF EPC

The translation of basic research into the clinical practice of EPCs has been limited, in part, by the lack of unambiguous and consistent definitions of EPCs. In general, two methods have been used to isolate EPCs: (1) cell selection based on surface markers; and (2) cell culture and then selection. Besides CD34, a variety of cell surface markers have been shown to be associated with EPCs.

Both $CD14^+$ monocytic and $CD14^-$ non-monocytic mononuclear cells have been used as the starting population for cultivation of EPCs[6]. Fernandez Pujol *et al*[8], demonstrated that $CD14^+$ monocytic cells underwent a morphological transformation to oval cells and showed a clear expression of EC markers after 1 wk. These markers include von Willebrand factor (vWF), VE-cadherin, CD105, acetylated low-density lipoprotein (ac-LDL)-receptor, CD36, vascular endothelial cell growth factor receptor-1 (VEGFR-1, Flt-1), and VEGF receptor-2 (VEGFR-2 or KDR). However, Urbich *et al*[6], showed that $CD14^-$ non-monocytic mononuclear cells also expressed endothelial marker proteins and were able to form colonies. $CD14^-$ cells were found to incorporate into vascular structures of nude mice after hind-limb ischemia and significantly improved neovascularization.

Kalka *et al*[9], cultured human peripheral blood mononuclear cells and characterized adherent EPCs. EPCs were able to up-take ac-LDL and expressed endothelial surface markers such as vWF, VEGFR-2, VE-cadherin, CD146, and CD31. In a similar approach, Hill *et al*[10], found that colonial formation EPCs expressed KDR, CD31, and TIE2.

Interestingly, Hur *et al*[3], identified two types of EPCs from the same source and labelled them as early EPC and late EPC. They expressed different level of VE-cadherin, Flt-1, KDR, and CD45 markers. Late EPC produced more nitric oxide, incorporated more into human umbilical vein ECs monolayer, and are able to better form capillary tube than early EPC[3]. However, early EPC secreted more angiogenic cytokines (VEGF and interleukin-8) than late EPC at culture[3]. These suggest that two types of EPC might have different roles in neovasculogenesis.

More recently, besides CD34, CD133, KDR and Ac-LDL up-take have been used more frequently as EPC markers for selection[11-14]. CD34 is a stem cell marker, CD133 an early EPC marker, KDR a marker for ECs, and Ac-LDL up-take, an endothelial function. Controversy remains on what are the most suitable makers for selecting EPC and what type of EPCs are most optimal for clinical application of cell therapy. Regardless of their cell surface markers, EPCs shall have the capacity to form tubular structure on Matrigel[3,4], take up Ac-LDL[3,4], form colonies[4-6] and have the capacity to form vessels *in vitro*[2,9,15,16].

EPC NUMBER AND FUNCTION IN CARDIOVASCULAR DISEASES

Clinical studies documented a decreased number of circulating EPCs in coronary artery disease (CAD) patients, suggesting that levels of circulating EPCs might be associated with vascular endothelial function and cardiovascular risk factors[17-21]. Hill *et al*[10] measured colony-forming units of EPCs from patients with different degrees of cardiovascular risk but without history of cardiovascular disease. A strong correlation was found between the number of circulating EPCs and the subjects' Framingham risk factor score and between the endothelial function and the number of EPCs. It was also found that EPCs from subjects at high risk for cardiovascular events had higher rates of *in vitro* senescence than cells from subjects at low risk.

Subsequently, it was demonstrated that reduced level of circulating EPCs independently predicts atherosclerotic disease progression and development of cardiovascular events[17-19]. Sen *et al*[17], suggested that EPC determines the quality of the coronary collateral circulation. Georgescu *et al*[18] found that hypertension with hypercholesterolemia is accompanied by the alteration of vascular tone, the expression of pro-inflammatory molecules by the vessel wall, and reduced circulating EPC number.

However, contrasting results were reported, by Güven *et al*[22] and Werner *et al*[23], on the association between the level of circulating EPCs and severity of CAD. Similarly, contrasting reports were also published in patients with peripheral arterial disease (PAD)[13,24-26]. This difference might be explained by different sampling time during the studies at different part of the disease process[27] Higher circulating EPC may indicate early stage of CAD and PAD, while lower circulating EPC indicates more severe and late stage of disease, and is associated with poorer outcome of these patients. It become clear that EPC cell number and function are reduced in subjects with cardiovascular risk factors and more severe cardiovascular disease[28-32]. These are also subjects whom may benefit from EPC harvest for autologous transplantation. Thus it is important to enhance EPC cell number and function for clinical use.

STRATEGIES TO ENHANCE EPC POTENCY

Though animal studies of autologous EPC transplantation is feasible in both coronary and peripheral artery diseases, clinical application of these therapies are limited. Asai *et al*[33] demonstrated that topical Sonic hedgehog (*Shh*) gene therapy enhanced wound healing

by promoting recruitment of bone marrow derived EPCs. Besides migration, Shh also enhances EPC proliferation, adhesion, and tubule formation. In contrast, Jujo *et al*[34], showed that AMD3100, a CXCR4 antagonist, enhanced neovascularization and functional recovery after myocardial infarction through enhanced mobilization of EPC. Interestingly, the combinational therapy of Shh gene transfer with AMD3100 improved cardiac functional recovery by enhanced progenitor cell mobilization[35].

Yao *et al*[12], modified EPCs with tissue kallikrein (TK) and found that TK protected EPCs from oxidative stress-induced apoptosis *via* inhibition of activation of caspase-3 and -9, induction of Akt phosphorylation, and secretion of vascular endothelial growth factor[12]. Moreover, Fu *et al*[36], demonstrated that TK can enhance EPC migration and adhesion by up-regulating the expression of integrin-$\alpha\beta$3. Thus, TK-modified EPCs may be another strategy to enhance therapeutic potency of EPC for tissue repair.

Other agents such as statin, adiponectin, thymosin β4 (Tβ4), losartan, aliskiren, hydrogen sulfide, GTP cyclohydrolase Ⅰ, and ephrin-B2/Fc have been used to enhance EPC[37-42]. Among these, statin, losartan, aliskiren, and Tβ4 have good potential to improve quality and quantity of EPCs in patients with diabetes. Statins, a commonly used class of drugs to lower cholesterol levels by inhibiting the enzyme HMG-CoA reductase, have pleiotropic beneficial effect on EPC[37,43], atorvastatin increased circulating EPC after just 4 wk of administration in patients with ischemic heart failure[37]. Rosuvastatin mobilized EPC which is shown to be Akt/endothelial nitric oxide synthase dependent[43].

Besides statins, losartan, an angiotensin II receptor antagonist drug, commonly used in hypertension, significantly improved impaired EPC function in hypertensive patients[42]. Tβ4, an actin sequestering protein, is found to possess angiogenic activity[44,45] and anti-diabetic property[46]. Tβ4 is angiogenic and can promote EC migration and adhesion, tubule formation, aortic ring sprouting, and angiogenesis[44,45]. Tβ4 ameliorates hyperglycemia and improves insulin resistance in mouse model of type 2 diabetes[46]. We showed that EPCs derived from Zucker diabetic fatty rat have reduced angiogenic potential. Treatment with Tβ4 *in vitro* improved EPC function and survival. It also appears to be beneficial *in vivo* (unpublished results). Tβ4 is a potential drug that can improve function of diabetic EPCs for cell therapy.

Clinically, EPC has been used in clinical trials[7,21,47]. In early phase clinical trials using EPCs for intramyocardial transplantation in subjects with refractory angina, Losordo *et al*[7,48] used G-CSF to mobilize bone marrow cells and selected $CD34^+$ cells using magnetic beads post-apheresis. Subsequently these are injected into the ischemic myocardium without enhancing the cells[7,48]. Feasibility and safety appears to be established. However, efficacy remains to be demonstrated in sizeable clinical trials, preferably in a randomized and blinded manner. As subjects who need EPC therapy has lower EPC numbers and more dysfunctional EPC, these cells may need to be augmented prior to autologous transplantation. There are already several agents discussed above, which can enhance mobilization (*e.g*., AMD3100) and function of these cells. For the latter, post-processing after harvesting, may be employed. However, it will be important to make sure the cells improve and no adverse effect on these cells as a result. *In vitro* assays and animal experiments appear to show enhancement. Whether these strategies can be translated into clinical use remain to be demonstrated. It is also important to define relevant clinical end-points and surrogate parameters. Beyond statistical significance in improving markers, these need to be clinical significance. Thus, EPC migration may increase by a few millimeter *in vitro* in a dish or the left ventricular longitudinal strain may increase by a couple of percent, it is important to show clinical relevance in translation. Besides autologous strategies, allogeneic transplantation, which has been used in animal models, may also be considered for clinical use[45,49].

REFERENCES

1 **Luttun A**, Carmeliet G, Carmeliet P. Vascular progenitors: from biology to treatment. *Trends Cardiovasc Med* 2002; **12**: 88-96 [PMID: 11852257 DOI: 10.1016/S1050-1738(01)00152-9]

2 **Asahara T**, Murohara T, Sullivan A, Silver M, van der Zee R, Li T, Witzenbichler B, Schatteman G, Isner JM. Isolation of putative progenitor endothelial cells for angiogenesis. *Science* 1997; **275**: 964-967 [PMID: 9020076 DOI: 10.1126/science.275.5302.964]

3 **Hur J**, Yoon CH, Kim HS, Choi JH, Kang HJ, Hwang KK, Oh BH, Lee MM, Park YB. Characterization of two types of endothelial progenitor cells and their different contributions to neovasculogenesis. *Arterioscler Thromb Vasc Biol* 2004; **24**: 288-293 [PMID: 14699017 DOI: 10.1161/01.ATV.0000114236.77009.06]

4 **Ingram DA**, Mead LE, Tanaka H, Meade V, Fenoglio A, Mortell K, Pollok K, Ferkowicz MJ, Gilley D, Yoder MC. Identification of a novel hierarchy of endothelial progenitor cells using human peripheral and umbilical cord blood. *Blood* 2004; **104**: 2752-2760 [PMID: 15226175 DOI: 10.1182/blood-2004-04-1396]

5 **Yoder MC**, Mead LE, Prater D, Krier TR, Mroueh KN, Li F, Krasich R, Temm CJ, Prchal JT, Ingram DA. Redefining endothelial progenitor cells via clonal analysis and hematopoietic stem/progenitor cell principals. *Blood* 2007; **109**: 1801-1809 [PMID: 17053059 DOI: 10.1182/blood-2006-08-043471]

6 **Urbich C**, Heeschen C, Aicher A, Dernbach E, Zeiher AM, Dimmeler S. Relevance of monocytic features for neovascularization capacity of circulating endothelial progenitor cells. *Circulation* 2003; **108**: 2511-2516 [PMID: 14581410 DOI: 10.1161/01.CIR.0000096483]

7 **Losordo DW**, Schatz RA, White CJ, Udelson JE, Veereshwarayya V, Durgin M, Poh KK, Weinstein R, Kearney M, Chaudhry M, Burg A, Eaton L, Heyd L, Thorne T, Shturman L, Hoffmeister P, Story K, Zak V, Dowling D, Traverse JH, Olson RE, Flanagan J, Sodano D, Murayama T, Kawamoto A, Kusano KF, Wollins J, Welt F, Shah P, Soukas P, Asahara T, Henry TD. Intramyocardial transplantation of autologous CD34+ stem cells for intractable angina: a phase I/IIa double-blind, randomized controlled trial. *Circulation* 2007; **115**: 3165-3172 [PMID: 17562958 DOI: 10.1161/CIRCULATIONAHA.106.687376]

8 **Fernandez Pujol B**, Lucibello FC, Gehling UM, Lindemann K, Weidner N, Zuzarte ML, Adamkiewicz J, Elsässer HP, Müller R, Havemann K. Endothelial-like cells derived from human CD14 positive monocytes. *Differentiation* 2000; **65**: 287-300 [PMID: 10929208 DOI: 10.1046/j.1432-0436.2000.6550287.x]

9 **Kalka C**, Masuda H, Takahashi T, Kalka-Moll WM, Silver M, Kearney M, Li T, Isner JM, Asahara T. Transplantation of ex vivo expanded endothelial progenitor cells for therapeutic neovascularization. *Proc Natl Acad Sci USA* 2000; **97**: 3422-3427

[PMID: 10725398 DOI: 10.1073/pnas.97.7.3422]
10 **Hill JM**, Zalos G, Halcox JP, Schenke WH, Waclawiw MA, Quyyumi AA, Finkel T. Circulating endothelial progenitor cells, vascular function, and cardiovascular risk. *N Engl J Med* 2003; **348**: 593-600 [PMID: 12584367 DOI: 10.1056/NEJMoa022287]
11 **Hager G**, Holnthoner W, Wolbank S, Husa AM, Godthardt K, Redl H, Gabriel C. Three specific antigens to isolate endothelial progenitor cells from human liposuction material. *Cytotherapy* 2013; **15**: 1426-1435 [PMID: 24094492 DOI: 10.1016/j.jcyt.2013.06.018]
12 **Yao Y**, Sheng Z, Li Y, Fu C, Ma G, Liu N, Chao J, Chao L. Tissue kallikrein-modified human endothelial progenitor cell implantation improves cardiac function via enhanced activation of akt and increased angiogenesis. *Lab Invest* 2013; **93**: 577-591 [PMID: 23508045 DOI: 10.1038/labinvest.2013.48]
13 **Morishita T**, Uzui H, Nakano A, Mitsuke Y, Geshi T, Ueda T, Lee JD. Number of endothelial progenitor cells in peripheral artery disease as a marker of severity and association with pentraxin-3, malondialdehyde-modified low-density lipoprotein and membrane type-1 matrix metalloproteinase. *J Atheroscler Thromb* 2012; **19**: 149-158 [PMID: 22123215 DOI: 10.5551/jat.10074]
14 **Hernandez SL**, Gong JH, Chen L, Wu IH, Sun JK, Keenan HA, King GL. Characterization of circulating and endothelial progenitor cells in patients with extreme-duration type 1 diabetes. *Diabetes Care* 2014; **37**: 2193-2201 [PMID: 24780357 DOI: 10.2337/dc13-2547]
15 **Kocher AA**, Schuster MD, Szabolcs MJ, Takuma S, Burkhoff D, Wang J, Homma S, Edwards NM, Itescu S. Neovascularization of ischemic myocardium by human bone-marrow-derived angioblasts prevents cardiomyocyte apoptosis, reduces remodeling and improves cardiac function. *Nat Med* 2001; **7**: 430-436 [PMID: 11283669 DOI: 10.1038/86498]
16 **Kawamoto A**, Gwon HC, Iwaguro H, Yamaguchi JI, Uchida S, Masuda H, Silver M, Ma H, Kearney M, Isner JM, Asahara T. Therapeutic potential of ex vivo expanded endothelial progenitor cells for myocardial ischemia. *Circulation* 2001; **103**: 634-637 [PMID: 11156872 DOI: 10.1161/01.CIR.103.5.634]
17 **Sen T**, Aksu T. Endothelial progenitor cell and adhesion molecules determine the quality of the coronary collateral circulation/ Endothelial progenitor cells (CD34+KDR+) and monocytes may provide the development of good coronary collaterals despite the vascular risk factors and extensive atherosclerosis. *Anadolu Kardiyol Derg* 2012; **12**: 447; author reply 447-448 [PMID: 22626655 DOI: 10.5152/akd.2012.134]
18 **Georgescu A**, Alexandru N, Andrei E, Titorencu I, Dragan E, Tarziu C, Ghiorghe S, Badila E, Bartos D, Popov D. Circulating microparticles and endothelial progenitor cells in atherosclerosis: pharmacological effects of irbesartan. *J Thromb Haemost* 2012; **10**: 680-691 [PMID: 22303879 DOI: 10.1111/j.1538-7836.2012.04650.x]
19 **Du F**, Zhou J, Gong R, Huang X, Pansuria M, Virtue A, Li X, Wang H, Yang XF. Endothelial progenitor cells in atherosclerosis. *Front Biosci* (Landmark Ed) 2012; **17**: 2327-2349 [PMID: 22652782 DOI: 10.2741/4055]
20 **Głowińska-Olszewska B**, Moniuszko M, Hryniewicz A, Jeznach M, Rusak M, Dąbrowska M, Łuczyński W, Bodzenta-Łukaszyk A, Bossowski A. Relationship between circulating endothelial progenitor cells and endothelial dysfunction in children with type 1 diabetes: a novel paradigm of early atherosclerosis in high-risk young patients. *Eur J Endocrinol* 2013; **168**: 153-161 [PMID: 23111589 DOI: 10.1530/EJE-12-0857]
21 **Lee PS**, Poh KK. Endothelial progenitor cells in cardiovascular diseases. *World J Stem Cells* 2014; **6**: 355-366 [PMID: 25126384 DOI: 10.4252/wjsc.v6.i3.355]
22 **Güven H**, Shepherd RM, Bach RG, Capoccia BJ, Link DC. The number of endothelial progenitor cell colonies in the blood is increased in patients with angiographically significant coronary artery disease. *J Am Coll Cardiol* 2006; **48**: 1579-1587 [PMID: 17045891 DOI: 10.1016/j.jacc.2006.04.101]
23 **Werner N**, Wassmann S, Ahlers P, Schiegl T, Kosiol S, Link A, Walenta K, Nickenig G. Endothelial progenitor cells correlate with endothelial function in patients with coronary artery disease. *Basic Res Cardiol* 2007; **102**: 565-571 [PMID: 17932708 DOI: 10.1007/s00395-007-0680-1]
24 **Herbrig K**, Haensel S, Oelschlaegel U, Pistrosch F, Foerster S, Passauer J. Endothelial dysfunction in patients with rheumatoid arthritis is associated with a reduced number and impaired function of endothelial progenitor cells. *Ann Rheum Dis* 2006; **65**: 157-163 [PMID: 15975971 DOI: 10.1136/ard.2005.035378]
25 **Fadini GP**, Sartore S, Albiero M, Baesso I, Murphy E, Menegolo M, Grego F, Vigili de Kreutzenberg S, Tiengo A, Agostini C, Avogaro A. Number and function of endothelial progenitor cells as a marker of severity for diabetic vasculopathy. *Arterioscler Thromb Vasc Biol* 2006; **26**: 2140-2146 [PMID: 16857948 DOI: 10.1161/01.ATV.0000237750.44469.88]
26 **Delva P**, De Marchi S, Prior M, Degan M, Lechi A, Trettene M, Arosio E. Endothelial progenitor cells in patients with severe peripheral arterial disease. *Endothelium* 2008; **15**: 246-253 [PMID: 19065316 DOI: 10.1080/10623320802487718]
27 **Lee LC**, Chen CS, Choong PF, Low A, Tan HC, Poh KK. Time-dependent dynamic mobilization of circulating progenitor cells during percutaneous coronary intervention in diabetics. *Int J Cardiol* 2010; **142**: 199-201 [PMID: 19157595 DOI: 10.1016/j.ijcard.2008.11.198]
28 **Cubbon RM**, Kahn MB, Wheatcroft SB. Effects of insulin resistance on endothelial progenitor cells and vascular repair. *Clin Sci* (Lond) 2009; **117**: 173-190 [PMID: 19630751 DOI: 10.1042/CS20080263]
29 **van den Oever IA**, Raterman HG, Nurmohamed MT, Simsek S. Endothelial dysfunction, inflammation, and apoptosis in diabetes mellitus. *Mediators Inflamm* 2010; **2010**: 792393 [PMID: 20634940 DOI: 10.1155/2010/792393]
30 **Yiu KH**, Tse HF. Specific role of impaired glucose metabolism and diabetes mellitus in endothelial progenitor cell characteristics and function. *Arterioscler Thromb Vasc Biol* 2014; **34**: 1136-1143 [PMID: 24743430 DOI: 10.1161/ATVBAHA.114.302192]
31 **Zhang J**, Zhang X, Li H, Cui X, Guan X, Tang K, Jin C, Cheng M. Hyperglycaemia exerts deleterious effects on late endothelial progenitor cell secretion actions. *Diab Vasc Dis Res* 2013; **10**: 49-56 [PMID: 22561229 DOI: 10.1177/1479164112444639]
32 **Vasa M**, Fichtlscherer S, Aicher A, Adler K, Urbich C, Martin H, Zeiher AM, Dimmeler S. Number and migratory activity of circulating endothelial progenitor cells inversely correlate with risk factors for coronary artery disease. *Circ Res* 2001; **89**: E1-E7 [PMID: 11440984 DOI: 10.1161/hh1301.093953]
33 **Asai J**, Takenaka H, Kusano KF, Ii M, Luedemann C, Curry C, Eaton E, Iwakura A, Tsutsumi Y, Hamada H, Kishimoto S, Thorne T, Kishore R, Losordo DW. Topical sonic hedgehog gene therapy accelerates wound healing in diabetes by enhancing endothelial progenitor cell-mediated microvascular remodeling. *Circulation* 2006; **113**: 2413-2424 [PMID: 16702471 DOI: 10.1161/CIRCULATIONAHA.105.603167]
34 **Jujo K**, Hamada H, Iwakura A, Thorne T, Sekiguchi H, Clarke T, Ito A, Misener S, Tanaka T, Klyachko E, Kobayashi K, Tongers J, Roncalli J, Tsurumi Y, Hagiwara N, Losordo DW. CXCR4 blockade augments bone marrow progenitor cell recruitment to the neovasculature and reduces mortality after myocardial infarction. *Proc Natl Acad Sci USA* 2010; **107**: 11008-11013 [PMID: 20534467 DOI: 10.1073/pnas.0914248107]
35 **Roncalli J**, Renault MA, Tongers J, Misener S, Thorne T, Kamide C, Jujo K, Tanaka T, Ii M, Klyachko E, Losordo DW. Sonic hedgehog-induced functional recovery after myocardial infarction is enhanced by AMD3100-mediated progenitor-cell mobilization. *J Am Coll Cardiol* 2011; **57**: 2444-2452 [PMID: 21658566]
36 **Fu SS**, Li FJ, Wang YY, You AB, Qie YL, Meng X, Li JR, Li BC, Zhang Y, Da Li Q. Kallikrein gene-modified EPCs induce angiogenesis in rats with ischemic hindlimb and correlate with integrin αvβ3 expression. *PLoS One* 2013; **8**: e73035 [PMID: 24019890 DOI: 10.1371/journal.pone.0073035]
37 **Oikonomou E**, Siasos G, Zaromitidou M, Hatzis G, Mourouzis K, Chrysohoou C, Zisimos K, Mazaris S, Tourikis P, Athanasiou D, Stefanadis C, Papavassiliou AG, Tousoulis D. Atorvastatin

treatment improves endothelial function through endothelial progenitor cells mobilization in ischemic heart failure patients. *Atherosclerosis* 2015; **238**: 159-164 [PMID: 25525743 DOI: 10.1016/j.atherosclerosis.2014.12.014]

38 **Tie L**, Chen LY, Chen DD, Xie HH, Channon KM, Chen AF. GTP cyclohydrolase I prevents diabetic-impaired endothelial progenitor cells and wound healing by suppressing oxidative stress/thrombospondin-1. *Am J Physiol Endocrinol Metab* 2014; **306**: E1120-E1131 [PMID: 24644242 DOI: 10.1152/ajpendo.00696.2013]

39 **Liu F**, Chen DD, Sun X, Xie HH, Yuan H, Jia W, Chen AF. Hydrogen sulfide improves wound healing via restoration of endothelial progenitor cell functions and activation of angiopoietin-1 in type 2 diabetes. *Diabetes* 2014; **63**: 1763-1778 [PMID: 24487028 DOI: 10.2337/db13-0483]

40 **Broquères-You D**, Leré-Déan C, Merkulova-Rainon T, Mantsounga CS, Allanic D, Hainaud P, Contrères JO, Wang Y, Vilar J, Virally M, Mourad JJ, Guillausseau PJ, Silvestre JS, Lévy BI. Ephrin-B2-activated peripheral blood mononuclear cells from diabetic patients restore diabetes-induced impairment of postischemic neovascularization. *Diabetes* 2012; **61**: 2621-2632 [PMID: 22596048 DOI: 10.2337/db11-1768]

41 **Leicht SF**, Schwarz TM, Hermann PC, Seissler J, Aicher A, Heeschen C. Adiponectin pretreatment counteracts the detrimental effect of a diabetic environment on endothelial progenitors. *Diabetes* 2011; **60**: 652-661 [PMID: 21270275 DOI: 10.2337/db10-0240]

42 **Suzuki R**, Fukuda N, Katakawa M, Tsunemi A, Tahira Y, Matsumoto T, Ueno T, Soma M. Effects of an angiotensin II receptor blocker on the impaired function of endothelial progenitor cells in patients with essential hypertension. *Am J Hypertens* 2014; **27**: 695-701 [PMID: 24200748 DOI: 10.1093/ajh/hpt208]

43 **Zhou J**, Cheng M, Liao YH, Hu Y, Wu M, Wang Q, Qin B, Wang H, Zhu Y, Gao XM, Goukassian D, Zhao TC, Tang YL, Kishore R, Qin G. Rosuvastatin enhances angiogenesis via eNOS-dependent mobilization of endothelial progenitor cells. *PLoS One* 2013; **8**: e63126 [PMID: 23704894 DOI: 10.1371/journal.pone.0063126]

44 **Philp D**, Huff T, Gho YS, Hannappel E, Kleinman HK. The actin binding site on thymosin beta4 promotes angiogenesis. *FASEB J* 2003; **17**: 2103-2105 [PMID: 14500546 DOI: 10.1096/fj.03-0121fje]

45 **Ye L**, Zhang P, Duval S, Su L, Xiong Q, Zhang J. Thymosin β4 increases the potency of transplanted mesenchymal stem cells for myocardial repair. *Circulation* 2013; **128**: S32-S41 [PMID: 24030419 DOI: 10.1161/CIRCULATIONAHA.112.000025]

46 **Zhu J**, Su LP, Ye L, Lee KO, Ma JH. Thymosin beta 4 ameliorates hyperglycemia and improves insulin resistance of KK Cg-Ay/J mouse. *Diabetes Res Clin Pract* 2012; **96**: 53-59 [PMID: 22217673 DOI: 10.1016/j.diabres.2011.12.009]

47 **Jujo K**, Ii M, Losordo DW. Endothelial progenitor cells in neovascularization of infarcted myocardium. *J Mol Cell Cardiol* 2008; **45**: 530-544 [PMID: 18755197 DOI: 10.1016/j.yjmcc.2008.08.003]

48 **Losordo DW**, Henry TD, Davidson C, Sup Lee J, Costa MA, Bass T, Mendelsohn F, Fortuin FD, Pepine CJ, Traverse JH, Amrani D, Ewenstein BM, Riedel N, Story K, Barker K, Povsic TJ, Harrington RA, Schatz RA. Intramyocardial, autologous CD34+ cell therapy for refractory angina. *Circ Res* 2011; **109**: 428-436 [PMID: 21737787 DOI: 10.1161/CIRCRESAHA.111.245993]

49 **Poh KK**, Sperry E, Young RG, Freyman T, Barringhaus KG, Thompson CA. Repeated direct endomyocardial transplantation of allogeneic mesenchymal stem cells: safety of a high dose, "off-the-shelf", cellular cardiomyoplasty strategy. *Int J Cardiol* 2007; **117**: 360-364 [PMID: 16889857 DOI: 10.1016/j.ijcard.2006.04.092]

P- Reviewer: de Mello RA, Su H **S- Editor**: Ji FF
L- Editor: A **E- Editor**: Liu SQ

World Journal of Stem Cells

Submit a Manuscript: http://www.wjgnet.com/esps/
Help Desk: http://www.wjgnet.com/esps/helpdesk.aspx
DOI: 10.4252/wjsc.v7.i6.899

World J Stem Cells 2015 July 26; 7(6): 899-921
ISSN 1948-0210 (online)

REVIEW

Importance of being Nernst: Synaptic activity and functional relevance in stem cell-derived neurons

Aaron B Bradford, Patrick M McNutt

Aaron B Bradford, Patrick M McNutt, Cell/Molecular Biology Branch, US Army Medical Research Institute of Chemical Defense, Aberdeen Proving Grounds-EA, MD 21010, United States

Author contributions: Bradford AB and McNutt PM collected relevant figure materials, wrote and edited the paper.

Conflict-of-interest statement: The authors declare no conflict of interest.

Correspondence to: Patrick M McNutt, PhD, Cell/Molecular Biology Branch, US Army Medical Research Institute of Chemical Defense, 3100 Ricketts Point Road, Aberdeen Proving Grounds-EA, MD 21010,
United States. patrick.m.mcnutt2.civ@mail.mil
Telephone: +1-410-4368044

Received: December 19, 2014
Peer-review started: December 21, 2014
First decision: February 7, 2015
Revised: February 28, 2015
Accepted: May 8, 2015
Article in press: May 11, 2015
Published online: July 26, 2015

Abstract

Functional synaptogenesis and network emergence are signature endpoints of neurogenesis. These behaviors provide higher-order confirmation that biochemical and cellular processes necessary for neurotransmitter release, post-synaptic detection and network propagation of neuronal activity have been properly expressed and coordinated among cells. The development of synaptic neurotransmission can therefore be considered a defining property of neurons. Although dissociated primary neuron cultures readily form functioning synapses and network behaviors *in vitro*, continuously cultured neurogenic cell lines have historically failed to meet these criteria. Therefore, *in vitro*-derived neuron models that develop synaptic transmission are critically needed for a wide array of studies, including molecular neuroscience, developmental neurogenesis, disease research and neurotoxicology. Over the last decade, neurons derived from various stem cell lines have shown varying ability to develop into functionally mature neurons. In this review, we will discuss the neurogenic potential of various stem cells populations, addressing strengths and weaknesses of each, with particular attention to the emergence of functional behaviors. We will propose methods to functionally characterize new stem cell-derived neuron (SCN) platforms to improve their reliability as physiological relevant models. Finally, we will review how synaptically active SCNs can be applied to accelerate research in a variety of areas. Ultimately, emphasizing the critical importance of synaptic activity and network responses as a marker of neuronal maturation is anticipated to result in *in vitro* findings that better translate to efficacious clinical treatments.

Key words: Synapses; Neurotransmission; *In vitro* techniques; Induced pluripotent stem cells; Neuronal networks; Neurogenesis; Neural stem cells; Embryonic stem cells; Induced neurons

Core tip: During stem cell neuronal differentiation, functional synaptogenesis and the emergence of coordinated, networked activity are critical behaviors in confirming that cells have developed into a relevant neuronal population. As the number of stem cell-derived neuron (SCN) models continues to proliferate, the use

of specific functional readouts to evaluate SCN maturity will become increasingly important compared to morphological or proteomic characterization of neuronal maturation. The review provides diverse options for reliably assaying the development of synaptic neurotransmission in derived neurons and describes the strengths, weaknesses and potential applications of several stem cell-based neuron models.

Bradford AB, McNutt PM. Importance of being Nernst: Synaptic activity and functional relevance in stem cell-derived neurons. *World J Stem Cells* 2015; 7(6): 899-921 Available from: URL: http://www.wjgnet.com/1948-0210/full/v7/i6/899.htm DOI: http://dx.doi.org/10.4252/wjsc.v7.i6.899

INTRODUCTION

Over the last few decades a large variety of *in vitro* models have been developed for use in basic and applied neuroscience. These neurogenic models originate from diverse sources, including dissociated primary neurons, immortalized cell lines derived from neuronal and non-neuronal tissues and, most recently, stem cells. The predictive value of these models is critically dependent on their ability to recapitulate fundamental neuronal behaviors exhibited by primary neurons. This is particularly important given the profound effects that subtle changes in neuron development or maturation can have on emergent network properties.

In vivo, the differentiation of neural precursors into synaptically active, post-mitotic neurons involves a complex developmental cascade of gene expression and morphological changes[1-3]. These changes ultimately orchestrate synaptic, neuronal and network behaviors to produce the emergent properties responsible for sustained central nervous system (CNS) function. Given the complex cellular behaviors involved in producing synaptically active neurons, it is not surprising that synaptogenesis and maintenance of synaptic activity are highly sensitive to genetic and environmental perturbation[4,5]. While many dissociated primary neuron cultures reliably form functioning networks that exhibit physiological behaviors, their use is limited by several factors, including the difficulty of dissection, variability among cultures, poor viability for longer-term studies and the regulatory, administrative and ethical burdens imposed by animal studies. In contrast, while immortalized cells have been extensively used as a replacement for primary neurons, they uniformly fail to recapitulate many neurotypic properties[6].

The advent of neurons derived from stem cells offers the potential for a unique experimental platform that combines the relevance of primary neurons with the flexibility and scalability of immortalized cells[6]. Stem cell-derived neuron (SCN) models that produce functionally mature neurons have multiple characteristics that render them exceedingly well-suited to the study of neural development, neuron function and human disease. For example, SCNs can recapitulate functional behaviors that are characteristic of primary neurons, such as synaptic neurotransmission and network emergence. Many stem cell lines can be maintained in culture for prolonged periods prior to differentiation, enabling scalable expansion to accommodate the demands of high-throughput approaches and endowing differentiated neurons with reduced inter-experimental phenotypic and genetic variability. The ability to convert primary cells to patient-specific induced pluripotent stem cells (iPSCs) has kindled the extraordinary potential of personalized medicine, in which iPSC-derived neurons (i-neurons) expressing cellular correlates of particular neurological pathologies can be studied *in vitro* in the context of the patient's genome[7]. Finally, SCNs have also been proposed to have a direct application in cell-based therapies, whereby partially differentiated neural progenitor cells or post-mitotic immature neurons can be directly injected into the CNS to integrate into existing architecture, supplement endogenous neurogenic processes and promote the repair of damaged neural tissues[8,9]. However, SCN models must be shown to be competent to form context-appropriate, functioning neurons before these approaches can be used as intended.

The signature characteristic of CNS neurons is action potential (AP)-induced synaptic neurotransmission that synchronizes neuron firing to give rise to emergent circuit behaviors. Since synaptic activity is a principal endpoint of neurogenesis, detection of synaptic events and/or synaptically driven network behaviors serves as a higher-order readout that confirms the proper elaboration of the full range of biochemical, proteomic and morphological properties that are required for neuron function. However, in many cases the rigor and specificity of techniques used to characterize the physiological relevance of SCNs have been highly variable[10,11]. Frequently, characterizations have been limited to expression of small sets of neurotypic genes or electrophysiological assessment of intrinsic electrical excitability, without evaluation of functional synaptogenesis or network formation[12,13]. SCNs are frequently described as physiologically relevant based on insufficient or incomplete characterizations, therefore producing data of uncertain value. These inconsistencies illuminate a critical need for the identification of appropriate assays to evaluate the functional maturity and physiological relevance of derived neuron models.

In this review we will discuss methods to characterize the progression of *in vitro* neurogenesis and propose specific functional assays to confirm the physiological relevance of SCNs. We will focus on SCNs derived from four sources (summarized in Figure 1): embryonic stem cells (ESCs); restricted-potency neural stem cells (NSCs); iPSCs; and direct conversion of post-mitotic cells into induced neurons (iNs). Note that although iNs do not explicitly incorporate a pluripotent phase, the derivation of iNs uses principles and techniques involved

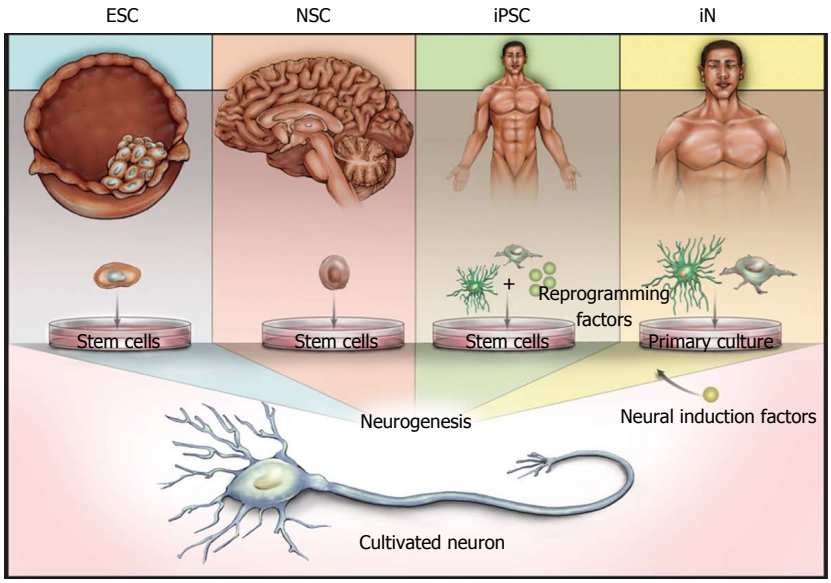

Figure 1 Illustration of the sources of derived neurons. Embryonic stem cells (ESCs) are derived from the inner cell mass of blastocysts, whereas neural stem cells (NSCs) are derived from several defined niches in the developing or adult brain. Both ESCs and NSCs are capable of neurogenesis without the forced expression of induction factors. Induced pluripotent stem cells (iPSCs) and induced neurons (iNs) can be derived from various tissues, and proceed to neuronal states via either reprogramming to a stem cell phenotype (iPSCs) or direct conversion using neuronal induction factors (iNs).

in production of other SCN models and therefore will be addressed in this review. We will also describe the current status of existing SCN models, and elaborate on reasons why synapse and network formations are critically important to SCN applications, even in cases where applications may not directly rely on neuronal function.

METHODS TO CHARACTERIZE NEUROGENESIS AND NEURONAL MATURATION

Measuring the maturation and relevance of neurogenic models

Developmentally regulated changes in proteomic, transcriptomic, biochemical and functional properties during embryonic neurogenesis can be repurposed to evaluate developmental progression *in vitro*[14]. The specific markers used may vary depending on the ultimate application, but at a minimum should include morphological characterization of neurotypic compartments; the development of electrical excitability; the detection of post-synaptic responses to pre-synaptic release of neurotransmitter; and, when appropriate, network-level behaviors (Figure 2). While functional confirmation of synaptic neurotransmission represents indisputable evidence of synaptogenesis, supplemental studies such as transcriptomic analysis, planar multi-electrode array (MEA) analysis or protein expression studies can also provide valuable contributions to the overall understanding of the maturity and nature of derived neuronal populations, as described below.

Although methods to validate the progression of neuronal maturation have been well-described in dissociated cultures of primary neurons, it is important to recognize that the source tissues for these neurons are often comprised of functionally mature neurons that are dissociated and plated[15]. In these cases, re-establishment of synaptic activity is primarily contingent on the temporal re-elaboration of appropriate morphological structures. In contrast, the differentiation of pluripotent stem cells into mature SCNs requires recapitulation of the full range of transcriptional, morphological and proteomic changes involved in functional neurogenesis. Neurogenic progression is an intricate process that is susceptible to misdirection *in vitro*, and unlike in dissociated primary neurons, there is a lower correlation between expression of intermediate developmental markers and the probability of functional maturation. Inappropriate differentiation conditions can cause neurogenic models to become developmentally arrested, expressing immature neurotypic properties but lacking the functional correlates of active synapses and network emergence[16]. Dissociated primary neuron cultures can also undergo developmental arrest if not properly maintained, despite having been functionally mature prior to dissociation[1]. Once neurons become functionally mature, their survival continues to depend on synaptic activity-induced neurotrophic signaling[17-20], as demonstrated by neurotoxicity following impaired synaptic function in neurodegenerative diseases[21-23]. Therefore, researchers characterizing SCN differentiation should be careful to avoid phenomenologically conflating the expression of intermediate developmental markers with the eventual likelihood of producing functionally mature neurons. For example, the ability to fire repeated APs with hyperpolarizing after shoots in response to

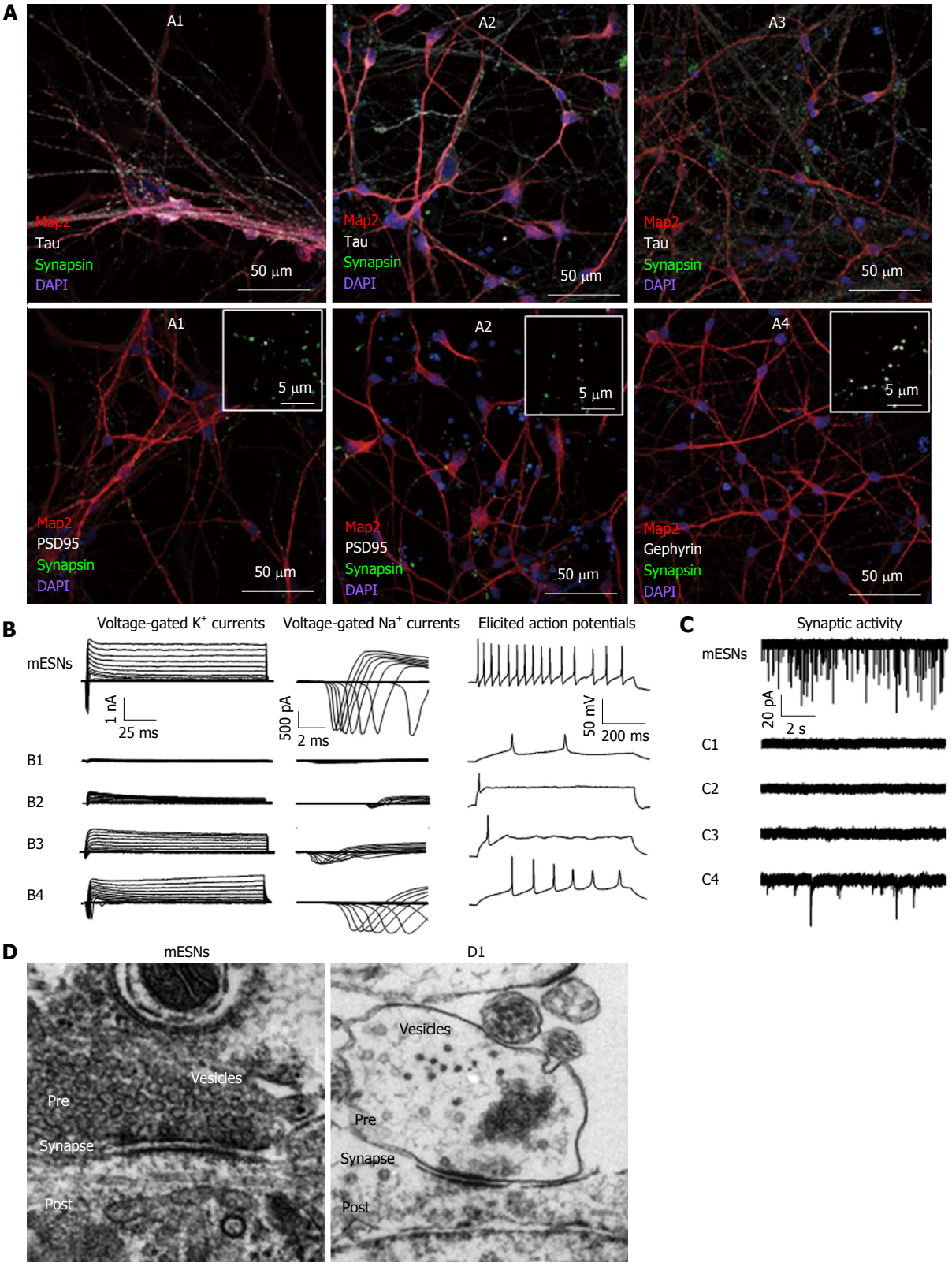

Figure 2 Neurotypic markers and passive membrane responses are not predictive of functional synaptogenesis. A: Representative fluorescent immunocytochemistry of i-neurons from several protocols (A1-A4) imaged at 43 d after plating (DAP). SCNs display neurotypic morphologies, including distinct dendrites (Map2) and axons (Tau) around cell nuclei [4',6-diamidino-2-phenylindole (DAPI)], with distributed and punctate synapsin (top panel) and PSD-95 or gephyrin (bottom panel) often expressed in close proximity to synapsin (insets); B: Although all four i-neuron models displayed intrinsic excitability, including voltage-gated currents, and produced action potentials following current injection, responses were smaller in amplitude and depolarization led to fewer repeated action potentials compared to responses displayed by mouse embryonic stem cell-derived neurons (mESNs, top row); C: Only one of four human i-neuron models displayed synaptic activity on DAP35 or later as indicated by miniature post-synaptic currents in the presence of tetrodotoxin, and those currents were smaller in amplitude, less frequent and slower to return to baseline when compared to mESNs; D: Transmission electron microscopy of single synapses in mESN and i-neuron models (D1) indicates that pre-synaptic compartments of mESNs are densely loaded with vesicles, while i1 is not. This indicates that while the model is capable of producing the morphology, synaptic markers and intrinsic characteristics of synaptogenesis, it lacks the capacity to maintain spontaneous activity and therefore is unable to model physiological synaptic transmission or network activity.

current injection is often associated with neuronal maturity. This may be valid in many well-characterized primary neuron cultures. However, there is no causal requirement that SCNs with this intrinsic behavior will exhibit functional synapses with synaptically driven network responses.

As the number of SCN models continues to proliferate, the deliberate use of specific functional readouts to evaluate SCN maturity will become increasingly important. By precisely and accurately associating neurotypic behaviors with stage-specific markers, researchers will be able to better ascertain the degree of relevance and applicability of SCN populations. Efforts to develop techniques to reliably determine the neurogenic potential of SCN differentiation models are currently underway[11,24]. However, in the absence of such functional validation, claims of neuronal maturation and therefore relevance should be reviewed with care.

Approaches for morphological and structural characterization of neurogenesis

Much of the current understanding of neuronal maturation comes from longitudinal studies of the formation of specialized neuronal structures in dissociated primary neurons[25]. These studies established that the progressive establishment of functionally specialized compartments (*e.g.,* axons, hillocks, dendrites, and pre- and post-synaptic compartments) provided the cellular substrates for polarized neurotransmission *in vitro*. Many of these morphological features can be distinguished by the localization expression of specific proteins and therefore immunocytochemistry (ICC) is often used to characterize developmental progression[26,27]. Morphological characterization may start with general neuronal markers, such as NeuN (post-mitotic neuronal nuclei) or βⅢ-tubulin (immature neuronal marker), and progress to more specialized markers of cellular compartments, such as synapsin (pre-synaptic), tau (axon), MAP2 (somatodendritic) and gephyrin or PSD-95 (inhibitory or excitatory post-synaptic markers, respectively). It can then extend to the use of well-described antibodies to distinguish among neuronal subtypes, such as markers of glutamatergic (vesicular glutamate transporter-1 or -2), cholinergic (choline acetyltransferase), GABAergic (glutamate decarboxylase 1), serotonergic (serotonin transporter), aminergic (vesicular monoamine transporters 1 or 2), or dopaminergic and/or adrenergic (tyrosine hydroxylase) neurons. Longitudinal studies using such markers are a regular feature of SCN differentiation studies and are an important aspect of verifying neuronal maturation, even though expression of specific markers are not indicative of functional behaviors[28,29].

In addition to providing information on the establishment of synaptic compartments, the morphological apposition of pre- and post-synaptic proteins can provide clear evidence of synaptic assembly[30]. Synaptic assembly begins with the contact of complementary cell adhesion molecules between potential pre- and post-synaptic compartments, which in turn requires the previous elaboration of axons and dendrites (with the exception of axosomatic synapses[31]). From this point, proteins necessary for synaptic architectures and function are recruited to the site of contact in both compartments[32,33]. In mature neuron cultures and *in vivo*, the establishment of new synapses can occur very quickly, with synaptic activity apparent almost immediately[34,35]. However, as demonstrated in Figure 2 and discussed above, SCNs can form synaptic structures but fail to develop synaptic function. Based on this positional apposition, ICC for synapsin and PSD-95 (for example) have been used to provide a low-resolution confirmation that pre- and post-synaptic compartments are in close proximity. More recently, the mammalian GFP reconstitution across synaptic partners (mGRASP) method has been used as a fluorescent indicator of the co-localization of synaptic adhesion proteins. mGRASP is based on functional complementation of split GFP separately expressed from pre- and post-synaptic membranes, and therefore is a highly specific marker of synaptic proximity[36]. Ultrastructural imaging using transmission electron microscopy (TEM) can also be used for advanced morphological analysis of synaptogenesis. TEM enables a definitive visualization of pre- and post-synaptic compartments, allowing researchers to search for characteristic intra-synaptic structures, such as pre- and post-synaptic densities, the presence of synaptic vesicles in the pre-synaptic compartment and possibly even vesicles docked or fused with the pre-synaptic membrane, suggesting neurotransmitter release. It is important to emphasize that positive confirmation of synaptic architectures by any of these methods is not prima facie evidence of synaptic function. Synapse assembly precedes onset of synaptic activity and is not indicative of the current or future development of synaptic function[37-39]. However, pairing these types of morphological studies with electrophysiology may allow the identification of benchmarks that can be used to correlate synaptic function with gene expression (*e.g.,* the onset of synaptic activity cannot precede the localization of protein X, *etc.*). While structural characterizations have rarely been used in the study of SCN maturation, they have the potential to offer highly specific and detailed correlations between structural and functional synaptogenesis when combined with synaptic activity assays.

While morphological characterization provides researchers with a visual confirmation of protein expression and compartmentalization, some neuronal markers (*e.g.,* βⅢ-tubulin[40], synapsin[41] or NeuN[42]) may also be expressed in non-neuronal or neoplastic cells. Morphological characterization of neurogenesis should therefore be used as a secondary method to confirm neurogenesis and be corroborated by more direct methods to measure the production of neurons. For example, we have found transcriptomic analysis to be invaluable in reconciling neuronal fate with expression of neurotypic markers and evaluating neurotypic responses, including: (1) longitudinal characterization

of neurogenic progression; (2) identification of neuronal subtypes; (3) determination of which neurotransmitter receptors subunits are expressed; and (4) measurement of activity-dependent responses to treatment with pharmacological regulators of network activity[43].

Measurements of intrinsic excitability

Functional evaluation of neuron maturation begins with electrophysiological characterization of intrinsic excitability, which is the ability to undergo the rapid, defined changes in ion flux that are necessary to repeatedly fire APs. These include measurements such as quantitation of Na^+ and K^+ voltage-gated responses, the ability to fire evoked APs, membrane resistance, membrane capacitance, sag (or I_h) currents, hyperpolarization-activated currents and establishment of a stable resting membrane potential. Another intrinsic neuronal characteristic that can be used as a developmental marker of maturation is the γ-aminobutyric acid (GABA) reversal potential (E_{GABA}). Immature neurons have high intracellular Cl^- levels, such that $GABA_A$ receptor activation triggers Cl^- efflux[44]. This excitatory GABA current has been proposed to contribute to the developmental activation of nascent excitatory synapses[45]. Neuron maturation is associated with increased expression of the potassium chloride co-transporter KCC2, which is an electroneutral Cl^- exporter that decreases intracellular Cl^- concentration, thereby shifting E_{GABA} to a value that is close to the mature resting membrane potential[46]. The developmental shift in E_{GABA} potentiates a transition from excitatory post-synaptic GABA currents to inhibitory GABA currents[47]. While the development of E_{GABA} is rarely used for neuronal characterization because of the relative difficulty in measuring Cl^- reversal potentials, the shift in E_{GABA} is an elegant marker of the developmental changes that are required for the establishment of network-level activities in many neuron subtypes.

Once neurons have been determined to exhibit mature characteristics of intrinsic excitability, analysis then expands to measuring cell behaviors under non-evoked conditions, such as spontaneous production of APs and miniature post-synaptic currents. It is important to note that the mere presence of spontaneous APs does not necessitate or signify synaptic function[48]. For example, dissociated primary neurons exhibit mature-appearing intrinsic characteristics and spontaneously fire APs prior to formation of active synapses[27]. In fact, spontaneous, non-evoked AP firing appears to be a developmental phenomenon involved in the maturation of ionic gradients[49,50]. Furthermore, the detection of APs can reflect a neuron with a membrane potential that is near to the threshold potential and therefore fires APs in response to subtle changes in the conductance of membrane ion channels, independent of synaptic activity[51,52]. Since APs may occur in the absence of synaptic function, pharmacological antagonists of neurotransmitter receptors must be used to experimentally confirm that APs originate from synaptically driven events as described below.

Synaptic activity is a functional signature of successful synaptogenesis

In some cases, SCNs produce morphological characteristics of synapse formation, exhibit evidence of intrinsic excitability and fire spontaneous APs, yet fail to develop synaptic activity[29,53]. As discussed below, this is currently a particularly vexing problem with human iPSC-derived neurons, which exhibit a wide array of morphological markers of neurogenesis, but often appear to be developmentally delayed or even arrested prior to the onset of synaptic activity. Consequently, measurements of synaptic activity are critical to providing unimpeachable confirmation of functional synaptogenesis.

The production of excitatory and/or inhibitory post-synaptic currents is a higher-order representation of the spatiotemporally precise elaboration of a large number of developmental processes required for synaptic activity, such as juxtaposition of pre-synaptic and post-synaptic compartments; loading and docking of neurotransmitter vesicles; and the appropriate localization and function of voltage-dependent ion channels. The two dominant modes of synaptic neurotransmission are spontaneous release and AP-evoked release. Under physiological conditions stochastic Ca^{2+} currents trigger synapses to spontaneously release neurotransmitter at approximate rates of 10^{-3} quanta per second (Hz) per CNS synapse[54,55] and 0.79 Hz per motor neuron synapse[56]. In a typical central neuron, which has 10^2-10^4 synapses, monosynaptic release probabilities result in a post-synaptic current detection rate of 0.1-10 Hz[57,58]. Similar rates have been reported in mouse SCNs[59]. In contrast, AP-induced pre-synaptic depolarization increases instantaneous quantal release rates increase to 10^3 Hz[54,55]. While either spontaneous or AP-evoked neurotransmission can be used to identify the presence of synaptic neurotransmission, the large currents generated by AP propagation can complicate rigorous characterization of post-synaptic behaviors, as described below. Consequently, detection and characterization of spontaneous post-synaptic events often provides a more reliable and quantifiable indicator of synaptic function than detection of synchronized release from many synapses following an AP.

Detection of post-synaptic events using whole-cell patch-clamp electrophysiology can involve characterization of excitatory post-synaptic potentials (EPSPs) in current-clamp mode or spontaneous miniature post-synaptic currents in voltage-clamp mode. For a number of technical reasons related to quantitation and characterization that will not be addressed here, we recommend the latter approach. Spontaneous release is a salient feature of all synapses *in vivo* and *in vitro* and direct measurement of spontaneous monosynaptic activity *via* detection of miniature excitatory or inhibitory post-synaptic currents (mEPSC or mIPSC, respectively) in the presence of tetrodotoxin (TTX) is an unambiguous indicator of synaptic function in neuron subtypes that utilize ionotropic neurotransmitter receptors (Figure

2)[54,60-62]. TTX blocks voltage-gated Na^+ channels, eliminating the large whole-cell currents caused by AP firing and enabling the detection of small post-synaptic currents resulting from the spontaneous activation of individual synapses. The addition of pharmacological agonists or antagonists for specific neurotransmitter receptors allows the contributions of different neuron subtypes to post-synaptic responses to be precisely determined.

Characterization of miniature post-synaptic currents (aka, minis) should include analysis of event rates and kinetics; functional responses to the addition of pharmacological modulators of post-synaptic function; and current:voltage relationships for well-characterized receptors[59]. Much is known about the functional mechanisms of synaptic neurotransmission in primary CNS and peripheral neurons and an extensive pharmacopeia is available to manipulate and characterize post-synaptic responses for most synapse subtypes. Thus, there is a wide array of resources to identify and develop electrophysiological approaches to evaluate synaptic function in SCNs.

While the kinetic analysis of minis can be used to unambiguously distinguish between synaptic and non-synaptic neurotransmission, in some instances (*e.g.,* synaptic potentiation studies) it would be valuable to simultaneously evaluate both pre- and post-synaptic behaviors. Paired recordings offer one means to do so. In paired recordings, two synaptically connected neurons are simultaneously patched, such that stimulation of one neuron elicits post-synaptic responses in the other. While this is a highly rigorous and reliable indicator of connectivity, it is a technically difficult method. Paired recordings are relatively feasible under conditions in which neuronal connectivity is well defined and the polarization of synaptic connections are known, such as in hippocampal slices[63]. In contrast, trans-synaptic connectivity and polarization are stochastic in dissociated neuron cultures, making it difficult to identify and record from synaptically coupled neurons, even when plated at very low densities[64]. Thus, while paired recordings are an effective method to characterize evoked synaptic neurotransmission, it is technically challenging to accomplish in neuron cultures and should be anticipated to have a high failure rate. Alternatively, the use of bipolar stimulating electrodes allows for the repeated stimulation of specific local synapses in vitro without requiring multiple patches[65]. However, this approach relies on the stimulation of multiple processes in proximity to a patched neuron and therefore may result in field stimulus-like artifacts and difficult to interpret post-synaptic responses.

The use of post-synaptic miniature currents to measure synaptic neurotransmission is not feasible in neuron subtypes that rely on metabotropic neurotransmitter receptors, such as dopaminergic or serotonergic neurons. While methods such as ultrafast voltammetry or the use of fluorescent false neurotransmitters can directly measure synaptic release of neurotransmitters[65,66], they are not a confirmation of synaptic neurotransmission, but rather are limited to providing information about the pre-synaptic release of neurotransmitter. Alternatively, indirect measurements of the activation of metabotropic synapses in cultures containing multiple neuron subtypes can be conducted based on changes in network behavior, as described in the next section.

Table 1 lists exemplar SCN models that have been evaluated for the existence of spontaneous post-synaptic currents in the absence of co-cultured primary neurons. The latter were excluded due to the difficulty in disambiguating neurotransmission and neuro-exception between SCNs and primary neurons[67]. Table 1 does not include references for putative SCNs that have only been characterized for morphological markers or for intrinsic excitability, since as described above these are poor surrogates for assaying functional synapses.

Network behaviors as higher-order signatures of neuron function

Similar to synaptic activity, emergence of network activity confirms successful elaboration of the developmental processes required for functional synaptogenesis. We define "network potential" as the ability of derived neurons to integrate post-synaptic events into APs (excitability), to transmit outgoing synaptic signals to other neurons (neurotransmission), and to elicit activity-dependent post-synaptic behaviors (adaptability). While the emergence of network activity is a function of the neuronal subtypes present, and therefore is not a required feature of mature neuron cultures, it does provide unambiguous confirmation of synaptic activity. Ideally, neuron cultures will incorporate both excitatory and inhibitory neuron subtypes whose activity is modulated by feedback mechanisms to produce an excitatory/inhibitory (E/I) balance. This condition is maintained by adaptation of pre- and post-synaptic properties and can be considered functional evidence of synaptic plasticity[68]. Alternatively, monotypic cultures comprised of excitatory or inhibitory neurons will result in unbalanced signaling and network inactivity[69] or seizurogenic bursting[70], conditions in which long-term neuronal viability may be compromised[71,72].

Mature network activity is typically observed in SCNs as synchronous AP propagation among multiple neurons, a phenomenon often referred to as network bursting. Since AP production is a stochastic process caused by the near-simultaneous occurrence of a sufficient number of excitatory EPSPs to exceed the firing threshold, *in vitro* quantitation of APs is influenced by a number of factors which determine neuron connectivity, such as the number, weight and type of functioning synapses. Several methods are available to quantify network activity. The most specific is the use of electrophysiological methods to directly measure AP production[59,73,74]. This can occur *via* simultaneous, multiple patch-clamp experiments, where the synchronicity of spontaneous AP production is compared among patched neurons. Alternatively, the effects of network modulators (*e.g.,* bicuculline, aminopyridine or CNQX, as described below) on the

Table 1 Stem cell-derived neurons characterized for synaptic activity

Cell type	Source	Technical approach	Post-synaptic measurement (days after differentiation)	Additional notes	Ref.
ESC	Human (BG01, BG03)	Stromal cell factors applied	mEPSCs (21)	Also dopaminergic Continued expression of NPC marker Msx1	[254]
	Human (WiCell H9, H1)	SHH application on ESCs or NPCs	mEPSCs, mIPSCs (30)	Also dopaminergic	[110]
	Human (H9 and SA121)	Dual SMAD inhibition, variable SHH, several additional neurotrophic factors	sEPSCs, sIPSCs (35)	SHH concentration-dependent GABAergic and glutamatergic, or dopaminergic fates	[240]
	Mouse (R1)	RA treatment, suspension culture	mEPSCs, mIPSCs (21)		[6,59,226]
	Mouse (J1)	FACS sorting for dopaminergic NPCs, SHH treatment	sEPSCs (22)	Also dopaminergic	[255]
NSC	Human (NSI-566RSC from fetal spinal cord)	9 component differentiation media	mEPSCs (12-48)		[256]
	Mouse (Adult C57/Bl6 SEZ)	BDNF treatment	mEPSCs, mIPSCs (11-28)	Perforated patch recording	[171]
iPSC	Human (normal and ALS fibroblasts)	Dual SMAD inhibition, RA and purmorphamine treatment	sEPSCs (21-42)	sEPSCs only detected with picrotoxin and 4-aminopyridine	[86]
	Human (normal and AD fibroblasts)	FACS sorting of NPCs, BDNF, GDNF and cAMP treatment	mIPSCs, mEPSCs (26)	Currents detected in approximately 40% of cells	[148]
iN	Human (postnatal and adult fibroblasts)	Two-stage Dox, bFGF, Noggin, GDNF, BDNF, forskolin treatments	mEPSCs (30)	Currents detected in 25%-43% of converted cells	[158]
	Mouse (perinatal tail tip fibroblasts)	Glial co-culture, FACS sorting	sEPSCs (15-27)		[156,157]
ESC + iPSC	Human (HES3, BioTime ESI, and WiCell H9 ESCs + melanocyte hiPSCs)	5 morphogenic factors, FACS sorting, glial co-culture	sIPSCs (42-84)	% of cells with currents increases over time Implanted neurons also received EPSCs	[28]
	Human (HUES9 ESCs + fibroblast hiPSCs)	Noggin and dorsomorphin treatment, recombinant human Dkk1 treatment of hiPSC EBs, glial co-culture	mEPSCs (35)	Currents detected in 33% of differentiated ESCs and 46% of differentiated iPSCs tested	[111]
	Human (WiCell H9 and SHEF4 ESCs + fibroblast hiPSCs)	3% O_2	mEPSCs (35)	Mature AMPA and GABA profiles	[47,116]

ESC: Embryonic stem cell; NSC: Neural stem cell; iPSC: Induced pluripotent stem cell; ALS: Amyotrophic lateral sclerosis; AD: Alzheimer's disease; SHH: Sonic hedgehog; NPC: Neural precursor cell; SMAD: Sma and Mad related proteins; RA: Retinoic acid; FACS: Fluorescence-activated cell sorting; BDNF: Brain-derived neurotrophic factor; GDNF: Glia-derived neurotrophic factor; iN: Induced neuron; cAMP: Cyclic adenosine monophosphate; bFGF: Basic fibroblast growth factor; mEPSC/mIPSC: Miniature excitatory/inhibitory post-synaptic current; sEPSC/sIPSC: Spontaneous excitatory/inhibitory post-synaptic current; GABA: Gamma aminobutyric acid; AMPA: Alpha-amino-3-hydroxy-5-methyl-4-isoxazolepropionic acid.

frequency or nature of synaptically driven APs can be evaluated in a single neuron in current-clamp mode, providing indirect evidence of the contribution of synaptic activity to AP production. A relatively new approach is the use of MEAs to quantify synchronized bursting behavior in two- and three-dimensional cultures, which provides a unique method for characterizing the effects of neuromodulatory compounds on longitudinal network responses[75,76]. A more limited alternative to MEAs is the use of live-imaging assays to quantify bursting behavior using fluorescence-based detection of neuronal activity reporters, such as fluorescent genetically encoded calcium indicators (GECIs) or voltage-gated dyes[77-79]. Calcium imaging is particularly useful for studying network activity, as it is capable of simultaneously monitoring up to thousands of neurons and their associated processes[80]. While the temporal resolution and sensitivity of calcium imaging can be limited by fluorophore kinetics, level of gene expression or equipment, it is an excellent complement to electrophysiology[81]. Recently described GECIs have been found to be able to detect individual APs[82]; however, improved detection of the small potential differences driven by sub-threshold events is still needed before calcium imaging can approach the resolution offered by whole-cell patch-clamp electrophysiology. The development of optical electrophysiology techniques that offer the throughput of GECIs with the sensitive of whole-cell recordings would represent a transformative approach in large population analyses that would be immediately applicable to synaptically active SCN models.

In all cases the presence of network activity must be confirmed by treatment with pharmacological modulators that alter synaptic activity without directly activating

post-synaptic receptors. This is particularly important for MEAs and calcium imaging, in which it is currently impractical to directly measure synaptic function. Such treatments could include bicuculline, which disinhibits the network by blocking GABAergic inhibitory activity; aminopyridines, which prolong APs by blocking K^+ efflux; or CNQX, which blocks AMPAR activation and therefore eliminates excitatory signaling in glutamatergic networks[83-85]. Depending on neuron maturity and the relative proportions of neuron subtypes in SCN cultures, the use of network modulators may be the only possible means to reveal excitatory synaptic activity exceeding the threshold of AP detection[86]. Thus, the inability to detect APs by methods such as fluorescent calcium imaging or MEAs should not be considered evidence of the absence of synaptic activity.

Activity-dependent responses as an indirect measure of synaptic function

A signature *in vivo* characteristic of network function is the elaboration of activity-induced changes in post-synaptic neurons. In healthy networks a variety of mechanisms are used to balance excitatory and inhibitory inputs, producing circuits that can respond to increases or decreases in input[68,87]. The best-described of these is Hebbian plasticity, which allows for the constant formation and strengthening of synchronously active synapses and weakening of asynchronous synapses and is mediated by altered phosphoproteomic signaling, changes in receptor function and expression and differential gene expression[88,89]. Functional Hebbian plasticity can be indirectly evaluated in cultured neurons by measuring changes in the biochemical correlates of plasticity under conditions that up- or down-regulate network activity. Molecular correlates of plasticity include the surface localization of glutamate-responsive AMPA receptors, which can be measured by surface biotinylation or antibody labeling of extracellular residues[47,90], or the phosphorylation state of post-synaptic kinases such as CaMKII, Akt or CREB, which can be quantified using routine immunoblot methods[91-93]. Activity-induced changes in the expression of plasticity-related immediate early genes (IEGs) can be monitored by transcriptomic and/or proteomic methods, including Arc, the EGR family, c-Fos, Jun and Homer-1a[69,70,94-96]. However, it is important to note that many of these genes have multiple functions and are regulated during development and other neuromodulatory treatments[97,98]. Thus, researchers should be careful to ensure they are evaluating IEG expression under conditions that precisely modulate network activity without inducing acute cytotoxicity or other forms of neuronal stress. Synaptic plasticity can be directly measured by whole-cell patch-clamp electrophysiology in neuron cultures using trans-synaptic patch clamping or bipolar stimulating electrode techniques[65]. Plasticity- and activity-related assays have rarely been described in SCN models or in primary neuron cultures, but do represent relevant physiological correlates of network function and they should be considered to be a valuable confirmatory tool when characterizing and validating activity in SCNs.

SCNS: TYPES AND CHARACTERISTICS

Approaches to SCN differentiation

The yield, neuronal subtype(s) and purity of SCNs are heavily influenced by an array of biochemical factors that affect the differentiation process by modulating progression through neurodevelopmental stages. In some cases these factors can be controlled very precisely, such as by the addition of small molecules to promote exit from the pluripotency state, whereas others are less amenable to rational control, such as longitudinal changes in neurogenic potential caused by the spontaneous emergence of mutated subpopulations during routine culturing of stem cell lines. Thus identifying confirmatory markers of neurogenic progression is critically important to validate that differentiation of specific stem cell lines successfully results in the desired neuronal products. Derivation of neurons from human and mouse stem cells lines has been shown to recapitulate many ontological markers described during *in vivo* neurogenesis[43]. These include markers of the different stages of neurodevelopment, starting from a stem cell state and expressing characteristics of a NSCs stage, neural progenitor cell (NPC) stage and an immature neuron stage before ultimately developing into functional mature neurons.

Neuronal differentiation typically starts with the induction of a neuroepithelial NSC phenotype by withdrawal of pluripotency factors, such as LIF (mouse stem cells) or FGF-2 (human stem cells). The resulting NSCs may be expanded in culture for a limited number of passages to increase neuronal yield[99-101]. Identifying compounds that sustain the neurogenic competency of NSCs in culture will be valuable for manufacturing purposes, since this will both streamline the differentiation process and increase the total yield. Methods of neural patterning vary wildly. Many protocols involve the use of retinoic acid (RA), which is an early developmental signal for rostral-caudal patterning of the embryonic brain[102-104]. Differentiation can be further enhanced or directed by a variety of techniques, including supplementation with growth factors, such as brain-derived neurotrophic factor or glia-derived growth factor[100,105-107]; forced expression of transcription factors that control neuronal fates[108,109]; or addition of small molecules such as Noggin, Sonic Hedgehog or dorsomorphin[74,110,111]. Neural patterning can also be influenced by secreted factors, such as the increased production of motor neurons by co-culture of NSCs with muscle cells[112]. While neuronal maturation can proceed without the deliberate addition of conditioned media or the presence of support cells, some studies suggest that synaptogenesis is significantly enhanced by co-culture with astrocytes[113,114].

ESCs

ESCs are derived from totipotent cells collected from the inner cell mass of embryos at the blastocyst stage[115]. Mouse ESC are frequently differentiated to neurons *via* the 4/4 method, which involves neural induction by the withdrawal of LIF and neural patterning by the addition of RA[116,117]. The resulting ESC-derived neurons (e-neurons) have been shown to produce highly active glutamatergic and GABAergic synapses with emergent network responses[59] and activity-dependent gene expression[74]. ESC differentiation protocols can be modified by the addition of exogenous growth factors to generate other neuronal phenotypes, ranging from a mixture of dopaminergic, glutamatergic, cholinergic and andrenergic neurons[118] to a homogenous GABAergic neuron population with immature, excitatory GABA signaling[119]. Mouse e-neurons have been found to reliably form functioning synapses and robust emergent networks within weeks, whereas methods to produce comparable levels of network activity in human e-neurons are still under investigation[28]. It has recently been suggested that many extant human ESC lines exhibit epigenetic markers of partially differentiated epiblasts rather than naïve ESCs, which could provide a plausible mechanism for their relatively poor and inconsistent neurogenic potential[120]. In contrast, neurons derived from monkey, canine, pig, chicken, worm or fly ESCs[121-127] have been found to develop neurotypic morphologies, although characterization of the resulting neurons has not included functional measure of synaptic activity and network emergence to date.

NSCs

NSCs are proliferating stem cells that are restricted to neural lineages. NSCs are isolated from fetal and adult CNS, and therefore their availability and use is limited and subject to ethical concerns[128-131]. One advantage of NSCs is that they appear to replicate *in vivo* mechanisms of adult neurogenesis and therefore may represent a more physiologically appealing model than neurons derived from pluripotent cell lines[132]. In the brain, slow cycling NSCs in the sub-ventricular zones and in the subgranular zone of the dentate gyrus produce neurogenic progeny that pass through sequential developmental stages with structurally and functionally distinct cellular properties[133]. For example, in the well-studied rodent hippocampal subgranular zone, $GFAP^+$ NSCs progressively differentiate into $Trb2^+$ transiently amplifying NPCs, DCX^+ migratory neuroblasts and finally into post-mitotic $NeuN^+$-neurons which functionally integrate into existing hippocampal circuits within 3 wk and adopt mature dentate gyrus characteristics within 6-8 wk[134]. A similar developmental progression has been shown to occur in cultured NSCs based on morphological analysis[132]. Some NSCs have been observed to be restricted to specific neural lineages *in vitro*, such as lines that only generate astrocytes and oligodendrocytes[135,136]. The mechanisms underlying this limited potency are unknown, and whether this is a consequence of culture conditions or representative of *in situ* behaviors is unclear. As with iPSC- or ESC-derived NSCs, primary NSCs have a limited ability to proliferate in culture before losing their neurogenic competence[137,138]. Despite the potential value of NSC models, few functional assays have been performed on neurons differentiated from these sources, making it unclear whether they reliably produce active synapses. Furthermore, the collection of human NSCs is only possible under limited conditions, such as from aborted fetuses, during brain surgery or immediately post-mortem, and consequently their use is likely to have limited clinical utility[139].

iPSCs

iPSCs are reprogrammed from differentiated tissues through the exogenous expression of pluripotency genes, such as the original Yamanaka reprogramming factors *Oct4*, *Sox2*, *Klf4* and *cMyc* or subsequently described variants[140,141]. While neurogenic iPSCs have been generated from a wide variety of animals and tissues, this review will specifically focus on human iPSCs, predominantly derived from fibroblasts. For reasons that appear to be attributable to stochastic variability in epigenetic changes that occurs during reprogramming, even iPSC clones derived from the same tissue typically exhibit a range of neurogenic potentials, requiring neurogenesis to be characterized from each individual line[142,143]. As with human ESCs, there has been a recent focus on converting human iPSCs to a naïve epigenetic state (aka, ground-state), with the objectives of establishing a truly pluripotent phenotype that exhibits greater reliability and reduced variability during differentiation[144-146]. Despite their current technical limitations, two characteristics of iPSCs render iPSC-derived neurons (i-neurons) highly valuable for clinical research. First is the ability to generate patient-specific i-neurons that express the specific genotypic and phenotypic characteristics for a given disease in the context of the patient's own genome. Second, the decreased risk of immunoreactivity following engraftment of autologous cells back to the patient renders iPSCs a viable model for cell replacement therapies. The clinical implications of these characteristics are described further in next section.

The production of i-neurons is relatively new and protocols to reliably generate synaptically active i-neurons are not yet currently available[147]. For example, neurons differentiated from both normal and Alzheimer's disease patient iPSCs display neurotypic intrinsic electrophysiological properties within a week after differentiation from NPC cultures, but derived neurons were unable to fire repetitive APs following current injection, so they were considered immature[148]. Similarly, iPSCs differentiated for 10 wk with standard stem cell derivation and differentiation directed towards cortical neurons were found to express abundant synaptic markers, but electron micrographs indicated sparse vesicles in pre-synaptic compartments, and no activity was reported[16]. In another example, the ability to fire repeated APs was not observed in differentiated iPSC neurons until

about 12 wk after plating[28]. These findings suggest that i-neurons produced using current methods tend to be developmentally arrested or undergo functional synaptogenesis much less quickly than rodent SCNs. In contrast, there are reports suggesting the robust production of synaptically active i-neurons; however, reproducible protocols have not been published nor have other labs validated these findings, making it unclear exactly what element(s) of the differentiation protocols promoted functional synaptogenesis[111,116].

Rationally designed improvements to the speed and efficiency of i-neuron differentiation would be exceedingly valuable for a wide variety of uses, including pharmaceutical screening and cell replacement strategies. The ideal approach would enable the reproducible yield of large quantities of synaptically active neurons of defined lineages in a relatively short period of time. Recent experiments have focused on the ability of transgenic transcription factors and/or small molecules to increase the speed and efficiency of differentiation. For example, overexpression of neurogenin (Ngn1 or 2) transcription factors accelerates maturation of intrinsic neuronal characteristics in i-neurons, but has mixed results on the appearance of post-synaptic currents, with one study finding such currents at 2-3 wk[149] while another did not find any until 7 wk[150]. The addition of small molecules to iPSCs during neuronal differentiation increases the efficiency of differentiation into intermediate neuronal precursors[151]. Small molecules may also be used to influence neuronal pattering, but to date this approach has only been successful in directing cells towards dopaminergic populations, and the resulting neurons have not been assessed for network activity[152,153]. While these approaches are still immature, the identification of methods that improve the speed and efficiency/specificity of neuronal differentiation has the potential to render i-neurons a transformative tool in basic and clinical sciences.

iNs

Recent work suggests that a neuronal phenotype can be differentiated directly from non-neuronal tissue by the expression of specific genes. Direct conversion, or trans-differentiation, works on many of the same principles as iPSCs, involving the forced expression of transcription factors associated with the target neurons or neuronal intermediates. As with iPSCs, a variety of transcriptional and biochemical factors have been used as neural induction factors for iNs. Initially, the transcription factors Ngn2, Ascl1 (Mash1), and Dlx2 were found to directly convert non-proliferative mouse astrocytes into populations of glutamatergic and GABAergic neurons[154,155]. Ascl1, along with the factors Brn2 and Mytl1 (collectively BAM), can convert mouse fibroblasts into active neuronal populations[156,157]. Human postnatal and adult fibroblasts appear to require expression of Brn2, Mytl1l and microRNA-124 to produce active glutamatergic synapses[158]. Alternatively, Nurr1, Lmx1a, Ngn2, Sox2 and Pitx3 have been found to induce fibroblasts to express dopaminergic markers[159-161], while BAM plus Lhx3, Hb9, Isl1, and Ngn2 promotes expression of motor neuron markers[162]. Like iPSC models, iNs can be used to replicate functional pathologies. For example, neuroligin-3 mutations associated with autism cause post-synaptic dysfunction in iNs when co-cultured with primary neurons[163].

The iN field is still new, and many of the challenges facing iPSC-based neuronal differentiation are likely to affect iN approaches as well. Only a small percentage of cells are successfully converted to neurons and most iNs retain epigenetic features of their non-neuronal origins[161]. Unlike differentiation of iPSCs which can be expanded during the stem cell stage iN conversion has frequently proven to have low efficiency, with only 1%-20% of starting cells successfully reprogrammed to become neurons, although some more recent work indicates conversion rates that exceed 200% (indicating a period of proliferation during the conversion process)[162,164]. Low success rates may complicate functional neurogenesis, leading to a sparser neuron population, variable intrinsic properties and little to no network activity, as demonstrated in electrophysiological profiling of iN populations with as few as five neuron-like conversions per coverslip[165]. Conversely, the limited scalability may also render iNs less likely to become tumorigenic following implantation or conversion *in vivo*. One potential way around limited scalability might be to induce differentiated cells into neuronal precursor cells rather than directly into neurons. While this approach has been used to produce presumptive precursors (based on gene expression studies and morphology), it remains to be seen if induced progenitors cells can differentiate into functionally mature neurons[166,167].

APPLICATIONS OF SCNS FOR NEUROSCIENCE AND THERAPEUTICS

General properties of SCN models that facilitate research applications

In addition to the clinical potential, SCNs have extensive potential for basic and applied neuroscience studies. In many cases, stem cells are genetically tractable, typically clonal and amenable to culturing in large numbers, facilitating the production of scalable quantities of synchronized SCNs that are genetically homogenous and amenable to forward and reverse genetics approaches as well as functional engineering for biotechnological studies[101,168,169]. While the stem cell stage of SCN differentiation is the most obvious target for genetic manipulation, allowing for isolation and expansion of genetically identical clones, post-mitotic neurons can also be modified using a variety of techniques that are well-described in primary neuron cultures[170]. Genetic manipulations have been used for a variety of studies. For example, exogenous expression of developmentally regulated transcription factors has been used to explicate the genetic regulators that influence neuronal patterning

and neuron subtype specification[171,172]. In addition to influencing cell type or development, functionality can be added to SCNs by the expression of transgenic proteins. These functional modifications enable a particular readout, such as fluorescent reporters of gene expression, synaptic assembly, synaptic activity, or metabolic function[77,173-175]. Recent advances that provide control over neuron activity *via* biologically orthogonal inducers, such as biophotonic or chemogenetic approaches, make it possible to measure and control synaptic activity in networked neuron cultures[176,177]. For example, expression of channelrhodopsin under the control of a dopaminergic promoter allows for the light-activated stimulation of grafted dopaminergic neurons[67]. The effects of these controlled stimuli on *in vitro* network behavior could be measured by whole-cell patch clamp or in MEAs, providing an indirect electrophysiological measure of the function of metabotropic synapses. Genetic manipulation may also be used to improve the therapeutic potential of SCNs. Targets include repairing the mutated huntingtin protein in models of Huntington's disease[178,179] or expressing factors enhancing neuron growth and repair in implanted SCNs[180,181]. Despite the utility of genetic modulation of stem cells, care must be taken in characterizing the resultant lines. For example, genetic modifications may alter differentiation outcomes, potentially producing cells that are morphologically and structurally neuronal, but lack intrinsic or synaptic electrophysiological characteristics[182]. Although below we will focus on applications that are not dependent on genetic modification, it is important to remember that in most applications the incorporation of genetically modified SCNs would complement basic and clinical studies.

Study of disease mechanisms in personalized SCN models

The *in vitro* analysis of i-neurons produced from patient-derived iPSCs is expected to be one of the early successes of personalized medicine. Autologous SCN models are already in use for applications such as population-wide phenotypic comparisons and drug screening studies[183]. Shortly after protocols became widespread to generate iPSCs, laboratories rushed to establish cell banks of iPSCs derived from patients with a wide variety of neurodevelopmental and neurodegenerative disorders, with the goal of developing diagnostics and assessing treatment efficacies *in vitro*[184-186]. This approach has the distinct advantage of studying the phenotypic disease in the native genetic environment and avoiding confounds that may influence disorder penetrance and prognosis. One example of a disease-specific approach is i-neurons derived from a patient with Dravet syndrome epilepsy, which is caused by a single protein mutation in the Nav1.1 sodium channel. Dravet SCNs exhibited altered excitability, with reductions in evoked AP amplitude and probability of firing[187]. Autologous iPSCs also facilitate the study of neuropsychiatric diseases with complex polygenic or unknown genetic origins, something difficult or impossible by the rational introduction of mutations[188]. For example, i-neurons derived from schizophrenia (SZ) patients have fewer post-synaptic markers and less neurite growth than controls, despite similar intrinsic electrophysiological profiles[189]. When maintained in an immature NPC-like state, SZ cells were also found to have abnormal cytoskeletal development, increased oxidative stress, and aberrant migration, indicative of developmental abnormalities[190]. These discoveries would have been considerably more difficult without access to a developmental SCN model.

Many neurodegenerative disorders originate from multiple genetic loci, including Alzheimer's disease, Parkinson's disease and other dementias[191]. They often exhibit variable penetrance, which is further compounded by a lifetime of unknown environmental interactions. Patient-derived iPSCs offer the potential to study the effects of complex and subtle genetic contributions to these variable disease phenotypes by replicating the genomic context from which the disease is expressed. In some cases, disorders have displayed relatively consistent pathophysiologies in SCN models, enabling high resolution characterization of the disease pathophysiology. For example, i-neurons derived from Parkinson's disease patients from diverse genetic backgrounds exhibit initial morphological characteristics of synaptogenesis, but subsequently degenerate *in vitro*, accumulating α-synuclein and other toxic intermediaries[192,193]. Other disorders have shown inconsistent pathophysiology *in vitro*, including iPSCs derived from Huntington's disease patients[194,195] and multiple sclerosis patients[196]. However, while sometimes confounding, this inconsistent pathology may also contribute to an improved understanding of disease mechanisms. For example, iPSC-derived motor neurons from a subset of amyotrophic lateral sclerosis (ALS) patients exhibit pathophysiological characteristics, while others ALS patient-derived motor neurons appear normal[86,197-199]. Derived ALS motor neurons cocultured with astrocytes have suggested that some ALS neuropathology is due to aberrant glial function[200-202]. Together, these studies suggest that ALS may originate from the interactions of multiple cell types and genetic loci, with potentially tissue-specific diagnoses and treatment requirements.

Two potential caveats to the general appeal of iPSCs for disease modeling are the possibility of selecting a non-representative line during reprogramming and increased risk of genomic changes during maintenance of reprogrammed iPSCs. For example, cultured iPSCs have been found to exhibit increased copy number variation, which is associated with a wide range of neuropsychiatric diseases[203]. Unfortunately, while a variety of assays have been used to characterize the phenotype of neuropsychiatric i-neuron models, few have emphasized differences in synaptic and network activity, in large part because reproducible protocols to generate synaptically active i-neurons are not widely available. In fact, recent reviews have noted that functional assays, such as calcium imaging or electrophysiology are infrequently

performed compared to gene expression studies[192]. This lack of rigor in characterizing SCN models may further contribute to discrepancies in translational interpretation. While i-neurons are not likely to be viable models for all neuropsychiatric diseases, particularly those that rely on multi-tissue interactions, the pathophysiological relevance of patient-specific SCN models has extraordinary potential to explicate complex disease mechanisms.

Neuro-reparative studies

Unlike the comparatively robust reparative mechanisms of the peripheral nervous system, intrinsic regenerative processes in the CNS do not appear to be capable of repairing damaged nervous tissue and restoring normal brain function in cases of severe or large-scale neural disease or injury[204]. Consequently, clinical management of traumatic brain injury or degenerative neurological diseases is predominantly limited to supportive or palliative care. One of the most promising treatment strategies for regeneration of neural function is targeted cell replacement (TCR), in which exogenously derived cells are administered to the CNS to ameliorate the disease or injury process, protect from further decline of function and possibly facilitate repair of lost capacity. In one aspect of TCR, *in vitro*-derived neural cells of defined maturity and fate are delivered to specific CNS locations, where in theory they will appropriately integrate into existing circuits. This approach is complicated by several factors, including the intricate and poorly understood physiology of the nervous system; the fact that ontogenic processes such as axonal pathfinding and circuit formation may not be appropriately recapitulated in adult brains; and the difficulty in specifying the character of the grafted cells. Nonetheless, in preliminary studies centrally administered SCNs have exhibited potential as a regenerative CNS therapy. Administration of human NSCs, such as the NSI-566RSC line, have proven safe and effective in animal models of ALS, spinal cord injury, and ischemia[205], and are currently undergoing clinical trials[206]. These NSCs appear to form functioning neurons that integrate into existing neuronal networks *in vivo*[207]. Studies using more mature dopaminergic neurons derived from fetal NSCs have also found that long-term integration and transplanted neurons conferred resistance to PD in mouse models[208].

TCR has been made more technically feasible by the recent development of autologous iPSCs, which are less likely to evoke undesired immune responses. The development of autologous SCN-based TCR therapies would be immensely valuable for traumatic CNS injury as well as for neurodegenerative diseases such as Parkinson's disease and ALS. However, despite the promise of SCN therapies, early studies suggest that implantation of stem cells and stem cell-derived tissue suffers from several complications, most notably cell survival and functional integration into target circuits[209,210]. For example, inappropriately integrated cells may disrupt existing circuits while cell death may trigger counterproductive inflammatory responses that further degrade central function[211,212]. More severe complications may arise if mitotically active donor cells proliferate to form non-neuronal, neoplastic tissues[213] or otherwise damage the engraftment site, provoking responses that impair the function of implants over time[214,215]. Despite these complications, SCN therapies have transformative potential now, and as protocols are established for improved graft survival and integration with reduced adverse host responses, such therapeutic modalities will be realized.

In vitro neurotoxicology

One of the most attractive uses of SCNs is as a scalable, relevant cell model of neuronal responses in pharmacological and toxicological testing[216]. For example, the physiological relevance imparted by SCNs for *in vitro* toxicology is anticipated to significantly reduce dependence on the use of animals to detect, diagnose or study lethal toxins, such as with the mouse lethality assay, or to conduct initial efficacy testing of candidate therapeutics[217,218]. Neuron-like immortalized cell lines, such as neuroblastomas and pheochromocytomas, have historically been used in *in vitro* toxicity studies and countermeasure screening protocols for the Tier 1 select agents collectively known as botulinum toxins (BoNTs)[219-222]. However, as described above, these cell lines have poor neurogenic competence and thus are not suitable to study neurotoxic substances whose modes of action are mediated by neurotypic behaviors, act in specific neuronal compartments or are evidenced through altered neurotransmission[223,224]. The various BoNT serotypes are good examples of neuron specific agents, as they are internalized at the pre-synaptic compartment and then specifically target and cleave SNARE proteins responsible for neurotransmitter release[225]. In the absence of a functioning pre-synaptic compartment, it is doubtful that non-neuronal models faithfully reflect the biochemistry and host interactions involved in intoxication. In contrast, mouse e-neurons differentiated into a synaptically active population of glutamatergic and GABAergic neurons with emergent network behavior undergo synaptic blockade within hours after intoxication with femtomolar concentrations of botulinum neurotoxins serotype A[6,226,227]. This represents the first *in vitro*-derived, cell-based model to manifest the functional pathophysiology responsible for the clinical symptoms of botulism, enabling novel *in vitro* studies on host: toxin interactions. This e-neuron model has also been shown to be highly sensitive to other neurotoxins, such as glutamate and latrotoxin, with mechanisms of injury, toxin sensitivities and cellular responses that are identical to those of primary neurons[59]. Similar glutamate excitotoxicity has been demonstrated in human e-neurons and i-neurons[228]. As these models are shown to be increasingly relevant neurotoxicological models, they are anticipated to rapidly become the primary approach for target discovery, drug screening and detection/diagnosis of neurotoxins and neurotoxic effects.

Another valuable application of SCNs in neurotoxin

studies is the modeling of developmental neurotoxicity. While primary neuron cultures may not recapitulate developmental vulnerabilities that occur during early stages of differentiation, SCNs are well-suited for studying specific mechanisms of early developmental toxicity, such as the effects of reactive oxygen production and alterations to specific cell signaling pathways during early stages of neurogenesis[229-232]. SCNs can also be used to evaluate toxicant-induced changes to relative neurogenic and gliogenic outcomes during neural differentiation, as well as to test for persistent changes in synaptic function, such as the chronic functional deficits resulting from developmental exposure to ethanol[233-235]. Taking advantage of the scalability of SCN models and high throughput detection platforms such as MEAs or calcium imaging, multiple neurotoxic compounds can be screened and compared in SCN systems over multiple stages of development to assess vulnerable stages and mechanisms[236-238]. In addition, the use of MEAs facilitates high-throughput monitoring of the development and interruption of network activity[75,76,239]. Finally by combining scalability with transgene expression, moderate-to-high throughput assays can be developed to rapidly assess the efficacy of candidate therapeutics on injury or disease at various stages of neurogenesis.

Histogenic models: A step beyond networks

Relevance is a key goal of neuronal models. In addition to functional relevance of neuronal monolayers, a relevant histotypic model can be generated by simultaneously producing or combining multiple nervous tissue types in two- or three-dimensional cultures. Depending on the differentiation protocol, multiple neural types, including glia and oligodendrocytes, can be produced simultaneously with neurons[137,138]. Multiple neuronal subtypes are generated in many SCN differentiation protocols[43,110,171,240]. The introduction of physicobiological techniques to differentiation methods may further enable the defined production of diverse neural cell types, such as the three-dimensional culture of neocortical-like organoids[241-245] and use of chemical or physical micropatterning of plates, including microfluidics[246,247].

Histogenic neuronal models are anticipated to produce more complex neuronal circuits by facilitating synaptic interactions among multiple neuron types. For instance, complex retinal tissue has been generated from iPSCs[248-250], including the formation of three-dimensional superstructures that facilitate the development of photoreceptor cells, multiple neuron types and other cells in the retina. The cells themselves respond to incident light with electrochemical and biochemical responses that are similar to those produced *in vivo*. Further elaboration of this retinal model would require optic nerve tissue as well as visual cortex tissue to more comprehensively model the circuits involved in sight. It may be that in producing SCN models with multiple active neuronal and glial types, researchers have incidentally begun to form specific regional patterning and developmental forms of neuroectodermal tissue that essentially produce many of the outcomes of a histogenic model. For example, the rosettes formed during neurogenesis *in vitro* may be patterned similar to neural tubes or cortical plates *in vivo*[251]. Similarly, three-dimensional cultures of some ESCs allow for the formation of stratified structures similar to fetal cortex[252], and even recapitulates the folding of neuroepithelium[253]. The functional generation of complex tissues such as retina and multi-layered cortex and neuroepithelium solely from stem cells suggests that generation of other complex CNS tissues may soon be feasible.

CONCLUSION

With available stem cell derivation and SCN differentiation techniques growing rapidly, researchers must be able to critically analyze and compare these models to *in vivo* neurons and circuits. Many SCN models, particularly those derived from human origins, still require optimized protocols to reproducibly generate synaptically active neurons. It may be a challenge for some researchers to functionally validate SCN models, but validation is essential for physiological relevance and to increase the translatability of findings regarding neurological development, function and dysfunction. It is encouraging to see newer research in the literature recognizing that functional endpoints, such as the establishment of a neuronal network, are highly sensitive and powerful tools. This review presents some variations in the approaches used to establish synaptic and network activity, but for now it should be apparent to those pursuing electrophysiological approaches that post-synaptic activity must be measured alongside intrinsic characteristics, followed by assays for networked activity. It is hoped that as techniques improve, the means of proving functional synaptogenesis and networked activity in SCNs will also expand. With expanding collections of validated models available, researchers will have excellent options for both basic neuroscience and therapeutic applications.

ACKNOWLEDGMENTS

We would like to acknowledge Kyle Hubbard and Megan Lyman (USAMRICD) for providing cells and exemplar images; Phillip Beske (USAMRICD) for providing exemplar traces; and Tracey Hamilton (USAMRICD) for electron microscopy images; James Abraham (USAMRICD) for illustration work; and Katie Hoffman and Cindy Kronman (USAMRICD) for editorial assistance.

REFERENCES

1 **Dodla MC**, Mumaw J, Stice SL. Role of astrocytes, soluble factors, cells adhesion molecules and neurotrophins in functional synapse formation: implications for human embryonic stem cell derived neurons. *Curr Stem Cell Res Ther* 2010; **5**: 251-260 [PMID: 20214556 DOI: 10.2174/157488810791824520]

2 **Dieni CV**, Chancey JH, Overstreet-Wadiche LS. Dynamic functions of GABA signaling during granule cell maturation. *Front Neural Circuits* 2012; **6**: 113 [PMID: 23316139 DOI: 10.3389/

fncir.2012.00113]
3 **Kaur P**, Karolina DS, Sepramaniam S, Armugam A, Jeyaseelan K. Expression profiling of RNA transcripts during neuronal maturation and ischemic injury. *PLoS One* 2014; **9**: e103525 [PMID: 25061880 DOI: 10.1371/journal.pone.0103525]
4 **Zuko A**, Kleijer KT, Oguro-Ando A, Kas MJ, van Daalen E, van der Zwaag B, Burbach JP. Contactins in the neurobiology of autism. *Eur J Pharmacol* 2013; **719**: 63-74 [PMID: 23872404 DOI: 10.1016/j.ejphar.2013.07.016]
5 **Telias M**, Segal M, Ben-Yosef D. Neural differentiation of Fragile X human Embryonic Stem Cells reveals abnormal patterns of development despite successful neurogenesis. *Dev Biol* 2013; **374**: 32-45 [PMID: 23219959 DOI: 10.1016/j.ydbio.2012.11.031]
6 **McNutt P**, Celver J, Hamilton T, Mesngon M. Embryonic stem cell-derived neurons are a novel, highly sensitive tissue culture platform for botulinum research. *Biochem Biophys Res Commun* 2011; **405**: 85-90 [PMID: 21215258 DOI: 10.1016/j.bbrc.2010.12.132]
7 **Lin M**, Hrabovsky A, Pedrosa E, Wang T, Zheng D, Lachman HM. Allele-biased expression in differentiating human neurons: implications for neuropsychiatric disorders. *PLoS One* 2012; **7**: e44017 [PMID: 22952857 DOI: 10.1371/journal.pone.0044017]
8 **Chau MJ**, Deveau TC, Song M, Gu X, Chen D, Wei L. iPSC Transplantation increases regeneration and functional recovery after ischemic stroke in neonatal rats. *Stem Cells* 2014; **32**: 3075-3087 [PMID: 25132189 DOI: 10.1002/stem.1802]
9 **Boucherie C**, Hermans E. Adult stem cell therapies for neurological disorders: benefits beyond neuronal replacement? *J Neurosci Res* 2009; **87**: 1509-1521 [PMID: 19115417 DOI: 10.1002/jnr.21970]
10 **Telias M**, Ben-Yosef D. Modeling neurodevelopmental disorders using human pluripotent stem cells. *Stem Cell Rev* 2014; **10**: 494-511 [PMID: 24728983 DOI: 10.1007/s12015-014-9507-2]
11 **Panchision DM**. Meeting report: using stem cells for biological and therapeutics discovery in mental illness, April 2012. *Stem Cells Transl Med* 2013; **2**: 217-222 [PMID: 23408104 DOI: 10.5966/sctm.2012-0149]
12 **Zeng H**, Guo M, Martins-Taylor K, Wang X, Zhang Z, Park JW, Zhan S, Kronenberg MS, Lichtler A, Liu HX, Chen FP, Yue L, Li XJ, Xu RH. Specification of region-specific neurons including forebrain glutamatergic neurons from human induced pluripotent stem cells. *PLoS One* 2010; **5**: e11853 [PMID: 20686615 DOI: 10.1371/journal.pone.0011853]
13 **Li H**, Liu H, Corrales CE, Risner JR, Forrester J, Holt JR, Heller S, Edge AS. Differentiation of neurons from neural precursors generated in floating spheres from embryonic stem cells. *BMC Neurosci* 2009; **10**: 122 [PMID: 19778451 DOI: 10.1186/1471-2202-10-122]
14 **Verstraelen P**, Pintelon I, Nuydens R, Cornelissen F, Meert T, Timmermans JP. Pharmacological characterization of cultivated neuronal networks: relevance to synaptogenesis and synaptic connectivity. *Cell Mol Neurobiol* 2014; **34**: 757-776 [PMID: 24748115 DOI: 10.1007/s10571-014-0057-6]
15 **Banker GA**, Cowan WM. Rat hippocampal neurons in dispersed cell culture. *Brain Res* 1977; **126**: 397-342 [PMID: 861729 DOI: 10.1016/0006-8993(77)90594-7]
16 **Mariani J**, Simonini MV, Palejev D, Tomasini L, Coppola G, Szekely AM, Horvath TL, Vaccarino FM. Modeling human cortical development in vitro using induced pluripotent stem cells. *Proc Natl Acad Sci USA* 2012; **109**: 12770-12775 [PMID: 22761314 DOI: 10.1073/pnas.1202944109]
17 **Lilienbaum A**, Israël A. From calcium to NF-kappa B signaling pathways in neurons. *Mol Cell Biol* 2003; **23**: 2680-2698 [PMID: 12665571 DOI: 10.1128/mcb.23.8.2680-2698.2003]
18 **Hagenston AM**, Bading H. Calcium signaling in synapse-to-nucleus communication. *Cold Spring Harb Perspect Biol* 2011; **3**: a004564 [PMID: 21791697 DOI: 10.1101/cshperspect.a004564]
19 **Arundine M**, Tymianski M. Molecular mechanisms of calcium-dependent neurodegeneration in excitotoxicity. *Cell Calcium* 2003; **34**: 325-337 [PMID: 12909079 DOI: 10.1016/s0143-4160(03)00141-6]
20 **Zhang SJ**, Zou M, Lu L, Lau D, Ditzel DA, Delucinge-Vivier C, Aso Y, Descombes P, Bading H. Nuclear calcium signaling controls expression of a large gene pool: identification of a gene program for acquired neuroprotection induced by synaptic activity. *PLoS Genet* 2009; **5**: e1000604 [PMID: 19680447 DOI: 10.1371/journal.pgen.1000604]
21 **Nie CL**, Wang XS, Liu Y, Perrett S, He RQ. Amyloid-like aggregates of neuronal tau induced by formaldehyde promote apoptosis of neuronal cells. *BMC Neurosci* 2007; **8**: 9 [PMID: 17241479 DOI: 10.1186/1471-2202-8-9]
22 **Cho DH**, Nakamura T, Fang J, Cieplak P, Godzik A, Gu Z, Lipton SA. S-nitrosylation of Drp1 mediates beta-amyloid-related mitochondrial fission and neuronal injury. *Science* 2009; **324**: 102-105 [PMID: 19342591 DOI: 10.1126/science.1171091]
23 **Léveillé F**, Papadia S, Fricker M, Bell KF, Soriano FX, Martel MA, Puddifoot C, Habel M, Wyllie DJ, Ikonomidou C, Tolkovsky AM, Hardingham GE. Suppression of the intrinsic apoptosis pathway by synaptic activity. *J Neurosci* 2010; **30**: 2623-2635 [PMID: 20164347 DOI: 10.1523/JNEUROSCI.5115-09.2010]
24 **Kozhich OA**, Hamilton RS, Mallon BS. Standardized generation and differentiation of neural precursor cells from human pluripotent stem cells. *Stem Cell Rev* 2013; **9**: 531-536 [PMID: 22388559 DOI: 10.1007/s12015-012-9357-8]
25 **Craig AM**, Banker G. Neuronal polarity. *Annu Rev Neurosci* 1994; **17**: 267-310 [PMID: 8210176 DOI: 10.1146/annurev.ne.17.030194.001411]
26 **Cáceres A**, Banker GA, Binder L. Immunocytochemical localization of tubulin and microtubule-associated protein 2 during the development of hippocampal neurons in culture. *J Neurosci* 1986; **6**: 714-722 [PMID: 3514816 DOI: 10.1016/0306-4522(85)90052-1]
27 **Fletcher TL**, Cameron P, De Camilli P, Banker G. The distribution of synapsin I and synaptophysin in hippocampal neurons developing in culture. *J Neurosci* 1991; **11**: 1617-1626 [PMID: 1904480]
28 **Nicholas CR**, Chen J, Tang Y, Southwell DG, Chalmers N, Vogt D, Arnold CM, Chen YJ, Stanley EG, Elefanty AG, Sasai Y, Alvarez-Buylla A, Rubenstein JL, Kriegstein AR. Functional maturation of hPSC-derived forebrain interneurons requires an extended timeline and mimics human neural development. *Cell Stem Cell* 2013; **12**: 573-586 [PMID: 23642366 DOI: 10.1016/j.stem.2013.04.005]
29 **Belinsky GS**, Moore AR, Short SM, Rich MT, Antic SD. Physiological properties of neurons derived from human embryonic stem cells using a dibutyryl cyclic AMP-based protocol. *Stem Cells Dev* 2011; **20**: 1733-1746 [PMID: 21226567 DOI: 10.1089/scd.2010.0501]
30 **Micheva KD**, Busse B, Weiler NC, O'Rourke N, Smith SJ. Single-synapse analysis of a diverse synapse population: proteomic imaging methods and markers. *Neuron* 2010; **68**: 639-653 [PMID: 21092855 DOI: 10.1016/j.neuron.2010.09.024]
31 **Burton SD**, Johnson JW, Zeringue HC, Meriney SD. Distinct roles of neuroligin-1 and SynCAM1 in synapse formation and function in primary hippocampal neuronal cultures. *Neuroscience* 2012; **215**: 1-16 [PMID: 22542674 DOI: 10.1016/j.neuroscience.2012.04.047]
32 **Bury LA**, Sabo SL. Dynamic mechanisms of neuroligin-dependent presynaptic terminal assembly in living cortical neurons. *Neural Dev* 2014; **9**: 13 [PMID: 24885664 DOI: 10.1186/1749-8104-9-13]
33 **Barrow SL**, Constable JR, Clark E, El-Sabeawy F, McAllister AK, Washbourne P. Neuroligin1: a cell adhesion molecule that recruits PSD-95 and NMDA receptors by distinct mechanisms during synaptogenesis. *Neural Dev* 2009; **4**: 17 [PMID: 19450252 DOI: 10.1186/1749-8104-4-17]
34 **Heine M**, Thoumine O, Mondin M, Tessier B, Giannone G, Choquet D. Activity-independent and subunit-specific recruitment of functional AMPA receptors at neurexin/neuroligin contacts. *Proc Natl Acad Sci USA* 2008; **105**: 20947-20952 [PMID: 19098102 DOI: 10.1073/pnas.0804007106]
35 **De Roo M**, Klauser P, Muller D. LTP promotes a selective long-term stabilization and clustering of dendritic spines. *PLoS Biol* 2008; **6**: e219 [PMID: 18788894 DOI: 10.1371/journal.pbio.0060219]

36 **Kim J**, Zhao T, Petralia RS, Yu Y, Peng H, Myers E, Magee JC. mGRASP enables mapping mammalian synaptic connectivity with light microscopy. *Nat Methods* 2012; **9**: 96-102 [PMID: 22138823 DOI: 10.1038/nmeth.1784]

37 **Rao A**, Kim E, Sheng M, Craig AM. Heterogeneity in the molecular composition of excitatory postsynaptic sites during development of hippocampal neurons in culture. *J Neurosci* 1998; **18**: 1217-1229 [PMID: 9454832]

38 **Harms KJ**, Craig AM. Synapse composition and organization following chronic activity blockade in cultured hippocampal neurons. *J Comp Neurol* 2005; **490**: 72-84 [PMID: 16041714 DOI: 10.1002/cne.20635]

39 **Valor LM**, Charlesworth P, Humphreys L, Anderson CN, Grant SG. Network activity-independent coordinated gene expression program for synapse assembly. *Proc Natl Acad Sci USA* 2007; **104**: 4658-4663 [PMID: 17360580 DOI: 10.1073/pnas.0609071104]

40 **Dráberová E**, Lukás Z, Ivanyi D, Viklický V, Dráber P. Expression of class III beta-tubulin in normal and neoplastic human tissues. *Histochem Cell Biol* 1998; **109**: 231-239 [PMID: 9541471 DOI: 10.1007/s004180050222]

41 **Bustos R**, Kolen ER, Braiterman L, Baines AJ, Gorelick FS, Hubbard AL. Synapsin I is expressed in epithelial cells: localization to a unique trans-Golgi compartment. *J Cell Sci* 2001; **114**: 3695-3704 [PMID: 11707521]

42 **Darlington PJ**, Goldman JS, Cui QL, Antel JP, Kennedy TE. Widespread immunoreactivity for neuronal nuclei in cultured human and rodent astrocytes. *J Neurochem* 2008; **104**: 1201-1209 [PMID: 17995928 DOI: 10.1111/j.1471-4159.2007.05043.x]

43 **Hubbard KS**, Gut IM, Lyman ME, McNutt PM. Longitudinal RNA sequencing of the deep transcriptome during neurogenesis of cortical glutamatergic neurons from murine ESCs. *F1000Res* 2013; **2**: 35 [PMID: 24358889 DOI: 10.12688/f1000research.2-35.v1]

44 **Owens DF**, Boyce LH, Davis MB, Kriegstein AR. Excitatory GABA responses in embryonic and neonatal cortical slices demonstrated by gramicidin perforated-patch recordings and calcium imaging. *J Neurosci* 1996; **16**: 6414-6423 [PMID: 8815920]

45 **Chancey JH**, Adlaf EW, Sapp MC, Pugh PC, Wadiche JI, Overstreet-Wadiche LS. GABA depolarization is required for experience-dependent synapse unsilencing in adult-born neurons. *J Neurosci* 2013; **33**: 6614-6622 [PMID: 23575858 DOI: 10.1523/jneurosci.0781-13.2013]

46 **Bortone D**, Polleux F. KCC2 expression promotes the termination of cortical interneuron migration in a voltage-sensitive calcium-dependent manner. *Neuron* 2009; **62**: 53-71 [PMID: 19376067 DOI: 10.1016/j.neuron.2009.01.034]

47 **Livesey MR**, Bilican B, Qiu J, Rzechorzek NM, Haghi G, Burr K, Hardingham GE, Chandran S, Wyllie DJ. Maturation of AMPAR composition and the GABAAR reversal potential in hPSC-derived cortical neurons. *J Neurosci* 2014; **34**: 4070-4075 [PMID: 24623784 DOI: 10.1523/JNEUROSCI.5410-13.2014]

48 **Moore AR**, Zhou WL, Jakovcevski I, Zecevic N, Antic SD. Spontaneous electrical activity in the human fetal cortex in vitro. *J Neurosci* 2011; **31**: 2391-2398 [PMID: 21325506 DOI: 10.1523/jneurosci.3886-10.2011]

49 **Picken Bahrey HL**, Moody WJ. Early development of voltage-gated ion currents and firing properties in neurons of the mouse cerebral cortex. *J Neurophysiol* 2003; **89**: 1761-1773 [PMID: 12611962 DOI: 10.1152/jn.00972.2002]

50 **Sipilä ST**, Huttu K, Soltesz I, Voipio J, Kaila K. Depolarizing GABA acts on intrinsically bursting pyramidal neurons to drive giant depolarizing potentials in the immature hippocampus. *J Neurosci* 2005; **25**: 5280-5289 [PMID: 15930375 DOI: 10.1523/JNEUROSCI.0378-05.2005]

51 **Beatty JA**, Sullivan MA, Morikawa H, Wilson CJ. Complex autonomous firing patterns of striatal low-threshold spike interneurons. *J Neurophysiol* 2012; **108**: 771-781 [PMID: 22572945 DOI: 10.1152/jn.00283.2012]

52 **Ovsepian SV**, Dolly JO, Zaborszky L. Intrinsic voltage dynamics govern the diversity of spontaneous firing profiles in basal forebrain noncholinergic neurons. *J Neurophysiol* 2012; **108**: 406-418 [PMID: 22496531 DOI: 10.1152/jn.00642.2011]

53 **Sonntag KC**, Simantov R, Kim KS, Isacson O. Temporally induced Nurr1 can induce a non-neuronal dopaminergic cell type in embryonic stem cell differentiation. *Eur J Neurosci* 2004; **19**: 1141-1152 [PMID: 15016073 DOI: 10.1111/j.1460-9568.2004.03204.x]

54 **Kaeser PS**, Regehr WG. Molecular mechanisms for synchronous, asynchronous, and spontaneous neurotransmitter release. *Annu Rev Physiol* 2014; **76**: 333-363 [PMID: 24274737 DOI: 10.1146/annurev-physiol-021113-170338]

55 **Peled ES**, Newman ZL, Isacoff EY. Evoked and spontaneous transmission favored by distinct sets of synapses. *Curr Biol* 2014; **24**: 484-493 [PMID: 24560571 DOI: 10.1016/j.cub.2014.01.022]

56 **Dolly JO**, Lande S, Wray DW. The effects of in vitro application of purified botulinum neurotoxin at mouse motor nerve terminals. *J Physiol* 1987; **386**: 475-484 [PMID: 3681717 DOI: 10.1113/jphysiol.1987.sp016546]

57 **Harris JJ**, Jolivet R, Attwell D. Synaptic energy use and supply. *Neuron* 2012; **75**: 762-777 [PMID: 22958818 DOI: 10.1016/j.neuron.2012.08.019]

58 **Otsu Y**, Murphy TH. Miniature transmitter release: accident of nature or careful design? *Sci STKE* 2003; **2003**: pe54 [PMID: 14657459 DOI: 10.1126/stke.2112003pe54]

59 **Gut IM**, Beske PH, Hubbard KS, Lyman ME, Hamilton TA, McNutt PM. Novel application of stem cell-derived neurons to evaluate the time- and dose-dependent progression of excitotoxic injury. *PLoS One* 2013; **8**: e64423 [PMID: 23691214 DOI: 10.1371/journal.pone.0064423]

60 **Shi Y**, Kirwan P, Livesey FJ. Directed differentiation of human pluripotent stem cells to cerebral cortex neurons and neural networks. *Nat Protoc* 2012; **7**: 1836-1846 [PMID: 22976355 DOI: 10.1038/nprot.2012.116]

61 **Fatt P**, Katz B. Spontaneous subthreshold activity at motor nerve endings. *J Physiol* 1952; **117**: 109-128 [PMID: 14946732]

62 **Paré D**, Lebel E, Lang EJ. Differential impact of miniature synaptic potentials on the soma and dendrites of pyramidal neurons in vivo. *J Neurophysiol* 1997; **78**: 1735-1739 [PMID: 9310459]

63 **Debanne D**, Boudkkazi S, Campanac E, Cudmore RH, Giraud P, Fronzaroli-Molinieres L, Carlier E, Caillard O. Paired-recordings from synaptically coupled cortical and hippocampal neurons in acute and cultured brain slices. *Nat Protoc* 2008; **3**: 1559-1568 [PMID: 18802437 DOI: 10.1038/nprot.2008.147]

64 **Bi GQ**, Poo MM. Synaptic modifications in cultured hippocampal neurons: dependence on spike timing, synaptic strength, and postsynaptic cell type. *J Neurosci* 1998; **18**: 10464-10472 [PMID: 9852584]

65 **Maximov A**, Pang ZP, Tervo DGR, Südhof TC. Monitoring synaptic transmission in primary neuronal cultures using local extracellular stimulation. *J Neurosci Meth* 2007 **161**: 75-87 [PMID: 17118459 DOI: 10.1016/j.jneumeth.2006.10.009]

66 **Cragg SJ**. Variable dopamine release probability and short-term plasticity between functional domains of the primate striatum. *J Neurosci* 2003; **23**: 4378-4385 [PMID: 12764127]

67 **Tønnesen J**, Parish CL, Sørensen AT, Andersson A, Lundberg C, Deisseroth K, Arenas E, Lindvall O, Kokaia M. Functional integration of grafted neural stem cell-derived dopaminergic neurons monitored by optogenetics in an in vitro Parkinson model. *PLoS One* 2011; **6**: e17560 [PMID: 21394212 DOI: 10.1371/journal.pone.0017560]

68 **Beggs JM**. The criticality hypothesis: how local cortical networks might optimize information processing. *Philos Trans A Math Phys Eng Sci* 2008; **366**: 329-343 [PMID: 17673410 DOI: 10.1098/rsta.2007.2092]

69 **Okuno H**, Akashi K, Ishii Y, Yagishita-Kyo N, Suzuki K, Nonaka M, Kawashima T, Fujii H, Takemoto-Kimura S, Abe M, Natsume R, Chowdhury S, Sakimura K, Worley PF, Bito H. Inverse synaptic tagging of inactive synapses via dynamic interaction of Arc/Arg3.1 with CaMKIIβ. *Cell* 2012; **149**: 886-898 [PMID: 22579289 DOI: 10.1016/j.cell.2012.02.062]

70 **DiFebo F**, Curti D, Botti F, Biella G, Bigini P, Mennini T,

Toselli M. Neural precursors (NPCs) from adult L967Q mice display early commitment to "in vitro" neuronal differentiation and hyperexcitability. *Exp Neurol* 2012; **236**: 307-318 [PMID: 22634210 DOI: 10.1016/j.expneurol.2012.05.010]

71 **Habas A**, Hahn J, Wang X, Margeta M. Neuronal activity regulates astrocytic Nrf2 signaling. *Proc Natl Acad Sci USA* 2013; **110**: 18291-18296 [PMID: 24145448 DOI: 10.1073/pnas.1208764110]

72 **Choi DW**. Excitotoxic cell death. *J Neurobiol* 1992; **23**: 1261-1276 [PMID: 1361523 DOI: 10.1002/neu.480230915]

73 **Barth L**, Sütterlin R, Nenniger M, Vogt KE. Reduced synaptic activity in neuronal networks derived from embryonic stem cells of murine Rett syndrome model. *Front Cell Neurosci* 2014; **8**: 79 [PMID: 24723848 DOI: 10.3389/fncel.2014.00079]

74 **Copi A**, Jüngling K, Gottmann K. Activity- and BDNF-induced plasticity of miniature synaptic currents in ES cell-derived neurons integrated in a neocortical network. *J Neurophysiol* 2005; **94**: 4538-4543 [PMID: 16293594 DOI: 10.1152/jn.00155.2005]

75 **Weiss D**. Neurotoxicity assessment by recording electrical activity from neuronal networks on microelectrode array neurochips. In: Aschner M, Suñol C, Bal-Price A. Cell culture techniques. Humana Press, 2011: 467-480 [DOI: 10.1007/978-1-61779-077-5_24]

76 **van Vliet E**, Stoppini L, Balestrino M, Eskes C, Griesinger C, Sobanski T, Whelan M, Hartung T, Coecke S. Electrophysiological recording of re-aggregating brain cell cultures on multi-electrode arrays to detect acute neurotoxic effects. *Neurotoxicology* 2007; **28**: 1136-1146 [PMID: 17692379 DOI: 10.1016/j.neuro.2007.06.004]

77 **Ikegaya Y**, Le Bon-Jego M, Yuste R. Large-scale imaging of cortical network activity with calcium indicators. *Neurosci Res* 2005; **52**: 132-138 [PMID: 15893573 DOI: 10.1016/j.neures.2005.02.004]

78 **Chen Q**, Cichon J, Wang W, Qiu L, Lee SJ, Campbell NR, Destefino N, Goard MJ, Fu Z, Yasuda R, Looger LL, Arenkiel BR, Gan WB, Feng G. Imaging neural activity using Thy1-GCaMP transgenic mice. *Neuron* 2012; **76**: 297-308 [PMID: 23083733 DOI: 10.1016/j.neuron.2012.07.011]

79 **Leão RN**, Reis A, Emirandetti A, Lewicka M, Hermanson O, Fisahn A. A voltage-sensitive dye-based assay for the identification of differentiated neurons derived from embryonic neural stem cell cultures. *PLoS One* 2010; **5**: e13833 [PMID: 21079795 DOI: 10.1371/journal.pone.0013833]

80 **Blum R**, Heinrich C, Sánchez R, Lepier A, Gundelfinger ED, Berninger B, Götz M. Neuronal network formation from reprogrammed early postnatal rat cortical glial cells. *Cereb Cortex* 2011; **21**: 413-424 [PMID: 20562320 DOI: 10.1093/cercor/bhq107]

81 **Matsumoto K**, Ishikawa T, Matsuki N, Ikegaya Y. Multineuronal spike sequences repeat with millisecond precision. *Front Neural Circuits* 2013; **7**: 112 [PMID: 23801942 DOI: 10.3389/fncir.2013.00112]

82 **Badura A**, Sun XR, Giovannucci A, Lynch LA, Wang SS. Fast calcium sensor proteins for monitoring neural activity. *Neurophotonics* 2014; **1**: 025008 [PMID: 25558464 DOI: 10.1117/1.NPh.1.2.025008]

83 **Odawara A**, Saitoh Y, Alhebshi AH, Gotoh M, Suzuki I. Long-term electrophysiological activity and pharmacological response of a human induced pluripotent stem cell-derived neuron and astrocyte co-culture. *Biochem Biophys Res Commun* 2014; **443**: 1176-1181 [PMID: 24406164 DOI: 10.1016/j.bbrc.2013.12.142]

84 **Piper DR**, Mujtaba T, Rao MS, Lucero MT. Immunocytochemical and physiological characterization of a population of cultured human neural precursors. *J Neurophysiol* 2000; **84**: 534-548 [PMID: 10899225]

85 **Song M**, Mohamad O, Chen D, Yu SP. Coordinated development of voltage-gated Na+ and K+ currents regulates functional maturation of forebrain neurons derived from human induced pluripotent stem cells. *Stem Cells Dev* 2013; **22**: 1551-1563 [PMID: 23259973 DOI: 10.1089/scd.2012.0556]

86 **Bilican B**, Serio A, Barmada SJ, Nishimura AL, Sullivan GJ, Carrasco M, Phatnani HP, Puddifoot CA, Story D, Fletcher J, Park IH, Friedman BA, Daley GQ, Wyllie DJ, Hardingham GE, Wilmut I, Finkbeiner S, Maniatis T, Shaw CE, Chandran S. Mutant induced pluripotent stem cell lines recapitulate aspects of TDP-43 proteinopathies and reveal cell-specific vulnerability. *Proc Natl Acad Sci USA* 2012; **109**: 5803-5808 [PMID: 22451909 DOI: 10.1073/pnas.1202922109]

87 **Levina A**, Herrmann JM, Geisel T. Dynamical synapses causing self-organized criticality in neural networks. *Nat Phys* 2007; **3**: 857-860 [DOI: 10.1038/Nphys758]

88 **Cullen DK**, Gilroy ME, Irons HR, Laplaca MC. Synapse-to-neuron ratio is inversely related to neuronal density in mature neuronal cultures. *Brain Res* 2010; **1359**: 44-55 [PMID: 20800585 DOI: 10.1016/j.brainres.2010.08.058]

89 **Marín-Burgin A**, Mongiat LA, Pardi MB, Schinder AF. Unique processing during a period of high excitation/inhibition balance in adult-born neurons. *Science* 2012; **335**: 1238-1242 [PMID: 22282476 DOI: 10.1126/science.1214956]

90 **Whitney NP**, Peng H, Erdmann NB, Tian C, Monaghan DT, Zheng JC. Calcium-permeable AMPA receptors containing Q/R-unedited GluR2 direct human neural progenitor cell differentiation to neurons. *FASEB J* 2008; **22**: 2888-2900 [PMID: 18403631 DOI: 10.1096/fj.07-104661]

91 **Barcomb K**, Buard I, Coultrap SJ, Kulbe JR, O'Leary H, Benke TA, Bayer KU. Autonomous CaMKII requires further stimulation by Ca2+/calmodulin for enhancing synaptic strength. *FASEB J* 2014; **28**: 3810-3819 [PMID: 24843070 DOI: 10.1096/fj.14-250407]

92 **Ma H**, Groth RD, Cohen SM, Emery JF, Li B, Hoedt E, Zhang G, Neubert TA, Tsien RW. γCaMKII shuttles Ca2+/CaM to the nucleus to trigger CREB phosphorylation and gene expression. *Cell* 2014; **159**: 281-294 [PMID: 25303525 DOI: 10.1016/j.cell.2014.09.019]

93 **Akchiche N**, Bossenmeyer-Pourié C, Pourié G, Koziel V, Nédélec E, Guéant JL, Daval JL. Differentiation and neural integration of hippocampal neuronal progenitors: signaling pathways sequentially involved. *Hippocampus* 2010; **20**: 949-961 [PMID: 19714568 DOI: 10.1002/hipo.20690]

94 **Wang CC**, Held RG, Hall BJ. SynGAP regulates protein synthesis and homeostatic synaptic plasticity in developing cortical networks. *PLoS One* 2013; **8**: e83941 [PMID: 24391850 DOI: 10.1371/journal.pone.0083941]

95 **Rao VR**, Pintchovski SA, Chin J, Peebles CL, Mitra S, Finkbeiner S. AMPA receptors regulate transcription of the plasticity-related immediate-early gene Arc. *Nat Neurosci* 2006; **9**: 887-895 [PMID: 16732277 DOI: 10.1038/nn1708]

96 **Inoue Y**, Udo H, Inokuchi K, Sugiyama H. Homer1a regulates the activity-induced remodeling of synaptic structures in cultured hippocampal neurons. *Neuroscience* 2007; **150**: 841-852 [PMID: 18006237 DOI: 10.1016/j.neuroscience.2007.09.081]

97 **Sanders JD**, Happe HK, Bylund DB, Murrin LC. Differential effects of neonatal norepinephrine lesions on immediate early gene expression in developing and adult rat brain. *Neuroscience* 2008; **157**: 821-832 [PMID: 18938224 DOI: 10.1016/j.neuroscience.2008.09.036]

98 **Saito TH**, Uda S, Tsuchiya T, Ozaki Y, Kuroda S. Temporal decoding of MAP kinase and CREB phosphorylation by selective immediate early gene expression. *PLoS One* 2013; **8**: e57037 [PMID: 23469182 DOI: 10.1371/journal.pone.0057037]

99 **Axell MZ**, Zlateva S, Curtis M. A method for rapid derivation and propagation of neural progenitors from human embryonic stem cells. *J Neurosci Methods* 2009; **184**: 275-284 [PMID: 19715727 DOI: 10.1016/j.jneumeth.2009.08.015]

100 **Cohen MA**, Itsykson P, Reubinoff BE. Neural differentiation of human ES cells. *Curr Protoc Cell Biol* 2007; **Chapter 23**: Unit 23.7 [PMID: 18228508 DOI: 10.1002/0471143030.cb2307s36]

101 **Niwa H**, Ogawa K, Shimosato D, Adachi K. A parallel circuit of LIF signalling pathways maintains pluripotency of mouse ES cells. *Nature* 2009; **460**: 118-122 [PMID: 19571885 DOI: 10.1038/nature08113]

102 **Bain G**, Kitchens D, Yao M, Huettner JE, Gottlieb DI. Embryonic stem cells express neuronal properties in vitro. *Dev Biol* 1995; **168**: 342-357 [PMID: 7729574 DOI: 10.1006/dbio.1995.1085]

103 **McBurney MW**, Jones-Villeneuve EM, Edwards MK, Anderson PJ. Control of muscle and neuronal differentiation in a cultured embryonal carcinoma cell line. *Nature* 1982; **299**: 165-167 [PMID: 7110336 DOI: 10.1038/299165a0]

104 **Jones-Villeneuve EM**, McBurney MW, Rogers KA, Kalnins VI. Retinoic acid induces embryonal carcinoma cells to differentiate into neurons and glial cells. *J Cell Biol* 1982; **94**: 253-262 [PMID: 7107698 DOI: 10.1083/jcb.94.2.253]

105 **Chambers SM**, Qi Y, Mica Y, Lee G, Zhang XJ, Niu L, Bilsland J, Cao L, Stevens E, Whiting P, Shi SH, Studer L. Combined small-molecule inhibition accelerates developmental timing and converts human pluripotent stem cells into nociceptors. *Nat Biotechnol* 2012; **30**: 715-720 [PMID: 22750882 DOI: 10.1038/nbt.2249]

106 **Gaspard N**, Bouschet T, Herpoel A, Naeije G, van den Ameele J, Vanderhaeghen P. Generation of cortical neurons from mouse embryonic stem cells. *Nat Protoc* 2009; **4**: 1454-1463 [PMID: 19798080 DOI: 10.1038/nprot.2009.157]

107 **Li XJ**, Hu BY, Jones SA, Zhang YS, Lavaute T, Du ZW, Zhang SC. Directed differentiation of ventral spinal progenitors and motor neurons from human embryonic stem cells by small molecules. *Stem Cells* 2008; **26**: 886-893 [PMID: 18238853 DOI: 10.1634/stemcells.2007-0620]

108 **Braun SM**, Machado RA, Jessberger S. Temporal control of retroviral transgene expression in newborn cells in the adult brain. *Stem Cell Reports* 2013; **1**: 114-122 [PMID: 24052947 DOI: 10.1016/j.stemcr.2013.06.003]

109 **Hong S**, Chung S, Leung K, Hwang I, Moon J, Kim KS. Functional roles of Nurr1, Pitx3, and Lmx1a in neurogenesis and phenotype specification of dopamine neurons during in vitro differentiation of embryonic stem cells. *Stem Cells Dev* 2014; **23**: 477-487 [PMID: 24172139 DOI: 10.1089/scd.2013.0406]

110 **Yan Y**, Yang D, Zarnowska ED, Du Z, Werbel B, Valliere C, Pearce RA, Thomson JA, Zhang SC. Directed differentiation of dopaminergic neuronal subtypes from human embryonic stem cells. *Stem Cells* 2005; **23**: 781-790 [PMID: 15917474 DOI: 10.1634/stemcells.2004-0365]

111 **Kim JE**, O'Sullivan ML, Sanchez CA, Hwang M, Israel MA, Brennand K, Deerinck TJ, Goldstein LS, Gage FH, Ellisman MH, Ghosh A. Investigating synapse formation and function using human pluripotent stem cell-derived neurons. *Proc Natl Acad Sci USA* 2011; **108**: 3005-3010 [PMID: 21278334 DOI: 10.1073/pnas.1007753108]

112 **Anjomshoa M**, Karbalaie K, Mardani M, Razavi S, Tanhaei S, Nasr-Esfahani MH, Baharvand H. Generation of motor neurons by coculture of retinoic acid-pretreated embryonic stem cells with chicken notochords. *Stem Cells Dev* 2009; **18**: 259-267 [PMID: 18422402 DOI: 10.1089/scd.2008.0049]

113 **Johnson MA**, Weick JP, Pearce RA, Zhang SC. Functional neural development from human embryonic stem cells: accelerated synaptic activity via astrocyte coculture. *J Neurosci* 2007; **27**: 3069-3077 [PMID: 17376968 DOI: 10.1523/jneurosci.4562-06.2007]

114 **Jordan PM**, Cain LD, Wu P. Astrocytes enhance long-term survival of cholinergic neurons differentiated from human fetal neural stem cells. *J Neurosci Res* 2008; **86**: 35-47 [PMID: 17729316 DOI: 10.1002/jnr.21460]

115 **Thomson JA**, Itskovitz-Eldor J, Shapiro SS, Waknitz MA, Swiergiel JJ, Marshall VS, Jones JM. Embryonic stem cell lines derived from human blastocysts. *Science* 1998; **282**: 1145-1147 [PMID: 9804556 DOI: 10.1126/science.282.5391.1145]

116 **Bilican B**, Livesey MR, Haghi G, Qiu J, Burr K, Siller R, Hardingham GE, Wyllie DJ, Chandran S. Physiological normoxia and absence of EGF is required for the long-term propagation of anterior neural precursors from human pluripotent cells. *PLoS One* 2014; **9**: e85932 [PMID: 24465796 DOI: 10.1371/journal.pone.0085932]

117 **Okada Y**, Shimazaki T, Sobue G, Okano H. Retinoic-acid-concentration-dependent acquisition of neural cell identity during in vitro differentiation of mouse embryonic stem cells. *Dev Biol* 2004; **275**: 124-142 [PMID: 15464577 DOI: 10.1016/j.ydbio.2004.07.038]

118 **Raye WS**, Tochon-Danguy N, Pouton CW, Haynes JM. Heterogeneous population of dopaminergic neurons derived from mouse embryonic stem cells: preliminary phenotyping based on receptor expression and function. *Eur J Neurosci* 2007; **25**: 1961-1970 [PMID: 17419751 DOI: 10.1111/j.1460-9568.2007.05489.x]

119 **Chatzi C**, Scott RH, Pu J, Lang B, Nakamoto C, McCaig CD, Shen S. Derivation of homogeneous GABAergic neurons from mouse embryonic stem cells. *Exp Neurol* 2009; **217**: 407-416 [PMID: 19348800 DOI: 10.1016/j.expneurol.2009.03.032]

120 **Schnerch A**, Cerdan C, Bhatia M. Distinguishing between mouse and human pluripotent stem cell regulation: the best laid plans of mice and men. *Stem Cells* 2010; **28**: 419-430 [PMID: 20054863 DOI: 10.1002/stem.298]

121 **Chen X**, Li T, Li X, Xie Y, Guo X, Ji S, Niu Y, Yu Y, Ding C, Yao R, Yang S, Ji W, Zhou Q. Neural progenitors derived from monkey embryonic stem cells in a simple monoculture system. *Reprod Biomed Online* 2009; **19**: 426-433 [PMID: 19778491 DOI: 10.1016/S1472-6483(10)60179-4]

122 **Wilcox JT**, Lai JK, Semple E, Brisson BA, Gartley C, Armstrong JN, Betts DH. Synaptically-competent neurons derived from canine embryonic stem cells by lineage selection with EGF and Noggin. *PLoS One* 2011; **6**: e19768 [PMID: 21611190 DOI: 10.1371/journal.pone.0019768]

123 **Yang JY**, Mumaw JL, Liu Y, Stice SL, West FD. SSEA4-positive pig induced pluripotent stem cells are primed for differentiation into neural cells. *Cell Transplant* 2013; **22**: 945-959 [PMID: 23043799 DOI: 10.3727/096368912x657279]

124 **Boast S**, Stern CD. Simple methods for generating neural, bone and endodermal cell types from chick embryonic stem cells. *Stem Cell Res* 2013; **10**: 20-28 [PMID: 23047046 DOI: 10.1016/j.scr.2012.08.008]

125 **Wu Y**, Ge C, Zeng W, Zhang C. Induced multilineage differentiation of chicken embryonic germ cells via embryoid body formation. *Stem Cells Dev* 2010; **19**: 195-202 [PMID: 19548770 DOI: 10.1089/scd.2008.0383]

126 **Tursun B**, Patel T, Kratsios P, Hobert O. Direct conversion of C. elegans germ cells into specific neuron types. *Science* 2011; **331**: 304-308 [PMID: 21148348 DOI: 10.1126/science.1199082]

127 **Schmidt H**, Lüer K, Hevers W, Technau GM. Ionic currents of Drosophila embryonic neurons derived from selectively cultured CNS midline precursors. *J Neurobiol* 2000; **44**: 392-413 [PMID: 10945895 DOI: 10.1002/1097-4695(20000915)44:4<392::AID-NEU3>3.0.CO;2-M]

128 **Horiguchi S**, Takahashi J, Kishi Y, Morizane A, Okamoto Y, Koyanagi M, Tsuji M, Tashiro K, Honjo T, Fujii S, Hashimoto N. Neural precursor cells derived from human embryonic brain retain regional specificity. *J Neurosci Res* 2004; **75**: 817-824 [PMID: 14994342 DOI: 10.1002/jnr.20046]

129 **Shihabuddin LS**, Horner PJ, Ray J, Gage FH. Adult spinal cord stem cells generate neurons after transplantation in the adult dentate gyrus. *J Neurosci* 2000; **20**: 8727-8735 [PMID: 11102479]

130 **Weiss S**, Dunne C, Hewson J, Wohl C, Wheatley M, Peterson AC, Reynolds BA. Multipotent CNS stem cells are present in the adult mammalian spinal cord and ventricular neuroaxis. *J Neurosci* 1996; **16**: 7599-7609 [PMID: 8922416]

131 **Coskun V**, Wu H, Blanchi B, Tsao S, Kim K, Zhao J, Biancotti JC, Hutnick L, Krueger RC, Fan G, de Vellis J, Sun YE. CD133+ neural stem cells in the ependyma of mammalian postnatal forebrain. *Proc Natl Acad Sci USA* 2008; **105**: 1026-1031 [PMID: 18195354 DOI: 10.1073/pnas.0710000105]

132 **Hermann A**, Maisel M, Wegner F, Liebau S, Kim DW, Gerlach M, Schwarz J, Kim KS, Storch A. Multipotent neural stem cells from the adult tegmentum with dopaminergic potential develop essential properties of functional neurons. *Stem Cells* 2006; **24**: 949-964 [PMID: 16373695 DOI: 10.1634/stemcells.2005-0192]

133 **Frisén J**, Johansson CB, Lothian C, Lendahl U. Central nervous system stem cells in the embryo and adult. *Cell Mol Life Sci* 1998; **54**: 935-945 [PMID: 9791537 DOI: 10.1007/s000180050224]

134 **Alvarez-Buylla A**, Seri B, Doetsch F. Identification of neural stem

cells in the adult vertebrate brain. *Brain Res Bull* 2002; **57**: 751-758 [PMID: 12031271 DOI: 10.1016/s0361-9230(01)00770-5]

135 **Rao MS**, Noble M, Mayer-Pröschel M. A tripotential glial precursor cell is present in the developing spinal cord. *Proc Natl Acad Sci USA* 1998; **95**: 3996-4001 [PMID: 9520481 DOI: 10.1073/pnas.95.7.3996]

136 **Laywell ED**, Rakic P, Kukekov VG, Holland EC, Steindler DA. Identification of a multipotent astrocytic stem cell in the immature and adult mouse brain. *Proc Natl Acad Sci USA* 2000; **97**: 13883-13888 [PMID: 11095732 DOI: 10.1073/pnas.250471697]

137 **Piao JH**, Odeberg J, Samuelsson EB, Kjaeldgaard A, Falci S, Seiger A, Sundström E, Akesson E. Cellular composition of long-term human spinal cord- and forebrain-derived neurosphere cultures. *J Neurosci Res* 2006; **84**: 471-482 [PMID: 16721767 DOI: 10.1002/jnr.20955]

138 **Sun Y**, Pollard S, Conti L, Toselli M, Biella G, Parkin G, Willatt L, Falk A, Cattaneo E, Smith A. Long-term tripotent differentiation capacity of human neural stem (NS) cells in adherent culture. *Mol Cell Neurosci* 2008; **38**: 245-258 [PMID: 18450476 DOI: 10.1016/j.mcn.2008.02.014]

139 **Schultz SS**, Lucas PA. Human stem cells isolated from adult skeletal muscle differentiate into neural phenotypes. *J Neurosci Methods* 2006; **152**: 144-155 [PMID: 16300830 DOI: 10.1016/j.jneumeth.2005.08.022]

140 **Takahashi K**, Yamanaka S. Induction of pluripotent stem cells from mouse embryonic and adult fibroblast cultures by defined factors. *Cell* 2006; **126**: 663-676 [PMID: 16904174 DOI: 10.1016/j.cell.2006.07.024]

141 **Yu J**, Vodyanik MA, Smuga-Otto K, Antosiewicz-Bourget J, Frane JL, Tian S, Nie J, Jonsdottir GA, Ruotti V, Stewart R, Slukvin II, Thomson JA. Induced pluripotent stem cell lines derived from human somatic cells. *Science* 2007; **318**: 1917-1920 [PMID: 18029452 DOI: 10.1126/science.1151526]

142 **Hu BY**, Weick JP, Yu J, Ma LX, Zhang XQ, Thomson JA, Zhang SC. Neural differentiation of human induced pluripotent stem cells follows developmental principles but with variable potency. *Proc Natl Acad Sci USA* 2010; **107**: 4335-4340 [PMID: 20160098 DOI: 10.1073/pnas.0910012107]

143 **Devine MJ**, Ryten M, Vodicka P, Thomson AJ, Burdon T, Houlden H, Cavaleri F, Nagano M, Drummond NJ, Taanman JW, Schapira AH, Gwinn K, Hardy J, Lewis PA, Kunath T. Parkinson's disease induced pluripotent stem cells with triplication of the α-synuclein locus. *Nat Commun* 2011; **2**: 440 [PMID: 21863007 DOI: 10.1038/ncomms1453]

144 **Gafni O**, Weinberger L, Mansour AA, Manor YS, Chomsky E, Ben-Yosef D, Kalma Y, Viukov S, Maza I, Zviran A, Rais Y, Shipony Z, Mukamel Z, Krupalnik V, Zerbib M, Geula S, Caspi I, Schneir D, Shwartz T, Gilad S, Amann-Zalcenstein D, Benjamin S, Amit I, Tanay A, Massarwa R, Novershtern N, Hanna JH. Derivation of novel human ground state naive pluripotent stem cells. *Nature* 2013; **504**: 282-286 [PMID: 24172903 DOI: 10.1038/nature12745]

145 **Ware CB**, Nelson AM, Mecham B, Hesson J, Zhou W, Jonlin EC, Jimenez-Caliani AJ, Deng X, Cavanaugh C, Cook S, Tesar PJ, Okada J, Margaretha L, Sperber H, Choi M, Blau CA, Treuting PM, Hawkins RD, Cirulli V, Ruohola-Baker H. Derivation of naive human embryonic stem cells. *Proc Natl Acad Sci USA* 2014; **111**: 4484-4489 [PMID: 24623855 DOI: 10.1073/pnas.1319738111]

146 **Valamehr B**, Robinson M, Abujarour R, Rezner B, Vranceanu F, Le T, Medcalf A, Lee TT, Fitch M, Robbins D, Flynn P. Platform for induction and maintenance of transgene-free hiPSCs resembling ground state pluripotent stem cells. *Stem Cell Reports* 2014; **2**: 366-381 [PMID: 24672758 DOI: 10.1016/j.stemcr.2014.01.014]

147 **Emdad L**, D'Souza SL, Kothari HP, Qadeer ZA, Germano IM. Efficient differentiation of human embryonic and induced pluripotent stem cells into functional astrocytes. *Stem Cells Dev* 2012; **21**: 404-410 [PMID: 21631388 DOI: 10.1089/scd.2010.0560]

148 **Israel MA**, Yuan SH, Bardy C, Reyna SM, Mu Y, Herrera C, Hefferan MP, Van Gorp S, Nazor KL, Boscolo FS, Carson CT, Laurent LC, Marsala M, Gage FH, Remes AM, Koo EH, Goldstein LS. Probing sporadic and familial Alzheimer's disease using induced pluripotent stem cells. *Nature* 2012; **482**: 216-220 [PMID: 22278060 DOI: 10.1038/nature10821]

149 **Zhang Y**, Pak C, Han Y, Ahlenius H, Zhang Z, Chanda S, Marro S, Patzke C, Acuna C, Covy J, Xu W, Yang N, Danko T, Chen L, Wernig M, Südhof TC. Rapid single-step induction of functional neurons from human pluripotent stem cells. *Neuron* 2013; **78**: 785-798 [PMID: 23764284 DOI: 10.1016/j.neuron.2013.05.029]

150 **Busskamp V**, Lewis NE, Guye P, Ng AH, Shipman SL, Byrne SM, Sanjana NE, Murn J, Li Y, Li S, Stadler M, Weiss R, Church GM. Rapid neurogenesis through transcriptional activation in human stem cells. *Mol Syst Biol* 2014; **10**: 760 [PMID: 25403753 DOI: 10.15252/msb.20145508]

151 **Menendez L**, Yatskievych TA, Antin PB, Dalton S. Wnt signaling and a Smad pathway blockade direct the differentiation of human pluripotent stem cells to multipotent neural crest cells. *Proc Natl Acad Sci USA* 2011; **108**: 19240-19245 [PMID: 22084120 DOI: 10.1073/pnas.1113746108]

152 **Chambers SM**, Fasano CA, Papapetrou EP, Tomishima M, Sadelain M, Studer L. Highly efficient neural conversion of human ES and iPS cells by dual inhibition of SMAD signaling. *Nat Biotechnol* 2009; **27**: 275-280 [PMID: 19252484 DOI: 10.1038/nbt.1529]

153 **Mak SK**, Huang YA, Iranmanesh S, Vangipuram M, Sundararajan R, Nguyen L, Langston JW, Schüle B. Small molecules greatly improve conversion of human-induced pluripotent stem cells to the neuronal lineage. *Stem Cells Int* 2012; **2012**: 140427 [PMID: 22567022 DOI: 10.1155/2012/140427]

154 **Berninger B**, Costa MR, Koch U, Schroeder T, Sutor B, Grothe B, Götz M. Functional properties of neurons derived from in vitro reprogrammed postnatal astroglia. *J Neurosci* 2007; **27**: 8654-8664 [PMID: 17687043 DOI: 10.1523/JNEUROSCI.1615-07.2007]

155 **Heinrich C**, Gascón S, Masserdotti G, Lepier A, Sanchez R, Simon-Ebert T, Schroeder T, Götz M, Berninger B. Generation of subtype-specific neurons from postnatal astroglia of the mouse cerebral cortex. *Nat Protoc* 2011; **6**: 214-228 [PMID: 21293461 DOI: 10.1038/nprot.2010.188]

156 **Vierbuchen T**, Ostermeier A, Pang ZP, Kokubu Y, Südhof TC, Wernig M. Direct conversion of fibroblasts to functional neurons by defined factors. *Nature* 2010; **463**: 1035-1041 [PMID: 20107439 DOI: 10.1038/nature08797]

157 **Chanda S**, Ang CE, Davila J, Pak C, Mall M, Lee QY, Ahlenius H, Jung SW, Südhof TC, Wernig M. Generation of induced neuronal cells by the single reprogramming factor ASCL1. *Stem Cell Reports* 2014; **3**: 282-296 [PMID: 25254342 DOI: 10.1016/j.stemcr.2014.05.020]

158 **Ambasudhan R**, Talantova M, Coleman R, Yuan X, Zhu S, Lipton SA, Ding S. Direct reprogramming of adult human fibroblasts to functional neurons under defined conditions. *Cell Stem Cell* 2011; **9**: 113-118 [PMID: 21802386 DOI: 10.1016/j.stem.2011.07.002]

159 **Liu X**, Huang Q, Li F, Li CY. Enhancing the efficiency of direct reprogramming of human primary fibroblasts into dopaminergic neuron-like cells through p53 suppression. *Sci China Life Sci* 2014; **57**: 867-875 [PMID: 25129808 DOI: 10.1007/s11427-014-4730-2]

160 **Liu X**, Li F, Stubblefield EA, Blanchard B, Richards TL, Larson GA, He Y, Huang Q, Tan AC, Zhang D, Benke TA, Sladek JR, Zahniser NR, Li CY. Direct reprogramming of human fibroblasts into dopaminergic neuron-like cells. *Cell Res* 2012; **22**: 321-332 [PMID: 22105488 DOI: 10.1038/cr.2011.181]

161 **Caiazzo M**, Dell'Anno MT, Dvoretskova E, Lazarevic D, Taverna S, Leo D, Sotnikova TD, Menegon A, Roncaglia P, Colciago G, Russo G, Carninci P, Pezzoli G, Gainetdinov RR, Gustincich S, Dityatev A, Broccoli V. Direct generation of functional dopaminergic neurons from mouse and human fibroblasts. *Nature* 2011; **476**: 224-227 [PMID: 21725324 DOI: 10.1038/nature10284]

162 **Son EY**, Ichida JK, Wainger BJ, Toma JS, Rafuse VF, Woolf CJ, Eggan K. Conversion of mouse and human fibroblasts into functional spinal motor neurons. *Cell Stem Cell* 2011; **9**: 205-218 [PMID: 21852222 DOI: 10.1016/j.stem.2011.07.014]

163 **Chanda S**, Marro S, Wernig M, Südhof TC. Neurons generated

by direct conversion of fibroblasts reproduce synaptic phenotype caused by autism-associated neuroligin-3 mutation. *Proc Natl Acad Sci USA* 2013; **110**: 16622-16627 [PMID: 24046374 DOI: 10.1073/pnas.1316240110]

164 **Ladewig J**, Mertens J, Kesavan J, Doerr J, Poppe D, Glaue F, Herms S, Wernet P, Kögler G, Müller FJ, Koch P, Brüstle O. Small molecules enable highly efficient neuronal conversion of human fibroblasts. *Nat Methods* 2012; **9**: 575-578 [PMID: 22484851 DOI: 10.1038/nmeth.1972]

165 **Koppensteiner P**, Boehm S, Arancio O. Electrophysiological profiles of induced neurons converted directly from adult human fibroblasts indicate incomplete neuronal conversion. *Cell Reprogram* 2014; **16**: 439-446 [PMID: 25437871 DOI: 10.1089/cell.2014.0054]

166 **Lujan E**, Chanda S, Ahlenius H, Südhof TC, Wernig M. Direct conversion of mouse fibroblasts to self-renewing, tripotent neural precursor cells. *Proc Natl Acad Sci USA* 2012; **109**: 2527-2532 [PMID: 22308465 DOI: 10.1073/pnas.1121003109]

167 **Tian C**, Liu Q, Ma K, Wang Y, Chen Q, Ambroz R, Klinkebiel DL, Li Y, Huang Y, Ding J, Wu J, Zheng JC. Characterization of induced neural progenitors from skin fibroblasts by a novel combination of defined factors. *Sci Rep* 2013; **3**: 1345 [PMID: 23439431 DOI: 10.1038/srep01345]

168 **Amit M**, Carpenter MK, Inokuma MS, Chiu CP, Harris CP, Waknitz MA, Itskovitz-Eldor J, Thomson JA. Clonally derived human embryonic stem cell lines maintain pluripotency and proliferative potential for prolonged periods of culture. *Dev Biol* 2000; **227**: 271-278 [PMID: 11071754 DOI: 10.1006/dbio.2000.9912]

169 **Hong S**, Kang UJ, Isacson O, Kim KS. Neural precursors derived from human embryonic stem cells maintain long-term proliferation without losing the potential to differentiate into all three neural lineages, including dopaminergic neurons. *J Neurochem* 2008; **104**: 316-324 [PMID: 17944878 DOI: 10.1111/j.1471-4159.2007.04952.x]

170 **Dhara SK**, Gerwe BA, Majumder A, Dodla MC, Boyd NL, Machacek DW, Hasneen K, Stice SL. Genetic manipulation of neural progenitors derived from human embryonic stem cells. *Tissue Eng Part A* 2009; **15**: 3621-3634 [PMID: 19795983 DOI: 10.1089/ten.tea.2009.0155]

171 **Berninger B**, Guillemot F, Götz M. Directing neurotransmitter identity of neurones derived from expanded adult neural stem cells. *Eur J Neurosci* 2007; **25**: 2581-2590 [PMID: 17561834 DOI: 10.1111/j.1460-9568.2007.05509.x]

172 **Sánchez-Danés A**, Consiglio A, Richaud Y, Rodríguez-Pizà I, Dehay B, Edel M, Bové J, Memo M, Vila M, Raya A, Izpisua Belmonte JC. Efficient generation of A9 midbrain dopaminergic neurons by lentiviral delivery of LMX1A in human embryonic stem cells and induced pluripotent stem cells. *Hum Gene Ther* 2012; **23**: 56-69 [PMID: 21877920 DOI: 10.1089/hum.2011.054]

173 **McNeish J**, Roach M, Hambor J, Mather RJ, Weibley L, Lazzaro J, Gazard J, Schwarz J, Volkmann R, Machacek D, Stice S, Zawadzke L, O'Donnell C, Hurst R. High-throughput screening in embryonic stem cell-derived neurons identifies potentiators of alpha-amino-3-hydroxyl-5-methyl-4-isoxazolepropionate-type glutamate receptors. *J Biol Chem* 2010; **285**: 17209-17217 [PMID: 20212047 DOI: 10.1074/jbc.M109.098814]

174 **Eiges R**, Schuldiner M, Drukker M, Yanuka O, Itskovitz-Eldor J, Benvenisty N. Establishment of human embryonic stem cell-transfected clones carrying a marker for undifferentiated cells. *Curr Biol* 2001; **11**: 514-518 [PMID: 11413002 DOI: 10.1016/s0960-9822(01)00144-0]

175 **Daadi MM**, Li Z, Arac A, Grueter BA, Sofilos M, Malenka RC, Wu JC, Steinberg GK. Molecular and magnetic resonance imaging of human embryonic stem cell-derived neural stem cell grafts in ischemic rat brain. *Mol Ther* 2009; **17**: 1282-1291 [PMID: 19436269 DOI: 10.1038/mt.2009.104]

176 **Dranias MR**, Ju H, Rajaram E, VanDongen AM. Short-term memory in networks of dissociated cortical neurons. *J Neurosci* 2013; **33**: 1940-1953 [PMID: 23365233 DOI: 10.1523/jneurosci.2718-12.2013]

177 **Dell'Anno MT**, Caiazzo M, Leo D, Dvoretskova E, Medrihan L, Colasante G, Giannelli S, Theka I, Russo G, Mus L, Pezzoli G, Gainetdinov RR, Benfenati F, Taverna S, Dityatev A, Broccoli V. Remote control of induced dopaminergic neurons in parkinsonian rats. *J Clin Invest* 2014; **124**: 3215-3229 [PMID: 24937431 DOI: 10.1172/jci74664]

178 **Nguyen GD**, Molero AE, Gokhan S, Mehler MF. Functions of huntingtin in germ layer specification and organogenesis. *PLoS One* 2013; **8**: e72698 [PMID: 23967334 DOI: 10.1371/journal.pone.0072698]

179 **Fink KD**, Crane AT, Lévêque X, Dues DJ, Huffman LD, Moore AC, Story DT, Dejonge RE, Antcliff A, Starski PA, Lu M, Lescaudron L, Rossignol J, Dunbar GL. Intrastriatal transplantation of adenovirus-generated induced pluripotent stem cells for treating neuropathological and functional deficits in a rodent model of Huntington's disease. *Stem Cells Transl Med* 2014; **3**: 620-631 [PMID: 24657963 DOI: 10.5966/sctm.2013-0151]

180 **Cenciarelli C**, Budoni M, Mercanti D, Fernandez E, Pallini R, Aloe L, Cimino V, Maira G, Casalbore P. In vitro analysis of mouse neural stem cells genetically modified to stably express human NGF by a novel multigenic viral expression system. *Neurol Res* 2006; **28**: 505-512 [PMID: 16808880 DOI: 10.1179/016164106X115161]

181 **Kim SU**. Human neural stem cells genetically modified for brain repair in neurological disorders. *Neuropathology* 2004; **24**: 159-171 [PMID: 15484694 DOI: 10.1111/j.1440-1789.2004.00552.x]

182 **Donato R**, Miljan EA, Hines SJ, Aouabdi S, Pollock K, Patel S, Edwards FA, Sinden JD. Differential development of neuronal physiological responsiveness in two human neural stem cell lines. *BMC Neurosci* 2007; **8**: 36 [PMID: 17531091 DOI: 10.1186/1471-2202-8-36]

183 **Haggarty SJ**, Perlis RH. Translation: screening for novel therapeutics with disease-relevant cell types derived from human stem cell models. *Biol Psychiatry* 2014; **75**: 952-960 [PMID: 23876186 DOI: 10.1016/j.biopsych.2013.05.028]

184 **Wray S**, Self M, Lewis PA, Taanman JW, Ryan NS, Mahoney CJ, Liang Y, Devine MJ, Sheerin UM, Houlden H, Morris HR, Healy D, Marti-Masso JF, Preza E, Barker S, Sutherland M, Corriveau RA, D'Andrea M, Schapira AH, Uitti RJ, Guttman M, Opala G, Jasinska-Myga B, Puschmann A, Nilsson C, Espay AJ, Slawek J, Gutmann L, Boeve BF, Boylan K, Stoessl AJ, Ross OA, Maragakis NJ, Van Gerpen J, Gerstenhaber M, Gwinn K, Dawson TM, Isacson O, Marder KS, Clark LN, Przedborski SE, Finkbeiner S, Rothstein JD, Wszolek ZK, Rossor MN, Hardy J. Creation of an open-access, mutation-defined fibroblast resource for neurological disease research. *PLoS One* 2012; **7**: e43099 [PMID: 22952635 DOI: 10.1371/journal.pone.0043099]

185 **Cao Z**, Hammock BD, McCoy M, Rogawski MA, Lein PJ, Pessah IN. Tetramethylenedisulfotetramine alters Ca2+ dynamics in cultured hippocampal neurons: mitigation by NMDA receptor blockade and GABA(A) receptor-positive modulation. *Toxicol Sci* 2012; **130**: 362-372 [PMID: 22889812 DOI: 10.1093/toxsci/kfs244]

186 **Park IH**, Arora N, Huo H, Maherali N, Ahfeldt T, Shimamura A, Lensch MW, Cowan C, Hochedlinger K, Daley GQ. Disease-specific induced pluripotent stem cells. *Cell* 2008; **134**: 877-886 [PMID: 18691744 DOI: 10.1016/j.cell.2008.07.041]

187 **Higurashi N**, Uchida T, Lossin C, Misumi Y, Okada Y, Akamatsu W, Imaizumi Y, Zhang B, Nabeshima K, Mori MX, Katsurabayashi S, Shirasaka Y, Okano H, Hirose S. A human Dravet syndrome model from patient induced pluripotent stem cells. *Mol Brain* 2013; **6**: 19 [PMID: 23639079 DOI: 10.1186/1756-6606-6-19]

188 **Schizophrenia Working Group of the Psychiatric Genomics Consortium**. Biological insights from 108 schizophrenia-associated genetic loci. *Nature* 2014; **511**: 421-427 [PMID: 25056061 DOI: 10.1038/nature13595]

189 **Marchetto MC**, Brennand KJ, Boyer LF, Gage FH. Induced pluripotent stem cells (iPSCs) and neurological disease modeling: progress and promises. *Hum Mol Genet* 2011; **20**: R109-R115 [PMID: 21828073 DOI: 10.1093/hmg/ddr336]

190 **Brennand K**, Savas JN, Kim Y, Tran N, Simone A, Hashimoto-

Torii K, Beaumont KG, Kim HJ, Topol A, Ladran I, Abdelrahim M, Matikainen-Ankney B, Chao SH, Mrksich M, Rakic P, Fang G, Zhang B, Yates JR, Gage FH. Phenotypic differences in hiPSC NPCs derived from patients with schizophrenia. *Mol Psychiatry* 2015; **20**: 361-368 [PMID: 24686136 DOI: 10.1038/mp.2014.22]

191 **Zou F**, Chai HS, Younkin CS, Allen M, Crook J, Pankratz VS, Carrasquillo MM, Rowley CN, Nair AA, Middha S, Maharjan S, Nguyen T, Ma L, Malphrus KG, Palusak R, Lincoln S, Bisceglio G, Georgescu C, Kouri N, Kolbert CP, Jen J, Haines JL, Mayeux R, Pericak-Vance MA, Farrer LA, Schellenberg GD, Petersen RC, Graff-Radford NR, Dickson DW, Younkin SG, Ertekin-Taner N. Brain expression genome-wide association study (eGWAS) identifies human disease-associated variants. *PLoS Genet* 2012; **8**: e1002707 [PMID: 22685416 DOI: 10.1371/journal.pgen.1002707]

192 **Badger JL**, Cordero-Llana O, Hartfield EM, Wade-Martins R. Parkinson's disease in a dish - Using stem cells as a molecular tool. *Neuropharmacology* 2014; **76 Pt A**: 88-96 [PMID: 24035919 DOI: 10.1016/j.neuropharm.2013.08.035]

193 **Peng J**, Liu Q, Rao MS, Zeng X. Using human pluripotent stem cell-derived dopaminergic neurons to evaluate candidate Parkinson' s disease therapeutic agents in MPP+ and rotenone models. *J Biomol Screen* 2013; **18**: 522-533 [PMID: 23364514 DOI: 10.1177/1087057112474468]

194 **Camnasio S**, Delli Carri A, Lombardo A, Grad I, Mariotti C, Castucci A, Rozell B, Lo Riso P, Castiglioni V, Zuccato C, Rochon C, Takashima Y, Diaferia G, Biunno I, Gellera C, Jaconi M, Smith A, Hovatta O, Naldini L, Di Donato S, Feki A, Cattaneo E. The first reported generation of several induced pluripotent stem cell lines from homozygous and heterozygous Huntington's disease patients demonstrates mutation related enhanced lysosomal activity. *Neurobiol Dis* 2012; **46**: 41-51 [PMID: 22405424 DOI: 10.1016/j.nbd.2011.12.042]

195 **Niclis JC**, Pinar A, Haynes JM, Alsanie W, Jenny R, Dottori M, Cram DS. Characterization of forebrain neurons derived from late-onset Huntington's disease human embryonic stem cell lines. *Front Cell Neurosci* 2013; **7**: 37 [PMID: 23576953 DOI: 10.3389/fncel.2013.00037]

196 **Song B**, Sun G, Herszfeld D, Sylvain A, Campanale NV, Hirst CE, Caine S, Parkington HC, Tonta MA, Coleman HA, Short M, Ricardo SD, Reubinoff B, Bernard CC. Neural differentiation of patient specific iPS cells as a novel approach to study the pathophysiology of multiple sclerosis. *Stem Cell Res* 2012; **8**: 259-273 [PMID: 22265745 DOI: 10.1016/j.scr.2011.12.001]

197 **Burkhardt MF**, Martinez FJ, Wright S, Ramos C, Volfson D, Mason M, Garnes J, Dang V, Lievers J, Shoukat-Mumtaz U, Martinez R, Gai H, Blake R, Vaisberg E, Grskovic M, Johnson C, Irion S, Bright J, Cooper B, Nguyen L, Griswold-Prenner I, Javaherian A. A cellular model for sporadic ALS using patient-derived induced pluripotent stem cells. *Mol Cell Neurosci* 2013; **56**: 355-364 [PMID: 23891805 DOI: 10.1016/j.mcn.2013.07.007]

198 **Egawa N**, Kitaoka S, Tsukita K, Naitoh M, Takahashi K, Yamamoto T, Adachi F, Kondo T, Okita K, Asaka I, Aoi T, Watanabe A, Yamada Y, Morizane A, Takahashi J, Ayaki T, Ito H, Yoshikawa K, Yamawaki S, Suzuki S, Watanabe D, Hioki H, Kaneko T, Makioka K, Okamoto K, Takuma H, Tamaoka A, Hasegawa K, Nonaka T, Hasegawa M, Kawata A, Yoshida M, Nakahata T, Takahashi R, Marchetto MC, Gage FH, Yamanaka S, Inoue H. Drug screening for ALS using patient-specific induced pluripotent stem cells. *Sci Transl Med* 2012; **4**: 145ra104 [PMID: 22855461 DOI: 10.1126/scitranslmed.3004052]

199 **Dimos JT**, Rodolfa KT, Niakan KK, Weisenthal LM, Mitsumoto H, Chung W, Croft GF, Saphier G, Leibel R, Goland R, Wichterle H, Henderson CE, Eggan K. Induced pluripotent stem cells generated from patients with ALS can be differentiated into motor neurons. *Science* 2008; **321**: 1218-1221 [PMID: 18669821 DOI: 10.1126/science.1158799]

200 **Christou YA**, Ohyama K, Placzek M, Monk PN, Shaw PJ. Wild-type but not mutant SOD1 transgenic astrocytes promote the efficient generation of motor neuron progenitors from mouse embryonic stem cells. *BMC Neurosci* 2013; **14**: 126 [PMID: 24134124 DOI: 10.1186/1471-2202-14-126]

201 **Hedlund E**, Isacson O. ALS model glia can mediate toxicity to motor neurons derived from human embryonic stem cells. *Cell Stem Cell* 2008; **3**: 575-576 [PMID: 19041769 DOI: 10.1016/j.stem.2008.11.004]

202 **Marchetto MC**, Muotri AR, Mu Y, Smith AM, Cezar GG, Gage FH. Non-cell-autonomous effect of human SOD1 G37R astrocytes on motor neurons derived from human embryonic stem cells. *Cell Stem Cell* 2008; **3**: 649-657 [PMID: 19041781 DOI: 10.1016/j.stem.2008.10.001]

203 **Närvä E**, Autio R, Rahkonen N, Kong L, Harrison N, Kitsberg D, Borghese L, Itskovitz-Eldor J, Rasool O, Dvorak P, Hovatta O, Otonkoski T, Tuuri T, Cui W, Brüstle O, Baker D, Maltby E, Moore HD, Benvenisty N, Andrews PW, Yli-Harja O, Lahesmaa R. High-resolution DNA analysis of human embryonic stem cell lines reveals culture-induced copy number changes and loss of heterozygosity. *Nat Biotechnol* 2010; **28**: 371-377 [PMID: 20351689 DOI: 10.1038/nbt.1615]

204 **Gomez-Nicola D**, Suzzi S, Vargas-Caballero M, Fransen NL, Al-Malki H, Cebrian-Silla A, Garcia-Verdugo JM, Riecken K, Fehse B, Perry VH. Temporal dynamics of hippocampal neurogenesis in chronic neurodegeneration. *Brain* 2014; **137**: 2312-2328 [PMID: 24941947 DOI: 10.1093/brain/awu155]

205 **Tajiri N**, Quach DM, Kaneko Y, Wu S, Lee D, Lam T, Hayama KL, Hazel TG, Johe K, Wu MC, Borlongan CV. Behavioral and histopathological assessment of adult ischemic rat brains after intracerebral transplantation of NSI-566RSC cell lines. *PLoS One* 2014; **9**: e91408 [PMID: 24614895 DOI: 10.1371/journal.pone.0091408]

206 **Feldman EL**, Boulis NM, Hur J, Johe K, Rutkove SB, Federici T, Polak M, Bordeau J, Sakowski SA, Glass JD. Intraspinal neural stem cell transplantation in amyotrophic lateral sclerosis: phase 1 trial outcomes. *Ann Neurol* 2014; **75**: 363-373 [PMID: 24510776 DOI: 10.1002/ana.24113]

207 **Xu L**, Ryugo DK, Pongstaporn T, Johe K, Koliatsos VE. Human neural stem cell grafts in the spinal cord of SOD1 transgenic rats: differentiation and structural integration into the segmental motor circuitry. *J Comp Neurol* 2009; **514**: 297-309 [PMID: 19326469 DOI: 10.1002/cne.22022]

208 **Hallett PJ**, Cooper O, Sadi D, Robertson H, Mendez I, Isacson O. Long-term health of dopaminergic neuron transplants in Parkinson's disease patients. *Cell Rep* 2014; **7**: 1755-1761 [PMID: 24910427 DOI: 10.1016/j.celrep.2014.05.027]

209 **Rong Z**, Fu X, Wang M, Xu Y. A scalable approach to prevent teratoma formation of human embryonic stem cells. *J Biol Chem* 2012; **287**: 32338-32345 [PMID: 22865887 DOI: 10.1074/jbc.M112.383810]

210 **Parsons XH**. Constraining the Pluripotent Fate of Human Embryonic Stem Cells for Tissue Engineering and Cell Therapy - The Turning Point of Cell-Based Regenerative Medicine. *Br Biotechnol J* 2013; **3**: 424-457 [PMID: 24926434 DOI: 10.9734/BBJ/2013/4309#sthash.6D8Rulbv.dpuf]

211 **Weerakkody TN**, Patel TP, Yue C, Takano H, Anderson HC, Meaney DF, Coulter DA, Wolfe JH. Engraftment of nonintegrating neural stem cells differentially perturbs cortical activity in a dose-dependent manner. *Mol Ther* 2013; **21**: 2258-2267 [PMID: 23831593 DOI: 10.1038/mt.2013.163]

212 **Hunt JA**, Fok M, Bryan N. Impact of cell purification technique of autologous human adult stem cells on inflammatory reaction. *Biomaterials* 2013; **34**: 7626-7631 [PMID: 23871537 DOI: 10.1016/j.biomaterials.2013.06.065]

213 **Roy NS**, Cleren C, Singh SK, Yang L, Beal MF, Goldman SA. Functional engraftment of human ES cell-derived dopaminergic neurons enriched by coculture with telomerase-immortalized midbrain astrocytes. *Nat Med* 2006; **12**: 1259-1268 [PMID: 17057709 DOI: 10.1038/nm1495]

214 **Dlouhy BJ**, Awe O, Rao RC, Kirby PA, Hitchon PW. Autograft-derived spinal cord mass following olfactory mucosal cell transplantation in a spinal cord injury patient: Case report. *J Neurosurg Spine* 2014; **21**: 618-622 [PMID: 25002238 DOI: 10.3171/2014.5.

SPINE13992]
215 **Molcanyi M**, Riess P, Bentz K, Maegele M, Hescheler J, Schäfke B, Trapp T, Neugebauer E, Klug N, Schäfer U. Trauma-associated inflammatory response impairs embryonic stem cell survival and integration after implantation into injured rat brain. *J Neurotrauma* 2007; **24**: 625-637 [PMID: 17439346 DOI: 10.1089/neu.2006.0180]
216 **McKim JM**. Building a tiered approach to in vitro predictive toxicity screening: a focus on assays with in vivo relevance. *Comb Chem High Throughput Screen* 2010; **13**: 188-206 [PMID: 20053163 DOI: 10.2174/138620710790596736]
217 **Bitz S**. The botulinum neurotoxin LD50 test - problems and solutions. *ALTEX* 2010; **27**: 114-116 [PMID: 20686744]
218 **Scott CW**, Peters MF, Dragan YP. Human induced pluripotent stem cells and their use in drug discovery for toxicity testing. *Toxicol Lett* 2013; **219**: 49-58 [PMID: 23470867 DOI: 10.1016/j.toxlet.2013.02.020]
219 **Laurenza I**, Pallocca G, Mennecozzi M, Scelfo B, Pamies D, Bal-Price A. A human pluripotent carcinoma stem cell-based model for in vitro developmental neurotoxicity testing: effects of methylmercury, lead and aluminum evaluated by gene expression studies. *Int J Dev Neurosci* 2013; **31**: 679-691 [PMID: 23501475 DOI: 10.1016/j.ijdevneu.2013.03.002]
220 **Lundqvist J**, El Andaloussi-Lilja J, Svensson C, Gustafsson Dorfh H, Forsby A. Optimisation of culture conditions for differentiation of C17.2 neural stem cells to be used for in vitro toxicity tests. *Toxicol In Vitro* 2013; **27**: 1565-1569 [PMID: 22542584 DOI: 10.1016/j.tiv.2012.04.020]
221 **Ma S**, Liu H, Jiao H, Wang L, Chen L, Liang J, Zhao M, Zhang X. Neuroprotective effect of ginkgolide K on glutamate-induced cytotoxicity in PC 12 cells via inhibition of ROS generation and Ca(2+) influx. *Neurotoxicology* 2012; **33**: 59-69 [PMID: 22120026 DOI: 10.1016/j.neuro.2011.11.003]
222 **Munir M**, Lu L, Mcgonigle P. Excitotoxic cell death and delayed rescue in human neurons derived from NT2 cells. *J Neurosci* 1995; **15**: 7847-7860 [PMID: 8613724]
223 **Eubanks LM**, Hixon MS, Jin W, Hong S, Clancy CM, Tepp WH, Baldwin MR, Malizio CJ, Goodnough MC, Barbieri JT, Johnson EA, Boger DL, Dickerson TJ, Janda KD. An in vitro and in vivo disconnect uncovered through high-throughput identification of botulinum neurotoxin A antagonists. *Proc Natl Acad Sci USA* 2007; **104**: 2602-2607 [PMID: 17293454 DOI: 10.1073/pnas.0611213104]
224 **Purkiss JR**, Friis LM, Doward S, Quinn CP. Clostridium botulinum neurotoxins act with a wide range of potencies on SH-SY5Y human neuroblastoma cells. *Neurotoxicology* 2001; **22**: 447-453 [PMID: 11577803 DOI: 10.1016/s0161-813x(01)00042-0]
225 **Pellizzari R**, Rossetto O, Schiavo G, Montecucco C. Tetanus and botulinum neurotoxins: mechanism of action and therapeutic uses. *Philos Trans R Soc Lond B Biol Sci* 1999; **354**: 259-268 [PMID: 10212474 DOI: 10.1098/rstb.1999.0377]
226 **Hubbard KS**, Gut IM, Lyman ME, Tuznik KM, Mesngon MT, McNutt PM. High yield derivation of enriched glutamatergic neurons from suspension-cultured mouse ESCs for neurotoxicology research. *BMC Neurosci* 2012; **13**: 127 [PMID: 23095170 DOI: 10.1186/1471-2202-13-127]
227 **Hubbard K**, Beske P, Lyman M, McNutt P. Functional evaluation of biological neurotoxins in networked cultures of stem cell-derived central nervous system neurons. *J Vis Exp* 2015; (**96**): e52361 [DOI: 10.3791/52361]
228 **Gupta K**, Hardingham GE, Chandran S. NMDA receptor-dependent glutamate excitotoxicity in human embryonic stem cell-derived neurons. *Neurosci Lett* 2013; **543**: 95-100 [PMID: 23518152 DOI: 10.1016/j.neulet.2013.03.010]
229 **Bai X**, Twaroski D, Bosnjak ZJ. Modeling anesthetic developmental neurotoxicity using human stem cells. *Semin Cardiothorac Vasc Anesth* 2013; **17**: 276-287 [PMID: 23859832 DOI: 10.1177/1089253213495923]
230 **Bosnjak ZJ**. Developmental neurotoxicity screening using human embryonic stem cells. *Exp Neurol* 2012; **237**: 207-210 [PMID: 22770995 DOI: 10.1016/j.expneurol.2012.06.023]
231 **Bai X**, Yan Y, Canfield S, Muravyeva MY, Kikuchi C, Zaja I, Corbett JA, Bosnjak ZJ. Ketamine enhances human neural stem cell proliferation and induces neuronal apoptosis via reactive oxygen species-mediated mitochondrial pathway. *Anesth Analg* 2013; **116**: 869-880 [PMID: 23460563 DOI: 10.1213/ANE.0b013e3182860fc9]
232 **Li T**, Wang W, Pan YW, Xu L, Xia Z. A hydroxylated metabolite of flame-retardant PBDE-47 decreases the survival, proliferation, and neuronal differentiation of primary cultured adult neural stem cells and interferes with signaling of ERK5 MAP kinase and neurotrophin 3. *Toxicol Sci* 2013; **134**: 111-124 [PMID: 23564643 DOI: 10.1093/toxsci/kft083]
233 **Sánchez-Alvarez R**, Gayen S, Vadigepalli R, Anni H. Ethanol diverts early neuronal differentiation trajectory of embryonic stem cells by disrupting the balance of lineage specifiers. *PLoS One* 2013; **8**: e63794 [PMID: 23724002 DOI: 10.1371/journal.pone.0063794]
234 **Nash R**, Krishnamoorthy M, Jenkins A, Csete M. Human embryonic stem cell model of ethanol-mediated early developmental toxicity. *Exp Neurol* 2012; **234**: 127-135 [PMID: 22227564 DOI: 10.1016/j.expneurol.2011.12.022]
235 **Taléns-Visconti R**, Sanchez-Vera I, Kostic J, Perez-Arago MA, Erceg S, Stojkovic M, Guerri C. Neural differentiation from human embryonic stem cells as a tool to study early brain development and the neuroteratogenic effects of ethanol. *Stem Cells Dev* 2011; **20**: 327-339 [PMID: 20491543 DOI: 10.1089/scd.2010.0037]
236 **Buzanska L**, Sypecka J, Nerini-Molteni S, Compagnoni A, Hogberg HT, del Torchio R, Domanska-Janik K, Zimmer J, Coecke S. A human stem cell-based model for identifying adverse effects of organic and inorganic chemicals on the developing nervous system. *Stem Cells* 2009; **27**: 2591-2601 [PMID: 19609937 DOI: 10.1002/stem.179]
237 **Choi YS**, Lee MC, Kim HS, Lee KH, Park YG, Kim HK, Jeong HS, Kim MK, Woo YJ, Kim SU, Ryu JK, Choi HB. Neurotoxicity screening in a multipotent neural stem cell line established from the mouse brain. *J Korean Med Sci* 2010; **25**: 440-448 [PMID: 20191045 DOI: 10.3346/jkms.2010.25.3.440]
238 **Breier JM**, Radio NM, Mundy WR, Shafer TJ. Development of a high-throughput screening assay for chemical effects on proliferation and viability of immortalized human neural progenitor cells. *Toxicol Sci* 2008; **105**: 119-133 [PMID: 18550602 DOI: 10.1093/toxsci/kfn115]
239 **Ylä-Outinen L**, Heikkilä J, Skottman H, Suuronen R, Aänismaa R, Narkilahti S. Human cell-based micro electrode array platform for studying neurotoxicity. *Front Neuroeng* 2010; **3**: pii: 111 [PMID: 20953240 DOI: 10.3389/fneng.2010.00111]
240 **Kirkeby A**, Grealish S, Wolf DA, Nelander J, Wood J, Lundblad M, Lindvall O, Parmar M. Generation of regionally specified neural progenitors and functional neurons from human embryonic stem cells under defined conditions. *Cell Rep* 2012; **1**: 703-714 [PMID: 22813745 DOI: 10.1016/j.celrep.2012.04.009]
241 **Cho MS**, Lee YE, Kim JY, Chung S, Cho YH, Kim DS, Kang SM, Lee H, Kim MH, Kim JH, Leem JW, Oh SK, Choi YM, Hwang DY, Chang JW, Kim DW. Highly efficient and large-scale generation of functional dopamine neurons from human embryonic stem cells. *Proc Natl Acad Sci USA* 2008; **105**: 3392-3397 [PMID: 18305158 DOI: 10.1073/pnas.0712359105]
242 **Choi YY**, Chung BG, Lee DH, Khademhosseini A, Kim JH, Lee SH. Controlled-size embryoid body formation in concave microwell arrays. *Biomaterials* 2010; **31**: 4296-4303 [PMID: 20206991 DOI: 10.1016/j.biomaterials.2010.01.115]
243 **Dubois-Dauphin ML**, Toni N, Julien SD, Charvet I, Sundstrom LE, Stoppini L. The long-term survival of in vitro engineered nervous tissue derived from the specific neural differentiation of mouse embryonic stem cells. *Biomaterials* 2010; **31**: 7032-7042 [PMID: 20591476 DOI: 10.1016/j.biomaterials.2010.06.017]
244 **Preynat-Seauve O**, Suter DM, Tirefort D, Turchi L, Virolle T, Chneiweiss H, Foti M, Lobrinus JA, Stoppini L, Feki A, Dubois-Dauphin M, Krause KH. Development of human nervous tissue upon differentiation of embryonic stem cells in three-dimensional

culture. *Stem Cells* 2009; **27**: 509-520 [PMID: 19074418 DOI: 10.1634/stemcells.2008-0600]

245 **Ylä-Outinen L**, Joki T, Varjola M, Skottman H, Narkilahti S. Three-dimensional growth matrix for human embryonic stem cell-derived neuronal cells. *J Tissue Eng Regen Med* 2014; **8**: 186-194 [PMID: 22611014 DOI: 10.1002/term.1512]

246 **Branch DW**, Corey JM, Weyhenmeyer JA, Brewer GJ, Wheeler BC. Microstamp patterns of biomolecules for high-resolution neuronal networks. *Med Biol Eng Comput* 1998; **36**: 135-141 [PMID: 9614762 DOI: 10.1007/bf02522871]

247 **Brunello CA**, Jokinen V, Sakha P, Terazono H, Nomura F, Kaneko T, Lauri SE, Franssila S, Rivera C, Yasuda K, Huttunen HJ. Microtechnologies to fuel neurobiological research with nanometer precision. *J Nanobiotechnology* 2013; **11**: 11 [PMID: 23575365 DOI: 10.1186/1477-3155-11-11]

248 **Lamba DA**, Karl MO, Ware CB, Reh TA. Efficient generation of retinal progenitor cells from human embryonic stem cells. *Proc Natl Acad Sci USA* 2006; **103**: 12769-12774 [PMID: 16908856 DOI: 10.1073/pnas.0601990103]

249 **Mellough CB**, Sernagor E, Moreno-Gimeno I, Steel DH, Lako M. Efficient stage-specific differentiation of human pluripotent stem cells toward retinal photoreceptor cells. *Stem Cells* 2012; **30**: 673-686 [PMID: 22267304 DOI: 10.1002/stem.1037]

250 **Meyer JS**, Howden SE, Wallace KA, Verhoeven AD, Wright LS, Capowski EE, Pinilla I, Martin JM, Tian S, Stewart R, Pattnaik B, Thomson JA, Gamm DM. Optic vesicle-like structures derived from human pluripotent stem cells facilitate a customized approach to retinal disease treatment. *Stem Cells* 2011; **29**: 1206-1218 [PMID: 21678528 DOI: 10.1002/stem.674]

251 **Karus M**, Blaess S, Brüstle O. Self-organization of neural tissue architectures from pluripotent stem cells. *J Comp Neurol* 2014; **522**: 2831-2844 [PMID: 24737617 DOI: 10.1002/cne.23608]

252 **Lancaster MA**, Renner M, Martin CA, Wenzel D, Bicknell LS, Hurles ME, Homfray T, Penninger JM, Jackson AP, Knoblich JA. Cerebral organoids model human brain development and microcephaly. *Nature* 2013; **501**: 373-379 [PMID: 23995685 DOI: 10.1038/nature12517]

253 **Kadoshima T**, Sakaguchi H, Nakano T, Soen M, Ando S, Eiraku M, Sasai Y. Self-organization of axial polarity, inside-out layer pattern, and species-specific progenitor dynamics in human ES cell-derived neocortex. *Proc Natl Acad Sci USA* 2013; **110**: 20284-20289 [PMID: 24277810 DOI: 10.1073/pnas.1315710110]

254 **Vazin T**, Becker KG, Chen J, Spivak CE, Lupica CR, Zhang Y, Worden L, Freed WJ. A novel combination of factors, termed SPIE, which promotes dopaminergic neuron differentiation from human embryonic stem cells. *PLoS One* 2009; **4**: e6606 [PMID: 19672298 DOI: 10.1371/journal.pone.0006606]

255 **Chung S**, Moon JI, Leung A, Aldrich D, Lukianov S, Kitayama Y, Park S, Li Y, Bolshakov VY, Lamonerie T, Kim KS. ES cell-derived renewable and functional midbrain dopaminergic progenitors. *Proc Natl Acad Sci USA* 2011; **108**: 9703-9708 [PMID: 21606375 DOI: 10.1073/pnas.1016443108]

256 **Guo X**, Johe K, Molnar P, Davis H, Hickman J. Characterization of a human fetal spinal cord stem cell line, NSI-566RSC, and its induction to functional motoneurons. *J Tissue Eng Regen Med* 2010; **4**: 181-193 [PMID: 19950213 DOI: 10.1002/term.223]

P- Reviewer: Sarkadi B **S- Editor**: Tian YL
L- Editor: A **E- Editor**: Liu SQ

World Journal of Stem Cells

Submit a Manuscript: http://www.wjgnet.com/esps/
Help Desk: http://www.wjgnet.com/esps/helpdesk.aspx
DOI: 10.4252/wjsc.v7.i6.922

World J Stem Cells 2015 July 26; 7(6): 922-944
ISSN 1948-0210 (online)

REVIEW

Stem cell autotomy and niche interaction in different systems

David C Dorn, August Dorn

David C Dorn, Department of Hematology, Hemostasis, Oncology, and Stem Cell Transplantation, Hannover Medical School, 30625 Hannover, Germany

August Dorn, Institute of Zoology, Johannes Gutenberg University, 55099 Mainz, Germany

Author contributions: Dorn DC and Dorn A contributed to this paper.

Conflict-of-interest statement: David C Dorn has not received fees for serving as a speaker. David C Dorn has only received research funding from the state and his home institution. David C Dorn is solely an employee of his home institution. David C Dorn owns no stocks and/or shares. David C Dorn owns patents to: (1) Synthesis of epothilones, intermediates thereto, analogues and uses thereof, patent number: 7384964; (2) Migrastatin analogs in the treatment of cancer, patent number: 8957056; (3) Isomigrastatin analogs in the treatment of cancer, patent number: 8188141.

Correspondence to: Dr. David C Dorn, MD, Department of Hematology, Hemostasis, Oncology, and Stem Cell Transplantation, Hannover Medical School, Carl-Neuberg-Straße 1, 30625 Hannover, Germany. ddorn_1999@yahoo.com
Telephone: +49-511-94085270
Fax: +49-511-5328041

Received: July 20, 2014
Peer-review started: July 20, 2014
First decision: October 14, 2014
Revised: March 30, 2015
Accepted: May 26, 2015
Article in press: May 27, 2015

Published online: July 26, 2015

Abstract

The best known cases of cell autotomy are the formation of erythrocytes and thrombocytes (platelets) from progenitor cells that reside in special niches. Recently, autotomy of stem cells and its enigmatic interaction with the niche has been reported from male germline stem cells (GSCs) in several insect species. First described in lepidopterans, the silkmoth, followed by the gipsy moth and consecutively in hemipterans, foremost the milkweed bug. In both, moths and the milkweed bug, GSCs form finger-like projections toward the niche, the apical cells (homologs of the hub cells in Drosophila). Whereas in the milkweed bug the projection terminals remain at the surface of the niche cells, in the gipsy moth they protrude deeply into the singular niche cell. In both cases, the projections undergo serial retrograde fragmentation with progressing signs of autophagy. In the gipsy moth, the autotomized vesicles are phagocytized and digested by the niche cell. In the milkweed bug the autotomized vesicles accumulate at the niche surface and disintegrate. Autotomy and sprouting of new projections appears to occur continuously. The significance of the GSC-niche interactions, however, remains enigmatic. Our concept on the signaling relationship between stem cell-niche in general and GSC and niche (hub cells and cyst stem cells) in particular has been greatly shaped by Drosophila melanogaster. In comparing the interactions of GSCs with their niche in Drosophila with those in species exhibiting GSC autotomy it is obvious that additional or alternative modes of stem cell-niche communication exist. Thus, essential signaling pathways, including niche-stem cell adhesion (E-cadherin) and the direction of asymmetrical GSC division - as they were found in Drosophila - can hardly be translated into the systems where GSC autotomy

was reported. It is shown here that the serial autotomy of GSC projections shows remarkable similarities with Wallerian axonal destruction, developmental axon pruning and dying-back degeneration in neurodegenerative diseases. Especially the hypothesis of an existing evolutionary conserved "autodestruction program" in axons that might also be active in GSC projections appears attractive. Investigations on the underlying signaling pathways have to be carried out. There are two other well known cases of programmed cell autotomy: the enucleation of erythroblasts in the process of erythrocyte maturation and the segregation of thousands of thrombocytes (platelets) from one megakaryocyte. Both progenitor cell types - erythroblasts and megakaryocytes - are associated with a niche in the bone marrow, erythroblasts with a macrophage, which they surround, and the megakaryocytes with the endothelial cells of sinusoids and their extracellular matrix. Although the regulatory mechanisms may be specific in each case, there is one aspect that connects all described processes of programmed cell autotomy and neuronal autodestruction: apoptotic pathways play always a prominent role. Studies on the role of male GSC autotomy in stem cell-niche interaction have just started but are expected to reveal hitherto unknown ways of signal exchange. Spermatogenesis in mammals advance our understanding of insect spermatogenesis. Mammal and insect spermatogenesis share some broad principles, but a comparison of the signaling pathways is difficult. We have intimate knowledge from Drosophila, but of almost no other insect, and we have only limited knowledge from mammals. The discovery of stem cell autotomy as part of the interaction with the niche promises new general insights into the complicated stem cell-niche interdependence.

Key words: Stem cell-niche interaction; Male germline stem cells; Spermatogenesis; Erythropoiesis; Stem cell autotomy; Thrombopoiesis

Core tip: A new mode of stem cell-niche interaction has been observed in insects. Male germline stem cells (GSCs) undergo autotomy by serial segregation of vesicles from finger-like projections. These vesicles either accumulate at the niche surface or are phagocytized by the niche cells. Autotomized projections are apparently replaced by newly sprouting ones. It is suggested that the unprecedented dynamics of GSC autotomy are involved in a not yet known form of information exchange between GSCs and niche. Apoptotic pathways and autodestruction programs could be involved in GSC autotomy.

Dorn DC, Dorn A. Stem cell autotomy and niche interaction in different systems. *World J Stem Cells* 2015; 7(6): 922-944 Available from: URL: http://www.wjgnet.com/1948-0210/full/v7/i6/922.htm DOI: http://dx.doi.org/10.4252/wjsc.v7.i6.922

EARLY OBSERVATIONS ON STEM CELL-NICHE RELATIONSHIPS PRIOR TO THE ESTABLISHMENT OF THE STEM CELL-NICHE HYPOTHESIS

When, in 1978, Schofield[1] put forward the hematopoietic stem cell (HSC)-"niche" hypothesis it was solely based on the assumed requirements the niche must fulfill, but he had no knowledge concerning the physical identity of the niche: "The location of the stem cell niche can, of course, only be a matter of speculation, although there are several items of data which suggest that they may well be in intimate association with the bone". It is astonishing how accurate some of his predictions turned out to be. However, up to date the HSC niche is not fully understood and is apparently composed of a variety of different cell types: osteogenic cells, endothelial cells, perivascular mesenchymal cells and adipocytes[2,3]. Recently, Chasis *et al*[4] pointed out that the first description of a hematopoietic niche actually took place 20 years earlier when, in 1958, Bessis[5] described erythroblastic islands. These represent microenvironmental niches for erythropoiesis. Erythroblasts, which represent oligopotent progenitors derived from a small population of HSCs, are arranged rosette-like around a reticular cell (macrophage) where they proliferate and differentiate (Figure 1A). Erythroblastic islands offer striking structural similarities with another significant model system for research on stem cell niche-interactions, the male germline stem cells (GSCs) and its niche in insects (Figure 1B).

Due to its anatomical simplicity and the advantageous genetic access, the male GSC-niche system of Drosophila proved as an invaluable tool to study stem cell-niche interactions on the molecular level[6]. In insects the GSC niche is located in the apex of testicular follicles and consists of the somatic apical cells (ACs) (called hub cells in Drosophila) and the cyst stem cells (CySCs). As in the case of the erythroblastic islands, apical complexes were described long before Drosophila became the model system. Figure 2 demonstrates the testicular GSC-niche complex of butterflies published in 1889 by Verson[7] and in 1911 by Zick[8], respectively (The first record of apical complexes stems from Spichardt[9] published in 1886 from studies on butterflies). The drawings in Figure 2, based on light microscopical observations, indicate intricate physical relationships between AC and GSCs which could not be clearly resolved with the techniques available at that time. It is remarkable that several of the early investigators already suggested that the ACs might regulate the fate of the GSCs: Zick[8] in 1911 believed that the spermatogonial pathway could only be entered after detachment of the germ cells from the AC, and Buder[10] and Schneider[11] in 1915 postulated that ACs release an inhibitory factor which prevents the differentiation of GSCs into spermatogonia; Nelsen[12] in 1931 considered the ACs as an activation center which controls the mitotic activity

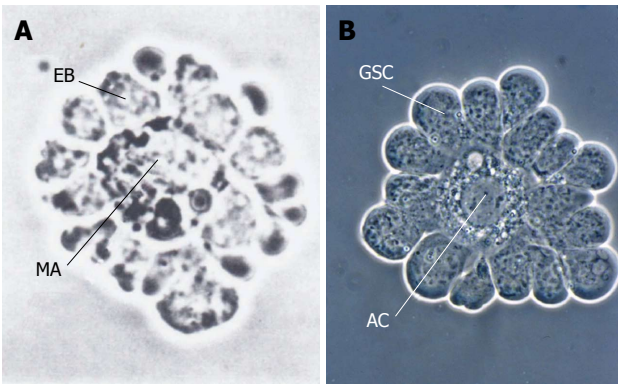

Figure 1 Simple systems of the stem cell/progenitor-niche interaction: isolated erythroblastic island and isolated apical complex from an insect exhibit strong resemblances. A: Erythroblastic island from dissociated rat bone marrow. A corona of erythroblasts (EB) has extensive cell-cell contact with their niche, the central macrophage (MA) (from Bessis *et al*[93] with kind permission of Springer Verlag, Berlin, Heidelberg); B: Isolated testicular apical complex from Locusta migratoria. Germline stem cells (GSC) surround the apical cell (AC), which represents the niche (besides the peripheral cyst stem cells, which were removed) (From Dorn *et al*[64]).

of the GSCs. Thus, main characteristics of a niche were already hypothesized at the beginning of cell research. Since the early investigations on butterfly apical complexes developmental studies have ascertained the identity of GSCs and the role of ACs as their niche (together with CySCs). Electron microscopic studies revealed complex physical interactions between ACs and stem cells which points to a hitherto not elucidated communication between these cells. Figure 3D demonstrates the complicated structure of lepidopteran apical complexes. In fact, enigmatic physical relationships between male GSCs and their niche have been observed in a number of insect species. One of the most astonishing phenomenons is the controlled autotomy of GSC projections which are directed toward the ACs. Examples of these cases are examined for their functional significance in this review. They are compared with other stem cell-niche systems where cell autotomy takes place, such as enucleation of erythroblasts and megakaryocyte fragmentation are discussed in respect to the suggested "autodestruction program" of neurons.

GSC-NICHE INTERACTION IN THE TESTIS OF THE MODEL INSECT DROSOPHILA MELANOGASTER

The testis of Drosophila has become one of the most successful models for the exploration of molecular stem cell-niche interaction. Comprehensive reviews on this matter have been published recently[13,14]. A summary of the structural and molecular relationships within the apical complex of Drosophila is presented here and compared with observations in other insects.

Figure 3A shows the apex of a testicular follicle of Drosophila. A longitudinal section of the testicular follicle shows the three cell types that constitute the germinal proliferation center. A small cluster of somatic cells, the hub cells (*i.e.*, ACs), is located in the follicular apex (the hub). Hub cells, together with CySCs, represent the niche for the row of bordering GSCs. Except for the region where hub cells and GSCs contact one another; each GSC is embraced by a pair of CySCs whose tips also contact the hub cells. CySCs are of somatic origin and, besides their niche function for GSCs, represent stem cells that generate the cyst cells by asymmetrical division. Hub cells only function as the CySC niche. Prior to an asymmetric division of a GSC (which produces a gonialblast that is directed toward the periphery of the apical complex and a daughter GSC that remains in contact with the niche) its two associated CySCs undergo a synchronized division resulting in a pair of daughter cells which encloses the forming gonialblast and becomes the cyst wall. The two cyst cells forming the wall no longer divide during subsequent spermatogenesis although the cysts enlarge considerably.

The fate of GSCs - maintenance, self-renewal (asymmetric and symmetric division), frequency of mitotic activity - is orchestrated by a multitude of factors and processes: (1) Short-range signaling between niche and GSCs. This was the first factor to be elucidated and proved to be exemplary for other stem cell-niche systems; (2) Niche-stem cell adhesion. Adherens junctions were found to play a crucial role in the regulation of signaling and asymmetric GSC division in addition to its physical adhesion function; (3) Cell intrinsic regulation. This has more recently come into focus; and (4) Systemic regulation. This may affect all aspects of niche-stem cell interaction, but is to date the least understood.

Short-range signaling

GSC maintenance and self-renewal are supported by a wide range of signals from the hub. The cytokine ligand unpaired (Upd), secreted by the hub cells activates Janus kinase-signal transducer and activator of transcription (JAK/STAT) signaling in GSCs and CySCs[15,16]. Gonialblast differentiation is caused by lower levels of Upd. In aging flies the number of GSCs and their proliferation rate declines in correlation with declining Upd levels in the hub cells. Upd secreted by hub cells also activates the JAK/STAT signaling in CySCs. Whereas JAK/STAT activation is sufficient for CySC maintenance and self-renewal, GSC self-renewal requires additional signals. Hub cells and CySCs both secrete glass bottom boat (Gbb) and decapentaplegic (Dpp). Both ligands activate the bone morphogenetic protein (BMP) signaling pathway in GSCs. BMP represses the transcription of the differentiation factor bag of marbles (Bam). Thus inhibition of differentiation to gonialblasts contributes to GSC self-renewal[17,18]. Hub cells also produce the ligand Hedgehog (Hh) that supports the self-renewal of CySCs in addition to JAK/STAT activation. GSC maintenance does not require Hh signaling[19,20]. Gbb and Dpp produced from CySCs contribute to the activation of BMP

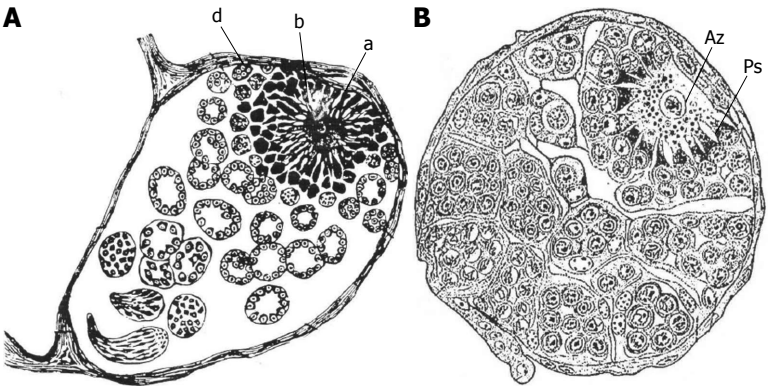

Figure 2 Early histological studies on testicular follicles in butterflies (Lepidoptera) that depict the complex structures of the apical complexes. A: Testicular follicle of the silkmoth *Bombyx mori* which includes the apical complex (a, b, d). The limited light microscopical resolution caused some misinterpretation concerning the identity of cell types: the central apical cell (a) was considered to be a "germ cell" ("Keimzelle") with radial extensions. The germline stem cells were described as clumps of protoplasm with nuclei (b, d) (from Verson[7]); B: Testicular follicle of the cabbage white butterfly *Pieris brassicae*. The relationship between apical cell (Az) (also called Verson cell) and germline stem cells (Ps) is correctly described: The germline stem cells send projections toward the apical cell and their tips penetrate the apical cell. A layer of cells surround the germline stem cells, the cyst stem cell which, however, were not identified as such (from Zick[8]).

in GSCs (besides Gbb and Dpp signaling from the hub cells)[18]. They are conceivably activated by STAT and/or zinc-finger homeodomain protein 1 which is targeted by STAT as is chinmo (chronologically inappropriate morphogenesis)[21,22] (Figure 4).

Niche-stem cell adhesion, adherens junctions, E-cadherin

GSCs and CySCs are both connected with hub cells *via* adherens junctions[23]. Hub cell-GSC connection plays are crucial role in GSC behavior. Tight contact of the GSCs with hub cells is correlated with high levels of E-cadherin and β-catenin at the interface (adherens junctions). Accumulation of both proteins at the interface is dependent upon guanine nucleotide exchange factor 26 (Gef26) for the Rap GTPase (Rap0-GEF)[24]. The intracellular domains of the cadherin molecules interact with cytoskeleton-associated proteins. JAK/STAT signaling is required in GSCs to maintain E-cadherin expression, niche anchorage and self-renewal and in CySCs to control BMP expression[25]. In addition, the leukocyte-antigen-related-like receptor tyrosine phosphatase has been proposed to regulate the attachment of GSCs to the hub cells[26]. It is responsible for the proper localization of tumor suppressor Adenomatous polyposis coli 2 (Apc2) and E-cadherin and the proper orientation of centrosomes in GSCs[23]. The BMP receptor complexes are localized to E-cadherin rich adherens junctions at the stem cell-niche junction, which might help restrict BMP signaling activity to the GSC niche interface[27]. Localized BMP signaling might be also affected by BMP signaling modulators that accumulate in the extracellular matrix such as the protein Magu (known to be involved in life span extension and late age female fecundity) which is transcribed in hub cells[28] and the heparin sulfate proteoglycans Dally (division abnormally delayed) and Dally-like[29]. Recently it was demonstrated that the actin-binding protein profilin is required cell autonomously to maintain GSCs, possibly facilitating localization or maintenance of E-cadherin to the GSC-hub cell interface[30].

The age dependent loss of GSC is accompanied by a decline in E-cadherin expression. Increased E-cadherin expression slows down GSC loss[31].

E-cadherin is also required in CySCs to maintain their adhesion to the hub. In addition, integrin-mediated adhesion exists between the hub and CySCs, and is limited by a negative regulator of STAT signaling[32].

Integrins: In the Drosophila testis, competition exists between GSCs and CySCs and among CySCs themselves for occupancy of the hub[33]. Interestingly, the CySCs with higher JAK/STAT signaling activity, which can be achieved experimentally by removing the function of the JAK/STAT negative regulator SOCS36E, can outcompete normal CySCs and can also push GSCs out of their niche. This JAK/STAT-regulated stem cell competition is dependent on the cell adhesion protein βPS integrin, but not E-cadherin. Integrin-mediated cell competition is thus thought to play a crucial role in balancing two stem cell populations in the same niche[33]. Integrins are also required for positioning the hub in the apical testis tip, but are dispensable for GSC or CySC anchorage to the niche[34]. The extracellular domains of integrins can bind directly to extracellular matrix (ECM) proteins, such as laminin, but there is no ECM between hub cells, GSCs and CySCs.

Gap junctions: The gap junction protein zero population growth is required for GSC maintenance and differentiation in Drosophila testes[35]. But it remains to be seen whether the function of gap junctions in the regulation of stem cell maintenance derives from their adhesion role, intercellular molecular transfer or electrical communication.

Cell intrinsic factors, hub cells

Upd levels in hub cells are regulated by IGF-Ⅱ mRNA

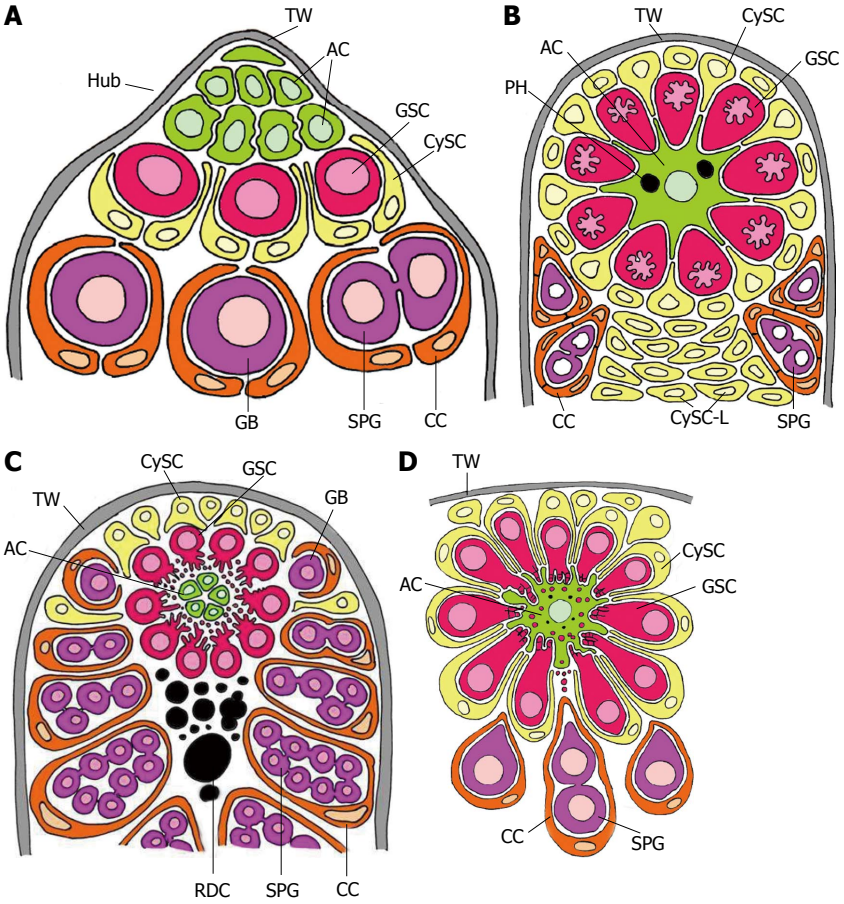

Figure 3 Schematized longitudinal sections through the apices of testicular follicles of four insect species. The order of the images from (A) to (D) is arranged according to increasing complexity of the structural relationships between germline stem cells (GSCs) and their niche. It should be noted that the order is not in congruence with the positions of the species in the natural insect system based on evolutionary progress. A: *Drosophila melanogaster*. The ACs (hub cells) are located in a small terminal appendix of the follicle, the hub (HUB), where many of them border the testicular wall (TW). (The testicular wall consists of an outer pigment layer resting on a basal lamina and a muscle cell layer sitting on an inner basal lamina.) The testicular wall does not provide a hemolymph-testis barrier. A spermatogonial is constituted by two CCs which protect the spermatogonia against hemolymph. Both GSCs and CySCs contact ACs (Adapted from Hardy *et al*[61]); B: *Locusta migratoria*. Depicted is the rosette-like arrangement of GSCs and CySCs with the single AC in the center. The AC of this example includes two phagocytized GSCs (see above). Besides GSCs also CySCs contact extensions of the star-like AC. A plug of CySC-like cells (CySC-L) is located below the apical rosette. The wall of the spermatogonial cysts is composed of numerous CCs (Adapted from Szöllösi *et al*[154] and Dorn *et al*[64]); C: *Oncopeltus fasciatus*. The cellular extensions of GSCs and segregated vesicles surround the surface of ACs. CySCs cover only the distal part of the apical rosette; they do not make contacts with the ACs. Proximal to the rosette, remnants of degraded GSCs and probably young cysts amass (RDC). Cysts form at the lateral parts of the rosette (Adapted from Schmidt *et al*[65]); D: *Lymantria dispar*. Note that the cellular extensions of GSCs protrude into the large singular AC. The extensions autotomize and the segregated vesicles are phagocytized by the AC. Each GSC is affiliated with one CySC. During early larval development the AC is attached to the TW [comparable to the situation in Drosophila, where ACs (*i.e.*, hub cells) are lifelong attached to the TW], but separates with progressing development. The apical complex then adopts a spherical organization. (Adapted from Klein[66]). AC: Apical cell (often called hub cell in Drosophila) (green); CC: Cyst cell (orange); CySC: Cyst stem cell (yellow); GB: Gonialblast (purple); GSC: Germline stem cell (red); SPG: Spermatogonia (purple); TW: Testicular wall (grey).

binding protein (Imp) that binds to upd mRNA and protects it from degradation caused by short interfering RNAs. Imp itself is repressed by let-7 microRNA (miRNA) that is expressed at higher levels in aging male GSCs[36]. epidermal growth factor (EGF) signaling negatively regulates GSC division frequency in adults, but not in larvae, and promotes gonialblast differentiation and enclosure of germ cells by somatic cyst cells. Stg (string, a Cdc 25 homolog-phosphatase) is essential for activating cyclin-dependent kinases and promoting the cell cycle and is therefore required for proliferation and maintenance of GSCs and CySCs. The transcriptional regulator lola (longitudinals lacking) is cell autonomously required for GSC (and CySC) maintenance[37]. MiRNAs control the stem cell differentiation pathway by regulating Bam[38]. Recently, the impact of epigenetic factors on male GSCs has been analyzed. Nucleosome remodeling factor promotes STAT expression while repressing Bam thus contributing to the maintenance of GSCs[39]. Additionally chromatin-associated proteins, such as no child left behind and PHD finger protein 7 are necessary for GSC maintenance[40,41]. CySCs. JAK/STAT signaling in CySCs is suppressed by suppressor of cytokine signaling at 36E (Socs36E) which may harmonize self-renewal of CySCs with that of GSCs[33,42]. Ken (ken and barbie, a transcriptional repressor) also promotes CySC identity[43]. Restriction of proliferation and maintenance of CySC identity are affected by polycomb repressive complex 1 genes posterior sex combs and suppressor of zeste two [Su(z)2][44].

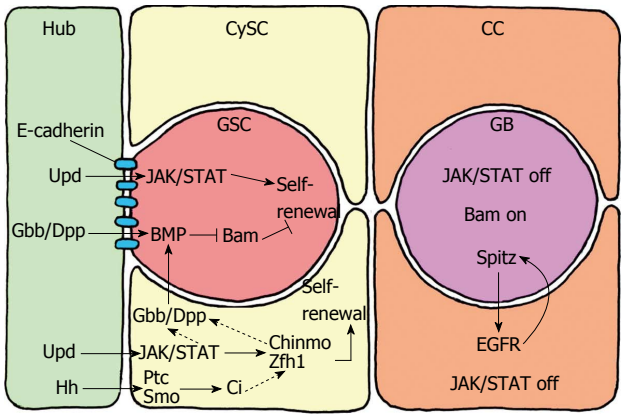

Figure 4 Short range signalling between the germline stem cells and their niche, which consists of the hub cells and the cyst stem cells. The hub cells secrete the ligand Upd, which activates JAK/STAT signalling in GSCs and CySCs. Whereas JAK/STAT activation is sufficient for CySC maintenance and self-renewal, GSC self-renewal requires additional signals. Hub cells and CySCs secrete the ligands Gbb and Dpp, which activate BMP in GSCs. BMP suppresses the transcription of Bam that inhibits the differentiation of GSCs to gonialblasts. BMP activation in GSCs is also supports by Gbb and Dpp produced by the CySCs. Gbb and Dpp in CySCs are conceivably activated by STAT and/or Zfh1 and Chinmo. Hub cells also secrete the ligand Hh (hedge hog), which supports CySC self-renewal in addition to, but independently of, JAK/STAT activity. Hh binds to the transmembrane receptor PTC (patched) of CySC, which releases Smo (smoothened) from repression. This leads to the activation of the transcription factor Ci (cubitus interruptus), which activates the transcription of target genes that support maintenance and self-renewal of CySCs besides JAK/STAT activity. The Hh signalling pathway in CySCs may also affect Zfh1 and, *via* Gbb/Dpp, influence BMP signalling in GSCs. Thus, Hh signalling in the testis niche apparently has a dual role. CC: Cyst cell; GSCs: Germline stem cells; CySCs: Cyst stem cells.

The histone variant His2Av and the ATP-dependent chromatin-remodeling factor Domino are also required for GSC and CySC maintenance. Furthermore, in a recent review Zoller *et al*[45] listed about 50 genes that were found (or expected) to be involved in the direction of CySC specification, CySC self-renewing divisions, cyst cell differentiation, and soma-germline interactions.

Systemic factors

Numerous environmental factors, such as changing seasons or periods of drought and rain, nutritional conditions (irregular food availability or starvation), injury or illness all affect tissue homeostasis. As a consequence niche and stem cell activity must be adapted to these changing demands. This is primarily accomplished *via* systemic factors that may influence any of the regulatory entities of the stem cell-niche complex.

Best known is the support of GSCs maintenance by insulin signaling[46,47]. The source of some insulin-like peptides is the brain others are synthesized in the fat body and other tissues probably including the GSCs themselves. Effects of the nutritional status on GSC maintenance are apparently exerted by insulin signaling pathway[48]. In the Drosophila female it has been shown that the nutrient-sensing insulin/FOXO signaling directly controls Notch activation in the GSC niche which maintains the niche and GSC identity[49]. In maintaining embryonic stem cell pluripotency and the modulation of adult stem cell quiescence nutrient-sensing pathways play an important role. They maintain energy production by inhibition and stimulation of crucial processes like oxidative phosphorylation and glycolysis. "This interplay is key to the maintenance of stem-ness"[50].

Recently it has been found that day-night cycles and alterations in sleep can influence the daily dynamics of GSC divisions in male Drosophila[51]. The GSC division rate increases, when the sleep-promoting factor, Sleepless, is lacking. This is mediated, in part, by the GABAergic signaling pathway.

A systemic signal that presumably plays a decisive role in testis development and spermatogenesis is the steroid hormone ecdysone[52]. It is synthesized in testicular tissue of many insects: *Heliothis virescens*[53], *Lymantria dispar*[54], *Ostrinia nubilalis*[55], *Spodoptera littoralis*[56], *Melanoplus sanguinipes*[57]. However, its significance in the regulation of male GSC proliferation and self-renewal in Drosophila is not known.

Ecdysteroids play a role in female GSC regulation in Drosophila. Ecdysteroids are synthesized by developing follicles of ovarioles and regulate directly GSC maintenance, proliferation and self-renewal. Ecdysteroids interact with the intrinsic epigenetic factor ISWI, a chromatin remodeling factor[58]. The survival of ecdysone-producing follicles of ovarioles depends on the availability of food which points to an interaction of the hormonal with the nutrient-sensing signaling pathways[59].

INCREASING COMPLEXITY OF STRUCTURAL RELATIONSHIPS BETWEEN MALE GSCS AND THEIR NICHE IN DIFFERENT INSECT SPECIES: DROSOPHILA MELANOGASTER, LOCUSTA MIGRATORIA, ONCOPELTUS FASCIATUS, LYMANTRIA DISPAR, AND THE CASE OF LAMPYRIS NOCTILUCA

Insects with their long evolutionary history may be expected to present great variations on a theme, in this case the organization of GSCs and their niche. And in deed, the Figure 3 exhibits an increasing complication of the physical interactions of the cells of the apical complex. However, the complexity of the structures is not correlated with the systematic position of a given species. In fact, whereas the hemipteran *Oncopeltus fasciatus* (Figure 3C) shows an astonishingly irregular and dynamic anatomy of GSCs[60], another hemipteran, *Corizus hyoscyami*, has a relatively "simple" apical complex which harbors only one small AC, sparsely equipped with cell organelles, surrounded by a corona of pear-shaped GSCs (Klein personal communication). Nonetheless, it appears self-evident that the enigmatic structures expressed especially in the GSCs of *Oncopeltus fasciatus* and the lepidopteran *Lymantria dispar* (Figure 3D) - as well as in many other lepidopterans (Figure 2) - have a

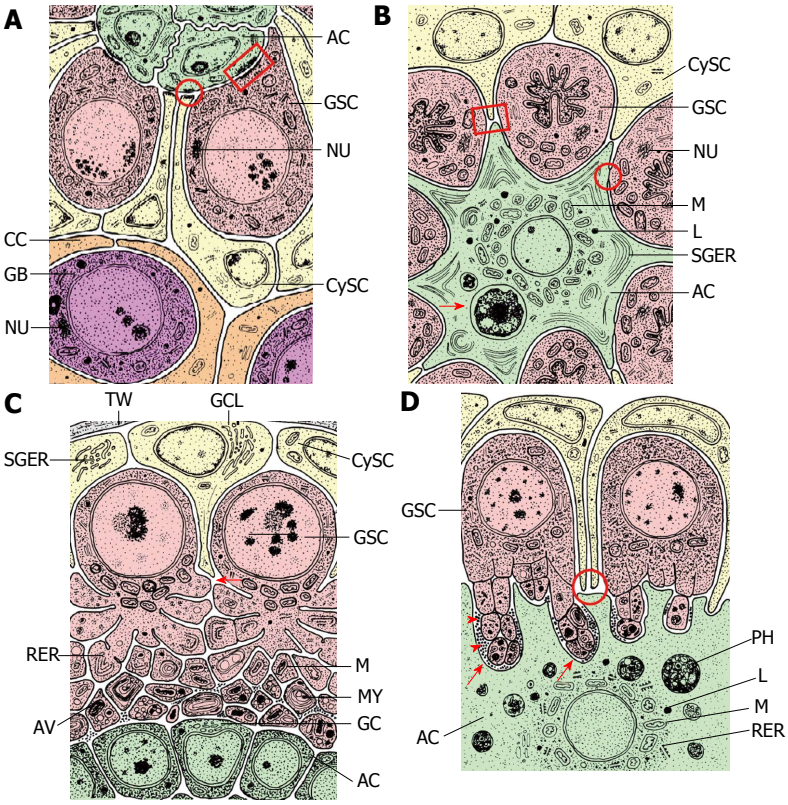

Figure 5 Fine structural organization (schematized) of the apical complexes (longitudinal sections) of four insect species. The order (A) to (D) is arranged according to the order in Figure 3. A: *Drosophila melanogaster*. ACs are "light" and interdigitate richly between themselves. Their organelle equipment is scarce. GSCs are "dark" due to many free ribosomes and characterized by "spongy bodies" which may represent nuage. Adherens junctions are expressed between ACs and GSCs (marked by a rectangle) and between ACs and CySCs (encircled). CySCs are "light" and include few cell organelles (Adapted from Hardy *et al*[61]); B: *Locusta migratoria*. The single apical cell of an apical complex is "light" and harbors a complex organelle equipment: in particular a ring of mitochondria (M) and lysosomes (L) around the nucleus, and stacks of sparsely granulated endoplasmic reticulum (SGER) at the cell periphery. Arrow marks a phagocytized and partly lysed GSC. ACs and GSCs are connected by gap-like junctions (encircled). The "dark" GSCs include extremely irregularly shaped nuclei and nuage-like material (NU). Extensions of the "light" CySCs reach to extensions of the star-shaped AC (marked by square) (Adapted from Dorn *et al*[64]); C: *Oncopeltus fasciatus*. The ACs are rather small and very "dark". Cell organelles are inconspicuous besides Golgi complexes (GC) that face bordering GSC vesicles. The "dark" GSCs form cytoplasmic projections toward the ACs that undergo progressing autotomy. In the course of vesicle segregation rough endoplasmic reticulum (RER) and mitochondria (M) increase. Later autophagic vacuoles (AV) and myelin-like bodies (MY) are formed. Arrow points to a presumably newly sprouting cell projection. The "light" CySCs are characterized by extensive Golgi complex-like structures (GCL) that bare often associated with sparsely granulated endoplasmic reticulum (SGER) (Adapted from Dorn *et al*[60]); D: Lymantria dispar. The single AC of an apical complex is "light" and exhibits a spherical organization: mitochondria (M), lysosomes (L) and rough endoplasmic reticulum (RER) surround the nucleus: The cell periphery shows deep indentations caused by invading, autotomizing GSC projections (arrows). Segregated GSC vesicles are taken up by the AC, and phagosomes (PH) accumulate in the cytoplasm. The "dense" GSCs exhibit projection formation and projection autotomy that closely resembles that of Oncopeltus (see Figure 4C). GSC projections that indent the AC are often surrounded by extracellular granules (arrow heads). CySCs are "light", and thin extensions reach the surface of the GSCs (encircled) (Adapted from Klein[66]). AC: Apical cell (green); CC: Cyst cell (orange); CySC: Cyst stem cell (yellow); GB: Gonialblast (purple); GSC: Germline stem cell (red); TW: Testicular wall (grey); AV: Autophagic vacuole; GC: Golgi complex; GCL: Golgi complex-like stricture; L: Lysosomes; M: Mitochondrion; MY: Myelin-like body; NU: Nuage; PH: Phagosomes; RER: Rough endoplasmic reticulum; SGER: Sparsely granulated endoplasmic reticulum.

specific function (see below), in reverse to the principle: no function without structure. We will briefly describe the portrayed apical complexes and characterize the cell types.

Drosophila melanogaster

Figure 3A demonstrates the rather "ordinary" organization of the apical complex and Figure 5A the fine structural characteristics of its different components. The niche consists of 8-16 small hub cells, which richly interdigitate and are anchored to the testicular wall. They are characterized by a "light" appearance and scarcity of cell organelles. No mitoses were observed. The GSCs are, in contrast, rather "dark" due to many free ribosomes. They have a spheroidal shape but are flattened where they contact the hub cells. Their cytoplasm includes "spongy bodies"[61] which may represent nuage material that is typical for germ cells[62]. Mitoses of GSCs were rarely observed by the above authors, *i.e.*, one mitotic GSC in 50 GSCs. E-cadherin-mediated adherens junctions (Figure 4A) attach GSCs to hub sells[26]. The CySCs are rather "light" and have inconspicuous organelle equipment. They also form adherens junctions with GSCs (Figure 5A). Among the 76 CySCs observed by Hardy *et al*[61] only two were in mitosis.

Locusta migratoria

The longitudinal section through the follicular apex (Figure 3B) shows that the apical complex has the shape of a rosette with a singular AC in the center. The pear-shaped GSCs reach deeply into the large star-like AC.

The CySCs are irregularly arranged around the GSCs and it is not clear how many CySCs are affiliated with a GSC. The ACs touch the protrusions of the CySCs between the GSCs. Remarkably, a plug of CySC-like cells is located beneath the rosette formed by AC, GSCs and CySCs. The CySC-like cells presumably participate in the formation of the cyst wall which consists of a higher number of cyst cells, up to 7 were counted on serial sections[63].

In contrast to the hub cells in Drosophila the large AC of *Locusta* (also "light") shows a complex organelle equipment (Figure 5B). Around the large centrally located nucleus there is a broad ring of mitochondria that also includes lysosomal bodies. The periphery of the AC shows an abundance of sparsely granulated endoplasmic reticulum, often arranged in stacks and whorls that are also found in the cellular extensions that reach deeply between the basal parts of GSCs. The AC includes regularly one or two engulfed and more or less lysed GSCs (Figures 3B and 5B). The GSCs, "darker" than the ACs, show a polar organization. The nuclei are located in broader peripheral parts of the cells and present extremely irregular outlines. In the direction to the AC, mitochondria aggregate and fibrous nuage-like material is discernible. Free ribosomes are abundant. AC and GSCs form gap-like junctions (Figure 5B) but adherens junctions are not apparent[63]. No specific junctions seem to exist between CySCs and GSCs. CySCs and CySC-like cells have the same fine structural characteristics but only the CySCs contact the AC. Both cell types are rather "light". Their cytoplasm is scant and shows no specifications. In mature males, many dividing GSCs, CySCs and CySC-like cells can be observed[64]. Both, asymmetrical and symmetrical divisions occur at the same time. Sometimes whole clusters of these cells are seen in mitosis.

Oncopeltus fasciatus

The longitudinal section through the follicular apex of *Oncopeltus* (Figure 3C) reveals an organization of the apical complex similar to that of *Locusta* (Figure 3B), however, with important cytological differences of the different cell types. The niche is represented by a small cluster of "dark" cells with a relatively thin cytoplasmic lining. Small areas of the cytoplasm include a Golgi complex in continuation with some strands of smooth endoplasmic reticulum which is directed toward the periphery where GSCs are bordering (Figure 5C). Specialized cell-cell contacts were not seen[60]. The GSCs reveal an extraordinary structure and astonishing dynamics. The GSCs have a polar structure, with a lobular perikaryon oriented toward the CySCs and prominent cytoplasmic projections toward the ACs (Figure 5C), which are reminiscent of neurons. The projections exhibit trabecular or septum-like ingrowths that are most advanced at their tips, next to the ACs. The process results in the segregation of free vesicles that amass around the niche. During the autotomy of the projection terminals, the number of mitochondria increases in these segments, lysosomal bodies and autophagic vacuole-like vesicles become abundant and rough endoplasmic reticulum is often arranged in whorls (Figure 5C). Degradation processes proceed, indicated by the presence of acid phosphatase and TPPase, resulting in myelin - and autophagosome-like bodies[60]. Autotomized vesicles aggregate at the surface of the ACs (Figure 6A). They finally rupture and release their content in the vicinity of the ACs. None of the debris is taken up by the ACs. Remarkably, intact-looking cytoplasm contains free ribosomes grouped in clusters. These clusters break up in slightly advanced stages of autotomy and the ribosomes are then evenly distributed. It is suggested that they give rise to electron dense granules of about 25 nm in diameter. These grana are sometimes enclosed in projection terminals; grana of lesser diameter occur free in the extracellular space between projection terminals and ACs (Figure 6A). This is of special interest, since morphologically similar grana were reported to be present at the same location in a number of apical complexes of different insect species (see *Lymantria dispar*, below). It is not clear whether or not these grana are taken up by ACs. After advanced autotomy of GSC projections new projections sprout at the "neck" of GSCs, where the projections arise from the perikaryon (Figure 5C). In this "neck" area of the cell there is an accumulation of mitochondria. CySCs surround only the apical part of the apical complex (Figure 3C). The ratio CySCs:GSCs is roughly 1:1, and only one cyst cell grows around a gonialblast. The cyst cell does not divide any more after its generation by division of a CySC but becomes highly polyploid as it enlarges during spermatogenesis[60]. Divisions of GSCs and CySCs are rarely observed. Asymmetrical divisions of GSCs, where the spindle axis is oriented perpendicularly to the niche, were never observed. During symmetrical GSC divisions, the cell projections are persistent. In the process of gonialblast formation one of the GSCs, that shows no structural difference to the remaining GSCs, moves away from the niche toward the periphery. It loses its projections as the cyst cell encloses it. The spermatogonial cysts now move proximally. Cyst cells, which are rather "light", like the CySCs, develop striking organelles, composed of multiple complexes consisting of a meshwork of branching and anastomosing tubules and budding off vesicles which partly enclose electron-dense material. The Golgi complex-like structures (about 2.8 μm long and 1.1 μm in diameter) are often associated with sparsely granulated endoplasmic reticulum. The mitochondria are exceptionally long and branched. Cyst cells take up apoptotic spermatogonia[65]. Follicular apices include regularly extensive clusters of degenerating GSCs and spermatogonia (Figure 3C).

Lymantria dispar

The niche of the apical complex consists of only one large AC (Figure 3D).The shape of the apical complex changes during development. During the first three larval stages the AC is attached to the envelope of the follicular apex,

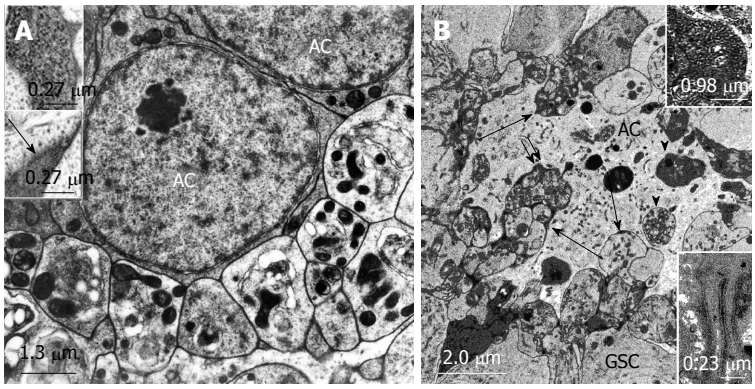

Figure 6 Structural relationships between apical cells and projections and autotomized vesicles of germline stem cells in *Oncopeltus fasciatus* and Lymantria dispar. A: Electron micrographs. *Oncopeltus fasciatus*. Vesicles that are segregated from GSC projections accumulate at the surface of ACs. The vesicles show signs of degeneration. Mitochondria are abundant and appear electron dense. (From Schmidt *et al*[65]). Upper inset: Intracellular granules in autotomizing GSC projections. Lower inset: Extracellular granules (arrow) between autotomizing GSC projections; B: Electron micrograph. *Lymantria dispar*. Numerous autotomized GSC projections protrude deeply into the AC (long arrows). Some of the segregated vesicles were apparently taken up by the AC and are being digested (arrow heads). Double arrow points to extracellular granules between GSC vesicles and the AC. Upper inset: Extracellular granules at higher magnification. Lower inset: Tubular indentations into the AC include electron dense material. (From Klein[66]). GSCs: Germline stem cells; AC: Apical cell.

and only the distal part of it is contacted by GSCs[66]. From third to forth larval stage the AC detaches from the follicle envelope and moves somewhat distally. Then it adopts a concentric organization, and the GSCs attach from all sides (Figure 6A). Each GSC is accompanied by one CySC whose perikaryon covers the peripheral part of the GSC and sends delicate projections to the AC, separating neighboring GSCs. Whereas the symmetry of the apical complex changes during larval development (from bipolar to rotationally symmetrical), the intricate relationships between AC and GSCs are largely similar until the pupal stage when signs of senescence become apparent and cyst formation seizes[66].

The large, "light" AC includes a centrally located nucleus around which the cell organelles are concentrically arranged (at progressed developmental stages) (Figure 5D). Mitochondria, rough endoplasmic reticulum and lysosomes are especially abundant. As a rule the cell contains phagosomes, exceedingly numerous during early larval stages, with cell fragments of variable degree of degradation (Figure 5D and 6B). The periphery of the AC shows many Golgi complexes. The pear-shaped GSCs are "darker" than the AC apparently due to the presence of many free ribosomes. Striking are the cell projections of GSCs that deeply invade the AC. Similar to the GSC projections in *Oncopeltus*, GSC projections of *Lymantria* autotomize. But, unlike to *Oncopeltus*, the separated vesicles are phagocytized by the AC (Figure 6B). The GSC projections contain whirls of rough endoplasmic reticulum, many free ribosomes, mitochondria and multivesicular bodies. Phagosomes of the AC include similar cell organelles before they are digested indicating their origin from GSC projections. The electron micrograph Figure 6B demonstrates the extremely complex interactions between GSCs and AC. Extracellular space between GSC projections and AC regularly contains electron dense granules of 25-38 nm in diameter (Figure 6B inset 1). Tubular invaginations of the AC also contain electron dense material which often exhibits a fibrillar consistency (Figure 6B). A relationship with the dense granules is unclear. The large nucleus of the GSCs is located in the peripheral part of the cells. The organelles in the perinuclear cytoplasm are inconspicuous. Symmetrical as well as asymmetrical divisions have been observed (see below). CySCs are "light". They divide apparently prior to the associated GSC[66].

Lampyris noctiluca

The glowworm represents a special case in as far as no niche cells (ACs) for the GSCs could be identified[67]. During early larval stages the gonadal follicles only include ("dark") GSCs but no ACs and no CySCs; male and female gonads can not be differentiated. The onset of testis differentiation is marked by the appearance of "light" cyst progenitor cells (CPCs) segregated from the apical part of the follicle wall[67,68]. Whereas a cluster of theses cells is located and multiplies in the apex of the follicle, a cluster of dividing GSCs is located at the basal part of the follicle. The ratio of GSCs/CPCs is about 1/1. At that stage of development there are no associations between individual GSCs and individual CPCs. ACs are never observed. In later larval development, CPCs form cell projections, move toward and between the germ cells, which now may represent gonialblasts, contact and ensheathe them, thus forming spermatogonial cysts[67]. During transformation from CPCs to cyst cells, the cells develop conspicuous stacks and whorls of smooth endoplasmic reticulum. It was speculated that the cyst cells may produce hormones, *i.e.*, juvenile hormone or ecdysone. Since all GSCs/gonialblasts and CPCs engage in cyst formation at approximately the same time, a precise temporal regulation of GSC division and gonialblast differentiation seems obsolete and the function of a niche therefore not necessary. The absence of ACs has also been reported from several other insect species[69].

In summary primarily electron microscopic studies

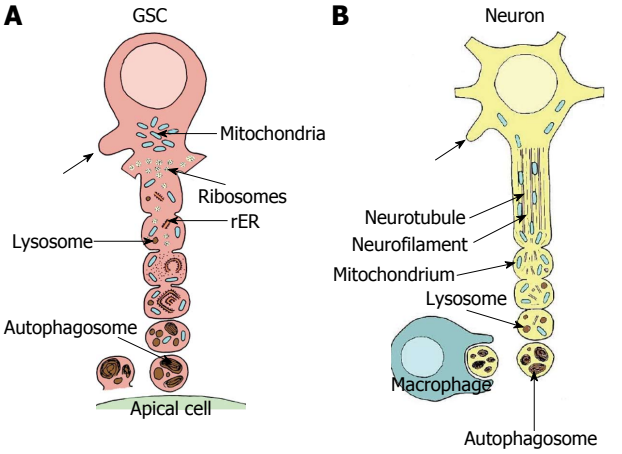

Figure 7 Comparison of autotomizing germline stem cell projection with autodestruction of an injured axon. A: Sequence of vesicle formation of a GSC projection in *Oncopeltus fasciatus*. The area of projection formation is characterized by an accumulation of mitochondria (blue). At the base of the projection ribosomes form small clusters (yellow), mitochondria are infrequent. Rough endoplasmic reticulum (rER, orange) and lysosomes (brown) are scarce. With progressing vesicle segregation mitochondria become more frequent and swollen, ribosomes form no longer clusters, rER becomes more prominent and lysosomal bodies increase. Segregated vesicles show many autophagosomes and myelin bodies. They accumulate at the surface of the apical cells (green) and disintegrate. Arrows point to newly sprouting projections (adapted from Dorn *et al*[60]); B: Sequence of progressive axonal fragmentation after injury. First neurotubules and neurofilaments break down. Then mitochondria accumulate and lysosomes (brown) become more abundant. Finally vesicles which mainly includ autophagosomes and myelin bodies are segregated and taken up by macrophages. Arrows points to newly sprouting axon (adapted from Lingor *et al*[155]; Beirowski *et al*[156]; Kerschensteiner *et al*[157]). GSC: Germline stem cell.

revealed the enigmatic relationship between GSCs and their niche in numerous insects. Identification of the different cell types and their interactions were facilitated by the profound differences in electron density between the components of the apical complex: GSCs, ACs and CySCs. In almost all species studied, the ACs and the CySCs were "light" and the GSCs "dark". *Oncopeltus* is an exception: here, ACs are "very dark" whereas GSCs are "dark" and the CySCs "light". But, whereas the "light" and "dark" marking facilitates identification of the cell types, the functional significance of these characteristics remains unclear. In contrast, the intriguing processes of GSC autotomy and the interaction of autotomized GSC vesicles with niche cells (ACs) point to a to date unknown form of communication between GSCs and their niche. Next we will examine the process of GSC autotomy and compare it with morphologically similar processes in other systems: axon autodestruction, erythropoiesis and thrombopoiesis.

THE AUTOTOMY OF GSC PROJECTIONS: ARE THERE COMPARABLE PROCESSES IN OTHER CELL TYPES?

Autotomy of GSC projections in Oncopeltus fasciatus and Lymantria dispar

In both species the autotomy process follows an apparently standardized pattern (see above). Figure 7A gives a schematized view of the process in *Oncopeltus*. At the base of the cell projections the cytoplasm exhibits similar organelle equipment as the GSC perikaryon: scattered mitochondria, few strands of rough endoplasmic reticulum, many free ribosomes, often forming typical clusters and few lysosomes. The fractionation of the projections that leads to vesicle formation starts with the sequential ingrowth of the plasma membrane from the periphery (described by Schmidt *et al*[65] in *Oncopeltus*). With progressing vesiculation of a projection, mitochondria and rough endoplasmic reticulum that often form concentric whorls, become more abundant, clusters of ribosomes dissolve and the ribosomes are scattered evenly. Mitochondria and vacuoles accumulate. With progressing projection segregation mitochondria become swollen and show signs of degradation and the number of lysosomal bodies increase. Finally, autophagosomal activity becomes evident[60] and secondary lysosomes and myelin-like become abundant. The terminal vesicles then completely segregate from the GSC projections.

In the case of *Oncopeltus* the separated vesicles amass at the surface of the ACs, where they eventually rupture and release their contents. In the case of *Lymantria* the GSC projections are embedded in the AC and the segregated vesicles are phagocytized and digested by the AC (Figure 6B).

The process of projection segregation of GSCs exhibits remarkable similarities with degenerative processes of axons that take place either after injury, in neurodegenerative diseases or during developmental axon pruning. In the following it will be discussed whether an autodestruction program that may underlie the axonal destruction processes could possibly also be active in the process of GSC autotomy.

INJURY-INDUCED AXON DESTRUCTION (WALLERIAN DESTRUCTION) AND THE HYPOTHESIS OF AN AUTODESTRUCTION PROGRAM

Programmed cell autotomy seems to be a rather rare process. It is best known in axon degeneration that occurs after nerve injury in vertebrates and invertebrates (Wallerian degeneration), developmental neuron pruning and as pathological symptoms of neurodegenerative diseases (multiple sclerosis, Parkinson's disease and others)[70]. Other examples of programmed cell autotomy are the formation of blood platelets and erythrocytes in mammals which are discussed later. Wallerian degeneration (Figure 7B) shares morphological similarities with axon degeneration during normal brain development (axon pruning) and with the "dying back" degeneration in neurodegenerative diseases.

Recent studies on the degeneration of injured axons strongly suggest that an active autodestruction program exists akin to apoptosis, and that the autodestruction pathway may be conserved between fly and human[71,72]. The sequence of progressing autodestruction of the

stumps of transected giant nerve fibers in the cockroach *Periplaneta americana*, for instance, follows closely the segregation of GSC projection terminals in *Oncopeltus* (Figure 7): swelling of mitochondria, accumulation of myelin bodies, accumulation of lysosomal vacuoles and sequential segregation of vesicles[73]. Vesicle formation at the axon stump starts like in GSC projections with cell membrane ingrowths. Whereas the distal nerve stump degenerates, the proximal stump produces sprouts that have been interpreted as axonal regeneration. This resembles the expected outgrowth of new GSC projections after exhaustive vesicle segregation (Figures 5C and 7A).

Although still little is known concerning the signaling pathway directing the autodestruction program, some progress has been reported recently. The *Wlds* gene protects severed axons from degeneration. It encodes dNmnat (nicotinamide mononucleotide adenylyltransferase 1). Nmnat is a critical enzyme in the NAD+ biosynthesis pathway and is essential for many cellular processes[74]. Nmnat is likely essential for normal axon maintenance. Down regulation of Nmnat in the wing nerve of *Drosophila* leads to robust dying back fragmentation that markedly resembles Wallerian degeneration, whereas upregulation of Nmnat protects axon degeneration. The function of WldS/Nmnat may involve its essential role in NAD+ biosynthesis. The question arises if the mitochondria are the site of Nmnat-mediated action and mechanism[71]. Also the ubiquitin proteasome system (UPS) plays a crucial role in axon and dendrite maintenance and neuropathology, but the precise effects of WldS/Nmnat and the effect of the UPS vary depending upon the situation, an acute injury, developmental pruning or disease context (for review see Fang *et al*[71]).

The UPS is a potent regulatory mechanism used to control protein stability in numerous cellular processes, including neural development[75]. Many neurodegenerative diseases are featured by the accumulation of UPS-associated proteins, suggesting the UPS dysfunction may be crucial for pathogenesis. Recent experiments have highlighted the UPS as a key player during synaptic development. Recent discoveries center on the role of UPS in synapse remodeling and draw attention to the potential link between synaptic UPS dysfunction and the pathology of neurodegenerative diseases: Parkinson, Alzheimer, Huntington's disease[75]. In Drosophila, the E3 ubiquitin ligase RPM-1 (disease resistance protein) targets DLK1 (delta homolog 1) which acts in the mitogen activated protein kinase (MAPK) cascade consisting of the MAPK MKK4 and the p38 kinase pMK3 or the MAPK c-Jun N-terminal kinase. Thereby RPM-1 regulates the organization and stabilization of presynaptic terminals and axon termination in mechano-sensory and motor neurons[76].

Regeneration of injured neurons can restore function, but most neurons regenerate poorly or not at all. The failure to regenerate in some cases is due to a lack of activation of cell-intrinsic regeneration pathways. These pathways might be targeted for the development of therapies that can restore neuron function after injury or disease. Hammarlund *et al*[77] showed that the DLK-1 MAPK pathway is essential for regeneration in *Caenorhabditis elegans* motor neurons. Loss of this pathway eliminates regeneration, whereas activating it improves regeneration. Further, these proteins also regulate the later steps of growth.

Osterloh *et al*[78] demonstrated that the ortholog genes sterile alpha and TIR motif-containing protein 1 (Sarm 1) in mouse and dSarm (sterile alpha/Armadillo/Toll-Interleukin receptor homology domain protein) in Drosophila promote cell autonomous axon destruction. The genes otherwise involved in innate immune response, are also players in a highly conserved axon destruction pathway. dSarm and Sarm 1 exhibit a punctate localization in neuronal cell bodies and a broad localization in neuritis of *Drosophila* and mouse respectively. An early event in the axon self-destruction pathway is the increase of intra-axonal calcium levels followed by a calcium-dependent cytoskeletal breakdown[72].

There is evidence that WldS enhances physiological functions of the mitochondria and that axonal mitochondria are required for WldS-dependent axon protection. WldS/Nmnat activity enhances mitochondrial motility and Ca^{2+} buffering and that the mitochondrion is an organelle necessary for WldS/Nmnat-mediated axonal protection[79,80].

DEVELOPMENTAL AXON PRUNING, DYING-BACK DEGENERATION AND NEURODEGENERATIVE DISEASES

Developmental axon pruning occurs at a large scale during metamorphosis of holometabolous insects, including Drosophila, where the process was studied in detail. Metamorphosis and axon pruning are controlled by ecdysone. Interestingly, in the mushroom body of the fly brain glia cells participate actively in axon pruning. Ecdysone stimulated axons extrinsically activate glial cells to infiltrate the axon branches and eliminate varicosities actively. They induce the fragmentation of axons, and engulf the fragments[81,82]. The process resembles the interaction of GSCs with the AC in *Lymantria* (Figure 6B). In both cases, the perikarya survive whereas the autotomy of cell projections/axons proceeds, and fragments are taken up by the AC and glia cells, respectively. In *Oncopeltus*, the GSC projections also autotomize but the severed and degrading vesicles are almost never phagocytized. It has been suggested that new projections sprout from the perikarya of *Oncopeltus* comparable to the sprouting of new neurites from pruned neurons. The neuron-glia interaction has an indispensable role in the pruning process of neurons in the mushroom body. The pruning proceeds in a neuron-autonomous manner. It resembles the interaction between phagocytes and apoptotic cells[81,82]. It was shown that dendrite-

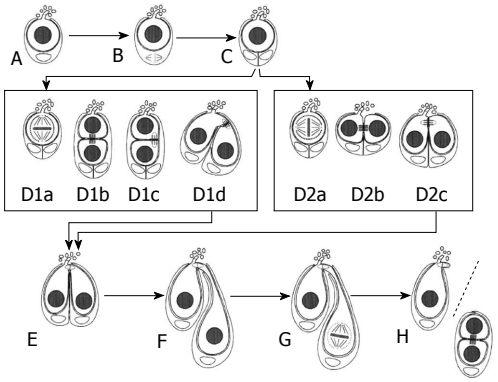

Figure 8 Symmetric and asymmetric germline stem cell division in *Lymantria dispar*. Both symmetric and asymmetric GSC divisions occur in this insect species. Both are preceded by the division of the single cyst stem cell that is associated with a GSC (A to C). Asymmetric division is depicted in D1a to D1d. One of the daughter cells is oriented toward the AC and still forms projections, whereas the other daughter cell has no contact with the AC and is devoid of projections (D1b). Then this daughter cell "swivels" round toward the AC (D1d) and adopts a similar position as daughter cells have after a symmetric GSC division (D2a to D2c). In each case, the daughter cell that doesn't form projections becomes the gonialblast (E to H) (from Klein[66]). GSCs: Germline stem cells; AC: Apical cell.

specific remodeling of *Drosophila* sensory neurons is controlled by two intracellular mechanisms: the ecdysone pathway and ubiquitin-proteasome system[83]. It should be noted that components of the ubiquitin-proteasome pathway has been linked to apoptosis[84].

A dying-back degeneration of axons can be induced in culture of mice neurons by removing nerve growth factor from the chamber. In the process, several distal ends of axons atrophy and undergo fragmentation while the neuronal somata survive. The controlling events are obviously confined to neurites and occur autonomously from the soma[85]. Many neurological deceases are accompanied by neurodegeneration. Although different factors might contribute to axon pathology in each case, what is clear is that the end result is always the same, the axon degenerates in a process that resembles Wallerian degeneration[86].

Wallerian degeneration is an evolutionary highly conserved process that is central to neurite autotomy occurring either regularly in developmental remodeling of neurons or pathologically in neurological diseases and experimental manipulations. The mechanism of serial autotomy of GSC projections in *Oncopeltus* and *Lymantria* (and probably butterflies in general) resembles closely axon autotomy described above. Molecular studies are necessary to uncover whether similar signaling pathways are involved.

CONSEQUENCES OF GSC AUTOTOMY ON SIGNAL EXCHANGE WITH THE NICHE AND GSC DIVISION (SYMMETRIC *VS* ASYMMETRIC DIVISION)

Until recently it was accepted that adult male GSCs in Drosophila only undergo asymmetric divisions[87]. GSCs attached to hub cells by adherens junctions provide a polarity cue that orients stem cells. The centrosome is oriented toward the hub cell-GSC interface throughout the cell cycle. The mother centrosome is always located close to the hub cells whereas the daughter centrosome moves to the opposite side. Consequently, GSC spindle orientation is predetermined during interphase[88]. The correct centrosome orientation toward the hub cells requires the adherens junction which is composed of E-cadherin and β-catenin, centrosomin, and Apc2. Apc2 is believed to connect astral microtubules to the adherens junction/actin cytoskeleton network formed between hub cells and GSCs thereby anchoring the centrosome[89]. Centrosome orientation prior to mitosis is accomplished by Par-1 (a serine/threonine kinase that regulates polarity in many systems) that regulates cyclin A localization[90]. Recently "symmetric renewal" of male GSCs in *Drosophila* has been observed[91]. In this process, GSC division starts like a typical asymmetric mitosis (the mitotic spindle is perpendicularly oriented toward the hub surface) but then the still interconnected pair of cells "swivel" such that both cells contact the hub. Studies on other insect testes revealed still different modes of GSC divisions and gonialblast differentiation.

Unique processes have been described in male GSCs of *Lymantria* (Figure 8). GSCs undergo either symmetrical divisions (the spindle is oriented parallel to the AC surface) or asymmetrical divisions (the spindle is oriented perpendicularly to the AC surface). Both types of mitosis can result in gonialblast formation but, surprisingly, after asymmetrical division GSC and daughter cell - interconnected by a fusome - "swivel", comparable to the process in *Drosophila* described by Sheng *et al*[91] in 2011, and both contact the AC. Whereas the mother GSC maintains its intense interaction with the AC, the daughter and presumptive gonialblast does not form cell projections. Finally, the daughter cell moves further to the periphery and differentiates to a gonialblast. Alternatively, after symmetrical division the daughter cell is again characterized by the lack of cell projections, develops to a gonialblast in a similar fashion as in the case of asymmetric GSC division[66]. Each GSC is associated with one CySC. CySC division precedes GSC division and the mitotic spindle is always oriented parallel to the AC surface. The mechanism destining the centrosome location is not known and adherens junctions between GSCs and AC have not been described - and are not likely to exist, given the complex relationship between GSCs and AC. Consequently, the regulation of spindle orientation must differ in *Lymantria* from Drosophila.

Also in *Oncopeltus* adherens junctions could not be identified in electron microscopic studies[92]. In this species, only symmetrical divisions of GSCs have been observed. GSC projections persist during division. Gonialblasts are formed when GSCS migrate toward the periphery of the apical complex. Its projections elongate, become thin and gradually degenerate before one cyst

cell encloses the gonialblast[92]. *Locusta* shows both symmetrical and asymmetrical divisions[64]. But again, besides tight junction-like connections, no adherens junctions have been detected between GSCs and AC. It should be mentioned, however, that GSCs and AC are extremely difficult to separate, either enzymatically or mechanically, in *Locusta*[64].

In summary, the mechanism for spindle orientation appears variable in insect male GSCs. But up to date, Drosophila is the main species studied in this respect in the evolutionary highly diversified group of insects.

Interactions between GSCs and ACs in the testes of various insects are diverse and it is evident that the mode of short range signaling between stem cell and niche differ in distinct species from that in *Drosophila*. In *Oncopeltus*, ACs are surrounded by vesicles segregated from GSC projections (Figure 6A). This poses the questions: how is the communication and information exchange organized between GSCs and AC? and how is the sequential projection autotomy, progressing degradation, and sprouting of new projections programmed? There are no studies on the molecular level concerning these questions. However, the ancient conserved axon destructing Wallerian pathway bears many similarities with GSC projection autotomy. Further, the outgrowth of new projections near the perikaryon of *Oncopeltus* GSCs parallels the outgrowth of new neuritis after Wallerian axon destruction. As described above, developmental axon pruning and neurite dying-back in neuronal diseases all appear to be governed by a related axon-autonomous program that carries characteristics of apoptotic processes. Extensive fragmentation of megakaryocyte projections takes place during platelet formation as described below. Also in this case apoptotic processes take place, *i.e.*, fragmentation of the nucleus. The segregation of platelets, however, appears to follow a different pattern than Wallerian axon fragmentation and GSC projection autotomy. In the latter cases, concentrically transverse ingrowing plasma membrane that finally fuses, cuts off vesicular fragments. Pinching off platelets apparently involves transverse microtubule arrangement and vesicle widening at the constriction zone (see below).

In *Lymantria*, segregation of GSC projection terminals resembles that in *Oncopeltus*. Thus, the underlying cell autotomy program is expected to be similar as in *Oncopeltus*. But in *Lymantria* and several other butterflies (see above) the AC embraces the GSC projections and engulfs and digests separated vesicles. In *Locusta*, ACs almost constantly include one or two phagocytized GSCs. The interactions of GSCs and ACs (their niche) are puzzling in *Oncopeltus* as well as in butterflies. We speculate that the AC sends signals that promote GSC autotomy and that in return the AC receives information concerning the surrounding GSC population. In response to that information the AC may regulate GSC self-renewal and maintenance. Unfortunately, none of these aspects have yet been tested. In about all insect apical complexes studied by electron microscopy, "dark" granules have been described in the interface between AC and GSCs (Figure 6). In *Lymantria*, the AC shows tubular invaginations filled with "dark" material of unknown fate. Due to the phagocytic processes and material exchange early investigators suggested a trophic role of ACs[92]. We believe that these processes are part of the information exchange and signaling pathways. In erythroblastic islands, after release of the reticulocyte, the pyrenocyte is phagocytized by the central macrophage. This is mandatory for continued erythropoiesis (see below). This indicates that the involvement of phagocytic processes in stem cell-niche interaction is existent but needs further investigation.

STEM CELL/PROGENITOR AUTOTOMY IN ERYTHROCYTE AND PLATELET FORMATION

Erythroblastic islands and enucleation of erythroblasts

In vivo, erythropoiesis occurs in specific units, the erythroblastic islands in the bone marrow of mammals[93]. Erythroblastic islands were also described in the spleen, yolk sac and fetal liver. They harbor a central macrophage that arises from a resident monocyte precursor with a unique immunophenotypic signature[94]. The central macrophage, representing the niche, is surrounded by one or more synchronously maturing cohorts of erythroid cells that undergo four or five divisions between proerythroblast and orthochromatic erythroblast stage. In their fine structural study Allen *et al*[95] describe gap junction-like contacts between the macrophage and erythroblasts and possible reciprocal vesicular activity. Several molecules indicate adhesive interactions within the erythroblastic islands[4]: (1) Erythroblast macrophage protein (Emp) forms macrophage/erythroblast attachments *via* hemophilic binding; (2) $\alpha 4\beta 1$ integrin in erythroblasts and vascular cell adhesion molecule-1 in the central macrophage mediate receptor/counter receptor cell-cell interactions; (3) Macrophage α integrin and erythroid intercellular adhesion molecule-4 are expected to contribute to the island integrity; and (4) Other macrophage adhesion glycoproteins, *i.e.*, CD69 and CD 163, have been detected[96] although their erythroid binding partners are unknown. It is expected that adhesive connections between erythroblasts and macrophages play a crucial role in signaling pathways as they do in Drosophila testes. The central macrophage secretes soluble factors, cytokines, that promote proliferation and maturation of erythroblasts (insulin-like growth factor-1 and others) and also negative regulatory factors [transforming growth factor-β1 (TGF-β), TNF-α, ILG and others][4] (Figure 9).

The most striking event in mammalian erythrocyte maturation is the enucleation of orthochromatic erythroblasts at the last stage of erythroblast differentiation. It results in multilobulated non-nuclear reticulocytes and

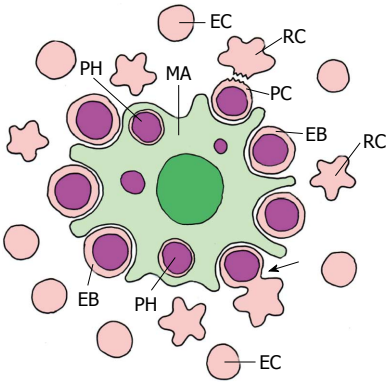

Figure 9 Erythropoiesis in mammal bone marrow (schematized). The erythroblastic island consists of a central macrophage (MA) that functions as the niche, and the peripheral erythroblasts (EB), that represent stem/progenitor cells. Erythroblasts undergo an enucleation process (arrow) that results in the pyrenocyte (PC) that mainly consists of the erythroblast nucleus, and the nucleus-free reticulocyte (RC). The pyrenocyte is phagocytized by the macrophage (PH, phagosome), whereas the reticulocyte develops to the erythrocyte (EC) (adapted from Chasis *et al*[4]; Keerthivasan *et al*[98]).

pyrenocytes which mainly consist of the nucleus and the enwrapping plasma membrane. Enucleation is regulated by retinoblastoma protein (Rb) but other signaling molecules, *e.g.*, p38 MAPK (p38) and Rac-1 GTPase, have been found to be involved in the enucleation[97]. Interestingly, sorting of protein and vesicle trafficking in the orthochromatic erythroblast in concert with nuclear positioning are essential for the enucleation process[98]. The pyrenocytes express phosphatidylserine, a recognition signal similar to apoptotic cells, on their surface that signals macrophages to engulf and digest them. The taken up DNA is digested by DNase Ⅱ from the macrophage[99]. The lack of DNase Ⅱ in DNase Ⅱ knockout mice is lethal *in utero* due to embryonic anemia. Digestion of engulfed pyrenocyte nuclei is vital for continued erythropoiesis[100].

Already in the 1990ties Hanspal *et al*[101,102] found that the interaction between erythroblasts and macrophages is needed for normal erythroblast proliferation and for enucleation. The authors showed that this interaction is mediated by Emp that prevents apoptosis of developing erythrocytes. Nonetheless, erythroblasts cultured *in vitro* in the absence of macrophages undergo complete differentiation including nuclear extrusion[103,104]. Although erythropoietin was used to start erythroblast amplification (and other factors were eventually added) erythropoiesis proceeded apparently normal without macrophages, however, at a much lower pace as it does in erythroblastic islands[93]. Thus the question arises: have macrophages merely a trophic function? As mentioned above, genetic manipulations of macrophage activity resulted in lethality due to anemia. It may be speculated that in these cases erythropoiesis was (only) insufficient (but not completely) suppressed. The "true" function of island macrophages is to optimize and accelerate erythrocyte production allowing effective erythrocyte supply and rapid adjustment to the actual need. Erythrocyte homeostasis might be largely regulated by systemic factors that convey the need or surplus of erythrocytes and affect short-range signaling within the erythroblast island which determines the pace of erythrocyte production.

We suggest that spermatocyte production in insect testes is regulated in a similar way. The example of *Lampyris* shows that no ACs are needed for GSC differentiation *per se*. The apparent reason: all GSCs differentiate at the same time and the process does not need any temporal regulation. Onset of GSC differentiation and production of CC progenitors occurs during larval development of *Lampyris* and is expectedly put in motion by the release of morphogenetic hormones, *e.g.*, ecdysone and juvenile hormone, representing systemic signals[67].

Another conspicuous interaction shared by the niche of erythroblastic islands and the niche of butterfly testes are spectacular phagocytic processes. In the case of erythroblastic islands, macrophages engulf the pyrenocytes; in the case of butterflies, ACs phagocytise large vesicles segregated from GSC projections. DNA taken up by macrophages plays a role in signaling, as described above. And there are also vesicle interactions with expected receptor exchange. In butterflies, the vivid autotomic activity of GSCs and the phagocytotic uptake of the autotomized vesicles are not understood. We propose that it represents an interaction/communication between niche and stem cell hitherto unknown. Noteworthy, whereas autotomy of GSC projections also takes place in *Oncopeltus* the segregated vesicles are not taken up by ACs, but degenerate in a distinct pattern as described above. We suggest that the degenerating vesicles provide specific signals that are recognized by the AC. Interestingly, the ACs of *Locusta* include, as a rule, one or two phagocytized GSCs (see above). Phagocytosis here may play a similar role as it does in *Lymantria*. The variations in stem cell-niche relation seem highly variable in insect testes, and the analysis of species beyond *Drosophila* might provide new insights.

Platelet formation by megakaryocyte fragmentation

The probably most spectacular case of programmed cell autotomy is the shedding of 5000-10000 platelets from one megakaryocyte. Platelets are characterized by the absence of a nucleus and by the accumulation of three types of granules: (1) Dense (or delta) granules, with a diameter of 150 nm, contain ADP or ATP, Ca and Serotonin. They are secreted to recruit other platelets; (2) Alpha-granules, with a diameter of 200-400 nm, contain P-selectin, platelet factor 4, TGF-β1, platelet-derived growth factor, fibronectin, B-thromboglobulin, von Willebrand factor (VWF), fibrinogen, coagulation factors Ⅴ and ⅩⅢ. They are responsible for adhesion and healing processes; and (3) Lambda granules, with a diameter of 175-250 nm, resemble lysosomes. They contain several hydrolytic enzymes that are able to eliminate circulating platelet aggregates (for review see Rendu *et al*[105]) (Figure 10).

Megakaryocytes mature from megakaryoblasts

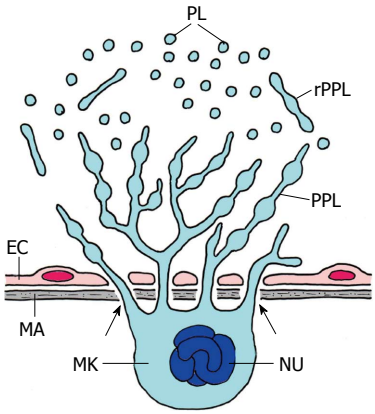

Figure 10 Thrombopoiesis (platelet formation) in mammal bone marrow (schematized). Platelets are produced by a most spectacular form of cell autotomy performed by the megakaryocyte (MK). Maturation and fragmentation of the megakaryocyte is orchestrated by the vascular niche which consists of the endothelial cells (EC) of sinusoids and the extracellular matrix (MA) of the endothelium. The megakaryocyte is located at the outer surface of the sinusoid epithelium and sends pseudopods through the pores of the endothelium into the lumen of the sinusoids (arrows). The pseudopods branch and form proplatelets (PPL). These are released into the sinusoids (rPPL) followed by the release of platelets (PL). Nu, polyploidy nucleus of the megakaryocyte (Adapted from Patel *et al*[115]).

via promegakaryocytes in the bone marrow. Megakaryoblasts reside in the osteoblastic niche where osteoblasts secrete the cytokine thrombopoietin (TPO) that regulates megakaryopoiesis and thrombopoiesis, *i.e.*, platelet formation, as well[106]. Stromal cell derived factor-1 from stromal fibroblasts and fibroblast growth factor-4 direct megakaryocyte interaction with the bone marrow stroma and regulate cytokine-independent megakaryocyte maturation[107]. A number of cytokines [interleukin-3 (IL-3), IL-6, IL-11, IL-13, leukemia inhibiting factor (LIF), stem cell factor, and others] affect megakaryopoiesis which was mostly tested in *in vitro* systems[108,109]. In the process of maturation, the precursors of the megakaryocytes migrate from the osteoblastic to the vascular niche along an oxygen gradient to the higher oxygen of the vascularized compartment of the bone marrow[110]. During maturation megakaryocyte progenitors undergo endomitosis, up to 128 times. Reaching the endothelium of the marrow sinusoids the strongly enlarged megakaryocytes form cytoplasmic projections that protrude through endothelial pores into the lumina of the sinusoids. There, the projections presumably (as inferred from *in vitro* observations) branch repeatedly forming formidable trees of proplatelets which segregate and release the platelets into the lumina of the sinusoids. The vascular niche that promotes platelet formation and shedding consists of the endothelial cells and the extracellular matrix of the endothelium[111].

The dynamic interactions of megakaryocytes with different extracellular matrix proteins seem to orchestrate their maturation in specific sites[111]. In the vascular niche such proteins include collagen type Ⅳ, fibronectin, laminin, fibrinogen and VWF. (VWF is secreted by endothelial cells and megakaryocytes into the blood and has a function in adhesion and aggregation of platelets.) In mice (*in vitro*) fibrinogen binding to the fibrinogen receptor $\alpha_{IIb}\beta_3$, which is expressed in megakaryocytes, is essential for proplatelet formation. However, the role of the interaction in humans is not fully understood[112]. Astonishingly, *in vitro* studies have shown that the cytokine TPO alone is required for thrombopoiesis and that extracellular matrix and other cytokines are not essential, although they may have regulatory functions *in vivo* that accommodates platelet homeostasis[113]. This is reminiscent of the niche function in erythroblastic islands and testes of insects where stem cell differentiation can proceed without niche but is adjusted to the actual need by niche interaction.

The process of proplatelet formation and platelet shedding is highly complicated and still not fully understood[114,115]. Electron microscopic studies on cultured megakaryocytes demonstrated that prior to proplatelet formation mature megakaryocytes have already a well-developed demarcation membrane system[116]. This elaborate membrane system is - as commonly believed - formed by invaginations of the plasma membrane, shows open cisternae and is at first randomly distributed throughout the cytoplasm. Randomly scattered α-granules and some dense granules are also present. Preparing for active platelet shedding, the peripheral demarcation membranes dilate and align at the cell periphery. Cytoplasmic sheets unfold and cell projections extend. The extensions display a beaded appearance with constriction points separating discrete platelet-like territories. A bundle of longitudinal microtubules runs through the center of the extensions. At the constriction zone transverse microtubules are observed near the longitudinal microtubules. Also, a vacuole of increasing size is formed at the constriction zone which may lead to the detachment of the platelet fragment. These observations of Cramer *et al*[116] suggest that vesiculation and microtubule force attribute to autotomy. Other studies emphasize even more the role of microtubules in platelet segregation[115,117]. Before proplatelet formation, microtubules align into bundles beneath the surface of megakaryocytes and, at projection formation, fill the cortex of outgrowing cones. Cell organelles are in direct contact with microtubules and are transported along these elements. Microtubules coil at the end of the projections, but their exact role in platelet segregation remains unresolved.

It should be mentioned that in an opposing view the membrane boundaries of platelets are not provided by involutions of the megakaryocyte plasma membrane but by vesicles from Golgi complexes. So-called proplatelets constitute within the megakaryocyte whose plasma membrane finally ruptures and releases the platelets. Extensions of the megakaryocyte with proplatelets and segregation of terminal platelets are considered as artifacts by some authors[114,118,119].

It is, however, the prevailing view that platelets segregate from ends of the megakaryocytes extensions that

offer a beaded structure, in as much platelet-sized and platelet-structured proplatelets are connected by string-like connections with longitudinally running microtubules (Figure 10). Interestingly, the process of platelet assembly is accompanied by some characteristics associated with apoptosis: cytoskeletal reorganization, membrane condensation and chromatin condensation. Microtubules and F-actin play supposedly a major role in proplatelet formation and fragmentation. The kinetics of platelet release *in vitro* corresponds to the onset of apoptosis in the megakaryocyte. Maximal platelet production and megakaryocyte apoptosis are closely related events[115,120,121]. Molecular evidence of apoptotic processes in megakaryocytes provided the detection of caspase 3. Before the platelet formation caspase 3 shows a punctuate cytoplasmic distribution (in a presumably inactive state) and a diffuse staining pattern (in a presumably active state) in senescent megakaryocytes. It was concluded, that proplatelet formation is regulated by caspase activation limited to only cellular compartments[122]. Further evidence for an involvement of apoptotic processes in platelet formation comes from the presence of the antiapoptotic protein BclxL which is upregulated during megakaryocyte differentiation but absent during late megakaryopoiesis. Bclxl overexpression causes a strong decrease in proplatelet formation[123]. Other apoptotic-related genes such as TGF-β1 and SMAD proteins are expressed during thrombopoiesis which supports the significance of apoptotic signaling in the process[124]. Besides, NO in conjunction with TPO facilitates platelet production[125]. Nagata *et al*[126] report that estradiol synthesized in megakaryocytes triggers proplatelet formation by autocrine action. Few transcription factors were reported to play major roles in thrombopoiesis. GATA-1, which interacts with friend of GATA-1 controls proliferation during megakaryopoiesis, and NF-E2 regulates platelet biosynthesis[127-129].

Cell autotomy in the process of erythrocyte formation (*i.e.*, enucleation) and platelet generation (by megalokaryocyte fragmentation) appear to follow quite different strategies. However, in both cases apoptotic processes play a prominent role. This offers parallels to the autodestructive processes in neurons (see above). Concerning GSC autotomy, no attempts have been made to demonstrate apoptotic processes in GSC projections. Schmidt *et al*[92] described apoptosis of GSCs and spermatogonia in *Oncopeltus* but its significance - apart from removal of surplus spermatogonia - remains obscure. Dying germ cells in Drosophila revealed mixed morphologies of apoptosis and necrosis that may indicate an alternative developmental cell death pathway[130]. The role of the cytoskeleton in cell autotomy is little understood although it may play a major role in all cases. Concerning megakaryocyte fragmentation, the cytoskeleton is obviously decisively involved in platelet segregation. Neurofilaments and microtubules are the first cell organelles that break down in axonal autodestruction following intracellular calcium increase after nerve injury. The role of the cytoskeleton in GSC autotomy is not known but is conceivably important and should be analyzed.

COMPARISON OF THE INSECT AND MAMMAL SPERMATOGENESIS

Testes of insects offer a rather simple architecture. One testis is composed of one to many testicular follicles, blind ending tubules that join into a common seminal duct. GSCs and niche exhibit a globular arrangement, mostly in the form of a rosette at the apex of a testicular follicle, representing the apical complex. Spermatogonial cysts move distally during spermatogenesis. The follicular epithelium that envelopes the apical complex and cysts is mostly thin and has, so far, not been considered as part of the niche for GSCs. However, as pointed out above, in a number of species, the envelope synthesizes and releases the steroid ecdysone at some point of development[53]. Although effects of ecdysone on spermatogenesis have been reported, a specific function or signaling pathway has not been elucidated. Nonetheless, it parallels the production of steroids, androgens, in Leydig cells of the testes of mammals.

Mammalian testes exhibit a complex epithelial organization (for review see Yoshida[131]). The long seminiferous tubules are convoluted and both ends open into the rete testis. Figure 11 shows the organization of a seminiferous tubule. The high epithelium of the tubules consists of the larger Sertoli cells, and the smaller spermatogonia and spermatocytes. The epithelium rests on a basement membrane, and below it stretches peritubular myoid cells. Located in the interstitial between the seminiferous tubules are Leydig cells, macrophages, lymphoid epithelial cells and connective tissue. Blood vessels form a network around the tubules and run in the interstitial spaces. Besides the germ cells all mentioned cell types and structures may be part of the GSC niche. The complexity of the niche, which doesn't offer spatial specifications, is reflected by the difficulty to define GSCs. They represent obviously a small population of spermatogonia. According to de Rooij *et al*[132] and Russell *et al*[132,133], spermatogenesis progresses uniformly all over the inner surface of the seminiferous epithelium, and stem cells are scattered all over. But how are GSCs identified? First, they are located in the basal compartment of the epithelium. All neighboring Sertoli cells form tight junctions at a distinct height separating a basal compartment which has contact with blood vessels and an adluminal compartment without blood contact. Thus, a blood-testis-barrier is installed at the level of tight junctions. Located in the basal compartment are "undifferentiated spermatogonia" (A_{undiff}), comprising singly located spermatogonia (A_s) and such that have undergone up to four mitotic divisions. The mitotic spermatogonia form syncytia due to incomplete cytokinesis. A_s have contact with the basement membrane and a subpopulation of them might represent yet-to-

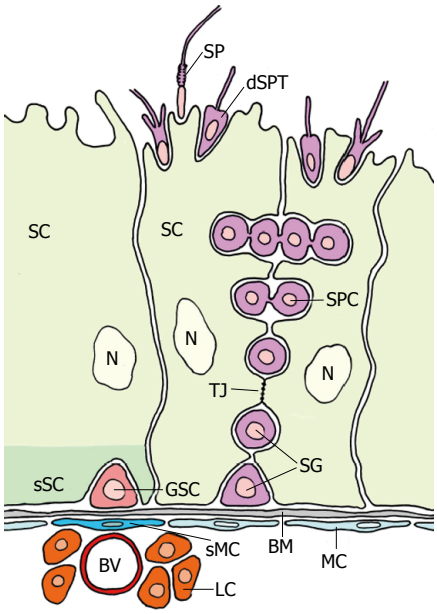

Figure 11 Organization of the mammalian testicular germline stem cell niche (adapted from Yoshida[131]). The seminiferous tubules exist of large sertoli cells (SC) and spermatocytes (SPC). The putative germline stem cell (GSC) is located at the basement membrane (BM) at an interstitium. It is in close vicinity of a blood vessel (BV) and leydig cells (LC). Myoid cells (MC) that line the BM are thought to be "specialized" MC (sMC) below the GSC. The basal part of the SC that surrounds the GSC presumably performs a specialized "domain" acting as (the main) part of the complex niche. The niche allegedly consists of several additional entities besides the specialized SC domain: the BM, the sMC, the BV, the LC and probably others (see text). Tight junctions (arrow) between SCs establish a blood-testis barrier: GSCs and spermatogonia are exposed to the vascular system, whereas primary spermatocytes (SPC) and the following stages of Spermatogenesis proceed behind the barrier. dSPT: Differentiating spermatid; SP: Spermatozoon; N: Nucleus of SC; Red: GSC; Light green: SC; Dark green: sSC domain surrounding the GSC; Purple: Spermatogonia and different stages of spermatogenesis; Dark blue: sMC; Light blue: MC; Light red: BV; Orange: LC; Grey: BM.

be-identified GSCs. At the transition from mitotic to meiotic divisions, spermatogonia move to the adluminal compartment and are now called spermatocytes. From there on spermatogenesis takes place behind the blood-testis-barrier. Round spermatids move to the luminal surface where they elongate. The accumulation of stags of spermatogonia and spermatocytes among the Sertoli cell epithelium results in a multilayered organization of the seminiferous tubules.

Since A_s are spread all over the tubules the question arises: which mechanisms provide uneven features within the basal compartment to specify the niche microenvironment for stem cells? Yoshida *et al*[100] demonstrated that A_{undiff} (and possibly GSCs) are preferentially localized to the area adjacent to the interstitium at branching points of blood vessels of medium thickness. Yoshida *et al*[131] suggests that Sertoli cells and myoid cells in this region might be "specialized". Theoretically, all parts of the niche could control stem cells directly by short-range signaling. Systemic signals could arrive *via* blood directly at the GSCs or indirectly by modulating the short-range signaling of other parts of the niche. The niche region might not be fixed.

Several signaling factors are known to have effects on spermatogenic cells (Figure 12). Most important is glial cell line-derived neurotrophic factor (GDNF), a member of the TGF-β superfamily[134]. The ligand GDNF is expressed in Sertoli cells and its receptor c-Ret and co-receptor GFRα1 is expressed in the least mature subsets of A_{undiff}, the putative GSC[135,136]. Thus, *via* GDNF signaling Sertoli cells control self-renewal, survival, and maintenance of GSCs. Another receptor highly expressed in GSCs is colony stimulating factor 1 receptor. Its ligand is expressed in Leydig cells of the interstitium and a subset of myoid cells[137]. It is suggested that CSF1 may cooperate with GDNF in supporting the self maintenance of GSCs. The tyrosine kinase receptor c-kit and its ligand KitL, which is expressed in Sertoli cells, have been recently shown to be involved in proliferation, survival and migration of spermatogonia. However, only KIT(-) spermatogonia have stem cell activity. Several factors have effects on GSCs *in vitro*: FGF, EGF and LIF, in the presence of GDNF, support the proliferation of GSCs[138]. LIF is probably also involved in the maturation of gonocytes into spermatogonia[139]. But a possible function *in vivo* is uncertain. The transcriptional regulator Ets related molecule has been detected in nuclei of Sertoli cells of adult testes. It is assumed that it regulates Sertoli cell function that mediates germ cell self-renewal[140].

Stem cells and spermatogonial populations express α6 and β1-integrin[136] which mediates the attachment to the basement membrane *via* binding of laminins, probably as a heterocomplex with α6-integrin[141]. Its significance in signaling *in vivo* is not known; GSCs lacking β1-integrins fail to develop spermatogenic colonies after transplantation[142]. E-cadherin is expressed in A_{undiff} but is dispensable for the normal functioning of stem cells[143].

Despite the profound differences between the organization of the insect Drosophila and the mammal mouse testis, several important common principles can be observed. In both cases, the stem cell-niche complex is exposed to blood: in insects hemolymph freely surrounds the testicular follicles whose envelope allows the passage of larger molecules[144]. In mammals blood vessels run through the niche of GSCs and release molecules in the vicinity of GSCs. In several adult stem cell-niche systems blood vessels and endothelial cells are an integral part of the niche: the HSC niche and the vascular niche of platelet producing megakaryocytes (see above), the neural stem cell (NSC) niche the B1 NSCs within the ventricular-subventricular zone sends out a basal process ending in a specialized end-foot that contacts blood vessels; blood-borne factors and endothelial-derived factors may act on B1 cells in this domain[145], intestinal stem cell and probably other niches[146,147]. Recently, it has been reported that an important function of endothelial cells in glioblastoma multiforme is to create a niche that helps to promote self-renewal in cancer stem-like cells[148]. In liver regeneration, endothelial cells establish an instructive vascular niche, which through elaboration of paracrine trophogenes stimulates organ regeneration,

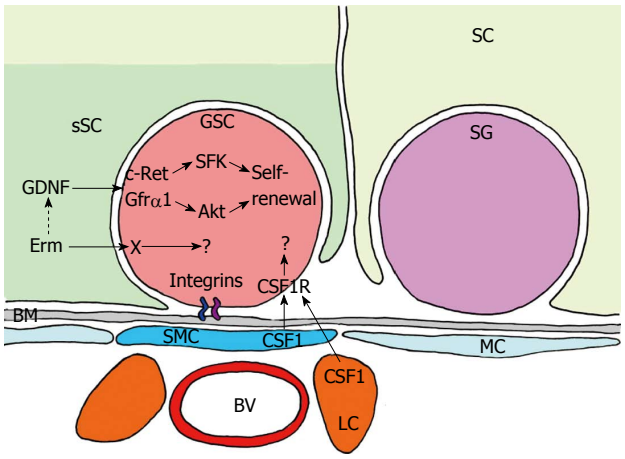

Figure 12 Short range signalling between germline stem cell and its niche. GDNF is the most important signal produced by the "specialized" basal compartment of SC. Its receptor - c-RET (transmembrane tyrosine kinase receptor) and co-receptor GFRα1, which functions as a glycosylphosphatidylinositol-anchored docking receptor that is needed for GDNF to bind with c-RET - is expressed in GSC, and SFK and Akt pathway are initiated. They control self-renewal and maintenance of GSCs. GSCs also express CSF1R (colony stimulating factor 1 receptor). Its ligand CSF1 is synthesized in "specialized" MCs (sMC) and in leydig cells (LC). Thus, CSF1 may cooperate with GDNF in supporting self-maintenance. Integrins attach the GSCs to the BM and may also contribute to signalling. Red: GSC; Light green: SC; Dark green: sSC domain surrounding the GSC; Purple: Spermatogonium (SG); Dark blue: sMC; Light blue: MC; Light red: BV; Orange: LC; Grey: BM.

in a manor similar to endothelial-cell-derived angiocrine factors that support hematopoiesis[149].

Meiotic divisions of spermatogonia in mammals and all mitotic and meiotic divisions after gonialblast formation in insects take place behind the blood-testis-barrier. Whereas tight junctions between neighboring Sertoli cells establish the barrier in mammals, it is the cyst cells that isolate the developing germ cells from the hemolymph in insects. There is little information on the necessity for a compartment in which spermatogenesis is protected from blood-borne factors.

Mouse and Drosophila differentiating germ cells share another astonishing potency: they can generate GSCs, *in vivo*. In mice "spermatogonial progenitors committed to differentiation" can generate functional GSCs that can repopulate germ cell-depleted testes when transplanted into adult males. GDNF and FGF2 are able to reprogram *in vitro* spermatogonial progenitors for reverse differentiation[150,151]. Amazingly, posttransplantation homing GSCs have to perform multiple steps: attachment to the Sertoli cell surface, retrograde translocation to the basal compartment across tight junctions, migration to the presumptive stem cell niche, survival, proliferation, and self-renewal within the niche, expansion of the transient amplifying spermatogonia and differentiation into sperm[131]. β1-intergin, which is expressed in spermatogonial cells, plays an essential role in GSC homing[142]. In Drosophila testes spermatogonia undergoing transit-amplifying divisions can be reverted to stem cell identity by conditionally manipulating Jak-STAT signaling[152]. In the process, the spermatogonia, which are enclosed in cysts and interconnected by fusomes, have to break up their connections, and the cyst wall has to disintegrate in order to release the dedifferentiating germ cells. These germ cells populate the orphaned niche and reestablish normal spermatogenesis. Spermatogonial dedifferentiation can be genetically induced by conditional loss of STAT or misexpression of the differentiation factor Bam within the testes. This causes the differentiation of all GSCs and free niche space. If normal signaling is restored differentiating spermatogonia revert to stem cells, as described above, adhere to hub cells and function normally[14,152]. Remarkably, dedifferentiation of oogonia has also been shown in the Drosophila ovary[153].

CONCLUSION

This review summarizes the current knowledge of a novel mode of interaction between GSCs and their niche, the ACs, in insects. In several insect species (Oncopeltus, Lymantria and other moths) male GSCs undergo autotomy of cell projections, which are directed toward the ACs. The segregated GSC vesicles degrade at the surface of the niche cells or are phagocytized by them. This unique stem cell-niche relationship has been compared with known examples of stem cell/progenitor autotomy (*i.e.*, erythrocyte and thrombocyte formation) and autotomy of neurons in developmental axon pruning or neurodegenerative processes. In all the cases described, apoptotic signalling is involved. Studies on injury-induced axon destruction (Wallerian degeneration) suggest that an active autodestruction program exists akin to apoptosis and that the autodestructive pathway maybe conserved between fly and human[71,72]. We propose that this pathway also exists and is active in male GSCs of Oncopeltus, Lymantria and other species. The analysis of signal exchange between autotomized GSC vesicles and niche cells is expected to reveal a new mechanism of stem cell-niche interaction.

REFERENCES

1 **Schofield R**. The relationship between the spleen colony-forming cell and the haemopoietic stem cell. *Blood Cells* 1978; **4**: 7-25 [PMID: 747780]
2 **Morrison SJ**, Scadden DT. The bone marrow niche for haematopoietic stem cells. *Nature* 2014; **505**: 327-334 [PMID: 24429631 DOI: 10.1038/nature12984]
3 **Park D**, Sykes DB, Scadden DT. The hematopoietic stem cell niche. *Front Biosci* (Landmark Ed) 2012; **17**: 30-39 [PMID: 22201730 DOI: 10.2741/3913]
4 **Chasis JA**, Mohandas N. Erythroblastic islands: niches for erythropoiesis. *Blood* 2008; **112**: 470-478 [PMID: 18650462]
5 **Bessis M**. [Erythroblastic island, functional unity of bone marrow]. *Rev Hematol* 1958; **13**: 8-11 [PMID: 13555228]
6 **Lin H**. The stem-cell niche theory: lessons from flies. *Nat Rev Genet* 2002; **3**: 931-940 [PMID: 12459723 DOI: 10.1038/nrg952]
7 **Verson E**. Zur spermatogenesis. *Zool Anz* 1889; **12**: 100-103
8 **Zick K**. Beitrage zur kenntnis der postembryonalen entwicklungsgeschichte der genitalorgane bei lepidopteren. *Zeitschrift fuer Wissenschaftliche Zoologie Leipzig* 1911; **98**: 430-477
9 **Spichardt C.** Beitrag zur entwicklung der männlichen genitalien und ihrer ausführungsgänge bei lepidopteren. *Verh Naturhist Verein*

Rheinland Bonn 1886; **43**: 1-43
10 **Buder JE**. Die spermatogenese von deilephila euphorbiae l. *Archiv f Zellforschung* 1915; **14**: 27-78
11 **Schneider K**. Die entwicklung des eierstockes und eies von deilephila euphorbiae. *Archiv f Zellforschun*g 1915; **14**: 79-143
12 **Nelsen OE**. Life cycle, sex differentiation, and testis development in melanoplus differentialis (acrididae, orthoptera). *Jour Morph and Physiol* 1931; **51**: 509-511
13 **Chen S**, Lewallen M, Xie T. Adhesion in the stem cell niche: biological roles and regulation. *Development* 2013; **140**: 255-265 [PMID: 23250203 DOI: 10.1242/dev.083139]
14 **Matunis EL**, Stine RR, de Cuevas M. Recent advances in Drosophila male germline stem cell biology. *Spermatogenesis* 2012; **2**: 137-144 [PMID: 23087833 DOI: 10.4161/spmg.21763]
15 **Kiger AA**, Jones DL, Schulz C, Rogers MB, Fuller MT. Stem cell self-renewal specified by JAK-STAT activation in response to a support cell cue. *Science* 2001; **294**: 2542-2545 [PMID: 11752574 DOI: 10.1126/science.1066707]
16 **Tulina N**, Matunis E. Control of stem cell self-renewal in Drosophila spermatogenesis by JAK-STAT signaling. *Science* 2001; **294**: 2546-2549 [PMID: 11752575 DOI: 10.1126/science.1066700]
17 **Chen D**, McKearin D. Dpp signaling silences bam transcription directly to establish asymmetric divisions of germline stem cells. *Curr Biol* 2003; **13**: 1786-1791 [PMID: 14561403 DOI: 10.1016/j.cub.2003.09.033]
18 **Kawase E**, Wong MD, Ding BC, Xie T. Gbb/Bmp signaling is essential for maintaining germline stem cells and for repressing bam transcription in the Drosophila testis. *Development* 2004; **131**: 1365-1375 [PMID: 14973292 DOI: 10.1242/dev.01025]
19 **Amoyel M**, Sanny J, Burel M, Bach EA. Hedgehog is required for CySC self-renewal but does not contribute to the GSC niche in the Drosophila testis. *Development* 2013; **140**: 56-65 [PMID: 23175633 DOI: 10.1242/dev.086413]
20 **Michel M**, Kupinski AP, Raabe I, Bökel C. Hh signalling is essential for somatic stem cell maintenance in the Drosophila testis niche. *Development* 2012; **139**: 2663-2669 [PMID: 22745310 DOI: 10.1242/dev.075242]
21 **Flaherty MS**, Salis P, Evans CJ, Ekas LA, Marouf A, Zavadil J, Banerjee U, Bach EA. chinmo is a functional effector of the JAK/STAT pathway that regulates eye development, tumor formation, and stem cell self-renewal in Drosophila. *Dev Cell* 2010; **18**: 556-568 [PMID: 20412771 DOI: 10.1016/j.devcel.2010.02.006]
22 **Leatherman JL**, Dinardo S. Zfh-1 controls somatic stem cell self-renewal in the Drosophila testis and nonautonomously influences germline stem cell self-renewal. *Cell Stem Cell* 2008; **3**: 44-54 [PMID: 18593558 DOI: 10.1016/j.stem.2008.05.001]
23 **Inaba M**, Yuan H, Salzmann V, Fuller MT, Yamashita YM. E-cadherin is required for centrosome and spindle orientation in Drosophila male germline stem cells. *PLoS One* 2010; **5**: e12473 [PMID: 20824213 DOI: 10.1371/journal.pone.0012473]
24 **Wang H**, Singh SR, Zheng Z, Oh SW, Chen X, Edwards K, Hou SX. Rap-GEF signaling controls stem cell anchoring to their niche through regulating DE-cadherin-mediated cell adhesion in the Drosophila testis. *Dev Cell* 2006; **10**: 117-126 [PMID: 16399083 DOI: 10.1016/j.devcel.2005.11.004]
25 **Leatherman JL**, Dinardo S. Germline self-renewal requires cyst stem cells and stat regulates niche adhesion in Drosophila testes. *Nat Cell Biol* 2010; **12**: 806-811 [PMID: 20622868 DOI: 10.1038/ncb2086]
26 **Srinivasan S**, Mahowald AP, Fuller MT. The receptor tyrosine phosphatase Lar regulates adhesion between Drosophila male germline stem cells and the niche. *Development* 2012; **139**: 1381-1390 [PMID: 22378638 DOI: 10.1242/dev.070052]
27 **Michel M**, Raabe I, Kupinski AP, Pérez-Palencia R, Bökel C. Local BMP receptor activation at adherens junctions in the Drosophila germline stem cell niche. *Nat Commun* 2011; **2**: 415 [PMID: 21811244 DOI: 10.1038/ncomms1426]
28 **Zheng Q**, Wang Y, Vargas E, DiNardo S. magu is required for germline stem cell self-renewal through BMP signaling in the Drosophila testis. *Dev Biol* 2011; **357**: 202-210 [PMID: 21723859 DOI: 10.1016/j.ydbio.2011.06.022]
29 **Hayashi Y**, Kobayashi S, Nakato H. Drosophila glypicans regulate the germline stem cell niche. *J Cell Biol* 2009; **187**: 473-480 [PMID: 19948496 DOI: 10.1083/jcb.200904118]
30 **Shields AR**, Spence AC, Yamashita YM, Davies EL, Fuller MT. The actin-binding protein profilin is required for germline stem cell maintenance and germ cell enclosure by somatic cyst cells. *Development* 2014; **141**: 73-82 [PMID: 24346697 DOI: 10.1242/dev.101931]
31 **Boyle M**, Wong C, Rocha M, Jones DL. Decline in self-renewal factors contributes to aging of the stem cell niche in the Drosophila testis. *Cell Stem Cell* 2007; **1**: 470-478 [PMID: 18371382 DOI: 10.1016/j.stem.2007.08.002]
32 **Voog J**, D'Alterio C, Jones DL. Multipotent somatic stem cells contribute to the stem cell niche in the Drosophila testis. *Nature* 2008; **454**: 1132-1136 [PMID: 18641633 DOI: 10.1038/nature07173]
33 **Issigonis M**, Tulina N, de Cuevas M, Brawley C, Sandler L, Matunis E. JAK-STAT signal inhibition regulates competition in the Drosophila testis stem cell niche. *Science* 2009; **326**: 153-156 [PMID: 19797664 DOI: 10.1126/science.1176817]
34 **Tanentzapf G**, Devenport D, Godt D, Brown NH. Integrin-dependent anchoring of a stem-cell niche. *Nat Cell Biol* 2007; **9**: 1413-1418 [PMID: 17982446 DOI: 10.1038/ncb1660]
35 **Gilboa L**, Forbes A, Tazuke SI, Fuller MT, Lehmann R. Germ line stem cell differentiation in Drosophila requires gap junctions and proceeds via an intermediate state. *Development* 2003; **130**: 6625-6634 [PMID: 14660550 DOI: 10.1242/dev.00853]
36 **Toledano H**, D'Alterio C, Czech B, Levine E, Jones DL. The let-7-Imp axis regulates ageing of the Drosophila testis stem-cell niche. *Nature* 2012; **485**: 605-610 [PMID: 22660319 DOI: 10.1038/nature11061]
37 **Davies EL**, Lim JG, Joo WJ, Tam CH, Fuller MT. The transcriptional regulator lola is required for stem cell maintenance and germ cell differentiation in the Drosophila testis. *Dev Biol* 2013; **373**: 310-321 [PMID: 23159836 DOI: 10.1016/j.ydbio.2012.11.004]
38 **Eun SH**, Stoiber PM, Wright HJ, McMurdie KE, Choi CH, Gan Q, Lim C, Chen X. MicroRNAs downregulate Bag of marbles to ensure proper terminal differentiation in the Drosophila male germline. *Development* 2013; **140**: 23-30 [PMID: 23154414 DOI: 10.1242/dev.086397]
39 **Cherry CM**, Matunis EL. Epigenetic regulation of stem cell maintenance in the Drosophila testis via the nucleosome-remodeling factor NURF. *Cell Stem Cell* 2010; **6**: 557-567 [PMID: 20569693 DOI: 10.1016/j.stem.2010.04.018]
40 **Casper AL**, Baxter K, Van Doren M. no child left behind encodes a novel chromatin factor required for germline stem cell maintenance in males but not females. *Development* 2011; **138**: 3357-3366 [PMID: 21752937 DOI: 10.1242/dev.067942]
41 **Yang SY**, Baxter EM, Van Doren M. Phf7 controls male sex determination in the Drosophila germline. *Dev Cell* 2012; **22**: 1041-1051 [PMID: 22595675 DOI: 10.1016/j.devcel.2012.04.013]
42 **Singh SR**, Zheng Z, Wang H, Oh SW, Chen X, Hou SX. Competitiveness for the niche and mutual dependence of the germline and somatic stem cells in the Drosophila testis are regulated by the JAK/STAT signaling. *J Cell Physiol* 2010; **223**: 500-510 [PMID: 20143337]
43 **Issigonis M**, Matunis E. The Drosophila BCL6 homolog Ken and Barbie promotes somatic stem cell self-renewal in the testis niche. *Dev Biol* 2012; **368**: 181-192 [PMID: 22580161 DOI: 10.1016/j.ydbio.2012.04.034]
44 **Morillo Prado JR**, Chen X, Fuller MT. Polycomb group genes Psc and Su(z)2 maintain somatic stem cell identity and activity in Drosophila. *PLoS One* 2012; **7**: e52892 [PMID: 23285219 DOI: 10.1371/journal.pone.0052892]
45 **Zoller R**, Schulz C. The Drosophila cyst stem cell lineage: Partners behind the scenes? *Spermatogenesis* 2012; **2**: 145-157 [PMID: 23087834 DOI: 10.4161/spmg.21380]
46 **Brogiolo W**, Stocker H, Ikeya T, Rintelen F, Fernandez R, Hafen

E. An evolutionarily conserved function of the drosophila insulin receptor and insulin-like peptides in growth control. *Current biology: CB* 2001; **11**: 213-221 [DOI: 10.1016/S0960-9822(01)00068-9]
47 **Ueishi S**, Shimizu H, Hi Y. Male germline stem cell division and spermatocyte growth require insulin signaling in drosophila. *Cell structure and function* 2009; **34**: 61-69 [DOI: 10.1247/csf.08042]
48 **Wang L**, McLeod CJ, Jones DL. Regulation of adult stem cell behavior by nutrient signaling. *Cell Cycle* 2011; **10**: 2628-2634 [PMID: 21814033 DOI: 10.4161/cc.10.16.17059]
49 **Yang SA**, Wang WD, Chen CT, Tseng CY, Chen YN, Hsu HJ. FOXO/Fringe is necessary for maintenance of the germline stem cell niche in response to insulin insufficiency. *Dev Biol* 2013; **382**: 124-135 [PMID: 23895933 DOI: 10.1016/j.ydbio.2013.07.018]
50 **Ochocki JD**, Simon MC. Nutrient-sensing pathways and metabolic regulation in stem cells. *J Cell Biol* 2013; **203**: 23-33 [PMID: 24127214 DOI: 10.1083/jcb.201303110]
51 **Tulina NM**, Chen WF, Chen JH, Sowcik M, Sehgal A. Day-night cycles and the sleep-promoting factor, Sleepless, affect stem cell activity in the Drosophila testis. *Proc Natl Acad Sci USA* 2014; **111**: 3026-3031 [PMID: 24516136 DOI: 10.1073/pnas.1316552111]
52 **De Loof A**. Ecdysteroids: The overlooked sex steroids of insects? Males: The black box. *Insect Science* 2006; **13**: 325-338 [DOI: 10.1111/j.1744-7917.2006.00101.x]
53 **Loeb MJ**, Woods CW, Brandt EP, Boakovec AB. Larval testes of the tobacco budworm: a new source of insect ecdysteroids. *Science* 1982; **218**: 896-898 [PMID: 17807143 DOI: 10.1126/science.218.4575.896]
54 **Loeb MJ**, Brandt EP, Woods CW, Bell RA. Secretion of ecdysteroid by sheaths of testes of the gypsy moth, lymantria dispar, and its regulation by testis ecdysiotropin. *J Exp Zool* 1988; **248**: 94-100 [DOI: 10.1002/jez.1402480112]
55 **Gelman DB**, Woods CW, Loeb MJ, Borkovec AB. Ecdysteroid synthesis by testes of 5th instars and pupae of the european corn borer, ostrinia nubilalis (hubner). *Invertebr Reprod Dev* 1989; **15**: 177-184 [DOI: 10.1080/07924259.1989.9672041]
56 **Jarvis TD**, Earley FGP, Rees HH. Ecdysteroid biosynthesis in larval testes of spodoptera littoralis. *Insect Biochem Mol Biol* 1994; **24**: 531-537 [DOI: 10.1016/0965-1748(94)90048-5]
57 **Gillott C**, Ismail PM. In vitro synthesis of ecdysteroid by the male accessory reproductive glands, testis and abdominal integument of the adult migratory grasshopper, melanoplus sanguinipes. *Invertebr Reprod Dev* 1995; **27**: 65-71 [DOI: 10.1080/07924259.1995.9672435]
58 **Ables ET**, Drummond-Barbosa D. The steroid hormone ecdysone functions with intrinsic chromatin remodeling factors to control female germline stem cells in Drosophila. *Cell Stem Cell* 2010; **7**: 581-592 [PMID: 21040900 DOI: 10.1016/j.stem.2010.10.001]
59 **Gancz D**, Gilboa L. Hormonal control of stem cell systems. *Annu Rev Cell Dev Biol* 2013; **29**: 137-162 [PMID: 23875645 DOI: 10.1146/annurev-cellbio-101512-122331]
60 **Dorn DC**, Dorn A. Structural polarity and dynamics of male germline stem cells in an insect (milkweed bug Oncopeltus fasciatus). *Methods Mol Biol* 2008; **450**: 71-94 [PMID: 18370052 DOI: 10.1007/978-1-60327-214-8_5]
61 **Hardy RW**, Tokuyasu KT, Lindsley DL, Garavito M. The germinal proliferation center in the testis of drosophila melanogaster. *J Ultra Res* 1979; **69**: 180-190 [DOI: 10.1016/S0022-5320(79)90108-4]
62 **Jaglarz MK**, Kloc M, Jankowska W, Szymanska B, Bilinski SM. Nuage morphogenesis becomes more complex: two translocation pathways and two forms of nuage coexist in Drosophila germline syncytia. *Cell Tissue Res* 2011; **344**: 169-181 [PMID: 21365220 DOI: 10.1007/s00441-011-1145-2]
63 **Zahn J**, Doormann P, Dorn A, Dorn DC. Apoptosis of male germline stem cells after laser ablation of their niche. *Stem Cell Res* 2007; **1**: 75-85 [PMID: 19383387 DOI: 10.1016/j.scr.2007.09.005]
64 **Dorn DC**, Dorn A. Structural characterization and primary in vitro cell culture of locust male germline stem cells and their niche. *Stem Cell Res* 2011; **6**: 112-128 [PMID: 21256099 DOI: 10.1016/j.scr.2010.11.002]
65 **Schmidt ED**, Sehn E, Dorn A. Differentiation and ultrastructure of the spermatogonial cyst cells in the milkweed bug, oncopeltus fasciatus. *Invert Reprod Develop* 2002; **42**: 163-178 [DOI: 10.1080/07924259.2002.9652773]
66 **Klein C.** Die postembryonale gonadenentwicklung und gametogenese bei lymantria dispar l. (lepidoptera) mit besonderer berücksichtigung des gonadensomas. Licht- und elektronenmikroskopische untersuchungen. *Thesis, Universität des Saarlandes* 2000
67 **Balles S**, Maas U, Sehn E, Dorn A. Testis differentiation in the glowworm, Lampyris noctiluca, with special reference to the apical tissue. *J Morphol* 2002; **251**: 22-37 [PMID: 11746466 DOI: 10.1002/jmor.1072]
68 **Naisse J**. [Endocrine control of sexual differentiation in the insect Lampyris noctiluca (Coleoptera Malacoderma Lampyridae). I. Androgenic role of the testes]. *Arch Biol* (Liege) 1966; **77**: 139-201 [PMID: 5908230]
69 **Roosen-Runge EC**. The process of spermatogenesis in animals. CUP Archive, 1977
70 **Coleman MP**, Freeman MR. Wallerian degeneration, wld(s), and nmnat. *Annu Rev Neurosci* 2010; **33**: 245-267 [PMID: 20345246 DOI: 10.1146/annurev-neuro-060909-153248]
71 **Fang Y**, Bonini NM. Axon degeneration and regeneration: insights from Drosophila models of nerve injury. *Annu Rev Cell Dev Biol* 2012; **28**: 575-597 [PMID: 22831639 DOI: 10.1146/annurev-cellbio-101011-155836]
72 **Wang JT**, Medress ZA, Barres BA. Axon degeneration: molecular mechanisms of a self-destruction pathway. *J Cell Biol* 2012; **196**: 7-18 [PMID: 22232700 DOI: 10.1083/jcb.201108111]
73 **Meiri H**, Dormann A, Spira ME. Comparison of ultrastructural changes in proximal and distal segments of transected giant fibers of the cockroach Periplaneta americana. *Brain Res* 1983; **263**: 1-14 [PMID: 6839162]
74 **Jayaram HN**, Kusumanchi P, Yalowitz JA. NMNAT expression and its relation to NAD metabolism. *Curr Med Chem* 2011; **18**: 1962-1972 [PMID: 21517776]
75 **Ding M**, Shen K. The role of the ubiquitin proteasome system in synapse remodeling and neurodegenerative diseases. *Bioessays* 2008; **30**: 1075-1083 [PMID: 18937340]
76 **Wakatsuki S**, Saitoh F, Araki T. ZNRF1 promotes Wallerian degeneration by degrading AKT to induce GSK3B-dependent CRMP2 phosphorylation. *Nat Cell Biol* 2011; **13**: 1415-1423 [PMID: 22057101 DOI: 10.1038/ncb2373]
77 **Hammarlund M**, Nix P, Hauth L, Jorgensen EM, Bastiani M. Axon regeneration requires a conserved MAP kinase pathway. *Science* 2009; **323**: 802-806 [PMID: 19164707 DOI: 10.1126/science.1165527]
78 **Osterloh JM**, Yang J, Rooney TM, Fox AN, Adalbert R, Powell EH, Sheehan AE, Avery MA, Hackett R, Logan MA, MacDonald JM, Ziegenfuss JS, Milde S, Hou YJ, Nathan C, Ding A, Brown RH, Conforti L, Coleman M, Tessier-Lavigne M, Züchner S, Freeman MR. dSarm/Sarm1 is required for activation of an injury-induced axon death pathway. *Science* 2012; **337**: 481-484 [PMID: 22678360 DOI: 10.1126/science.1223899]
79 **Avery MA**, Rooney TM, Pandya JD, Wishart TM, Gillingwater TH, Geddes JW, Sullivan PG, Freeman MR. WldS prevents axon degeneration through increased mitochondrial flux and enhanced mitochondrial Ca2+ buffering. *Curr Biol* 2012; **22**: 596-600 [PMID: 22425157 DOI: 10.1016/j.cub.2012.02.043]
80 **Fang Y**, Soares L, Teng X, Geary M, Bonini NM. A novel Drosophila model of nerve injury reveals an essential role of Nmnat in maintaining axonal integrity. *Curr Biol* 2012; **22**: 590-595 [PMID: 22425156 DOI: 10.1016/j.cub.2012.01.065]
81 **Awasaki T**, Ito K. Engulfing action of glial cells is required for programmed axon pruning during Drosophila metamorphosis. *Curr Biol* 2004; **14**: 668-677 [PMID: 15084281 DOI: 10.1016/j.cub.2004.04.001]
82 **Watts RJ**, Schuldiner O, Perrino J, Larsen C, Luo L. Glia engulf degenerating axons during developmental axon pruning. *Curr Biol* 2004; **14**: 678-684 [PMID: 15084282 DOI: 10.1016/

j.cub.2004.03.035]
83 **Kuo CT**, Jan LY, Jan YN. Dendrite-specific remodeling of Drosophila sensory neurons requires matrix metalloproteases, ubiquitin-proteasome, and ecdysone signaling. *Proc Natl Acad Sci USA* 2005; **102**: 15230-15235 [PMID: 16210248 DOI: 10.1073/pnas.0507393102]
84 **Orlowski RZ**. The role of the ubiquitin-proteasome pathway in apoptosis. *Cell Death Differ* 1999; **6**: 303-313 [PMID: 10381632 DOI: 10.1038/sj.cdd.4400505]
85 **Deckwerth TL**, Johnson EM. Neurites can remain viable after destruction of the neuronal soma by programmed cell death (apoptosis). *Dev Biol* 1994; **165**: 63-72 [PMID: 8088451 DOI: 10.1006/dbio.1994.1234]
86 **Coleman MP**, Perry VH. Axon pathology in neurological disease: A neglected therapeutic target. *Trends in neurosciences* 2002; **25**: 532-537 [DOI: 10.1016/S0166-2236(02)02255-5]
87 **Yamashita YM**, Jones DL, Fuller MT. Orientation of asymmetric stem cell division by the APC tumor suppressor and centrosome. *Science* 2003; **301**: 1547-1550 [PMID: 12970569 DOI: 10.1126/science.1087795]
88 **Yamashita YM**, Mahowald AP, Perlin JR, Fuller MT. Asymmetric inheritance of mother versus daughter centrosome in stem cell division. *Science* 2007; **315**: 518-521 [PMID: 17255513 DOI: 10.1126/science.1134910]
89 **Pereira G**, Yamashita YM. Fly meets yeast: checking the correct orientation of cell division. *Trends Cell Biol* 2011; **21**: 526-533 [PMID: 21705221 DOI: 10.1016/j.tcb.2011.05.004]
90 **Yuan H**, Chiang CY, Cheng J, Salzmann V, Yamashita YM. Regulation of cyclin A localization downstream of Par-1 function is critical for the centrosome orientation checkpoint in Drosophila male germline stem cells. *Dev Biol* 2012; **361**: 57-67 [PMID: 22024320 DOI: 10.1016/j.ydbio.2011.10.010]
91 **Sheng XR**, Matunis E. Live imaging of the Drosophila spermatogonial stem cell niche reveals novel mechanisms regulating germline stem cell output. *Development* 2011; **138**: 3367-3376 [PMID: 21752931 DOI: 10.1242/dev.065797]
92 **Schmidt ED**, Papanikolaou A, Dorn A. The relationship between germline cells and apical complex in the testes of the milkweed bug throughout postembryonic development. *Invertebr Reprod Dev* 2001; **39**: 109-126 [DOI: 10.1080/07924259.2001.9652474]
93 **Bessis M**, Mize C, Prenant M. Erythropoiesis: comparison of in vivo and in vitro amplification. *Blood Cells* 1978; **4**: 155-174 [PMID: 747769]
94 **Manwani D**, Bieker JJ. The erythroblastic island. *Curr Top Dev Biol* 2008; **82**: 23-53 [DOI: 10.1016/S0070-2153(07)00002-6]
95 **Allen TD**, Dexter TM. Ultrastructural aspects of erythropoietic differentiation in long-term bone marrow culture. *Differentiation* 1982; **21**: 86-94 [PMID: 7084572]
96 **Crocker PR**, Werb Z, Gordon S, Bainton DF. Ultrastructural localization of a macrophage-restricted sialic acid binding hemagglutinin, SER, in macrophage-hematopoietic cell clusters. *Blood* 1990; **76**: 1131-1138 [PMID: 2205308]
97 **Ji P**, Lodish HF. Rac GTPases play multiple roles in erythropoiesis. *Haematologica* 2010; **95**: 2-4 [PMID: 20065075 DOI: 10.3324/haematol.2009.015511]
98 **Keerthivasan G**, Wickrema A, Crispino JD. Erythroblast enucleation. *Stem Cells Int* 2011; **2011**: 139851 [PMID: 22007239]
99 **Porcu S**, Manchinu MF, Marongiu MF, Sogos V, Poddie D, Asunis I, Porcu L, Marini MG, Moi P, Cao A, Grosveld F, Ristaldi MS. Klf1 affects DNase II-alpha expression in the central macrophage of a fetal liver erythroblastic island: a non-cell-autonomous role in definitive erythropoiesis. *Mol Cell Biol* 2011; **31**: 4144-4154 [PMID: 21807894 DOI: 10.1128/MCB.05532-11]
100 **Yoshida H**, Okabe Y, Kawane K, Fukuyama H, Nagata S. Lethal anemia caused by interferon-beta produced in mouse embryos carrying undigested DNA. *Nat Immunol* 2005; **6**: 49-56 [PMID: 15568025 DOI: 10.1038/ni1146]
101 **Hanspal M**, Hanspal JS. The association of erythroblasts with macrophages promotes erythroid proliferation and maturation: a 30-kD heparin-binding protein is involved in this contact. *Blood* 1994; **84**: 3494-3504 [PMID: 7949103]
102 **Hanspal M**, Smockova Y, Uong Q. Molecular identification and functional characterization of a novel protein that mediates the attachment of erythroblasts to macrophages. *Blood* 1998; **92**: 2940-2950 [PMID: 9763581]
103 **Kang JA**, Zhou Y, Weis TL, Liu H, Ulaszek J, Satgurunathan N, Zhou L, van Besien K, Crispino J, Verma A, Low PS, Wickrema A. Osteopontin regulates actin cytoskeleton and contributes to cell proliferation in primary erythroblasts. *J Biol Chem* 2008; **283**: 6997-7006 [PMID: 18174176 DOI: 10.1074/jbc.M706712200]
104 **Miharada K**, Hiroyama T, Sudo K, Nagasawa T, Nakamura Y. Efficient enucleation of erythroblasts differentiated in vitro from hematopoietic stem and progenitor cells. *Nat Biotechnol* 2006; **24**: 1255-1256 [PMID: 16980975 DOI: 10.1038/nbt1245]
105 **Rendu F**, Brohard-Bohn B. The platelet release reaction: granules' constituents, secretion and functions. *Platelets* 2001; **12**: 261-273 [PMID: 11487378 DOI: 10.1080/09537100120068170]
106 **Yu M**, Cantor AB. Megakaryopoiesis and thrombopoiesis: an update on cytokines and lineage surface markers. *Methods Mol Biol* 2012; **788**: 291-303 [PMID: 22130715 DOI: 10.1007/978-1-61779-307-3_20]
107 **Schulze H**, Shivdasani RA. Mechanisms of thrombopoiesis. *J Thromb Haemost* 2005; **3**: 1717-1724 [PMID: 16102038]
108 **Ellis MH**, Avraham H, Groopman JE. The regulation of megakaryocytopoiesis. *Blood Rev* 1995; **9**: 1-6 [PMID: 7795420 DOI: 10.1016/0268-960X(95)90034-9]
109 **Matsumura I**, Kanakura Y. Molecular control of megakaryopoiesis and thrombopoiesis. *Int J Hematol* 2002; **75**: 473-483 [PMID: 12095146]
110 **Chow DC**, Wenning LA, Miller WM, Papoutsakis ET. Modeling pO(2) distributions in the bone marrow hematopoietic compartment. II. Modified Kroghian models. *Biophys J* 2001; **81**: 685-696 [PMID: 11463617 DOI: 10.1016/S0006-3495(01)75733-5]
111 **Pallotta I**, Lovett M, Rice W, Kaplan DL, Balduini A. Bone marrow osteoblastic niche: a new model to study physiological regulation of megakaryopoiesis. *PLoS One* 2009; **4**: e8359 [PMID: 20027303 DOI: 10.1371/journal.pone.0008359]
112 **Bury L**, Malara A, Gresele P, Balduini A. Outside-in signalling generated by a constitutively activated integrin αIIbβ3 impairs proplatelet formation in human megakaryocytes. *PLoS One* 2012; **7**: e34449 [PMID: 22539947 DOI: 10.1371/journal.pone.0034449]
113 **Kaushansky K**, Drachman JG. The molecular and cellular biology of thrombopoietin: the primary regulator of platelet production. *Oncogene* 2002; **21**: 3359-3367 [PMID: 12032774 DOI: 10.1038/sj.onc.1205323]
114 **Kosaki G**, Kambayashi J. Thrombocytogenesis by megakaryocyte; Interpretation by protoplatelet hypothesis. *Proc Jpn Acad Ser B Phys Biol Sci* 2011; **87**: 254-273 [PMID: 21558761 DOI: 10.2183/pjab.87.254]
115 **Patel SR**, Hartwig JH, Italiano JE. The biogenesis of platelets from megakaryocyte proplatelets. *J Clin Invest* 2005; **115**: 3348-3354 [PMID: 16322779]
116 **Cramer EM**, Norol F, Guichard J, Breton-Gorius J, Vainchenker W, Massé JM, Debili N. Ultrastructure of platelet formation by human megakaryocytes cultured with the Mpl ligand. *Blood* 1997; **89**: 2336-2346 [PMID: 9116277]
117 **Italiano JE**, Lecine P, Shivdasani RA, Hartwig JH. Blood platelets are assembled principally at the ends of proplatelet processes produced by differentiated megakaryocytes. *J Cell Biol* 1999; **147**: 1299-1312 [PMID: 10601342 DOI: 10.1083/jcb.147.6.1299]
118 **Kosaki G**. In vivo platelet production from mature megakaryocytes: does platelet release occur via proplatelets? *Int J Hematol* 2005; **81**: 208-219 [PMID: 15814332 DOI: 10.1532/IJH97.04177]
119 **Kosaki G**. Platelet production by megakaryocytes: protoplatelet theory justifies cytoplasmic fragmentation model. *Int J Hematol* 2008; **88**: 255-267 [PMID: 18751873 DOI: 10.1007/s12185-008-0147-7]
120 **Falcieri E**, Bassini A, Pierpaoli S, Luchetti F, Zamai L, Vitale M, Guidotti L, Zauli G. Ultrastructural characterization of maturation, platelet release, and senescence of human cultured

megakaryocytes. *Anat Rec* 2000; **258**: 90-99 [PMID: 10603452]
121 **Kaluzhny Y**, Ravid K. Role of apoptotic processes in platelet biogenesis. *Acta Haematol* 2004; **111**: 67-77 [PMID: 14646346 DOI: 10.1159/000074487]
122 **De Botton S**, Sabri S, Daugas E, Zermati Y, Guidotti JE, Hermine O, Kroemer G, Vainchenker W, Debili N. Platelet formation is the consequence of caspase activation within megakaryocytes. *Blood* 2002; **100**: 1310-1317 [PMID: 12149212 DOI: 10.1182/blood-2002-03-0686]
123 **Kaluzhny Y**, Yu G, Sun S, Toselli PA, Nieswandt B, Jackson CW, Ravid K. BclxL overexpression in megakaryocytes leads to impaired platelet fragmentation. *Blood* 2002; **100**: 1670-1678 [PMID: 12176887 DOI: 10.1182/blood-2001-12-0263]
124 **Kim JA**, Jung YJ, Seoh JY, Woo SY, Seo JS, Kim HL. Gene expression profile of megakaryocytes from human cord blood CD34(+) cells ex vivo expanded by thrombopoietin. *Stem Cells* 2002; **20**: 402-416 [PMID: 12351811 DOI: 10.1634/stemcells.20-5-402]
125 **Battinelli E**, Willoughby SR, Foxall T, Valeri CR, Loscalzo J. Induction of platelet formation from megakaryocytoid cells by nitric oxide. *Proc Natl Acad Sci USA* 2001; **98**: 14458-14463 [PMID: 11734646 DOI: 10.1073/pnas.241427398]
126 **Nagata Y**, Yoshikawa J, Hashimoto A, Yamamoto M, Payne AH, Todokoro K. Proplatelet formation of megakaryocytes is triggered by autocrine-synthesized estradiol. *Genes Dev* 2003; **17**: 2864-2869 [PMID: 14665668 DOI: 10.1101/gad.1128003]
127 **Crispino JD**. GATA1 in normal and malignant hematopoiesis. *Semin Cell Dev Biol* 2005; **16**: 137-147 [PMID: 15659348 DOI: 10.1016/j.semcdb.2004.11.002]
128 **Shivdasani RA**, Fujiwara Y, McDevitt MA, Orkin SH. A lineage-selective knockout establishes the critical role of transcription factor GATA-1 in megakaryocyte growth and platelet development. *EMBO J* 1997; **16**: 3965-3973 [PMID: 9233806 DOI: 10.1093/emboj/16.13.3965]
129 **Shivdasani RA**, Rosenblatt MF, Zucker-Franklin D, Jackson CW, Hunt P, Saris CJ, Orkin SH. Transcription factor NF-E2 is required for platelet formation independent of the actions of thrombopoietin/MGDF in megakaryocyte development. *Cell* 1995; **81**: 695-704 [PMID: 7774011]
130 **Yacobi-Sharon K**, Namdar Y, Arama E. Alternative germ cell death pathway in Drosophila involves HtrA2/Omi, lysosomes, and a caspase-9 counterpart. *Dev Cell* 2013; **25**: 29-42 [PMID: 23523076 DOI: 10.1016/j.devcel.2013.02.002]
131 **Yoshida S**. Stem cell niche system in mouse spermatogenesis. Male Germline Stem Cells: Developmental and Regenerative Potential Stem Cell Biology and Regenerative Medicine, 2011
132 **de Rooij DG**, Russell LD. All you wanted to know about spermatogonia but were afraid to ask. *J Androl* 2000; **21**: 776-798 [PMID: 11105904]
133 **Russell LD**, Ettlin RA, Hikim APS, Clegg ED. Histological and histopathological evaluation of the testis. *Int J Androl* 1993; **16**: 83-83 [DOI: 10.1111/j.1365-2605.1993.tb01156.x]
134 **Paratcha G**, Ledda F. The GTPase-activating protein Rap1GAP: a new player to modulate Ret signaling. *Cell Res* 2011; **21**: 217-219 [PMID: 20956997 DOI: 10.1038/cr.2010.143]
135 **Hofmann MC**, Braydich-Stolle L, Dym M. Isolation of male germ-line stem cells; influence of GDNF. *Dev Biol* 2005; **279**: 114-124 [PMID: 15708562 DOI: 10.1016/j.ydbio.2004.12.006]
136 **Tokuda M**, Kadokawa Y, Kurahashi H, Marunouchi T. CDH1 is a specific marker for undifferentiated spermatogonia in mouse testes. *Biol Reprod* 2007; **76**: 130-141 [PMID: 17035642 DOI: 10.1095/biolreprod.106.053181]
137 **Oatley JM**, Oatley MJ, Avarbock MR, Tobias JW, Brinster RL. Colony stimulating factor 1 is an extrinsic stimulator of mouse spermatogonial stem cell self-renewal. *Development* 2009; **136**: 1191-1199 [PMID: 19270176 DOI: 10.1242/dev.032243]
138 **Kanatsu-Shinohara M**, Ogonuki N, Inoue K, Miki H, Ogura A, Toyokuni S, Shinohara T. Long-term proliferation in culture and germline transmission of mouse male germline stem cells. *Biol Reprod* 2003; **69**: 612-616 [PMID: 12700182 DOI: 10.1095/biolreprod.103.017012]
139 **Kanatsu-Shinohara M**, Inoue K, Ogonuki N, Miki H, Yoshida S, Toyokuni S, Lee J, Ogura A, Shinohara T. Leukemia inhibitory factor enhances formation of germ cell colonies in neonatal mouse testis culture. *Biol Reprod* 2007; **76**: 55-62 [PMID: 17021343 DOI: 10.1095/biolreprod.106.055863]
140 **Chen C**, Ouyang W, Grigura V, Zhou Q, Carnes K, Lim H, Zhao GQ, Arber S, Kurpios N, Murphy TL, Cheng AM, Hassell JA, Chandrashekar V, Hofmann MC, Hess RA, Murphy KM. ERM is required for transcriptional control of the spermatogonial stem cell niche. *Nature* 2005; **436**: 1030-1034 [PMID: 16107850 DOI: 10.1038/nature03894]
141 **Shinohara T**, Orwig KE, Avarbock MR, Brinster RL. Spermatogonial stem cell enrichment by multiparameter selection of mouse testis cells. *Proc Natl Acad Sci USA* 2000; **97**: 8346-8351 [PMID: 10900001 DOI: 10.1073/pnas.97.15.8346]
142 **Kanatsu-Shinohara M**, Takehashi M, Takashima S, Lee J, Morimoto H, Chuma S, Raducanu A, Nakatsuji N, Fässler R, Shinohara T. Homing of mouse spermatogonial stem cells to germline niche depends on beta1-integrin. *Cell Stem Cell* 2008; **3**: 533-542 [PMID: 18983968 DOI: 10.1016/j.stem.2008.08.002]
143 **Lassalle B**, Bastos H, Louis JP, Riou L, Testart J, Dutrillaux B, Fouchet P, Allemand I. 'Side Population' cells in adult mouse testis express Bcrp1 gene and are enriched in spermatogonia and germinal stem cells. *Development* 2004; **131**: 479-487 [PMID: 14681185 DOI: 10.1242/dev.00918]
144 **Szollosi A**, Marcaillou C. Electron microscope study of the blood-testis barrier in an insect: Locusta migratoria. *J Ultrastruct Res* 1977; **59**: 158-172 [PMID: 864819]
145 **Fuentealba LC**, Obernier K, Alvarez-Buylla A. Adult neural stem cells bridge their niche. *Cell Stem Cell* 2012; **10**: 698-708 [PMID: 22704510 DOI: 10.1016/j.stem.2012.05.012]
146 **Fuchs E**, Tumbar T, Guasch G. Socializing with the neighbors: stem cells and their niche. *Cell* 2004; **116**: 769-778 [PMID: 15035980]
147 **Mills JC**, Gordon JI. The intestinal stem cell niche: there grows the neighborhood. *Proc Natl Acad Sci USA* 2001; **98**: 12334-12336 [PMID: 11675485 DOI: 10.1073/pnas.231487198]
148 **Zhu TS**, Costello MA, Talsma CE, Flack CG, Crowley JG, Hamm LL, He X, Hervey-Jumper SL, Heth JA, Muraszko KM, DiMeco F, Vescovi AL, Fan X. Endothelial cells create a stem cell niche in glioblastoma by providing NOTCH ligands that nurture self-renewal of cancer stem-like cells. *Cancer Res* 2011; **71**: 6061-6072 [PMID: 21788346 DOI: 10.1158/0008-5472.CAN-10-4269]
149 **Ding BS**, Nolan DJ, Butler JM, James D, Babazadeh AO, Rosenwaks Z, Mittal V, Kobayashi H, Shido K, Lyden D, Sato TN, Rabbany SY, Rafii S. Inductive angiocrine signals from sinusoidal endothelium are required for liver regeneration. *Nature* 2010; **468**: 310-315 [PMID: 21068842 DOI: 10.1038/nature09493]
150 **Barroca V**, Lassalle B, Coureuil M, Louis JP, Le Page F, Testart J, Allemand I, Riou L, Fouchet P. Mouse differentiating spermatogonia can generate germinal stem cells in vivo. *Nat Cell Biol* 2009; **11**: 190-196 [PMID: 19098901 DOI: 10.1038/ncb1826]
151 **Nakagawa T**, Sharma M, Nabeshima Y, Braun RE, Yoshida S. Functional hierarchy and reversibility within the murine spermatogenic stem cell compartment. *Science* 2010; **328**: 62-67 [PMID: 20299552 DOI: 10.1126/science.1182868]
152 **Brawley C**, Matunis E. Regeneration of male germline stem cells by spermatogonial dedifferentiation in vivo. *Science* 2004; **304**: 1331-1334 [PMID: 15143218 DOI: 10.1126/science.1097676]
153 **Spradling A**, Fuller MT, Braun RE, Yoshida S. Germline stem cells. *Cold Spring Harb Perspect Biol* 2011; **3**: a002642 [PMID: 21791699 DOI: 10.1101/cshperspect.a002642]
154 **Szöllösi A**, Marcaillou C. The apical cell of the locust testis: an ultrastructural study. *J Ultrastruct Res* 1979; **69**: 331-342 [PMID: 513185]
155 **Lingor P**, Koch JC, Tönges L, Bähr M. Axonal degeneration as a therapeutic target in the CNS. *Cell Tissue Res* 2012; **349**: 289-311 [PMID: 22392734 DOI: 10.1007/s00441-012-1362-3]
156 **Beirowski B**, Adalbert R, Wagner D, Grumme DS, Addicks K,

Ribchester RR, Coleman MP. The progressive nature of Wallerian degeneration in wild-type and slow Wallerian degeneration (WldS) nerves. *BMC Neurosci* 2005; **6**: 6 [PMID: 15686598 DOI: 10.1186/1471-2202-6-6]

157 **Kerschensteiner M**, Schwab ME, Lichtman JW, Misgeld T. In vivo imaging of axonal degeneration and regeneration in the injured spinal cord. *Nat Med* 2005; **11**: 572-577 [PMID: 15821747 DOI: 10.1038/nm1229]

P- Reviewer: Li SC, Song GB **S- Editor**: Song XX
L- Editor: A **E- Editor**: Liu SQ

World Journal of Stem Cells

Submit a Manuscript: http://www.wjgnet.com/esps/
Help Desk: http://www.wjgnet.com/esps/helpdesk.aspx
DOI: 10.4252/wjsc.v7.i6.945

World J Stem Cells 2015 July 26; 7(6): 945-955
ISSN 1948-0210 (online)

REVIEW

New insights into the epigenetic control of satellite cells

Viviana Moresi, Nicoletta Marroncelli, Sergio Adamo

Viviana Moresi, Nicoletta Marroncelli, Sergio Adamo, Department of Anatomical, Histological, Forensic and Orthopaedic Sciences, Sapienza University of Rome, 00161 Rome, Italy

Author contributions: Moresi V, Marroncelli N and Adamo S wrote the paper.

Supported by The following grants: SA: Sapienza University 2012 (# C26A125ENW) and PRIN 2012 (# 2012N8YJC3); NM: Sapienza University "Avvio alla ricerca" 2014; and VM: EU Marie Curie "Muscle repair-Mdx", Italian Ministry of Instruction, University and Research FIRB project and Italian Ministry of Health "Ricerca finalizzata" grants.

Conflict-of-interest statement: The authors declare no conflicts of interest.

Correspondence to: Sergio Adamo, MD, Department of Anatomical, Histological, Forensic and Orthopaedic Sciences, Sapienza University of Rome, Via Antonio Scarpa 16, 00161 Rome, Italy. sergio.adamo@uniroma1.it
Telephone: +39-6-49766756
Fax: +39-6-4462854

Received: November 26, 2014
Peer-review started: November 26, 2014
First decision: December 12, 2014
Revised: February 12, 2015
Accepted: May 8, 2015
Article in press: May 11, 2015
Published online: July 26, 2015

Abstract

Epigenetics finely tunes gene expression at a functional level without modifying the DNA sequence, thereby contributing to the complexity of genomic regulation. Satellite cells (SCs) are adult muscle stem cells that are important for skeletal post-natal muscle growth, homeostasis and repair. The understanding of the epigenome of SCs at different stages and of the multiple layers of the post-transcriptional regulation of gene expression is constantly expanding. Dynamic interactions between different epigenetic mechanisms regulate the appropriate timing of muscle-specific gene expression and influence the lineage fate of SCs. In this review, we report and discuss the recent literature about the epigenetic control of SCs during the myogenic process from activation to proliferation and from their commitment to a muscle cell fate to their differentiation and fusion to myotubes. We describe how the co-ordinated activities of the histone methyltransferase families Polycomb group (PcG), which represses the expression of developmentally regulated genes, and Trithorax group, which antagonizes the repressive activity of the PcG, regulate myogenesis by restricting gene expression in a time-dependent manner during each step of the process. We discuss how histone acetylation and deacetylation occurs in specific loci throughout SC differentiation to enable the time-dependent transcription of specific genes. Moreover, we describe the multiple roles of microRNA, an additional epigenetic mechanism, in regulating gene expression in SCs, by repressing or enhancing gene transcription or translation during each step of myogenesis. The importance of these epigenetic pathways in modulating SC activation and differentiation renders them as promising targets for disease interventions. Understanding the most recent findings regarding the epigenetic mechanisms that regulate SC behavior is useful from the perspective of pharmacological manipulation for improving muscle regeneration and for promoting muscle homeostasis under pathological conditions.

Key words: Histone methylation; Histone acetylation; Muscle stem cells; Adult stem cells; Noncoding RNAs; Satellite cell activation; Satellite cell differentiation; Satellite cell quiescence

Core tip: Skeletal muscle needs to efficiently respond to internal and external stimuli, and satellite cells (SCs), the stem cells of muscle, play key roles in the preservation of muscle mass under both physiological and pathological conditions. Epigenetic pathways participate in co-ordinating the precise time-dependent expression of different subsets of myogenic genes in SCs. Thus, these pathways represent promising targets for therapeutic interventions. In this review, we focus on the epigenetic changes mediated by histone modifications - methylation or acetylation - and by noncoding mRNAs throughout SC differentiation.

Moresi V, Marroncelli N, Adamo S. New insights into the epigenetic control of satellite cells. *World J Stem Cells* 2015; 7(6): 945-955 Available from: URL: http://www.wjgnet.com/1948-0210/full/v7/i6/945.htm DOI: http://dx.doi.org/10.4252/wjsc.v7.i6.945

SATELLITE CELLS

The first report and ultrastructural description of satellite cells (SCs) was in 1961 when Mauro reported the presence of cells containing a scant cytoplasm that were "intimately associated with the muscle fiber wedged between the plasma membrane of the muscle fiber and the basement membrane"; Mauro termed them SCs[1]. In the same report, despite the absence of direct functional evidence, Mauro proposed that SCs "might be pertinent to the vexing problem of skeletal muscle regeneration".

In subsequent decades, Mauro's hypothesis proved true, and a number of studies demonstrated that SCs are the key mediators of post-natal skeletal muscle growth, homeostasis and repair[2-4]. The core functions of SCs are the repair of damaged muscle fibers and the maintenance of an adequate pool of stem cells. In fact, dividing SCs were shown by autoradiographic studies to supply both new nuclei within growing or regenerating muscle fibers and new SCs adjacent to the muscle fibers[5,6].

Quiescent SCs express the transcription factor Pax7[7]. However, quiescent SCs constitute a heterogeneous population: most SCs are committed to the myogenic lineage ($Pax7^+$, $Myf5^+$), whereas a small subpopulation of SCs ($Pax7^+$, $Myf5^-$) are interpreted as representing satellite stem cells, whose asymmetric division produces both $Pax7^+$, $Myf5^-$ stem cells and $Pax7^+$, $Myf5^+$ committed SCs. SCs are also capable of maintaining or expanding their number *via* symmetric division[8,9]. The observation that SC proliferation contributes to both the growth or repair of the muscle fiber and the maintenance of the SC pool provided the basis for considering SCs as muscle stem cells[10]. The equilibrium between asymmetric and symmetric division is therefore relevant to the maintenance of a homeostatic population of stem cells. In SCs, this equilibrium is influenced by signaling that includes WNT7A and its receptor Frizzled 7 (Fzd7) *via* the -catenin-independent, non-canonical planar cell polarity pathway[11]. Such signals dictate the polarity (parallel or perpendicular) of the orientation of mitotic division with respect to the fiber sarcolemma (and the basal lamina). WNT7A activity induces stem cells to divide in a planar orientation, parallel to the fiber sarcolemma, thereby favoring symmetric division, which produces two $Pax7^+$, $Myf5^-$ stem cells. Conversely, in the absence of WNT7A activity, the mitotic spindle is oriented perpendicular to the fiber sarcolemma, thereby favoring asymmetric division into two daughter cells; the daughter cell that contacts the basal lamina retains stem cell characteristics ($Pax7^+$, $Myf5^-$), whereas the other daughter cells, which contacts the fiber sarcolemma, becomes a $Pax7^+$, $Myf5^+$ committed SC.

SCs in muscle regeneration

Many stimuli, such as those present in injured or diseased muscle, induce SCs to activate, expand and contribute to new fiber formation. Importantly, SC activation is not restricted to the damaged area; rather, SC proliferation and migration to the regeneration site have been observed along entire fibers of injured muscles[12]. Muscle regeneration is absolutely dependent upon muscle-resident $Pax7^+$ cells[13], which predominantly, although not exclusively, consist of SCs[14]. The absolute requirement of $Pax7^+$ SCs for muscle regeneration was demonstrated in different studies[13,15,16]. In the absence of $Pax7^+$ SCs, regeneration does not take place; instead, fibro-adipogenic cells invade the tissue. In keeping with the notion that SC-dependent muscle regeneration processes are similar to those of embryonic myogenesis, SC activation involves the upregulation of myogenic basic helix-loop-helix transcription factors and SC differentiation[17]. In particular, at the molecular level, the activation of SCs is characterized by the rapid expression of *MyoD* and *Myf5*, which is triggered by Pax7 (and its paralog Pax3)[18] and is modulated by epigenetic mechanisms[19].

After the proliferation phase, the expression of the myogenesis regulatory factor (MRF) members myogenin and MRF4 is upregulated, leading to terminal SC differentiation[20]. This event is concomitant with the activation of the cell cycle arrest protein p21 and permanent exit from the cell cycle. The completion of the SC differentiation program includes the activation of muscle-specific proteins, such as myosin heavy chains, and the fusion of SCs to each other or the repair of damaged muscle. SC fusion, which is a complex and tightly controlled process[21], is regulated by numerous proteins involved in cell-cell adhesion and actin dynamics[22-25], as well as muscle-specific membrane proteins[26].

The depletion of SCs is a common occurrence in

chronic muscle degenerative diseases, and these cells cannot be replaced. Thus, the regulation of SC renewal is central to the promotion of muscle regeneration in muscle diseases, such as muscular dystrophies.

EPIGENETIC MECHANISMS OF GENE REGULATION

Epigenetics is responsible for the identity of distinct cell types despite the same genetic information by modulating gene expression without altering the genetic code. In other words, the ensemble of epigenetic characteristics, referred to as the epigenome, determines the gene expression pattern that defines the distinct characteristics and functions of each cell type[27]. In fact, although their genomes are essentially identical, the cell types in a multicellular organism perform strikingly different behaviors over extended periods. Lineage commitment during development is the most extreme example of epigenetics. During embryogenesis, cells progress from totipotency to terminal differentiation, and each step of this progression involves the establishment of a stable state in which specific developmental commitments that can be transmitted to daughter cells are encoded. The understanding of the epigenome of different cell types and the complexity of the post-transcriptional control of gene expression is constantly expanding due to the development of new technologies and the continuous discovery of noncoding RNAs that participate in epigenetic regulation.

Histone methylation

The eukaryotic genome is packaged into chromatin, a chain of nucleosomes composed of four core histones - H2A, H2B, H3, and H4 - whose amino-terminal tails are exposed on the surface of nucleosomes and are subjected to a wide range of post-translational modifications[28,29]. Gene activation and repression, as well as transcriptional initiation and elongation, are regulated by many such histone modifications. In the last decade, studies of human and mouse embryonic stem cells have delineated the role of the histone methyltransferase (HMT) families Polycomb group (PcG) and Trithorax group (TrxG) in modulating the pluripotency and lineage restriction of several cell types[30]. For instance, numerous trimethylations of histone 3 lysine 4 (H3K4me3) mediated by the TrxG family surrounding the transcription start sites indicate transcriptional gene activation, and trimethylations of histone 3 lysine 36 (H3K36me3) in the gene body are generally associated with active gene transcription; alternatively, the trimethylation of histone 3 lysine 27 (H3K27me3) mediated by the PcG complex is associated with transcriptional repression[28]. Although the repressive H3K27me3 mark is transmitted to daughter cells[31] and is dominant over the permissive H3K4me3 mark[32], transcriptional gene activation requires the demethylation of H3K27me3, which is mediated by the demethylase families lysine-specific demethylase 6A (Kdm6a) and KDM1 lysine-specific demethylase 6B (Kdm6b)[33-35]. Thus, whereas polycomb repressive complex 2 (PRC2) establishes gene silencing at developmentally regulated loci, the TrxG and Kdm6a/Kdm6b families work together to antagonize the repressive activity of PRC2 and to promote gene expression in specific cell types.

Histone acetylation

Histone acetylation modulates transcription *via* multiple mechanisms. The acetylation of lysine residues within histone tails neutralizes their positive charge, thereby facilitating chromatin relaxation and increasing the accessibility of transcription factors to their target genes[36]. Acetylated histones are also recognized as binding sites for transcriptional activators. Conversely, histone deacetylation induces transcriptional repression by compacting the chromatin structure[37]. The combined activities of two enzyme families, histone acetyltransferases (HATs) and deacetylases (HDACs), determine the overall levels of histone acetylation in the genome. Both HATs and HDACs act on chromatin by associating with a variety of DNA-binding transactivator proteins. In some cases, DNA targeting involves other chromatin-modifying activities, such as histone methylation. Thus, the effects of HATs and HDACs on gene regulation depend on the cell type and the spectrum of available partners[38].

Noncoding RNAs

Advances in the field of gene regulation mediated by single-stranded noncoding RNA molecules have demonstrated their importance in gene regulatory networks. Until recently, small noncoding RNAs (miRNAs) were believed to solely negatively regulate target mRNAs[39]. However, published studies are increasingly indicating that miRNAs can also stimulate gene expression in response to specific cellular conditions or cofactors[40]. miRNAs are able to reduce gene expression *via* multiple mechanisms. At the transcriptional level, miRNAs repress gene expression by pairing nucleotides 2 to 8, termed the seed region, to the seed match site in the target mRNA, typically positioned at the 3' UTR or, less frequently, at the 5' UTR or the coding region[41]. In addition to transcriptional effects, miRNAs can repress translation initiation *via* multiple mechanisms, such as promoting mRNA degradation or interfering with the formation of closed-loop mRNA or other translation initiation factors[41]. Moreover, increasing evidence indicates that some miRNAs can upregulate gene expression in specific cell types and under certain conditions *via* the direct action of miRNAs or *via* the indirect inhibition of repressive miRNA activity[42]. Another class of noncoding RNAs, long noncoding RNAs, has been shown to take part in many transcription regulatory processes[43] and post-transcriptional events, such as mRNA stability and translational control[44-46], and to function as competing endogenous RNA[47-49] by acting as an miRNA sponge to participate with coding RNA in a regulatory circuit that controls the binding of RNA to

miRNA.

Reciprocal and dynamic interactions between different epigenetic mechanisms and transcription factors modulate gene expression. For instance, changes in histone modifications are caused by the recruitment of chromatin-modifying enzymes, such as HATs or HMTs, by transcription factors and the RNA polymerase Ⅱ complex[28]; at the same time, combinations of histone modifications in the proximity of consensus sequences may anticipate and direct the binding of the transcription factor, facilitating the transcriptional activation of a given gene[50].

Numerous epigenetic mechanisms regulate the different phases of myogenesis, including chromatin remodeling and post-transcriptional gene regulation mediated by noncoding RNAs[51-53]. Such orchestrated regulation permits the correct timing of muscle-specific gene expression and influences the fate of muscle progenitors into muscle or non-muscle cell lineages[54,55]. In this review, we report and discuss the recent literature about the epigenetic regulation of the myogenic process from activation to proliferation and SC commitment. We focus on the epigenetic changes, specifically those mediated by chromatin methylation or acetylation and noncoding RNA function to regulate gene expression, that occur during the different steps of SC differentiation.

EPIGENETICS IN SCs

Epigenetics mediates most of the signaling integrating the regeneration cues released by interstitial cells and by the external environment within the SC niche. Our understanding of the highly coordinated layers of epigenetic regulation of SC maintenance, activation and differentiation and cross-talk of epigenetic regulatory mechanisms with muscle-specific transcriptional machinery has tremendously increased due to the recent results obtained *via* next-generation genome-wide sequencing[56]. Using ChIP-Seq experiments, chipped chromatin can currently be entirely mapped across the genome to identify the regions that are over-represented among these sequences, revealing the interactions between chromatin-remodeling enzymes, transcription factors and DNA, thereby facilitating the production of chromatin-state maps.

Epigenetic control of SC quiescence

In quiescent SCs, while the *Pax7* gene must be expressed, modulators of cell cycle progression and transcription factors of the myogenic lineage need to remain silenced. Increasing studies have suggested that quiescent SCs are not in a dormant state but rather are primed for activation and differentiation in response to external stimuli[57,58]. At the chromatin level, this primed state is maintained by the general lack of the repressive mark H3K27me3 across the genome and the concomitant presence of H3K4me3 at the transcription start sites of a large number of genes (nearly 50% of all annotated genes)[59], including myogenic regulatory factors such as MyoD, SRF and Myf5[60], whose encoded proteins are the primary activators of the myogenic program. Consistent with the notion that H3K4me3 alone does not predict the transcriptional state of a gene but rather marks the gene for transcriptional activation[61], neither the number nor the identity of genes marked by H3K4me3 is significantly different between activated and quiescent SCs. Indeed, SC activation is accompanied by the retention of H3K4me3 and the acquisition of H3K27me3 *via* PcG members[62], often in association with the transcriptional repressors YY1 and HDAC1. Interestingly, low levels of H3K27me3 are associated with the pluripotency of embryonic stem cells[56,63]. The current understanding is that the general lack of repressive H3K27me3 marks and the concomitant presence of H3K4me3 at the transcription start sites of a large number of genes may establish a permissive chromatin state that underlies and permits the pluripotency of stem cells. In addition, numerous transcription start sites across the genome of quiescent SCs contain bivalent chromatin domains[59], which are characterized by the concomitant presence of both H3K4me3 and H3K27me3 marks. Consistent with the presence of H3K27me3 marks, these genes are either not transcribed or transcribed at very low levels. Interestingly, bivalent domains correspond to genes that are associated with the development of other organs and tissues aside from muscle, suggesting that SCs retain the potential to adopt a non-myogenic fate because of the presence of bivalent domains that contribute to the determination of cell lineage[59].

miRNAs also contribute to the generation of an epigenetic state that enables the maintenance of the myogenic lineage in quiescent SCs and that facilitates the activation of muscle gene expression and the formation of differentiated myotubes in response to SC activation. An important role in the maintenance of muscle stem-cell quiescence has been demonstrated for microRNA-489, which is highly expressed in quiescent SCs, in which it suppresses the expression of the oncogene DEK, and which is rapidly downregulated upon SC differentiation[57]. Additionally, miR-31 has been demonstrated to play an important role in quiescent SCs[58]. In quiescent SCs, the *Myf5* gene has already been transcribed but cannot be expressed because miR-31 functionally inactivates Myf5 mRNA by retaining it inside cytoplasmic mRNP granules, thereby preventing its translation and blocking myogenic differentiation[58].

Epigenetic control of SC activation

In response to different stimuli, *e.g.,* muscle damage, SCs become activated, begin to express cell cycle markers, which are readily marked by the permissive H3K4me3[64], and re-enter the cell cycle. SCs that divide in a parallel orientation to the myofibers, undergo a symmetrical cell division and give rise to two SCs that can return to the quiescent state[8]. In contrast, cells that divide in the sagittal orientation undergo asymmetric cell division to produce one cell that returns to the

quiescent state and one proliferating myoblast[8]. The latter cell expresses the *Myf5* and *MyoD* genes, as well as genes that regulate cell cycle progression, all of which are characterized by the enrichment of the transcriptionally permissive H3K4me3 mark within their associated chromatin[19]; Pax7 is progressively silenced while transitioning from a transcriptionally permissive state of H3K4me3 to a repressive state of H3K27me3 throughout cell differentiation[65]. Additional mechanisms that regulate SC proliferation include p38-gamma MAPK, which phosphorylates the MyoD protein to reinforce the interaction between MyoD and the HMT KMT1A, and the consequent inhibition of the premature expression of the myogenin gene. Consistently, in p38-gamma MAPK-null SCs, KMT1A cannot associate with the myogenin promoter; therefore, myogenin is expressed earlier, resulting in decreased SC proliferation and defective differentiation[66].

During myoblast proliferation, distinct classes of HDACs are also involved in the repression of muscle gene transcription by countering the activities of HATs. Whereas local hyper-acetylation at consensus MyoD-binding sites in myoblasts likely predetermines the regions of chromatin accessibility, class Ⅰ and Ⅱ HDACs contribute to the hypo-acetylation of the *MyoD* gene and the inhibition of *MEF2* transcription and activation, respectively. In undifferentiated SCs, *MyoD* interacts with HDAC1, and this interaction is responsible for silencing the MyoD-dependent transcription of p21 and muscle-specific genes[67,68]. Moreover, class Ⅱ HDACs are localized to the nucleus during SC proliferation and are responsible for blocking the activity of the myogenic co-factor MEF2[69]. A recent study of HDAC4 function and SC proliferation reported that the HDAC4 levels positively correlate with the expression of *Pax7* and *Lix1*, both of which are important for appropriate SC proliferation[70]; however, the molecular mechanism underlying this phenomenon remains unclear.

SC proliferation is also promoted and maintained by miR-27a/b, which targets and downregulates myostatin mRNA[71]. Consistently, SCs treated with antagomirs specific to miR-27a/b displayed increased myostatin expression and reduced proliferation. In activated SCs, miR-27b plays an important role in determining the appropriate timing of myogenic gene expression and regulates the Pax3 protein levels to control the entry of these cells into the myogenic differentiation program[72]. SC proliferation is also promoted by miR-133a, which represses the expression of serum response factor[73], and by miR-682, which is highly upregulated during myoblast proliferation both *in vitro* and *in vivo*; the inhibition of miR-682 results in reduced myoblast proliferation[74]. Moreover, in activated SCs, tissue inhibitor of metalloproteinase 3 (TIMP3), an inhibitor of tumor necrosis factor (TNF)-alpha-converting enzyme, regulates TNF-alpha release and acts as a switch for myogenic differentiation. miR-206 promotes TIMP3 downregulation[75] and suppresses Pax3 expression[74], thereby promoting SC differentiation. Paradoxically, quiescent SCs express high levels of both Pax3 and miR-206. An additional layer of gene regulation explains these contradictory data. In fact, it has been shown that in quiescent SCs, Pax3 transcripts are alternatively polyadenylated and are expressed as shorter 3' UTR transcripts, thereby resulting in the resistance of *Pax3* expression to miR-206-mediated regulation[76].

Epigenetic control of SC differentiation

As a general rule, genes no longer required for lineage progression are targeted for stable repression[59,62]. Accordingly, during differentiation, SC chromatin converts to a more repressed state by accumulating H3K27me3 across the genome at both transcription start sites and intergenic regions. In fact, in contrast to the level of H3K4me3, the level of the repressive mark H3K27me3 is low in quiescent SCs and is dramatically increased in differentiating SCs. In particular, when SCs differentiate, PRC2 is released from muscle differentiation genes (*MyoD* and *SRF*) to translocate to loci that are typically repressed in differentiated myotubes, *e.g.,* Pax7. By inducing a transition from the transcriptionally permissive mark H3K4me3 to the repressive mark H3K27me3 on the *Pax7* gene, PRC2 contributes to the switching off of SC proliferation[65]. Similarly, a switch from the permissive mark H3K4me3 to the repressive mark H3K27me3 on genes involved in the cell cycle is mediated by the E2F family of transcription factors and by the retinoblastoma protein as the SC exits the cell cycle to terminally differentiate[64,77,78]. Moreover, Pax7 associates with the Wdr5-Ash2L-MLL2 HMT complex, which mediates H3K4me3[19]. The binding of the Pax7-HMT complex to Myf5 results in the formation of H3K4me3 on the surrounding chromatin. Thus, Pax7 also participates in the induction of chromatin modifications that stimulate transcriptional activation of target genes to regulate the entry into the myogenic developmental program. Concomitantly, lysine-specific demethylase 4A, together with heterochromatin protein 1 alpha, promotes the demethylation of H3K9me3 at myogenic promoters, facilitating myoblast commitment[79].

The Ezh2 subunit of PCR2 complex has been demonstrated to play a critical role in mediating SC differentiation into the skeletal muscle lineage by suppressing a subset of regulators of non-muscle cell fate. Indeed, Ezh2-mediated H3K27me3 marks are specifically present on genes associated with alternative lineage selection, although Ezh2 dos not suppress terminal differentiation into skeletal muscle[80]. In contrast to PRC2-Ezh2, PRC2-Ezh1 is required for the myogenic differentiation of SCs; specifically, PRC2-Ezh1 replaces PRC2-Ezh2 on the myogenin promoter to regulate the appropriate timing of the transcriptional activation of myogenin[81].

When SCs differentiate, HDAC1 downregulation and pRb hypo-phosphorylation occurs, enabling the formation of the pRb-HDAC1 complex in differentiated myotubes. The pRb-HDAC1 interaction coincides with the disruption of the MyoD-HDAC1 complex, the

transcriptional activation of muscle-specific genes, and the differentiation of myoblasts[68]. Muscle differentiation also induces the nuclear-to-cytoplasmic translocation of class Ⅱ HDACs, thereby releasing the inhibitory constraints on MEF2 and consequently activating the expression of muscle-specific genes[69].

Over the course of differentiation, p38 alpha/beta MAPK activity increases and is required for complete myoblast differentiation and fusion, which is partially due to its regulation of the epigenetic mechanisms controlling gene expression[82]. In particular, p38alpha/beta MAPK, by selectively enabling the recruitment of SWI-SNF to the gene promoters of myogenin and creatine kinase, facilitates chromatin remodeling and the consequent expression of muscle genes. Indeed, p38-alpha-null SCs display increased Pax7 expression, persistent proliferation, and impaired differentiation and fusion[83], highlighting the distinct role of different members of the p38 MAPK family in SC proliferation and differentiation. It appears likely that the relative abundance of p38-alpha and p38-gamma MAPK activity in activated SCs serves as a balance between SC proliferation and differentiation.

As SCs differentiate, the downregulation of the enzymatic subunit of PRC2-Ezh2 and its partner YY1 is mediated by the combined action of miR-214[84], miR-26a[85] and miR-29[86], thereby relieving PRC2-mediated repression of muscle genes. Once SCs differentiate, miR-128a, miR-1 and miR-206 cooperate to block cell proliferation by inhibiting the expression of several targets in the insulin signaling pathway and Pax7 expression[87,88]. Indeed, the loss of miR-1 and miR-206 increases Pax7 expression, enhances SC proliferation and significantly inhibits myoblast differentiation[87,89]. The inhibition of cell proliferation is also achieved *via* the downregulation of the *Ccnd1* gene by both miR-26a and miR-1[90]. In addition, miR-133a and miR-133b inhibit cell proliferation and promote myoblast differentiation by negatively regulating the FGFR1 and PP2AC proteins, which participate in ERK1/2-mediated signal transduction[91]. In addition to inhibiting Pax7, miR-206 promotes SC differentiation and fusion to muscle fibers *via* the suppression of a collection of negative regulators of myogenesis, such as notch3, igfbp5, Meox2, RARB, Fzd7, MAP4K3, CLCN3, and NFAT5[89,92]. An important role in determining SC lineage commitment has been attributed to miR-133[93]. By targeting the mRNA of PRDM16, a master gene for brown fat determination, miR-133 modulates the choice between the myogenic and brown adipose lineages during SC differentiation. In SCs, HDAC4 expression correlates with that of miR-133, and HDAC4 inhibition induces SCs to partially differentiate into adipocytes[70]; however, the link between HDAC4 and miR-133 has not been yet characterized. Moreover, by modulating the insulin-like growth factor (IGF)-1 pathway *via* the downregulation of the IGF-1 receptor, miR-133a promotes SC differentiation[94] and sarcomeric actin organization[95]. In differentiating myoblasts, the repression of tumor growth factor-beta signaling, which is known to negatively affect SC differentiation, is ensured by the combined activity of miR-26a, which represses Smad1 and Smad4 expression[96], miR-206 and miR-29, which are capable of inhibiting Smad3 expression[97]. Together with myomiRs whose expression is upregulated during SC differentiation, the expression of other microRNAs needs to be down-regulated in order to achieve SC terminal differentiation. One such example is miR-23a, which directly regulates the expression of myosin heavy chain genes[98].

CONCLUSION

The maintenance of skeletal muscle homeostasis is a key survival factor, considering that skeletal muscle accounts for approximately 40% of body mass. Skeletal muscle needs to efficiently respond to internal and external stimuli - such as changes in levels of blood sugar, circulating hormones, or growth factors or mechanical insults - or to pathological conditions to maintain homeostasis, particularly in muscle. Unequivocally, SCs play central roles in adult regenerative myogenesis and in the preservation of muscle mass. Different epigenetic marks contribute to the coordination of the precise time-dependent expression of different subsets of myogenic genes in SCs (Table 1 and Figure 1). For instance, the PcG catalytic subunit Ezh2 is specifically distributed on the regulatory regions of late but not early muscle genes[60], whereas the methyltransferases PRMT5 and CARM1 are detected on promoters of early and late muscle genes, respectively[99].

Despite the observation that most muscular diseases do not have an epigenetic cause *per se*, the importance of epigenetic pathways in modulating muscle-specific gene expression renders them as excellent candidate targets for disease interventions. For instance, an elegant study demonstrated that epigenetic commitment mediated by SMARCD3, a member of the SWI/SNF family of proteins, and MyoD is required for the efficient generation of skeletal muscle cells from human embryonic stem cells[100]. Several drugs that target epigenetic mechanisms are currently undergoing clinical trials for many diseases. These drugs include HDAC inhibitors[101] and HMT inhibitors alone[102] or in combination[103]. In amyotrophic lateral sclerosis, HDAC inhibitors have been proposed as potential drugs to ameliorate patient symptoms[104,105]. In the case of muscular dystrophy, HDAC inhibitors have been extensively studied using the mdx mouse model[106]; currently, these drugs are under review in a clinical trial for muscular dystrophy[107]. Their effects are believed to be primarily due to the inhibition of class Ⅰ HDACs[108]. However, the prolonged treatment of patients with drugs that inhibit these ubiquitously required chromatin-modifying enzymes is a potential concern. An alternative approach ideally relies on the identification of small molecules that interfere with the epigenetic enzymes to specific loci within the genome. This approach may provide similar benefits

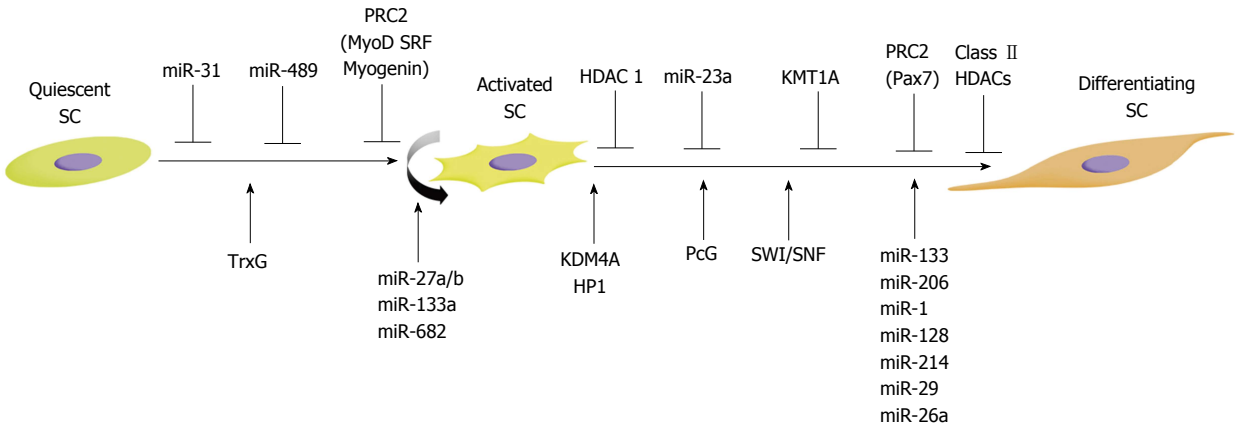

Figure 1 Schematic diagram of the epigenetic control of satellite cells during their activation and differentiation. SC: Satellite cells; PRC2: Polycomb repressive complex 2; TrxG: Trithorax group; PcG: Polycomb group; HDAC: Histone deacetylase.

Table 1 Summary of the main epigenetic events regulating the satellite cells status during myogenesis

SC status	Epigenetic regulation	Ref.
Quiescent	↓ H3K27me3[1] and ↑ H3K4me3[2]	[59,60]
	Bivalent domains (H3K27me3 + H3K4me3)	[59]
	↑ miR-489 ⊣ DEK[3]	[57]
	↑ miR-31 ⊣ Myf5[4]	[58]
Activated	↑ H3K4me3 on cell cycle genes	[19]
	↑ H3K27me3 on the *Pax7*[5] gene	[65]
	↑ P38 γ-MAPK[6] → p-MyoD[7] + KMT1A[8] ⊣ myogenin	[66]
	MyoD + HDAC1[9] ⊣ p21[10] and muscle genes	[67,68]
	HDAC4/5[11] ⊣ MEF2[12]	[69]
	HDAC4 → Pax7, Lix1[13]	[70]
	↑ miR-27a/b ⊣ myostatin and Pax3[13]	[71,72]
	↑ miR-133a ⊣ serum response factor	[73]
	↑ miR-206 ⊣ TIMP3[14] and Pax3	[75,76]
Differentiating	↑ H3K27me3 on cell cycle and alternative fate genes	[59,64,65,76-78]
	↑ H3K43me on Myf5	[19]
	↓ HDAC1 → MyoD-dependent genes	[68]
	HDAC4/5 in the cytoplasm → MEF2	[69]
	↑ P38 α/β-MAPK[15] → SWI-SNF[16] → myogenin and creatine kinase genes	[82,83]
	↑ miR-214, miR-26a, and miR-29 ⊣ Ezh2[17] and YY1[18]	[84-86]
	↑ miR-128a, miR-26a, miR-1, miR-206, miR-133a, and miR-133b ⊣ cell cycle	[87,88,90,91]
	↑ miR-206 ⊣ notch3[19], igfbp5[20], Meox2[21], RARB[22], Fzd7[23],MAP4K3[24],CLCN3[25], and NFAT5[26]	[59,89]
	↑ miR-133a ⊣ PRDM16[27] and the IGF-1[28] receptor	[78,80]
	↑ miR-26a ⊣ Smad1[29] and Smad4[30]	[96]
	↑ miR-206 and miR-29 ⊣ Smad3[31]	[97]
	↓ miR-23a ⊣ myosin heavy chain	[98]

[1]Trimethylated histone H3 lysine 27 (H3K27me3); [2]Trimethylated histone H3 lysine 4 (H3K4me3); [3]DEK oncogene; [4]Myogenic factor 5; [5]Paired box 7; [6]p38 gamma mitogen-activated protein kinase (P38 MAPK); [7]Phospho-myogenic differentiation; [8]Also referred to as suppressor of variegation 3-9 homolog 1 (Suv39h1); [9]Histone deacetylase 1; [10]Cyclin-dependent kinase inhibitor 1A; [11]Histone deacetylase 4/5; [12]Limb expression 1 homolog (chicken); [13]Paired box 3; [14]TIMP metallopeptidase inhibitor 3; [15]p38 alpha/gamma mitogen-activated protein kinase; [16]SWI/SNF complex; [17]Enhancer of zeste homolog 2; [18]YY1 transcription factor; [19]Neurogenic locus notch homolog protein 3 gene; [20]Insulin-like growth factor binding protein 5; [21]Mesenchyme homeobox 2 (Meox2); [22]Retinoic acid receptor, beta (RARB); [23]Frizzled class receptor 7 (Fzd7); [24]Mitogen-activated protein kinase kinase kinase kinase 3 (MAP4K3); [25]Chloride channel, voltage-sensitive 3 (CLCN3); [26]Nuclear factor of activated T-cells 5, tonicity-responsive (NFAT5); [27]PR domain containing 16 (PRDM16); [28]Insulin-like growth factor 1 (IGF-1); [29]SMAD family member 1; [30]SMAD family member 4; [31]SMAD family member 3. HDAC: Histone deacetylase.

without exerting side effects caused by the modification of gene expression in other cell types. In the last few years, numerous studies involving RNA-seq or ChIP-seq have contributed to provide a picture of the epigenetic characteristics of muscle-specific gene promoters during the different stages of myogenesis. However, most of these studies were performed using muscle cell lines and remain to be validated using *in vivo* models, for instance by analyzing mice in which individual epigenetic regulators are inactivated in a muscle-specific manner. The elucidation of the epigenetic mechanisms regulating SC function might reveal new targets for pharmacological manipulation to improve muscle regeneration and to promote muscle homeostasis under pathological

conditions.

REFERENCES

1 **Mauro A**. Satellite cell of skeletal muscle fibers. *J Biophys Biochem Cytol* 1961; **9**: 493-495 [PMID: 13768451 DOI: 10.1083/jcb.9.2.493]
2 **Brack AS**, Rando TA. Tissue-specific stem cells: lessons from the skeletal muscle satellite cell. *Cell Stem Cell* 2012; **10**: 504-514 [PMID: 22560074 DOI: 10.1016/j.stem.2012.04.001]
3 **Kuang S**, Rudnicki MA. The emerging biology of satellite cells and their therapeutic potential. *Trends Mol Med* 2008; **14**: 82-91 [PMID: 18218339 DOI: 10.1016/j.molmed.2007.12.004]
4 **Pannérec A**, Formicola L, Besson V, Marazzi G, Sassoon DA. Defining skeletal muscle resident progenitors and their cell fate potentials. *Development* 2013; **140**: 2879-2891 [PMID: 23739133 DOI: 10.1242/dev.089326]
5 **Reznik M**. Thymidine-3H uptake by satellite cells of regenerating skeletal muscle. *J Cell Biol* 1969; **40**: 568-571 [PMID: 5812478 DOI: 10.1083/jcb.40.2.568]
6 **Snow MH**. Myogenic cell formation in regenerating rat skeletal muscle injured by mincing. II. An autoradiographic study. *Anat Rec* 1977; **188**: 201-217 [PMID: 869238 DOI: 10.1002/ar.1091880206]
7 **Seale P**, Sabourin LA, Girgis-Gabardo A, Mansouri A, Gruss P, Rudnicki MA. Pax7 is required for the specification of myogenic satellite cells. *Cell* 2000; **102**: 777-786 [PMID: 11030621 DOI: 10.1016/S0092-8674(00)00066-0]
8 **Kuang S**, Kuroda K, Le Grand F, Rudnicki MA. Asymmetric self-renewal and commitment of satellite stem cells in muscle. *Cell* 2007; **129**: 999-1010 [PMID: 17540178 DOI: 10.1016/j.cell.2007.03.044]
9 **Wang YX**, Rudnicki MA. Satellite cells, the engines of muscle repair. *Nat Rev Mol Cell Biol* 2012; **13**: 127-133 [PMID: 22186952 DOI: 10.1038/nrm3265]
10 **Lipton BH**, Schultz E. Developmental fate of skeletal muscle satellite cells. *Science* 1979; **205**: 1292-1294 [PMID: 472747 DOI: 10.1126/science.472747]
11 **Le Grand F**, Jones AE, Seale V, Scimè A, Rudnicki MA. Wnt7a activates the planar cell polarity pathway to drive the symmetric expansion of satellite stem cells. *Cell Stem Cell* 2009; **4**: 535-547 [PMID: 19497282 DOI: 10.1016/j.stem.2009.03.013]
12 **Schultz E**, Jaryszak DL, Valliere CR. Response of satellite cells to focal skeletal muscle injury. *Muscle Nerve* 1985; **8**: 217-222 [PMID: 4058466 DOI: 10.1002/mus.880080307]
13 **Lepper C**, Partridge TA, Fan CM. An absolute requirement for Pax7-positive satellite cells in acute injury-induced skeletal muscle regeneration. *Development* 2011; **138**: 3639-3646 [PMID: 21828092 DOI: 10.1242/dev.067595]
14 **Mitchell KJ**, Pannérec A, Cadot B, Parlakian A, Besson V, Gomes ER, Marazzi G, Sassoon DA. Identification and characterization of a non-satellite cell muscle resident progenitor during postnatal development. *Nat Cell Biol* 2010; **12**: 257-266 [PMID: 20118923 DOI: 10.1038/ncb2025]
15 **Murphy MM**, Lawson JA, Mathew SJ, Hutcheson DA, Kardon G. Satellite cells, connective tissue fibroblasts and their interactions are crucial for muscle regeneration. *Development* 2011; **138**: 3625-3637 [PMID: 21828091 DOI: 10.1242/dev.064162]
16 **Sambasivan R**, Yao R, Kissenpfennig A, Van Wittenberghe L, Paldi A, Gayraud-Morel B, Guenou H, Malissen B, Tajbakhsh S, Galy A. Pax7-expressing satellite cells are indispensable for adult skeletal muscle regeneration. *Development* 2011; **138**: 3647-3656 [PMID: 21828093 DOI: 10.1242/dev.067587]
17 **Braun T**, Gautel M. Transcriptional mechanisms regulating skeletal muscle differentiation, growth and homeostasis. *Nat Rev Mol Cell Biol* 2011; **12**: 349-361 [PMID: 21602905 DOI: 10.1038/nrm3118]
18 **Bajard L**, Relaix F, Lagha M, Rocancourt D, Daubas P, Buckingham ME. A novel genetic hierarchy functions during hypaxial myogenesis: Pax3 directly activates Myf5 in muscle progenitor cells in the limb. *Genes Dev* 2006; **20**: 2450-2464 [PMID: 16951257 DOI: 10.1101/gad.382806]
19 **McKinnell IW**, Ishibashi J, Le Grand F, Punch VG, Addicks GC, Greenblatt JF, Dilworth FJ, Rudnicki MA. Pax7 activates myogenic genes by recruitment of a histone methyltransferase complex. *Nat Cell Biol* 2008; **10**: 77-84 [PMID: 18066051 DOI: 10.1038/ncb1671]
20 **Le Grand F**, Rudnicki MA. Skeletal muscle satellite cells and adult myogenesis. *Curr Opin Cell Biol* 2007; **19**: 628-633 [PMID: 17996437 DOI: 10.1016/j.ceb.2007.09.012]
21 **Chen EH**, Olson EN. Unveiling the mechanisms of cell-cell fusion. *Science* 2005; **308**: 369-373 [PMID: 15831748 DOI: 10.1126/science.1104799]
22 **Charrasse S**, Meriane M, Comunale F, Blangy A, Gauthier-Rouvière C. N-cadherin-dependent cell-cell contact regulates Rho GTPases and beta-catenin localization in mouse C2C12 myoblasts. *J Cell Biol* 2002; **158**: 953-965 [PMID: 12213839 DOI: 10.1083/jcb.200202034]
23 **Charrasse S**, Comunale F, Fortier M, Portales-Casamar E, Debant A, Gauthier-Rouvière C. M-cadherin activates Rac1 GTPase through the Rho-GEF trio during myoblast fusion. *Mol Biol Cell* 2007; **18**: 1734-1743 [PMID: 17332503 DOI: 10.1091/mbc.E06-08-0766]
24 **Griffin CA**, Kafadar KA, Pavlath GK. MOR23 promotes muscle regeneration and regulates cell adhesion and migration. *Dev Cell* 2009; **17**: 649-661 [PMID: 19922870 DOI: 10.1016/j.devcel.2009.09.004]
25 **Schwander M**, Leu M, Stumm M, Dorchies OM, Ruegg UT, Schittny J, Müller U. Beta1 integrins regulate myoblast fusion and sarcomere assembly. *Dev Cell* 2003; **4**: 673-685 [PMID: 12737803 DOI: 10.1016/S1534-5807(03)00118-7]
26 **Millay DP**, O'Rourke JR, Sutherland LB, Bezprozvannaya S, Shelton JM, Bassel-Duby R, Olson EN. Myomaker is a membrane activator of myoblast fusion and muscle formation. *Nature* 2013; **499**: 301-305 [PMID: 23868259 DOI: 10.1038/nature12343]
27 **Spivakov M**, Fisher AG. Epigenetic signatures of stem-cell identity. *Nat Rev Genet* 2007; **8**: 263-271 [PMID: 17363975 DOI: 10.1038/nrg2046]
28 **Kouzarides T**. Chromatin modifications and their function. *Cell* 2007; **128**: 693-705 [PMID: 17320507 DOI: 10.1016/j.cell.2007.02.005]
29 **Tan M**, Luo H, Lee S, Jin F, Yang JS, Montellier E, Buchou T, Cheng Z, Rousseaux S, Rajagopal N, Lu Z, Ye Z, Zhu Q, Wysocka J, Ye Y, Khochbin S, Ren B, Zhao Y. Identification of 67 histone marks and histone lysine crotonylation as a new type of histone modification. *Cell* 2011; **146**: 1016-1028 [PMID: 21925322 DOI: 10.1016/j.cell.2011.08.008]
30 **Mohn F**, Weber M, Rebhan M, Roloff TC, Richter J, Stadler MB, Bibel M, Schübeler D. Lineage-specific polycomb targets and de novo DNA methylation define restriction and potential of neuronal progenitors. *Mol Cell* 2008; **30**: 755-766 [PMID: 18514006 DOI: 10.1016/j.molcel.2008.05.007]
31 **Hansen KH**, Bracken AP, Pasini D, Dietrich N, Gehani SS, Monrad A, Rappsilber J, Lerdrup M, Helin K. A model for transmission of the H3K27me3 epigenetic mark. *Nat Cell Biol* 2008; **10**: 1291-1300 [PMID: 18931660 DOI: 10.1038/ncb1787]
32 **Barski A**, Cuddapah S, Cui K, Roh TY, Schones DE, Wang Z, Wei G, Chepelev I, Zhao K. High-resolution profiling of histone methylations in the human genome. *Cell* 2007; **129**: 823-837 [PMID: 17512414 DOI: 10.1016/j.cell.2007.05.009]
33 **Agger K**, Cloos PA, Christensen J, Pasini D, Rose S, Rappsilber J, Issaeva I, Canaani E, Salcini AE, Helin K. UTX and JMJD3 are histone H3K27 demethylases involved in HOX gene regulation and development. *Nature* 2007; **449**: 731-734 [PMID: 17713478 DOI: 10.1038/nature06145]
34 **De Santa F**, Totaro MG, Prosperini E, Notarbartolo S, Testa G, Natoli G. The histone H3 lysine-27 demethylase Jmjd3 links inflammation to inhibition of polycomb-mediated gene silencing. *Cell* 2007; **130**: 1083-1094 [PMID: 17825402 DOI: 10.1016/j.cell.2007.08.019]
35 **Lan F**, Bayliss PE, Rinn JL, Whetstine JR, Wang JK, Chen S, Iwase S, Alpatov R, Issaeva I, Canaani E, Roberts TM, Chang

HY, Shi Y. A histone H3 lysine 27 demethylase regulates animal posterior development. *Nature* 2007; **449**: 689-694 [PMID: 17851529 DOI: 10.1038/nature06192]
36 **Shahbazian MD**, Grunstein M. Functions of site-specific histone acetylation and deacetylation. *Annu Rev Biochem* 2007; **76**: 75-100 [PMID: 17362198 DOI: 10.1146/annurev.biochem.76.052705.162114]
37 **Ruthenburg AJ**, Li H, Patel DJ, Allis CD. Multivalent engagement of chromatin modifications by linked binding modules. *Nat Rev Mol Cell Biol* 2007; **8**: 983-994 [PMID: 18037899 DOI: 10.1038/nrm2298]
38 **Haberland M**, Montgomery RL, Olson EN. The many roles of histone deacetylases in development and physiology: implications for disease and therapy. *Nat Rev Genet* 2009; **10**: 32-42 [PMID: 19065135 DOI: 10.1038/nrg2485]
39 **Nilsen TW**. Mechanisms of microRNA-mediated gene regulation in animal cells. *Trends Genet* 2007; **23**: 243-249 [PMID: 17368621 DOI: 10.1016/j.tig.2007.02.011]
40 **Vasudevan S**. Posttranscriptional upregulation by microRNAs. *Wiley Interdiscip Rev RNA* 2012; **3**: 311-330 [PMID: 22072587 DOI: 10.1002/wrna.121]
41 **Valinezhad Orang A**, Safaralizadeh R, Kazemzadeh-Bavili M. Mechanisms of miRNA-Mediated Gene Regulation from Common Downregulation to mRNA-Specific Upregulation. *Int J Genomics* 2014; **2014**: 970607 [PMID: 25180174 DOI: 10.1155/2014/970607]
42 **Vasudevan S**, Steitz JA. AU-rich-element-mediated upregulation of translation by FXR1 and Argonaute 2. *Cell* 2007; **128**: 1105-1118 [PMID: 17382880 DOI: 10.1016/j.cell.2007.01.038]
43 **Rinn JL**, Chang HY. Genome regulation by long noncoding RNAs. *Annu Rev Biochem* 2012; **81**: 145-166 [PMID: 22663078 DOI: 10.1146/annurev-biochem-051410-092902]
44 **Gong C**, Maquat LE. lncRNAs transactivate STAU1-mediated mRNA decay by duplexing with 3' UTRs via Alu elements. *Nature* 2011; **470**: 284-288 [PMID: 21307942 DOI: 10.1038/nature09701]
45 **Wang J**, Gong C, Maquat LE. Control of myogenesis by rodent SINE-containing lncRNAs. *Genes Dev* 2013; **27**: 793-804 [PMID: 23558772 DOI: 10.1101/gad.212639.112]
46 **Yoon JH**, Abdelmohsen K, Srikantan S, Yang X, Martindale JL, De S, Huarte M, Zhan M, Becker KG, Gorospe M. LincRNA-p21 suppresses target mRNA translation. *Mol Cell* 2012; **47**: 648-655 [PMID: 22841487 DOI: 10.1016/j.molcel.2012.06.027]
47 **Cesana M**, Cacchiarelli D, Legnini I, Santini T, Sthandier O, Chinappi M, Tramontano A, Bozzoni I. A long noncoding RNA controls muscle differentiation by functioning as a competing endogenous RNA. *Cell* 2011; **147**: 358-369 [PMID: 22000014 DOI: 10.1016/j.cell.2011.09.028]
48 **Kallen AN**, Zhou XB, Xu J, Qiao C, Ma J, Yan L, Lu L, Liu C, Yi JS, Zhang H, Min W, Bennett AM, Gregory RI, Ding Y, Huang Y. The imprinted H19 lncRNA antagonizes let-7 microRNAs. *Mol Cell* 2013; **52**: 101-112 [PMID: 24055342 DOI: 10.1016/j.molcel.2013.08.027]
49 **Poliseno L**, Salmena L, Zhang J, Carver B, Haveman WJ, Pandolfi PP. A coding-independent function of gene and pseudogene mRNAs regulates tumour biology. *Nature* 2010; **465**: 1033-1038 [PMID: 20577206 DOI: 10.1038/nature09144]
50 **Guccione E**, Martinato F, Finocchiaro G, Luzi L, Tizzoni L, Dall' Olio V, Zardo G, Nervi C, Bernard L, Amati B. Myc-binding-site recognition in the human genome is determined by chromatin context. *Nat Cell Biol* 2006; **8**: 764-770 [PMID: 16767079 DOI: 10.1038/ncb1434]
51 **Perdiguero E**, Sousa-Victor P, Ballestar E, Muñoz-Cánoves P. Epigenetic regulation of myogenesis. *Epigenetics* 2009; **4**: 541-550 [PMID: 20009536 DOI: 10.4161/epi.4.8.10258]
52 **Saccone V**, Puri PL. Epigenetic regulation of skeletal myogenesis. *Organogenesis* 2010; **6**: 48-53 [PMID: 20592865 DOI: 10.4161/org.6.1.11293]
53 **Segalés J**, Perdiguero E, Muñoz-Cánoves P. Epigenetic control of adult skeletal muscle stem cell functions. *FEBS J* 2015; **282**: 1571-1588 [PMID: 25251895 DOI: 10.1111/febs.13065]
54 **Giordani L**, Puri PL. Epigenetic control of skeletal muscle regeneration: Integrating genetic determinants and environmental changes. *FEBS J* 2013; **280**: 4014-4025 [PMID: 23745685 DOI: 10.1111/febs.12383]
55 **Palacios D**, Puri PL. The epigenetic network regulating muscle development and regeneration. *J Cell Physiol* 2006; **207**: 1-11 [PMID: 16155926 DOI: 10.1002/jcp.20489]
56 **Mikkelsen TS**, Ku M, Jaffe DB, Issac B, Lieberman E, Giannoukos G, Alvarez P, Brockman W, Kim TK, Koche RP, Lee W, Mendenhall E, O'Donovan A, Presser A, Russ C, Xie X, Meissner A, Wernig M, Jaenisch R, Nusbaum C, Lander ES, Bernstein BE. Genome-wide maps of chromatin state in pluripotent and lineage-committed cells. *Nature* 2007; **448**: 553-560 [PMID: 17603471 DOI: 10.1038/nature06008]
57 **Cheung TH**, Quach NL, Charville GW, Liu L, Park L, Edalati A, Yoo B, Hoang P, Rando TA. Maintenance of muscle stem-cell quiescence by microRNA-489. *Nature* 2012; **482**: 524-528 [PMID: 22358842 DOI: 10.1038/nature10834]
58 **Crist CG**, Montarras D, Buckingham M. Muscle satellite cells are primed for myogenesis but maintain quiescence with sequestration of Myf5 mRNA targeted by microRNA-31 in mRNP granules. *Cell Stem Cell* 2012; **11**: 118-126 [PMID: 22770245 DOI: 10.1016/j.stem.2012.03.011]
59 **Liu L**, Cheung TH, Charville GW, Hurgo BM, Leavitt T, Shih J, Brunet A, Rando TA. Chromatin modifications as determinants of muscle stem cell quiescence and chronological aging. *Cell Rep* 2013; **4**: 189-204 [PMID: 23810552 DOI: 10.1016/j.celrep.2013.05.043]
60 **Caretti G**, Di Padova M, Micales B, Lyons GE, Sartorelli V. The Polycomb Ezh2 methyltransferase regulates muscle gene expression and skeletal muscle differentiation. *Genes Dev* 2004; **18**: 2627-2638 [PMID: 15520282 DOI: 10.1101/gad.1241904]
61 **Guenther MG**, Levine SS, Boyer LA, Jaenisch R, Young RA. A chromatin landmark and transcription initiation at most promoters in human cells. *Cell* 2007; **130**: 77-88 [PMID: 17632057 DOI: 10.1016/j.cell.2007.05.042]
62 **Dilworth FJ**, Blais A. Epigenetic regulation of satellite cell activation during muscle regeneration. *Stem Cell Res Ther* 2011; **2**: 18 [PMID: 21542881 DOI: 10.1186/scrt59]
63 **Marks H**, Kalkan T, Menafra R, Denissov S, Jones K, Hofemeister H, Nichols J, Kranz A, Stewart AF, Smith A, Stunnenberg HG. The transcriptional and epigenomic foundations of ground state pluripotency. *Cell* 2012; **149**: 590-604 [PMID: 22541430 DOI: 10.1016/j.cell.2012.03.026]
64 **Sebastian S**, Sreenivas P, Sambasivan R, Cheedipudi S, Kandalla P, Pavlath GK, Dhawan J. MLL5, a trithorax homolog, indirectly regulates H3K4 methylation, represses cyclin A2 expression, and promotes myogenic differentiation. *Proc Natl Acad Sci USA* 2009; **106**: 4719-4724 [PMID: 19264965 DOI: 10.1073/pnas.0807136106]
65 **Palacios D**, Mozzetta C, Consalvi S, Caretti G, Saccone V, Proserpio V, Marquez VE, Valente S, Mai A, Forcales SV, Sartorelli V, Puri PL. TNF/p38α/polycomb signaling to Pax7 locus in satellite cells links inflammation to the epigenetic control of muscle regeneration. *Cell Stem Cell* 2010; **7**: 455-469 [PMID: 20887952 DOI: 10.1016/j.stem.2010.08.013]
66 **Gillespie MA**, Le Grand F, Scimè A, Kuang S, von Maltzahn J, Seale V, Cuenda A, Ranish JA, Rudnicki MA. p38-{gamma}-dependent gene silencing restricts entry into the myogenic differentiation program. *J Cell Biol* 2009; **187**: 991-1005 [PMID: 20026657 DOI: 10.1083/jcb.200907037]
67 **Mal A**, Sturniolo M, Schiltz RL, Ghosh MK, Harter ML. A role for histone deacetylase HDAC1 in modulating the transcriptional activity of MyoD: inhibition of the myogenic program. *EMBO J* 2001; **20**: 1739-1753 [PMID: 11285237 DOI: 10.1093/emboj/20.7.1739]
68 **Puri PL**, Iezzi S, Stiegler P, Chen TT, Schiltz RL, Muscat GE, Giordano A, Kedes L, Wang JY, Sartorelli V. Class I histone deacetylases sequentially interact with MyoD and pRb during skeletal myogenesis. *Mol Cell* 2001; **8**: 885-897 [PMID: 11684023 DOI: 10.1016/S1097-2765(01)00373-2]
69 **Lu J**, McKinsey TA, Zhang CL, Olson EN. Regulation of skeletal myogenesis by association of the MEF2 transcription factor with class II histone deacetylases. *Mol Cell* 2000; **6**: 233-244 [PMID: 10983972 DOI: 10.1016/S1097-2765(00)00025-3]

70 **Choi MC**, Ryu S, Hao R, Wang B, Kapur M, Fan CM, Yao TP. HDAC4 promotes Pax7-dependent satellite cell activation and muscle regeneration. *EMBO Rep* 2014; **15**: 1175-1183 [PMID: 25205686 DOI: 10.15252/embr.201439195]

71 **McFarlane C**, Vajjala A, Arigela H, Lokireddy S, Ge X, Bonala S, Manickam R, Kambadur R, Sharma M. Negative auto-regulation of myostatin expression is mediated by Smad3 and microRNA-27. *PLoS One* 2014; **9**: e87687 [PMID: 24498167 DOI: 10.1371/journal.pone.0087687]

72 **Crist CG**, Montarras D, Pallafacchina G, Rocancourt D, Cumano A, Conway SJ, Buckingham M. Muscle stem cell behavior is modified by microRNA-27 regulation of Pax3 expression. *Proc Natl Acad Sci USA* 2009; **106**: 13383-13387 [PMID: 19666532 DOI: 10.1073/pnas.0900210106]

73 **Chen JF**, Mandel EM, Thomson JM, Wu Q, Callis TE, Hammond SM, Conlon FL, Wang DZ. The role of microRNA-1 and microRNA-133 in skeletal muscle proliferation and differentiation. *Nat Genet* 2006; **38**: 228-233 [PMID: 16380711 DOI: 10.1038/ng1725]

74 **Chen Y**, Gelfond J, McManus LM, Shireman PK. Temporal microRNA expression during in vitro myogenic progenitor cell proliferation and differentiation: regulation of proliferation by miR-682. *Physiol Genomics* 2011; **43**: 621-630 [PMID: 20841498 DOI: 10.1152/physiolgenomics.00136.2010]

75 **Liu H**, Chen SE, Jin B, Carson JA, Niu A, Durham W, Lai JY, Li YP. TIMP3: a physiological regulator of adult myogenesis. *J Cell Sci* 2010; **123**: 2914-2921 [PMID: 20682640 DOI: 10.1242/jcs.057620]

76 **Boutet SC**, Cheung TH, Quach NL, Liu L, Prescott SL, Edalati A, Iori K, Rando TA. Alternative polyadenylation mediates microRNA regulation of muscle stem cell function. *Cell Stem Cell* 2012; **10**: 327-336 [PMID: 22385659 DOI: 10.1016/j.stem.2012.01.017]

77 **Blais A**, Dynlacht BD. E2F-associated chromatin modifiers and cell cycle control. *Curr Opin Cell Biol* 2007; **19**: 658-662 [PMID: 18023996 DOI: 10.1016/j.ceb.2007.10.003]

78 **Blais A**, van Oevelen CJ, Margueron R, Acosta-Alvear D, Dynlacht BD. Retinoblastoma tumor suppressor protein-dependent methylation of histone H3 lysine 27 is associated with irreversible cell cycle exit. *J Cell Biol* 2007; **179**: 1399-1412 [PMID: 18166651 DOI: 10.1083/jcb.200705051]

79 **Sdek P**, Oyama K, Angelis E, Chan SS, Schenke-Layland K, MacLellan WR. Epigenetic regulation of myogenic gene expression by heterochromatin protein 1 alpha. *PLoS One* 2013; **8**: e58319 [PMID: 23505487 DOI: 10.1371/journal.pone.0058319]

80 **Woodhouse S**, Pugazhendhi D, Brien P, Pell JM. Ezh2 maintains a key phase of muscle satellite cell expansion but does not regulate terminal differentiation. *J Cell Sci* 2013; **126**: 565-579 [PMID: 23203812 DOI: 10.1242/jcs.114843]

81 **Stojic L**, Jasencakova Z, Prezioso C, Stützer A, Bodega B, Pasini D, Klingberg R, Mozzetta C, Margueron R, Puri PL, Schwarzer D, Helin K, Fischle W, Orlando V. Chromatin regulated interchange between polycomb repressive complex 2 (PRC2)-Ezh2 and PRC2-Ezh1 complexes controls myogenin activation in skeletal muscle cells. *Epigenetics Chromatin* 2011; **4**: 16 [PMID: 21892963 DOI: 10.1186/1756-8935-4-16]

82 **Simone C**, Forcales SV, Hill DA, Imbalzano AN, Latella L, Puri PL. p38 pathway targets SWI-SNF chromatin-remodeling complex to muscle-specific loci. *Nat Genet* 2004; **36**: 738-743 [PMID: 15208625 DOI: 10.1038/ng1378]

83 **Perdiguero E**, Ruiz-Bonilla V, Gresh L, Hui L, Ballestar E, Sousa-Victor P, Baeza-Raja B, Jardí M, Bosch-Comas A, Esteller M, Caelles C, Serrano AL, Wagner EF, Muñoz-Cánoves P. Genetic analysis of p38 MAP kinases in myogenesis: fundamental role of p38alpha in abrogating myoblast proliferation. *EMBO J* 2007; **26**: 1245-1256 [PMID: 17304211 DOI: 10.1038/sj.emboj.7601587]

84 **Juan AH**, Kumar RM, Marx JG, Young RA, Sartorelli V. Mir-214-dependent regulation of the polycomb protein Ezh2 in skeletal muscle and embryonic stem cells. *Mol Cell* 2009; **36**: 61-74 [PMID: 19818710 DOI: 10.1016/j.molcel.2009.08.008]

85 **Wong CF**, Tellam RL. MicroRNA-26a targets the histone methyltransferase Enhancer of Zeste homolog 2 during myogenesis. *J Biol Chem* 2008; **283**: 9836-9843 [PMID: 18281287 DOI: 10.1074/jbc.M709614200]

86 **Wang H**, Garzon R, Sun H, Ladner KJ, Singh R, Dahlman J, Cheng A, Hall BM, Qualman SJ, Chandler DS, Croce CM, Guttridge DC. NF-kappaB-YY1-miR-29 regulatory circuitry in skeletal myogenesis and rhabdomyosarcoma. *Cancer Cell* 2008; **14**: 369-381 [PMID: 18977326 DOI: 10.1016/j.ccr.2008.10.006]

87 **Chen JF**, Tao Y, Li J, Deng Z, Yan Z, Xiao X, Wang DZ. microRNA-1 and microRNA-206 regulate skeletal muscle satellite cell proliferation and differentiation by repressing Pax7. *J Cell Biol* 2010; **190**: 867-879 [PMID: 20819939 DOI: 10.1083/jcb.200911036]

88 **Motohashi N**, Alexander MS, Shimizu-Motohashi Y, Myers JA, Kawahara G, Kunkel LM. Regulation of IRS1/Akt insulin signaling by microRNA-128a during myogenesis. *J Cell Sci* 2013; **126**: 2678-2691 [PMID: 23606743 DOI: 10.1242/jcs.119966]

89 **Liu N**, Williams AH, Maxeiner JM, Bezprozvannaya S, Shelton JM, Richardson JA, Bassel-Duby R, Olson EN. microRNA-206 promotes skeletal muscle regeneration and delays progression of Duchenne muscular dystrophy in mice. *J Clin Invest* 2012; **122**: 2054-2065 [PMID: 22546853 DOI: 10.1172/JCI62656]

90 **Jash S**, Dhar G, Ghosh U, Adhya S. Role of the mTORC1 complex in satellite cell activation by RNA-induced mitochondrial restoration: dual control of cyclin D1 through microRNAs. *Mol Cell Biol* 2014; **34**: 3594-3606 [PMID: 25047835 DOI: 10.1128/MCB.00742-14]

91 **Feng Y**, Niu LL, Wei W, Zhang WY, Li XY, Cao JH, Zhao SH. A feedback circuit between miR-133 and the ERK1/2 pathway involving an exquisite mechanism for regulating myoblast proliferation and differentiation. *Cell Death Dis* 2013; **4**: e934 [PMID: 24287695 DOI: 10.1038/cddis.2013.462]

92 **Goljanek-Whysall K**, Pais H, Rathjen T, Sweetman D, Dalmay T, Münsterberg A. Regulation of multiple target genes by miR-1 and miR-206 is pivotal for C2C12 myoblast differentiation. *J Cell Sci* 2012; **125**: 3590-3600 [PMID: 22595520 DOI: 10.1242/jcs.101758]

93 **Yin H**, Pasut A, Soleimani VD, Bentzinger CF, Antoun G, Thorn S, Seale P, Fernando P, van Ijcken W, Grosveld F, Dekemp RA, Boushel R, Harper ME, Rudnicki MA. MicroRNA-133 controls brown adipose determination in skeletal muscle satellite cells by targeting Prdm16. *Cell Metab* 2013; **17**: 210-224 [PMID: 23395168 DOI: 10.1016/j.cmet.2013.01.004]

94 **Huang MB**, Xu H, Xie SJ, Zhou H, Qu LH. Insulin-like growth factor-1 receptor is regulated by microRNA-133 during skeletal myogenesis. *PLoS One* 2011; **6**: e29173 [PMID: 22195016 DOI: 10.1371/journal.pone.0029173]

95 **Mishima Y**, Abreu-Goodger C, Staton AA, Stahlhut C, Shou C, Cheng C, Gerstein M, Enright AJ, Giraldez AJ. Zebrafish miR-1 and miR-133 shape muscle gene expression and regulate sarcomeric actin organization. *Genes Dev* 2009; **23**: 619-632 [PMID: 19240126 DOI: 10.1101/gad.1760209]

96 **Dey BK**, Gagan J, Yan Z, Dutta A. miR-26a is required for skeletal muscle differentiation and regeneration in mice. *Genes Dev* 2012; **26**: 2180-2191 [PMID: 23028144 DOI: 10.1101/gad.198085.112]

97 **Winbanks CE**, Wang B, Beyer C, Koh P, White L, Kantharidis P, Gregorevic P. TGF-beta regulates miR-206 and miR-29 to control myogenic differentiation through regulation of HDAC4. *J Biol Chem* 2011; **286**: 13805-13814 [PMID: 21324893 DOI: 10.1074/jbc.M110.192625]

98 **Wang L**, Chen X, Zheng Y, Li F, Lu Z, Chen C, Liu J, Wang Y, Peng Y, Shen Z, Gao J, Zhu M, Chen H. MiR-23a inhibits myogenic differentiation through down regulation of fast myosin heavy chain isoforms. *Exp Cell Res* 2012; **318**: 2324-2334 [PMID: 22771720 DOI: 10.1016/j.yexcr.2012.06.018]

99 **Dacwag CS**, Bedford MT, Sif S, Imbalzano AN. Distinct protein arginine methyltransferases promote ATP-dependent chromatin remodeling function at different stages of skeletal muscle differentiation. *Mol Cell Biol* 2009; **29**: 1909-1921 [PMID: 19188441 DOI: 10.1128/MCB.00742-08]

100 **Albini S**, Coutinho P, Malecova B, Giordani L, Savchenko A, Forcales SV, Puri PL. Epigenetic reprogramming of human embryonic stem cells into skeletal muscle cells and generation of contractile myospheres. *Cell Rep* 2013; **3**: 661-670 [PMID: 23478022 DOI: 10.1016/j.celrep.2013.02.012]

101 **Colussi C**, Illi B, Rosati J, Spallotta F, Farsetti A, Grasselli A, Mai A, Capogrossi MC, Gaetano C. Histone deacetylase inhibitors: keeping momentum for neuromuscular and cardiovascular diseases treatment. *Pharmacol Res* 2010; **62**: 3-10 [PMID: 20227503 DOI: 10.1016/j.phrs.2010.02.014]

102 **Biancotto C**, Frigè G, Minucci S. Histone modification therapy of cancer. *Adv Genet* 2010; **70**: 341-386 [PMID: 20920755 DOI: 10.1016/B978-0-12-380866-0.60013-7]

103 **Falchook GS**, Fu S, Naing A, Hong DS, Hu W, Moulder S, Wheler JJ, Sood AK, Bustinza-Linares E, Parkhurst KL, Kurzrock R. Methylation and histone deacetylase inhibition in combination with platinum treatment in patients with advanced malignancies. *Invest New Drugs* 2013; **31**: 1192-1200 [PMID: 23907406 DOI: 10.1007/s10637-013-0003-3]

104 **Bruneteau G**, Simonet T, Bauché S, Mandjee N, Malfatti E, Girard E, Tanguy ML, Behin A, Khiami F, Sariali E, Hell-Remy C, Salachas F, Pradat PF, Fournier E, Lacomblez L, Koenig J, Romero NB, Fontaine B, Meininger V, Schaeffer L, Hantaï D. Muscle histone deacetylase 4 upregulation in amyotrophic lateral sclerosis: potential role in reinnervation ability and disease progression. *Brain* 2013; **136**: 2359-2368 [PMID: 23824486 DOI: 10.1093/brain/awt164]

105 **Cavallaro S**. Editorial: Emerging biomarkers for drug development in amyotrophic lateral sclerosis. *Curr Med Chem* 2014; **21**: 3507 [PMID: 25245511 DOI: 10.2174/0929867321311409181418 24]

106 **Minetti GC**, Colussi C, Adami R, Serra C, Mozzetta C, Parente V, Fortuni S, Straino S, Sampaolesi M, Di Padova M, Illi B, Gallinari P, Steinkühler C, Capogrossi MC, Sartorelli V, Bottinelli R, Gaetano C, Puri PL. Functional and morphological recovery of dystrophic muscles in mice treated with deacetylase inhibitors. *Nat Med* 2006; **12**: 1147-1150 [PMID: 16980968 DOI: 10.1038/nm1479]

107 **Consalvi S**, Mozzetta C, Bettica P, Germani M, Fiorentini F, Del Bene F, Rocchetti M, Leoni F, Monzani V, Mascagni P, Puri PL, Saccone V. Preclinical studies in the mdx mouse model of duchenne muscular dystrophy with the histone deacetylase inhibitor givinostat. *Mol Med* 2013; **19**: 79-87 [PMID: 23552722 DOI: 10.2119/molmed.2013.00011]

108 **Colussi C**, Gurtner A, Rosati J, Illi B, Ragone G, Piaggio G, Moggio M, Lamperti C, D'Angelo G, Clementi E, Minetti G, Mozzetta C, Antonini A, Capogrossi MC, Puri PL, Gaetano C. Nitric oxide deficiency determines global chromatin changes in Duchenne muscular dystrophy. *FASEB J* 2009; **23**: 2131-2141 [PMID: 19264835 DOI: 10.1096/fj.08-115618]

P- Reviewer: Liu SH, Yao CL, Zou ZM **S- Editor**: Tian YL
L- Editor: A **E- Editor**: Liu SQ

World Journal of Stem Cells

Submit a Manuscript: http://www.wjgnet.com/esps/
Help Desk: http://www.wjgnet.com/esps/helpdesk.aspx
DOI: 10.4252/wjsc.v7.i6.956

World J Stem Cells 2015 July 26; 7(6): 956-975
ISSN 1948-0210 (online)

ORIGINAL ARTICLE

Basic Study

Evaluation of biodegradable electric conductive tube-guides and mesenchymal stem cells

Jorge Ribeiro, Tiago Pereira, Ana Rita Caseiro, Paulo Armada-da-Silva, Isabel Pires, Justina Prada, Irina Amorim, Sandra Amado, Miguel França, Carolina Gonçalves, Maria Ascensão Lopes, José Domingos Santos, Dina Morais Silva, Stefano Geuna, Ana Lúcia Luís, Ana Colette Maurício

Jorge Ribeiro, Tiago Pereira, Ana Rita Caseiro, Miguel França, Ana Lúcia Luís, Ana Colette Maurício, Departmento de Clínicas Veterinárias and [+]UPVet, Instituto de Ciências Biomédicas de Abel Salazar (ICBAS) and Centro de Estudos de Ciência Animal (CECA), Instituto de Ciências, Tecnologias e Agroambiente da Universidade do Porto (ICETA), Rua de Jorge Viterbo Ferreira, 4050-313 Porto, Portugal

Paulo Armada-da-Silva, Sandra Amado, Centro Interdisciplinar de Estudo de Performance Humana (CIPER), Faculdade de Motricidade Humana (FMH), Universidade de Lisboa (UL), Estrada da Costa, 1499-002 Cruz Quebrada, Dafundo, Portugal

Isabel Pires, Justina Prada, CECAV and Departamento de Ciências Veterinárias, Universidade de Trás-os-Montes e Alto Douro (UTAD), 5001-801 Vila Real, Portugal

Irina Amorim, Departmento de Patologia e de Imunologia Molecular, Instituto de Ciências Biomédicas de Abel Salazar, Rua de Jorge Viterbo Ferreira, 4050-313 Porto, Portugal

Irina Amorim, Instituto Português de Patologia e Imunologia Molecular da Universidade do Porto (IPATIMUP), Rua Dr. Roberto Frias s/n, 4200-465 Porto, Portugal

Sandra Amado, UIS-IPL: Unidade de Investigação em Saúde da Escola Superior de Saúde de Leiria, Instituto Politécnico de Leiria, 2411-901 Leiria, Portugal

Carolina Gonçalves, Maria Ascensão Lopes, José Domingos Santos, CEMUC, Departamento de Engenharia Metalúrgica e Materiais, Faculdade de Engenharia da Universidade do Porto (FEUP), Rua Dr. Roberto Frias, 4200-465 Porto, Portugal

Dina Morais Silva, Biosckin, Molecular and Cell Therapies S.A. TecMaia, Rua Engenheiro Frederico Ulrich 2650, 4470-605 Maia, Portugal

Stefano Geuna, Neuroscience Institute of the Cavalieri Ottolenghi Foundation and Department of Clinical and Biological Sciences, University of Turin, 10124 Turin, Italy

Author contributions: Ribeiro J and Pereira T equally contributed; all authors contributed to this manuscript.

Supported by System of Incentives for Research and Technological development of QREN in the scope of project n° 38853/2013 - DEXGELERATION: "Soluções avançadas de regeneração óssea com base em hidrogéis de dextrin"; by the European Community FEDER fund through ON2 - O Novo Norte - North Portugal Regional Operational Program 2007-2013; by Project n° 34128 - BEPIM II: "Microdispositivos biomédicos com capacidade osteointegrativa por μPIM"; funded by AdI, and by the program COMPETE - Programa Operacional Factores de Competitividade, projects Pest-OE/AGR/UI0211/2011; PTDC/CVT/103081/2008; and CDRsp's Strategic Project - UI-4044-2011-2012 (Pest-OE/EME/UI4044/2011) funding from FCT.

Institutional review board statement: The article describes a basic research study involving animal subjects and was reviewed and was approved by the Instituto de Ciências Biomédicas Abel Salazar (ICBAS) - University of Porto (UP) and CECA-ICETA scientific boards. All procedures involving the experimental animals were performed with the approval of the Veterinary Authorities of Portugal in accordance with the European Communities Council Directive of November 1986 (86/609/EEC), and the NIH guidelines for the care and use of laboratory animals have been observed.

Institutional animal care and use committee statement: The article describes a basic research study involving animal subjects and was approved by the Veterinary Authorities of Portugal in accordance with the European Communities Council Directive of November 1986 (86/609/EEC), and the NIH guidelines for the care and use of laboratory animals have been observed. Also all the authors involved in the *in vivo* tasks have a degree in Veterinary Medicine and are accredited by the Veterinary Authorities of Portugal (Direcção Geral de Alimentação e Veterinária - DGAV) and by Felasa - Category C for working with laboratory animals. Humane end points were always followed in accordance to the OECD Guidance Document on the Recognition, Assessment and Use of Clinical Signs as Humane Endpoints for Experimental Animals Used in Safety Evaluation (2000).

Adequate measures were taken to minimize pain and discomfort taking into account human endpoints for animal suffering and distress. Animals were housed for two weeks before entering the experiment.

Conflict-of-interest statement: The authors state that they do not have any conflict of interests, including commercial, personal, political, intellectual, or religious interests that are related to the work submitted for consideration of publication.

Data sharing statement: This work is original in that it has not been published before or submitted for publication elsewhere, and will not be submitted elsewhere before a decision has been taken as to its acceptability in this Journal where you are Editor. Each author meets the criteria for authorship and assumes the corresponding responsibility. Technical appendix, statistical code, and dataset available from the corresponding author at Dryad repository, who will provide a permanent, citable and open-access home for the dataset is provided.

Correspondence to: Ana Colette Maurício, Professor, Departmento de Clínicas Veterinárias and +UPVet, Instituto de Ciências Biomédicas de Abel Salazar (ICBAS) and Centro de Estudos de Ciência Animal (CECA), Instituto de Ciências, Tecnologias e Agroambiente da Universidade do Porto (ICETA), Rua de Jorge Viterbo Ferreira, n° 228, 4050-313 Porto, Portugal. ana.colette@hotmail.com
Telephone: +351-220-428000

Received: February 2, 2015
Peer-review started: February 2, 2015
First decision: March 6, 2015
Revised: April 17, 2015
Accepted: May 5, 2015
Article in press: May 6, 2015
Published online: July 26, 2015

Abstract

AIM: To study the therapeutic effect of three tube-guides with electrical conductivity associated to mesenchymal stem cells (MSCs) on neuro-muscular regeneration after neurotmesis.

METHODS: Rats with 10-mm gap nerve injury were tested using polyvinyl alcohol (PVA), PVA-carbon nanotubes (CNTs) and MSCs, and PVA-polypyrrole (PPy). The regenerated nerves and tibialis anterior muscles were processed for stereological studies after 20 wk. The functional recovery was assessed serially for gait biomechanical analysis, by extensor postural thrust, sciatic functional index and static sciatic functional index (SSI), and by withdrawal reflex latency (WRL). *In vitro* studies included cytocompatibility, flow cytometry, reverse transcriptase polymerase chain reaction and karyotype analysis of the MSCs. Histopathology of lung, liver, kidneys, and regional lymph nodes ensured the biomaterials biocompatibility.

RESULTS: SSI remained negative throughout and independently from treatment. Differences between treted groups in the severity of changes in WRL existed, showing a faster regeneration for PVA-CNTs-MSCs ($P < 0.05$). At toe-off, less acute ankle joint angles were seen for PVA-CNTs-MSCs group ($P = 0.051$) suggesting improved ankle muscles function during the push off phase of the gait cycle. In PVA-PPy and PVA-CNTs groups, there was a 25% and 42% increase of average fiber area and a 13% and 21% increase of the "minimal Feret's diameter" respectively. Stereological analysis disclosed a significantly ($P < 0.05$) increased myelin thickness (M), ratio myelin thickness/axon diameter (M/d) and ratio axon diameter/fiber diameter (d/D; g-ratio) in PVA-CNT-MSCs group ($P < 0.05$).

CONCLUSION: Results revealed that treatment with MSCs and PVA-CNTs tube-guides induced better nerve fiber regeneration. Functional and kinematics analysis revealed positive synergistic effects brought by MSCs and PVA-CNTs. The PVA-CNTs and PVA-PPy are promising scaffolds with electric conductive properties, bio- and cytocompatible that might prevent the secondary neurogenic muscular atrophy by improving the reestablishment of the neuro-muscular junction.

Key words: Nerve regeneration; Neurotmesis; Tube-guides; Mesenchymal stem cells; Carbon nanotubes; Functional assessment; Gait biomechanical analysis; Histomorfometry; Polyvinyl alcohol

Core tip: The rat sciatic injury neurotmesis injury model is an appropriate model to evaluate the nerve regeneration when electric conductive tube-guides of polyvinyl alcohol (PVA)-carbon nanotubes (CNTs) and PVA-polypyrrole (PPy) associated to mesenchymal stem cells (MSCs) are used as scaffolds. The results obtained revealed that treatment with MSCs associated to PVA-CNTs tube-guides induced an increased number of regenerated fibers and thickening of the myelin sheet. Functional and kinematics analysis revealed positive synergistic effects brought by MSCs and PVA-CNTs. The PVA-CNTs and PVA-PPy are promising scaffolds with electric conductive properties, bio- and cytocompatible that might prevent the secondary neurogenic muscular atrophy by improving the reestablishment of the neuro-muscular junction.

Ribeiro J, Pereira T, Caseiro AR, Armada-da-Silva P, Pires I, Prada J, Amorim I, Amado S, França M, Gonçalves C, Lopes

MA, Santos JD, Silva DM, Geuna S, Luís AL, Maurício AC. Evaluation of biodegradable electric conductive tube-guides and mesenchymal stem cells. *World J Stem Cells* 2015; 7(6): 956-975 Available from: URL: http://www.wjgnet.com/1948-0210/full/v7/i6/956.htm DOI: http://dx.doi.org/10.4252/wjsc.v7.i6.956

INTRODUCTION

Functional recovery is rarely satisfactory in patients where peripheral nerve repair is needed, remaining a challenging task in neurosurgery[1,2]. Direct repair is the procedure of choice but only when a tension-free end-to-end suture is possible. However, for patients with loss of nerve tissue, resulting in a gap it is necessary to reconstruct the injured nerve using an autograft or a graft from a compatible donor[1,3]. One of the disadvantages of grafting is the necessity of a second surgery for collecting the nerve sample and respective donor site morbidity. In addition, non-matching donor and recipient nerve diameters often occur, which might be the reason for an incomplete functional recovery[4]. Entubulation offers advantages compared to graft implantation, including the potential to manipulate and to improve the regeneration environment within the tube-guide by adding to the lumen, growth factors and/or cellular systems[5]. Consequently, guidance of regenerating axons is improved by a mechanical effect but also by cellular growth factors, a chemical[6] and electrical cues[7]. Natural and synthetic biomaterials have been used as tube-guides, being the later sub-divided into two major groups: biodegradable and non-biodegradable[8,9]. The development of tube-guides is a consequence of the limitations inherent in the use of grafts, in terms of length, diameter and type of fiber, preventing damage to the sampling local, as it was previously referred[10]. For a correct nerve regeneration some important physical properties of tube-guides have been listed and referred by several authors like: the tube-guides should be made of biodegradable biomaterials with appropriate porous dimensions; the ability to deliver growth factors and drugs and allow the incorporation of cellular systems; an internal geometry to support an organized cell migration or intraluminal structures similar to nerve fascicles; and with some electrical activity in order to promote axon regeneration[11]. The use of electric conductive biomaterials to achieve nerve regeneration is a promising research area[12]. The goal of this work was to evaluate the therapeutic effect (by morphological and functional analysis) of three previously developed tube-guides with electrical conductivity for nerve regeneration associated to mesenchymal stem cells (MSCs) isolated from the Wharton's jelly of umbilical cord (UC) on neuro-muscular regeneration after neurotmesis injury using the rat sciatic nerve model. The three tube-guides used *in vivo* where those made of polyvinyl alcohol (PVA), PVA loaded with MWCNTs [functionalized carbon nanotubes (CNTs), PVA-CNTs], and PVA loaded with polypyrrole (PVA-PPy). Such composites with electric conductivity can be used to host cell therapies, and beneficial regenerative electrical stimulation can be applied directly to the cells through the composite[13]. PVA is a polymer used as a biomaterial due to its biocompatibility, non-toxic, non-carcinogenic, swelling properties, and bio-adhesive characteristics. PVA can also be used as host material in order to increase the solubility as well as the mechanical strength of conductive materials, and it is approved by Food and Drug Administration[14,15]. PPy and CNTs are two of the most studied conductive polymers for tissue engineering, especially for nerve tissue engineering[16]. The authors previously to *in vivo* application, focused on tube-guides design and *in vitro* characterization. The PVA-CNTs and PVA-PPy tube-guides presented conductivity advantages, important for nerve regeneration. The developed electrical conductive nerve tube-guides was achieved by loading PVA with 0.05% of PPy or COOH-functionalized CNTs. The inclusion of CNTs and PPy brought a significant increase of electrical conductivity of the simple PVA tube-guide. The PVA-CNTs tube-guides showed the rougher topography. The DSC and X-ray diffraction (XRD) studies revealed that all materials have similar low crystallinity. The wettability studies indicated a hydrophilic behaviour of all nerve tube-guides, being the PVA-PPy slightly more hydrophobic. In terms of surface charge, the zeta potential measurements revealed that both COOH-functionalized CNTs and PPy loads turned the surface charge slightly more positive. Regarding the elastic behaviour, the COOH-functionalized CNTs load caused a slight decrease of the rigidity of PVA. PVA-CNTs and PVA-PPy might present a regenerative potential and were tested in the rat sciatic nerve neurotmesis injury model[17]. Also, since the PVA-CNTs presented the rougher topography, which is important for the association and viability of the associated cellular systems[9], where also tested associated to the MSCs-based therapy[3,18].

Considering the peripheral nerve system (PNS), MSCs are promising cell-based therapies to be applied alone or associated to scaffolds. MSCs have a high plasticity, proliferative and differentiation capacity, and also have the advantage of presenting immuno-suppressive properties[3,19,20]. For these reasons, MSCs have been used in experimental trials as cell-based therapies, including pathologies of PNS and central nervous system (CNS). Furthermore, nowadays the characterization of MSCs is well defined by recommendations and standards stated by the international society for cellular therapy (ISCT)[19]. The MSCs therapeutic effect resides on their capacity to replace original cells of damaged tissues, and also by the physiologic secretion of growth factors and cytokines that modify the microenvironment inducing the activity of endogenous progenitor cells within the injured tissue, and by modulating the inflammatory and immune responses. The inflammatory modulation includes the Wallerian degeneration, a crucial step for nerve regeneration after neurotmesis injury[3]. Therefore, the use of cellular systems is a rational approach for promoting nerve

Figure 1 Synthetic biodegradable tubes of polyvinyl alcohol, polyvinyl alcohol loaded with COOH-functionalized multiwall carbon nanotubes MWCNTs (polyvinyl alcohol-carbon nanotubes, polyvinyl alcohol-carbon nanotubes tube-guides), and polyvinyl alcohol loaded with polypyrrole (polyvinyl alcohol-polypyrrole, polyvinyl alcohol-polypyrrole tube-guides).

regeneration by delivering growth-promoting factors and cytokines at the nerve lesion site[9]. MSCs can be isolated from several tissues, including bone marrow (BM), umbilical cord blood (UCB) and umbilical cord tissue (UCT), dental pulp, and adipose tissue[9]. BM collection has several disadvantages, since the BM include a high percentage of adipocytes and a heterogeneous cell population, there is the possibility of morbidity associated to donor collection, as well as it is observed a decreasing number of BM-MSCs along the adult life and available for therapeutic applications. The research concerning other sources of MSCs has been intensively performed for the past years for identifying tissues that will allow MSCs isolation, and safe and controlled *ex vivo* expansion of these cells for potential allogeneic and autologous application[9]. MSCs isolated from the Wharton's jelly UCT have been tested for the clinical application in CNS and PNS, including neurodegenerative diseases[21]. It has been reported that MSCs from the UCT are still viable 4 mo after transplantation and there is no need for immunological suppression of the patients and experimental animals[22]. The reason for this advantage is the fact that these cells are negative for major histocompatibility complex (MHC), and have low expression of MHC class Ⅰ[19] with potential application for MSC-based therapies in allogeneic treatments. *In vivo* studies involving these MSCs are limited but encouraging, especially what concerns PNS. Also, there are an increasing number of high quality cryopreserved cord tissue units in Cord Blood Banks worldwide. In addition, these cells represent a non-controversial source of MSCs, without neither ethical nor religious issues that are routinely harvested after birth, cryogenically stored, thawed, and can be expanded for therapeutic uses[9]. On the other hand, it was demonstrated in some studies, that grafted MSCs have a signalling role which initiates the recruitment and direction of endogenous cells by growth factors production, promoting the local regeneration and modulating the inflammatory process[23]. Nowadays it is believed that factors secreted by MSCs are primarily responsible for their therapeutic action, so it is particularly important to understand and fully characterize the MSCs secretome[18,24,25]. Recent studies demonstrated that MSCs produce and secrete multiple paracrine factors like interleukine-2 (IL-2), IL-6, IL-8, IL-12, IL-15, monocyte chemoattractant protein-1, macrophage inflammatory protein-1β, regulated on activation, normal T cell expressed and secreted, and platelet-derived growth factor-AA. The several secreted factors previously listed that are present in MSCs conditioned medium (CM) was already described by others[26] and more recently, by our research group[18]. These paracrine factors are important to promote the MSCs therapeutic effects identified by the scientific community, like immunomodulatory and chemoattractive, anti-apoptotic, anti-fibrotic, angiogenic, and anti-oxidants activities. The hypothesis that MSCs and the growth factors produced during expansion in culture (CM) is an appropriate therapeutic product for local application in severe peripheral lesions seemed to be a rational approach and was studied in the present experimental work.

MATERIALS AND METHODS

Tube-guide preparation

Synthetic biodegradable tubes of PVA (Aldrich, Mowiol 10-98), PVA loaded with COOH-functionalized multiwall carbon nanotubes MWCNTs (Nanothinx, NTX5, MWCNTs 97% - COOH) (PVA-CNTs tube-guides), and PVA loaded with PPy (Aldrich, 10-40 S/cm of conductivity) (PVA-PPy tube-guides) were prepared using a casting technique to a silicone mould. A 15% (%w/v) aqueous solution of PVA was prepared. Then the solution of PVA was mixed with 0.05% of COOH-functionalized MWCNTs and 0.05% of PPy. The tube-guides were produced by freezing/thawing process. The treatment consisted in three cycles of freezer (-30 ℃)/ incubator (25 ℃), and an annealing treatment started with a stage of 14 h on an incubator (25 ℃) followed by a ramp rate of 0.1 ℃ /min until 80 ℃, and then a stage of 20 h at 80 ℃. The tube-guides were sterilized by gama-radiation and hydrated in a sterile saline solution during 2 h before microsurgical application in the rat neurotmesis injuries (Figure 1).

MSCs cell culture and in vitro characterization

MSCs culture and expansion: Human MSCs isolated from the Wharton jelly (WJ) of UCT from PromoCell GmbH (C-12971, lot-number: 8082606.7) were cultured and expanded in a humidified atmosphere with 5% CO_2 at 37 ℃ by replacing the mesenchymal stem cell medium, PromoCell (C-28010) every 48 h. At 80% confluence, normally obtained after 4 d in culture (Figure 2), MSCs were harvested with 0.25% trypsin with EDTA (GIBCO) for further expansion at an initial concentration of 1×10^4 cells/cm^2. Immediately previously to *in vivo* application, a MSCs suspension was prepared in 1 mL syringes. Each syringe contained MSCs at a concentration

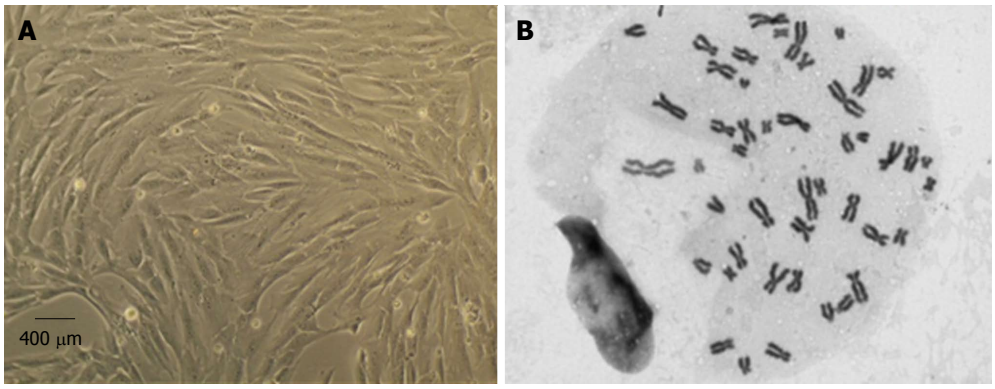

Figure 2 Mesenchymal stem cells culture and expansion. A: Isolated mesenchymal stem cells (MSCs) from the Wharton's jelly of umbilical cord presented a fusiform, fibroblast-like morphology in culture (magnification: 100 ×); B: Selected metaphases from MSCs in culture, showing normal number of chromossomes (46, XY) (magnification: 1000 ×).

of 1 × 10^6/μL for posterior intra-operatively nerve injection.

The MSCs lot used in the present experimental study was characterized by flow cytometry analysis for a comprehensive panel of markers by PromoCell as previously reported[18,25]. The MSCs exhibited a mesenchymal-like shape with a flat and polygonal morphology during cell culture expansion. Their phenotype was evaluated by flow cytometry for PE anti-human cluster of differentiation-105 (CD105); APC anti-human CD73; PE anti-human CD90; PerCP/Cy5.5 anti-human CD45: FITC anti-human CD34; PerCP/Cy5.5 anti-human CD14; Pacific Blue anti-human CD19 and pacific-blue anti-human Human Leukocyte Antigen-DR (HLA-DR) (antibodies and their respective isotypes from BioLegend).

MSCs karyotype by cytogenetic analysis: Cytogenetic analysis was carried out before *in vivo* application between passages 4 and 5 as previously reported[18,25]. Chromosome analysis was performed by one scorer on 20 Giemsa-stained metaphases and each MSC cell was scored for chromosome number. For determination of the karyotype, a routine chromosome G-banding analysis was also carried out and no structural alterations were observed which demonstrates the chromosomal stability to the cell culture procedures and also that the *in vivo* applied MSCs are not neoplastic (Figure 2).

Cytocompatibility evaluation of biomaterials: Intracellular free Ca^{2+} concentration ($[Ca^{2+}]_i$) by using dual wavelength spectrofluorometry as previously described[27] was measured in Fura-2-loaded MSCs cells. $[Ca^{2+}]_i$ from MSCs cultured without the presence of any biomaterial, sub-cultured over PVA discs, over PVA loaded with CNTs (PVA-CNTs) and PVA loaded with PPy (PVA-PPy) discs of 10 mm diameter are results obtained from epifluorescence technique confirming that the MSCs did not begin the apoptosis process.

Reverse transcriptase polymerase chain reaction to confirm that MSCs are undifferentiated: Reverse transcriptase polymerase chain reaction (RT-PCR) and quantitative PCR (qPCR) targeting specific genes expressed by the MSCs that were *in vivo* applied was performed to certify that the MSCs used *in vivo* were not differentiated. For that, primers were designed targeting seven human genes based on the literature[18]. DNA sequences from growth associated protein-43 (GAP-43), neurofilament-H (NF-H), Nestin, Glyceraldehyde-3-Phosphate Dehydrogenase (GAPDH), β-actin, neuronal nuclear (*NeuN*) and glial fibrillary acidic protein (*GFAP*) genes from mice (*Mus musculus*), rat (Rattus novergicus) and human (Homo sapiens) were downloaded from GenBank (www.ncbi.nlm.nih.gov/genbank) and aligned using the Clustal Omega bioinformatic tool from EMBL-EBI (http://www.ebi.ac.uk/Tools/msa/clustalo). MSCs culture was harvested with 0.25% trypsin EDTA solution (Gibco) and centrifuged at 2000 rpm 4 ℃ during 5 min. Cell pellets were used for total RNA extraction using an adequate extraction kit, high pure RNA Isolation kit (Roche). Briefly, cell pellets were lysed with a lysis buffer, loaded into a High Pure Filter Tube, DNA was removed with DNase I enzyme, washed twice on column, and eluted with 100 μL of Elution Buffer. RNA was quantified and its quality assessed by using a Nanodrop ND-1000 Spectrophotometer and reads from 220 nm to 350 nm, and then stored at -80 ℃ until further use. In the following step, cDNA was synthesized from the purified RNA. To fulfill that issue, the kit Ready-To-Go You-Prime First-Strand Beads (GE Healthcare) was used following the manufacturer instructions. Briefly, 1.5 μg of total RNA was used and diluted in DEPC-treated water to a 30 μL final volume in a RNase-free microcentrifuge tube; then heated at 65 ℃ for 10 min and then chilled in ice; transfer the RNA solution to the kit tube containing the first-strand reaction mix beads; add 0.2 μg of Oligo(dT) primer and DEPC-treated water to a 33 μL final volume; mix the content and incubate at 37 ℃ for 60 min. cDNA was synthesized and stored at -20 ℃ until further use. Of referring that, due to the use of the Oligo(dT) primer, the synthesized cDNA corresponds to the mRNA present in the sample at the time of collection. cDNA synthesized from undifferentiated MSCs was used to

check the expression of seven genes, two housekeeping genes (β-actin and *GAPDH*) and five specific of neuronal cells (GFAP, NeuN, Nestin, NF-H and GAP-43). Primers were designed in house and then synthesized in an external laboratory (MWG Operon, Germany). The primers were rehydrated in DNase/RNase free water in a concentration of 100 pmol/μL. qPCR was performed in a iCycler® iQ5TM (BioRad) apparatus using the iQTM SYBR® Green Supermix (BioRad). Each pair of primers targeting a gene was used to analyze its expression in the MSCs cDNA, in triplicate, along with a negative control. The plates containing the mix targeting the seven genes for both types of cells were submitted to the following cycles of temperatures: 95 ℃ during 4 min, 35 cycles comprising 95 ℃ during 20 s, 55 ℃ during 20 s and 72 ℃ during 20 s ending with Real-Time acquisition, and final extension of 75 ℃ for 7 min. After cycling temperatures, the number of cycle threshold for each well was recorded. The plate containing the amplified genes or qPCR products was kept in ice and observed in a 2% agarose gel to check and reinforce the identity of the amplicons. Briefly, 2 g of NuSieve® 3:1 Agarose (Lonza) were mixed with 100 mL Tris-Acetate-EDTA buffer, melted, mixed with ethidium bromide in a final concentration of 0.2 μg/mL, and loaded in a horizontal electrophoresis apparatus. After solidification, 15 μL of the qPCR products were loaded in the agarose wells, and submitted to a 120 V potential difference during 40 min to separate the amplicons. Gel was then observed under UV light and pictures recorded using the GelDoc® 2000 (BioRad) and Quantity One® software (BioRad). In the MSCs, the molecular analysis showed a very small amplification of *GFAP* gene, absence of amplification of the *NF-H* and *GAP-43* genes, and reasonable amplification of *NeuN*, β-actin, *GAPDH* and Nestin genes. Amplification of a given gene is correlated with its expression seeing that the template DNA is the one generated from mRNA. The RT-PCR results confirmed that the MSCs used *in vivo* were not differentiated into neuro-glial cells.

Surgical procedure for the rat sciatic nerve model for neurotmesis

The article describes a basic research study involving animal subjects and was approved by the Veterinary Authorities of Portugal [Direcção Geral de Alimentação e Veterinária (DGAV)] in accordance with the European Communities Council Directive of November 1986 (86/609/EEC), and the National Institutes of Health (NIH) guidelines for the care and use of laboratory animals have been observed. Also all the authors involved in the *in vivo* tasks have a degree in Veterinary Medicine and are accredited by the Veterinary Authorities of Portugal (DGAV) and by Felasa - Category C for working with laboratory animals.

The OECD Guidance Document on the Recognition, Assessment and Use of Clinical Signs as Humane Endpoints for Experimental Animals Used in Safety Evaluation (2000) were always followed by the authors by taking adequate measures to minimize pain and discomfort.

Polycarbonate cages type 3 were used for housing under standard laboratory conditions adult male Sasco Sprague Dawley rats with 300 g (Charles River Laboratories, Barcelona, Spain) always in a temperature and humidity controlled room with 12-12 h light/dark cycles. The rats were fed with standard chow and water *ad libitum* until the day of surgery. For surgery, the rats were anesthetized with ketamine 9 mg/100 g and xylazine 1.25 mg/100 g (body weight), by intraperitoneal administration. In lateral recumbence, the right sciatic nerve was exposed unilaterally and a transection injury was performed above the terminal nerve ramification using a straight microsurgical scissors, for creating a neurotmesis injury with 10 mm gap. Six experimental groups were studied: in groups 1, 2 and 3 after neurotmesis the proximal and distal nerve stumps were inserted 3 mm into PVA (group 1: PVA), PVA loaded with 0.05% (%w/v) of COOH-functionalized MWCNTs (group 2: PVA-CNTs), and PVA loaded with PPy 0.05% (%w/v) tube-guides (group 3: PVA-PPY), respectively, and tube-guides were sutured with two epineural sutures using 7/0 polypropylene monofilament, maintaining a nerve gap of 10 mm; in group 4 after neurotmesis, an autologous 180° inverted graft was sutured between both nerve stumps (group 4: Graft); in group 5 after neurotmesis, immediate cooptation with 7/0 monofilament polypropylene suture (group 5: End-to-End); in group 6 after neurotmesis the proximal and distal nerve stumps were inserted 3 mm in a PVA loaded with 0.05% (%w/v) of COOH-functionalized MWCNTs tube-guide kept in place with 2 epineural sutures using 7/0 monofilament polypropylene suture and the interior of the tube-guide was filled with 100 μm of MSCs at a concentration of 1×10^6 cells/μL in culture medium, also 100 μm of MSCs at a concentration of 1×10^6 cells/μL in culture medium were infiltrated in both nerve stumps inserted in the tube-guide (group 6: PVA-CNTs-MSCs) (Figure 3).

Functional assessment

After injury and sciatic nerve microsurgery reconstruction using the developed scaffolds in standardized neurotmesis injuries, a follow-up consisting in functional parameters measurements are important to evaluate the regeneration process and recovery. The animals were tested in an appropriate environment to minimize stress and handled by a single operator already trained for that purpose. Animals have been tested before the surgery at week 0, and after the surgery, at week 1, at week 2 and then every two weeks until the end of follow-up time of 20 wk.

Evaluation of motor performance and nociceptive function: Motor performance was evaluated by measuring extensor postural thrust (EPT) and nociceptive function using the withdrawal reflex latency (WRL). The EPT included in the neurological recovery evaluation

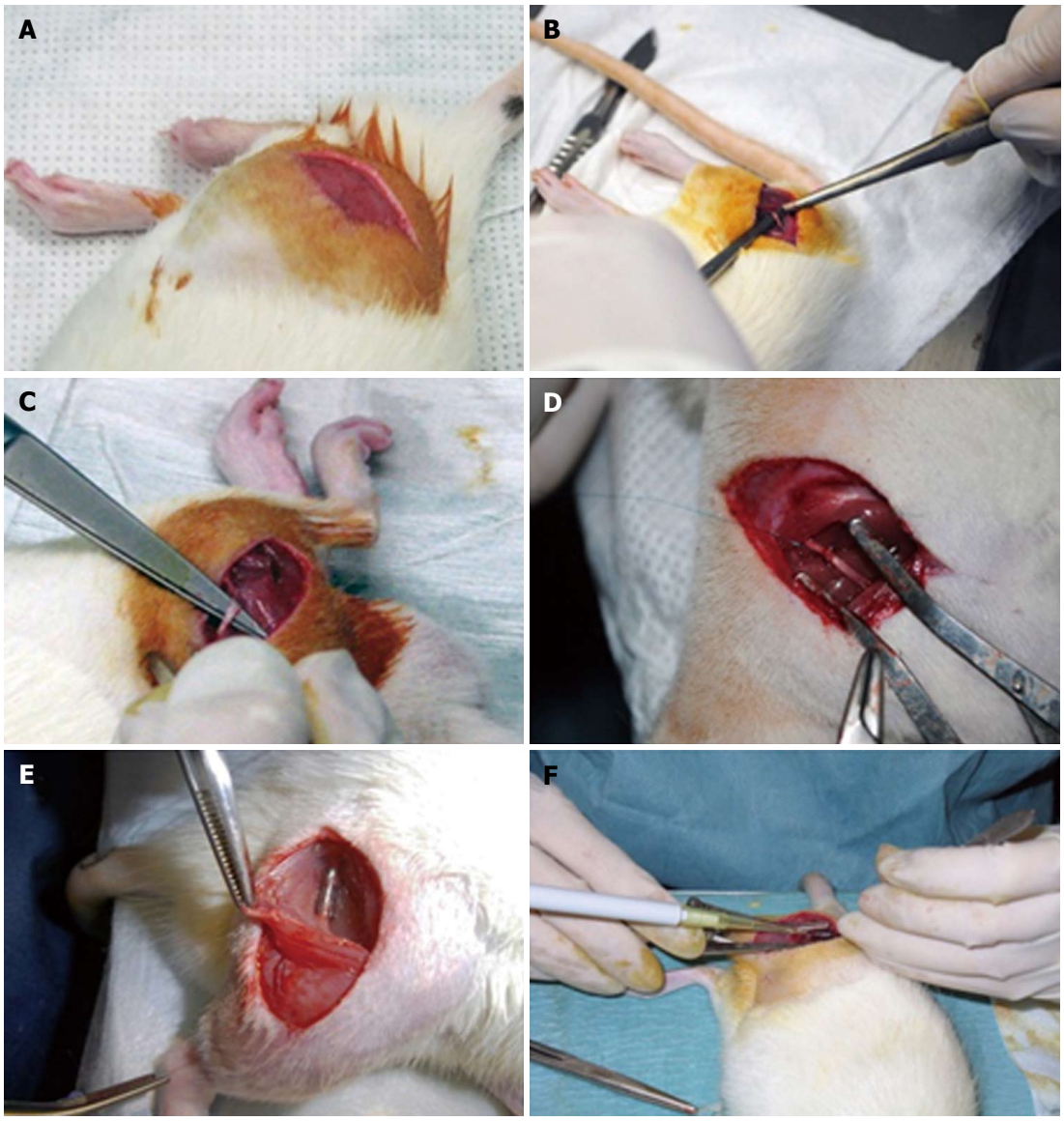

Figure 3 Surgery of the rat sciatic nerve neurotmesis injury model. Under deep anesthesia the right sciatic nerve was exposed unilaterally through a skin incision extending from the greater trochanter to the mid-half distally followed by a muscle splitting incision (A). After nerve mobilization (B), a transection injury was performed (neurotmesis) using a straight microsurgical scissors (C). In group 5 (End-to-End) after neurotmesis, immediate cooptation with 7/0 monofilament polypropylene suture was performed (D). Implantation of the tube-guide in the 10 mm gap (E). Local application of the mesenchymal stem cells (MSCs), the MSCs suspension filled the polyvinyl alcohol (PVA)-carbon nanotubes (CNTs) tube-guide lumen (group 6: PVA-CNTs-MSCs) (F).

of the rat after sciatic nerve injury was first described by[28]. EPT is induced by lowering the affected hind-limb towards the platform of a digital balance supporting the animal by the thorax. During the test, the rat extends the hind-limb and the distal metatarsus and digits contact with digital platform balance. The force in grams (g) applied is recorded individually and the results for both hind-limbs (affected and un-affected hind-limb) are taken for equation 1 calculation. The normal (unaffected limb) EPT (NEPT) and experimental EPT (EEPT) values considered for equation (1) and the percentage of functional deficit is calculated[9,28-31].

$$\% \text{ Motor deficit} = [(\text{NEPT} - \text{EEPT})/\text{NEPT}] \times 100 \quad (1)$$

To assess the nociceptive WRL, the hotplate test described by Masters *et al*[32] was used with some modifications and previously described by the authors[3,9,17,25,31,33]. Also, it is considered by the scientific bibliography that rats without sciatic nerve injury withdraw their paws from the hotplate within 4.3 s or less[9,17,31,33]. If there was no paw withdrawal after 12 s, the animal was assigned the maximal WRL of 12 s and the heat stimulus was removed to prevent tissue damage[34-36].

For sciatic functional index (SFI), a confined walkway measuring 42 cm long and 8.2 cm wide with a dark shelter at the end (own fabrication) that the rats cross was used. The footprints from the experimental (E) and normal (N) sides are measured: (1) distance from the heel to the third toe, the print length; (2) distance from the first to the fifth toe, the toe spread (TS); and (3) distance from the second to the fourth toe,

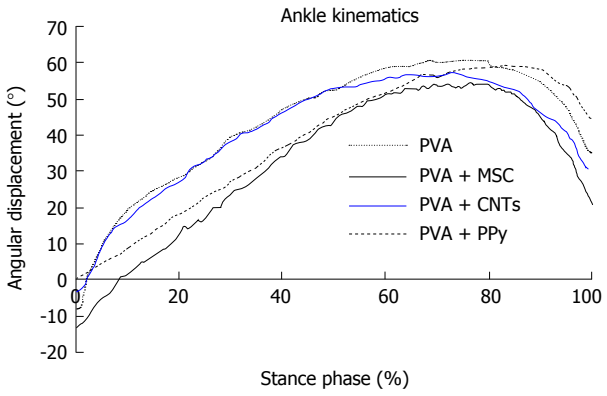

Figure 4 Kinematic plots in the sagittal plane for the ankle angle (°) as it moves through the stance phase, during the transection injury study. The mean of each group is plotted. PVA: Polyvinyl alcohol; CNTs: Carbon nanotubes; PPy: Polypyrrole; MSCs: Mesenchymal stem cells.

the intermediary toe spread (ITS). In the static sciatic functional index (SSI) is a simpler test where only the parameters TS and ITS are the measurements included in equation (6). Prints for measurements are chosen at the time of walking based on precise, clear and completeness of footprints[9,36,37]. The mean distances of 3 measurements are used to calculate the following factors (dynamic and static):

$$TSF = (ETS - NTS)/NTS \quad (2)$$

$$ITSF = (EITS - NITS)/NITS \quad (3)$$

$$PLF = (EPL - NPL)/NPL \quad (4)$$

TSF: Toe spread factor; ITSF: Intermediate toe spread factor; PLF: Print length factor; ETS: Experimental toe spread; NTS: Normal toe spread; NITS: Normal intermediary toe spread; EITS: Experimental Intermediary toe spread; NPL: Normal print length; EPL: Experimental print length.

SFI is calculated as described by Bain *et al*[38] according to the following equation:

$$SFI = -38.3 \times (EPL - NPL)/NPL + 109.5 \times (ETS - NTS)/NTS + 13.3 \times (EITS - NITS)/NITS - 8.8 = (-38.3 \times PLF) + (109.5 \times TSF) + (13.3 \times ITSF) - 8.8 \quad (5)$$

Considering the SFI measurements, it was not possible to obtain values during the 20 wk follow-up after the surgery procedure, due to autotomy of the fingers. As a matter of fact, the rat sciatic nerve model for neurotmesis has this disadvantage; the autotomy observed in several experimental animals even when a repellant substance is applied routinely[9]. SSI was calculated as described by[39] according to the following equation (equation 6):

$$SSI = 108.4 \times TSF + 31.85 \times ITF - 5.49 \quad (6)$$

For SFI and SSI, when no footprints are measurable, the index score of -100 is given considering total impairment, on the other hand, a score of 0 means that there is no alteration and the footprint is normal.

Kinematic analysis: Ankle kinematics was carried out at the end of the 20-wk follow-up time in the following experimental groups: PVA, PVA-CNTs, PVA-PPy, Graft, End-to-End, and PVA-CNTs-MSCs. A Perspex track with length, width (adjustable) and height of 120, 12, and 15 cm, respectively was used to record the rat locomotion in a straight line. The animals' gait was video recorded at a rate of 300 Hz images per second (Casio Exilim PRO EX-F1, Japan) by a camera with a visualization field of 14 cm wide, that was positioned at the track half-length, and 1 m distant from the track, where gait velocity was steady. The software APAS® (Ariel Performance Analysis System, Ariel Dynamics, San Diego, United States) was used for data analysis. The authors used a two-segment model of the ankle joint, adopted from the model firstly developed by[40] (2D biomechanical analyses in sagittal plan), and the rat ankle angle was determined using the scalar product between a vector representing the foot and a vector representing the lower leg. Dorsiflexion and plantarflexion is considered for positive and negative values of position of the ankle joint (θ°). Initial contact (IC), opposite toe off (OT), and heel rise (HR) and toe-off (TO)[33,40] were the time points analyzed for each step cycle, the values were time normalized for 100% of step cycle. The normalized temporal parameters were averaged over all recorded trials (Figure 4). Since the animal's normal walking velocity is 20-60 cm/sA[33,40], stance phases lasting between 150 and 400 ms were considered for analysis.

Morphological analysis and histopathology: For histomorphometric analysis, nerve samples obtained from the 10-mm-long sciatic nerve segments distal to the neurotmesis site and from un-operated controls[41-44]. The histological nerve preparation followed the previously reported protocol[3,9,17,25,31,33,35] and a systematic random sampling and D-disector were adopted[41-44].

At the end of the healing period tested (week 20), tibialis anterior (TA) muscles of all experimental (PVA, PVA-CNTs, PVA-PPy, Graft, End-to-End, and PVA-CNTs-MSCs) and Control (no lesion) groups were collected, and the tissue samples were fixed in 10% buffered formalin, routinely processed, dehydrated and embedded in paraffin wax. Consecutive 3 μm transverse sections from the mid-belly of each muscle were cut, stained with haematoxylin and eosin (HE) and used for morphometry evaluation and determination of the degree of atrophy. For the morphometric analysis, an unbiased sampling procedure was applied and the following measures were calculated: area, perimeter, "Feret's angle" and "minimal Feret's diameter" (which is the minimum distance of parallel tangents at opposing borders of the muscle fiber). These parameters were evaluated from the cross sections using the ImageJ© software (NIH) which allowed to apply this set of individual fiber measurements. A

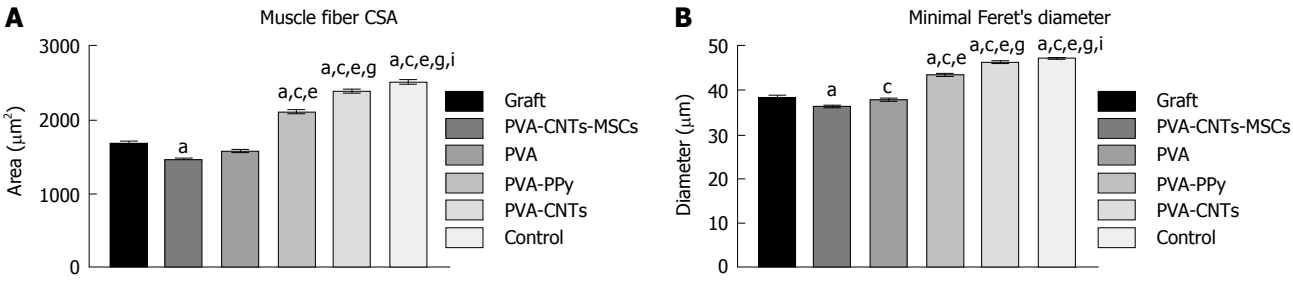

Figure 5 Graphical representation of the mean of area (A) and "minimal Feret's diameter" (B) of control, regenerated tibialis anterior muscle fibers at week-20 after neurotmesis (Graft) and neurotmesis with the proximal and distal nerve stumps sutured to a polyvinyl alcohol (polyvinyl alcohol) tube and polyvinyl alcohol coated tubes (polyvinyl alcohol, polyvinyl alcohol polypyrrole and polyvinyl alcohol carbon nanotubes). Values are presented as mean ± SEM. $^{a}P < 0.05$ *vs* Graft; $^{c}P < 0.05$ *vs* Graft PVA CNTs MSCs; $^{e}P < 0.05$ *vs* Graft PVA; $^{g}P < 0.05$ *vs* Graft PVA PPy; $^{i}P < 0.05$ *vs* Graft PVA CNTs. PVA: Polyvinyl alcohol; CNTs: Carbon nanotubes; PPy: Polypyrrole; MSCs: Mesenchymal stem cells.

minimum of 1000 skeletal muscle fibers was measured from each group. This assessment was performed by 2 independent operators. Each one of the operators measured, blindly and randomly, an average of 50 fibers in each section. Images were acquired using a Nikon® microscope connected to a Nikon® digital camera DXM1200, at low magnification (100 ×) under the same conditions that were used to acquire a reference ruler.

At the end of the study, all animals were subjected to a complete necropsy examination in order to evaluate the presence of possible internal anomalies and/or injuries. Lung, heart, kidneys, liver and spleen were collected and weighed and then submitted to histological analysis to check whether there were related microscopic changes such as inflammation, degeneration, or accumulation of biological material. The organs were fixed in 10% buffered formalin and processed for routine histology with HE stain. Microscopically, massive carbon deposits generally appear as well-recognized anthracotic black pigment, especially in the lung. A recent report described that some types of carbon nanotubes may appear as small punctuated accumulations inside Kupfer cells (liver) and in the intermediate zone of the spleen, when intravenously administered[45]. Special stains, such as Von Kossa (method that demonstrates phosphates and carbonates) and Masson-Fontana (method used for distinguish carbon deposits from melanin) were also performed in consecutive sections.

Statistical analysis

The statistical review of the study was performed by a biomedical statistician [PAS Armada-da-Silva, CIPER-Faculdade de Motricidade Humana (FMH): Centro Interdisciplinar de Estudo de Performance Humana, FMH, Universidade de Lisboa, Estrada da Costa, 1499-002, Cruz Quebrada - Dafundo, Portugal].

A mixed model repeated measures ANOVA was used to test for differences across time and sciatic nerve treatment. Sphericity was assessed by Mauchly's test and Greenhouse-Geisser degrees of freedom correction was used in cases sphericity could not be assumed or when corrected *P*-values were below the accepted level of significance ($P < 0.05$). Tukey's HSD test was used for pairwise comparisons. All data is presented as mean and standard deviation, unless otherwise stated. These statistical tests were carried out with IBM SPSS Statistics version 19. For stereology, statistical comparisons of quantitative data were subjected to one-way ANOVA test, followed by pairwise comparisons using Tukey's HSD test. Statistical significance was established as $P < 0.05$. Stereological data was analyzed using the software using the SPSS version 19.0 (SPSS, Chicago, IL). For muscle morphometry, statistical analysis was performed using the SPSS version 19.0 (SPSS, Chicago, IL). Results are presented as mean ± scanning electron microscope (SEM) in Figures 5 and 6. Multiple comparisons between groups were performed by one-way ANOVA supplemented with Tukey's HSD post hoc test. Differences were considered statistically significant at $P < 0.05$.

RESULTS

Development and characterization of MSCs isolated from UC WJ

MSCs are defined by the ISCT which includes the following characteristics: (1) their capacity to adhere to plastic surfaces during cell culture; (2) expression of the specific surface markers (positive for CD73, CD90, and CD105, and no expression of CD14, CD19, CD34, CD45 and HLA-DR); and (3) are able to undergo tri-lineage differentiation into adipocytes, chondrocytes and osteoblasts[19]. MSCs isolated from the UCT were expanded to P5-P6 where the culture appeared homogeneous and cells presented their typical fusiform, fibroblast-like, morphology (Figure 1). Flow cytometry analysis performed previously to *in vivo* application to expanded MSCs showed that over 95% of the cells in the population were consistently positive for the cell surface markers CD44, CD73, CD90 and CD105 and less than 2% positive for CD14, CD19, CD31, CD34, CD45 and HLA-DR. Also, the phenotype of MSCs was assessed by PromoCell by flow cytometry analysis for an additional comprehensive panel of markers: PECAM (CD31), HCAM (CD44), CD45, and Endoglin (CD105). Overall, these results are the ones expected for MSC-type stem cells according to ISCT[19].

Giemsa-stained cells of MSCs at P5 were analyzed

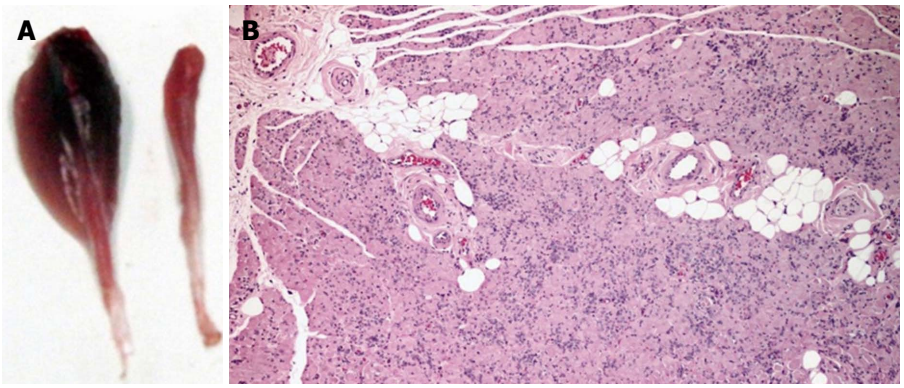

Figure 6 Macroscopic appearance of control tibialis anterior muscle and histological haematoxylin and eosin staining of a transverse section of tibialis anterior muscle. A: Macroscopic appearance of control tibialis anterior (TA) muscle (left) and 20 wk following neurotmesis and surgical treatment with PVA CNTs MSCs (right); B: Histological haematoxylin and eosin staining of a transverse section of TA muscle from PVA CNTs MSCs group. Magnification 40 ×. PVA: Polyvinyl alcohol; CNTs: Carbon nanotubes; MSCs: Mesenchymal stem cells.

for cytogenetic characterization. The karyotype of MSCs was determined previously to *in vivo* application to ensure that no neoplastic cells were used proving the cell therapy safety. The karyotype analysis demonstrated that no structural alterations were found, as well as chromosomal stability in terms of number and structure of the somatic and sexual chromosomes, to the cell culture procedures. The transplanted MSCs also presented normal morphology and flow cytometry markers for MSCs according to ISCT[19].

Results obtained from epifluorescence technique confirmed that MSCs did not begin the apoptosis process, showing that the *in vivo* applied MSCs were viable even in the presence of the tube-guides biomaterials. The $[Ca^{2+}]_i$ measured was 47.9 ± 4.5 (n = 25), 46.2 ± 3.5 (n = 25) and 48.1 ± 3.9 (n = 25) for MSCs cultured in the presence of PVA, PVA-CNTs, and PVA-PPy discs after 7 d of culture, respectively. The MSCs cultured and expanded in the presence of the three tested biomaterials reached confluence and exhibited a normal star-like shape with a flat morphology in culture. According to these results, it is reasonable to conclude that the three biomaterials (PVA, PVA-CNTs, and PVA-PPy) are viable substrate for MSCs culture and survival and may be used in the pre-clinical trials.

The MSCs were harvested and its RNA purified and converted to cDNA using adequate procedures. Primers targeting markers, two housekeeping genes (β-actin and *GAPDH*) and five specific of neuronal cells (GFAP, NeuN, Nestin, NF-H and GAP-43) were used to support the fact that the MSCs used *in vivo* were not differentiated into neuro-glial cells. The molecular analysis showed a very small amplification of GFAP gene, absence of amplification of the NF-H and GAP-43 genes, and reasonable amplification of *NeuN*, β-actin, *GAPDH* and Nestin genes. Amplification of a given gene is correlated with its expression seeing that the template DNA is the one generated from mRNA. According to the results of RT-PCR, the molecular analysis showed a small expression of *GFAP* gene and absence of expression of the NF-H and *GAP-43* genes in the expanded MSCs.

Biomaterials characterization

The electrical conductivity achieved for the different tube-guides (PVA, PVA-CNTs and PVA-PPy) was the following: 1.5 ± 0.5 × 10^{-6} S/m, 579 ± 0.6 × 10^{-6} S/m, and 1837.5 ± 0.7 × 10^{-6} S/m, respectively. Therefore these three tube-guide [simple PVA, PVA loaded with 0.05% (%w/v) of COOH-functionalized CNTs and PPy] compositions were chosen for further characterization and for *in vivo* application in the rat sciatic nerve neurotmesis injury model. The thermal characteristics of simple PVA and loaded PVA materials was examined by differential scanning calorimetry and enthalpy of fusion (ΔH) was calculated, and the percentage of crystallinity was near 7.4% for all analyzed nerve guide tubes. Fourier transform infrared spectroscopy analysis the bands identified for PVA loaded with COOH-functionalized CNTs were similar of the bands detected for simple PVA. For PVA loaded with PPy new bands appeared at 1313/cm (C - N stretching vibration in the ring) and 1170/cm (C - H in-plane deformation). Compared with simple PVA the other nerve guide tubes showed a less intensity of the peaks, especially between 2237 and 2380/cm (unpublished data). Considering the XRD analysis previously performed, the broad peak observed at 20° corresponded to a typical diffraction peak of PVA, and it could be also observed in all tube-guides. Near 26° a broad scattering peak appeared for the tube loaded with PPy, and it was an indication of the presence of PPy as supported in literature[46]; (unpublished data).

Both PVA and PVA loaded with PPy when analyzed by SEM exhibited similar surface appearance. On the other hand, the PVA loaded with COOH-functionalized CNTs showed a rougher surface as expected due to the presence of CNTs on PVA matrix, with oriented features. This characteristic was determinant to choose this biomaterial to be associated to the MSCs (PVA-CNTs-MSCs group). The Wettability analysis showed a hydrophilic behavior for the three biomaterials used for tube-guide tested, also the three materials showed negative zeta potential being the PVA the most negative

Table 1 Static sciatic functional index

SSI		Time											
		T0	T1	T2	T4	T6	T8	T10	T12	T14	T16	T18	T20
Group 1: PVA	Mean	-3.13	-40.52	-52.76	-69.60	-60.30	-56.59	-63.51	-54.89	-40.25	-44.03	-57.34	-48.23
(n = 7)	SD	24.17	19.25	17.78	9.56	19.69	13.19	8.05	11.96	13.33	9.07	21.81	7.25
Group 2: PVA-CNTs	Mean	12.10	-41.85	-45.81	-68.07	-51.18	-52.22	-49.31	-44.52	-48.73	-37.65	-38.47	-38.99
(n = 7)	SD	34.10	20.82	23.21	17.00	11.41	41.96	21.11	17.62	26.31	20.78	17.97	31.11
Group 3: PVA-PPy	Mean	5.31	-41.40	-50.95	-45.76	-47.40	-34.56	-39.51	-31.52	-32.47	-43.17	-50.00	-36.08[b]
(n = 7)	SD	17.51	17.52	23.99	29.92	22.53	14.00	25.05	15.10	20.78	25.52	11.77	16.09
Group 4: Graft	Mean	-6.29	-56.46	-52.18	-55.41	-63.81	-59.79	-75.56	-53.15	-64.53	-67.22	-57.95	-52.07
(n = 4)	SD	1.59	28.10	27.54	27.99	19.06	11.00	10.45	15.44	12.14	12.17	8.31	9.76
Group 5: End-to-End	Mean	-5.78	-44.21	-33.72	-58.28	-73.92	-70.22	-52.47	-68.04	-41.91	-46.56	-43.04	-59.97
(n = 5)	SD	12.91	15.34	15.72	22.25	6.82	6.44	27.43	11.02	24.55	16.79	12.31	2.64
Group 6: PVA-CNTs-MSCs	Mean	3.46	-31.48	-23.75	-28.57	-39.97	-40.30	-62.32	-34.71	-26.28	-42.87	-37.54	-36.16[b]
(n = 7)	SD	12.35	21.89	19.70	9.96	9.20	21.72	18.07	16.44	15.31	25.75	10.06	14.87

Static sciatic functional index (SSI) measured pre-operatively (week-0), and every week after the surgical procedure until week-20. An index score of 0 is considered normal and an index of 100 indicates total impairment. The measurements of the toe spread (TS), and the intermediary TS, were taken from the experimental (E) and normal (N) sides. Results are presented as mean and SD. n corresponds to the number of rats within the experimental group. PVA: Polyvinyl alcohol; CNTs: Carbon nanotubes; PPy: Polypyrrole; MSCs: Mesenchymal stem cells. [b]$P < 0.01$ *vs* Graft.

surface (-4.97 mV) (Figure 2).

Functional analysis during the healing period of 20 wk

SFI and SSI analysis: A few SSI data were missing due to inability to collect visible fingerprints as it was previously referred. As a result of the limited number of animals and the limitations of repeated measures analysis, missing SSI values were replaced using interpolation. Nine of a total of 275 SSI values were interpolated with only one animal having two missing values replace using the linear interpolation procedure. Also because of missing values, the 2-wk time point was not considered for statistical analysis. Sciatic nerve neurotmesis caused a steep decrease in SSI scores in every experimental group and therefore a significant effect of time could be found [F(10, 200) = 20.445; $P < 0.001$]. SSI scores remained negative and with little changes throughout the time following sciatic nerve neurotmesis and independently from sciatic nerve treatment, leading to a non-significant time *vs* treatment interaction effect [F(40, 190) = 279.581; $P < 0.651$]. However, there was significant differences in the extent of SSI scores' decrease between the experimental groups [F(4, 20) = 5.848; $P < 0.01$], with PVA-PPy tube-guides ($P < 0.01$) and PVA-CNTs-MSCs ($P < 0.01$) groups showing less severe SSI scores compared with Graft group (Table 1).

The motor performance by SFI was not possible to perform due to autotomy observed in all treated animals.

Evaluation of motor performance (EPT) and nociceptive function (WRL): In the weeks following sciatic nerve neurotmesis there was a large increase in the time latency to withdraw the paw in response to the thermal stimulus, with most animals reaching the cut-off time of 12 s and leading to a significant effect of time [F(11, 341) = 17.944; $P < 0.001$]. A mild improvement in latency times occurred over the weeks of recovery at a rate that was similar between the experimental groups so that no significant interaction effect existed [F(55, 341) = 5.727; $P < 0.503$]. According to ANOVA results, differences between treated groups (PVA, PVA-CNTs, PVA-PPy, PVA-CNTs-MSCs, Graft and End-to-End) in the severity of changes in WRL times existed [F(5, 31) = 2.942; $P < 0.05$], but these differences were not large enough to be detected by the pairwise comparisons (Table 2).

The motor performance by EPT was not possible to perform due to autotomy observed in all treated animals.

Ankle joint kinematics: Measures of ankle joint angle at the four selected instants of the stance phase (IC, OT, HR and TO) were collected at the end of 20-wk recovery period. This analysis was carried out only for biomaterial (PVA, PVA-CNTs and PVA-PPy groups, n = 7) and biomaterial plus MSCs-treated animals (PVA-CNTs-MSCs group, n = 7). Ankle joint angle values were similar across the experimental groups at the times of IC, OT and HR (P = non-significant). However, at TO less acute ankle joint angles were seen for PVA-CNTs-MSCs group, compared with PVA-PPy group ($P < 0.01$) and with PVA-CNTs group showing similar trend also compared with PVA-PPy group ($P = 0.051$). Such less acute ankle joint angles might suggest improved ankle muscles function during the push off phase of the rat's gait cycle (Table 3 and Figure 4).

Morphological analysis

Muscle results: After the healing period of 20 wk, TA muscle of all treated rats from the experimental groups (PVA, PVA-CNTs, PVA-PPy, PVA-CNTs-MSCs, Graft and End-to-End) was collect for histological analysis and morphometry to evaluate the secondary neurogenic muscle atrophy associated to neurotmesis injury. It was also evaluated the muscle healing process that followed the sciatic nerve regeneration where the scaffold

Table 2 Withdrawal reflex latency

WRL		Time											
		T0	T1	T2	T4	T6	T8	T10	T12	T14	T16	T18	T20
Group 1: PVA	Mean	3.71	10.95	10.81	10.68	9.74	10.23	9.85	8.15	7.78	9.99	7.88	6.98[a]
(n = 7)	SD	0.93	1.45	2.04	2.26	2.89	2.50	2.81	2.70	3.50	2.49	3.72	3.72
Group 2: PVA-CNTs	Mean	5.36	9.91	8.98	7.50	8.40	9.48	9.51	6.92	6.60	8.43	5.88	5.83[a]
(n = 7)	SD	1.50	3.57	3.65	3.36	3.22	3.41	3.01	3.49	3.41	3.40	3.09	2.80
Group 3: PVA-PPy	Mean	4.86	11.42	9.37	7.10	7.85	8.82	9.72	6.87	7.02	7.09	6.06	7.02[a]
(n = 7)	SD	1.69	1.54	3.31	2.51	3.40	2.53	2.35	3.50	3.92	3.23	4.43	3.89
Group 4: Graft	Mean	4.53	12.00	10.14	11.17	11.50	10.67	10.83	11.16	9.81	10.46	9.92	9.68[a]
(n = 4)	SD	1.14	0.00	3.72	1.66	1.01	2.65	2.35	1.27	2.84	1.78	1.82	1.88
Group 5: End-to-End	Mean	4.28	12.00	11.85	12.00	10.22	10.45	8.78	10.48	9.26	8.57	9.82	7.50
(n = 5)	SD	0.86	0.00	0.34	0.00	2.50	2.12	2.22	2.86	3.07	0.98	2.02	0.87
Group 6: PVA-CNTs-MSCs	Mean	3.93	12.00	8.89	9.23	9.30	9.90	7.65	7.41	10.06	8.33	8.28	8.02[a]
(n = 7)	SD	0.86	0.00	2.36	1.63	2.72	2.66	2.51	2.33	1.85	2.86	2.34	1.20

Values in seconds were obtained performing withdrawal reflex latency (WRL) test to evaluate the nociceptive function. This test has been performed pre-operatively (week-0), at week 1, week 2 and every 2 week after the surgical procedure until week-20, when the animals were sacrificed for morphological analysis. Results are presented as mean and standard error of the mean (SD). n corresponds to the number of animals within each experimental group. PVA: Polyvinyl alcohol; CNTs: Carbon nanotubes; PPy: Polypyrrole; MSCs: Mesenchymal stem cells. [a]$P < 0.05$ *vs* End-to-End.

Table 3 Ankle kinematics

Temporal events	Group	Week 20
IC	Group 1: PVA	-3.23 ± 20.65
	Group 2: PVA-CNTs	-8.32 ± 17.36
	Group 3: PVA + PPy	0.82 ± 26.33
	Group 6: PVA-MSCs	-13.68 ± 8.57
OT	Group 1: PVA	28.30 ± 19.52
	Group 2: PVA-CNTs	27.67 ± 12.91
	Group 3: PVA + PPy	17.66 ± 13.20
	Group 6: PVA-MSCs	11.43 ± 9.69
HR	Group 1: PVA	46.67 ± 14.81
	Group 2: PVA-CNTs	47.69 ± 11.19
	Group 3: PVA + PPy	36.46 ± 10.14
	Group 6: PVA-MSCs	34.07 ± 6.85
TO	Group 1: PVA	33.99 ± 9.57
	Group 2: PVA-CNTs	27.01 ± 10.99
	Group 3: PVA + PPy	43.90 ± 8.76
	Group 6: PVA-MSCs	20.56 ± 11.31

Values were obtained performing video analysis at 20-wk of the healing period. Results are presented as mean and standard deviation (SD) (n = 7). For each step cycle the following time points were identified: Initial contact (IC), opposite toe off (OT), heel rise (HR) and toe-off (TO). PVA: Polyvinyl alcohol; CNTs: Carbon nanotubes; PPy: Polypyrrole.

was applied. It was possible to observe by muscle morphometry that there was a significant difference ($P < 0.05$) in terms of the increase in mean fiber size between some of the treatment (PVA-PPy and PVA-CNTs) groups and the Graft group. In fact, in the PVA-PPy group there was a 25% increase in terms of average fiber area and a 13% increase in terms of the "minimal Feret's diameter", when compared to the Graft group. Whereas in the PVA-CNTs treatment group there was a 42% increase in terms of average fiber area and a 21% increase in term of the "minimal Feret's diameter", when compared to the Graft group. Although both these two treatment groups (PVA-PPy and PVA-CNTs) exhibited significant improvement in fiber size, approaching the values for normal muscles (collected from rats with no sciatic nerve neurotmesis lesion), both of them were still significantly different ($P < 0.05$) from the control group (without lesion) at 20 wk after lesion. PVA treatment without any coating (PVA group) revealed no regeneration benefit since the mean fiber size was lower (with significant difference in terms of "minimal Feret's diameter"; $P < 0.05$) when compared to the Graft group (Figure 5). However, unexpected results were observed with PVA-CNTs-MSCs, which showed the worst results in terms of muscular atrophy after denervation, results not correlated with functional analysis (considering mostly kinematics gait analysis and SSI) (Figure 5). The decreased fiber size observed in these animals' TA muscles was coincident with the smaller sized muscles that were collected at 20 wk after surgery macroscopically evaluated during the collection for histological evaluation. Histologically it was also possible to detect a considerable amount of necrosis with delayed muscle regeneration in this group's muscles (Figure 6).

Histomorphometry of the regenerated sciatic nerve: Histological analysis showed that nerve fiber regeneration occurred in all reconstructed nerves. In comparison to controls (sciatic nerve without neurotmesis injuries, data not shown)[3], in all repaired nerves regenerated fibers showed small axons with thin myelin sheaths and microfasciculation (Figure 7). Microfasciculation was more evident in the PVA-CNTs-MSCs repaired group (Figure 7 and Table 4). Also, stereological analysis disclosed a significantly ($P < 0.05$) larger axon diameter, but not fiber diameter, in the regenerated nerves from PVA-PPy group compared with those from PVA-CNT-MSC group (Table 4). On the other hand, as it was previously reported[3,25], the application of MSCs-based cell therapy to neurotmesis nerve injuries resulted in a significantly increased myelin thickness (M), ratio myelin thickness/axon diameter (M/d) and ratio axon diameter/fiber diamenter (d/D; g-ratio) when compared to PVA, PVA-CNTs, PVA-PPy groups ($P < 0.05$). The results clearly demonstrate a

Table 4 Stereological quantitative assessment

Group		Density	Total number	Axon diameter (d)	Fiber diameter (D)	Myelin thickness (M)	M/d	D/d	d/D (g-ratio)	Area (mm^2)
Group 1: PVA	Mean	42872	16596	2.95	3.56	0.31[a]	0.11[a]	1.23	0.82[a]	0.3862
(n = 7)	SD	4007	1741	0.25	0.28	0.03	0.01	0.02	0.01	0.0772
Group 2: PVA-CNTs	Mean	36261	16049	2.98	3.71	0.37[a]	0.14[a]	1.28	0.79[a]	0.4455
(n = 7)	SD	4267	1172	0.25	0.27	0.01	0.01	0.03	0.01	0.1856
Group 3: PVA-PPy	Mean	40289	22588	3.03[a]	3.70	0.33[a]	0.12[a]	1.24	0.81[a]	0.5720
(n = 7)	SD	2686	3157	0.21	0.23	0.02	0.01	0.01	0.00	0.2565
Group 4: Graft	Mean	37041	21939	2.58	3.56	0.49	0.21	1.41	0.71	0.5936
(n = 4)	SD	1214	1302	0.06	0.08	0.02	0.01	0.02	0.01	0.0694
Group 5: End-to-end	Mean	38762	22729	2.65	3.58	0.47	0.19	1.38	0.73	0.5990
(n = 5)	SD	1524	2308	0.14	0.16	0.01	0.01	0.01	0.01	0.2082
Group 6: PVA-CNTs-MSCs	Mean	43373	25731	2.44	3.34	0.45[c,e]	0.21[c,e]	1.41	0.72[c,e]	0.5942
(n = 7)	SD	3881	3386	0.20	0.21	0.06	0.04	0.08	0.01	0.1940

Density, total number, axon diameter (d), fiber diameter (D), myelin thickness (M), ratio myelin thickness and axon diameter (M/d), ratio fiber diameter and axon diameter (D/d), ratio axon diameter and fiber diameter (d/D, g-ratio) of regenerated sciatic nerve fibers at week-20 after neurotmesis. Values are presented as mean ± SD. n corresponds to the number of animals within each experimental group. PVA: Polyvinyl alcohol; CNTs: Carbon nanotubes; PPy: Polypyrrole. [a]$P < 0.05$ *vs* PVA-CNT-MSC; [c]$P > 0.05$ *vs* End-to-End; [e]$P > 0.05$ *vs* Graft.

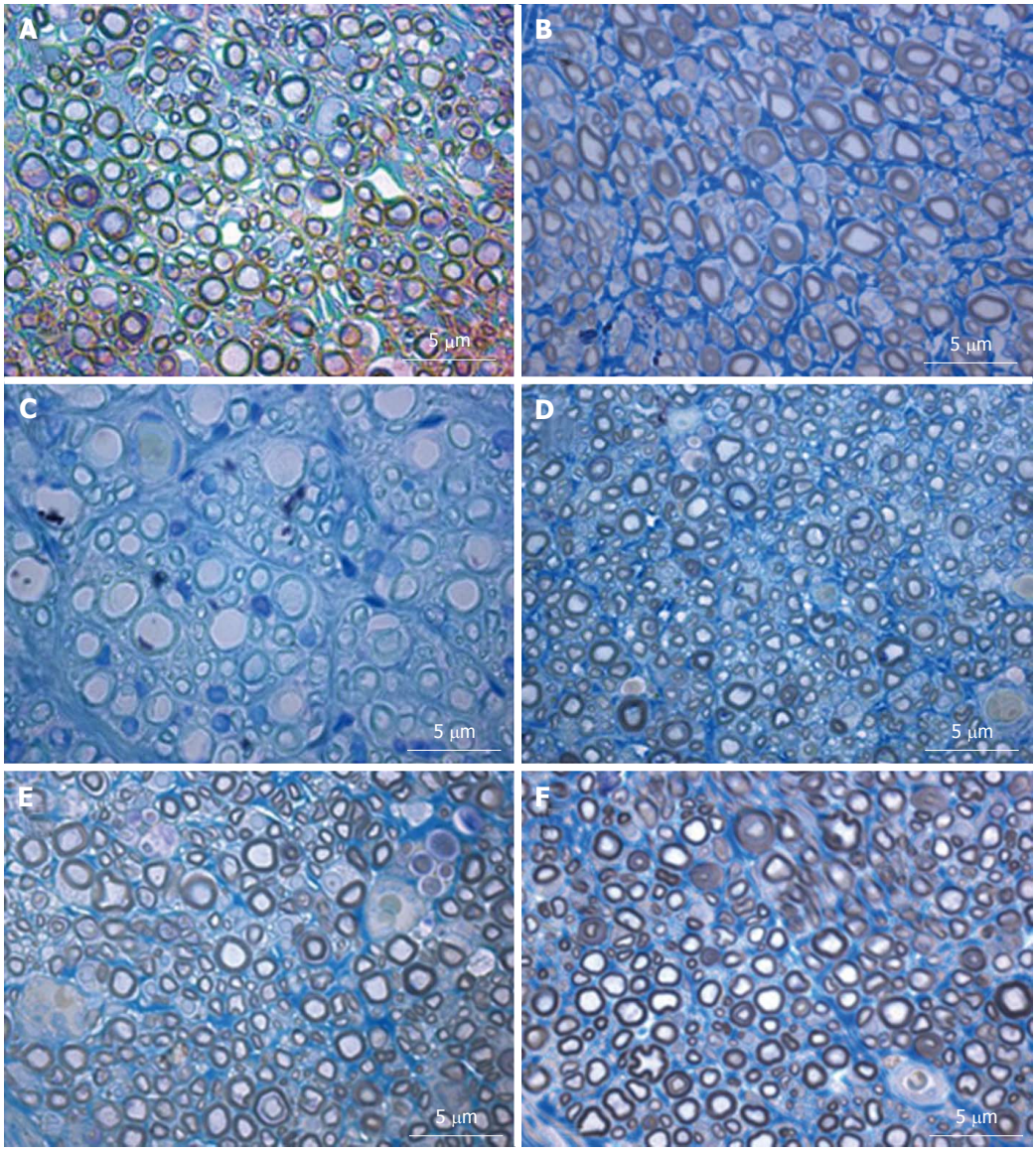

Figure 7 Histological appearance of regenerated nerve fiber in the different groups of neurotmesis. A: PVA; B: PVA-CNTs; C: PVA-PPy; D: PVA-CNTs-MSCs; E: Graft; F: End-to-end suture (magnification: 1000 ×). PVA: Polyvinyl alcohol; CNTs: Carbon nanotubes; PPy: Polypyrrole; MSCs: Mesenchymal stem cells.

synergistic positive effect on regenerated nerve fibers resulting from combined use of MSCs with the PVA-CNTs tube-guides. Also, in the PVA-CNTs-MSCs group these three stereological parameters (M, M/d, and g-ratio) were not significantly different from the values obtained from End-to-End and Graft groups (Table 4). The total number of nerve fibers and nerve fibers density were similar in all groups.

Histology of internal organs: At the microscopic exam, no alterations were observed. The histology sections of all organs confirmed the absence of inflammation, cell degeneration, necrosis and fibrosis. No signs of nanotubes, neither carbon deposits were detected in all organs.

DISCUSSION

An organ re-innervation and functional recovery after nerve injury has been intensively studied worldwide and regenerative medicine methods including cellular systems and new biomaterials concerning the peripheral nerve have been developed. The involved mechanisms in the regeneration process and the ideal scaffold have not been discovered yet. Peripheral nerve might regenerate after some types of injury like axonotmesis but it is difficult to achieve functional recovery after neurotmesis, especially when there is loss of nerve tissue and a gap is created. In the peripheral nervous system, nerves after axonotmesis injuries can regenerate, without any treatment but in most clinical cases a muscle regional neurogenic atrophy occurs. When neurotmesis injuries occur, the nerves must be surgically treated by direct end-to-end suture[33,47,48], using appropriate microsurgery techniques and suturing material. Nowadays most tissue engineered nerve grafts are composed of a neural scaffold prepared with a variety of biomaterials, and surgically applied in neurotmesis injuries with loss of nervous tissue where the direct end-to-end suture is not possible creating tension in the suture line and compromising the nerve regeneration[9]. The introduction of cell therapies should be delivered by appropriate vehicles promoting an important biochemical and physical cue. MSCs represent an appealing source of adult stem cells for cell therapy and tissue engineering including peripheral nerve. Because MSCs are present in low percentage in the adult BM and also because of some of the disadvantages previously listed, alternative sources have been studied, like the UCT (also called Wharton's jelly). MSCs were defined by the ISCT in 2006, and since that time it is considered that MSCs must adhere to plastic; have a specific profile for the specific surface markers (positive for CD73, CD90, and CD105, and negative for CD14, CD19, CD34, CD45 and HLA-DR). Other important characteristic is that MSCs are also able to undergo tri-lineage differentiation into adipocytes, chondrocytes and osteoblasts[19]. I*n vivo* and *in vitro* studies referred that MSCs have the capacity to induce the regeneration of cartilage, bone, tendon, and meniscus[18]. The MSCs are also able to differentiate into neuro-glial cells, which have been studied *in vitro* and *in vivo* using animal models, by our research group[25]. Children and adult clinical trials have been performed where MSCs were used to treat a wide range of pathologies, including neurological disorders, PNS and CNS injuries (access www.clinicaltrials.gov). In fact, nowadays, the cryopreservation of UCB, and UCT is performed worldwide in private and public cord blood banks. Furthermore, the MSCs from the UCT and hematopoietic stem cells from the UCB have positive clinical outcomes not only in hematologic malignancy patients, where the MSCs work as a co-adjuvant for the hematopoietic transplant success, but also in PNS injuries and neurologic disorders. For that reason, the crucial role of MSCs in tissue renewal and regeneration has been well established for several limiting pathologies, not treated by the traditional therapeutic approaches[49]. The *in vivo* application of MSCs performed by the authors was intended to improve the regeneration process in the rat sciatic nerve after a neurotmesis injury which was surgically reconstructed using electric conductive tube-guides of PVA-CNTs composition. At that moment there are several nerve tube-guides in the market, however they still have limitations and the functional outcome of the patients is still not complete. In this work the previously developed tube-guides with high electrical conductivity for nerve regeneration (unpublished data) were used *in vivo* using the rat sciatic nerve neurotmesis injury model. A matrix of PVA was used loaded with the following electrical conductive materials: COOH-functionalized multiwall carbon nanotubes (MWCNTs) and PPy PVA-CNTs and PVA-PPy tube, guides, respectively. The tubes production was carried out by a freezing/thawing process (physical cross-linking) and a final annealing treatment. After producing the tube-guides, the physicochemical characterization was performed. The most interesting results were achieved by loading PVA with 0.05% of PPy or COOH-functionalized CNTs, by combining the electrical conductivity of CNTs and PPy with the biocompatibility of PVA matrix, which seems to have potential to be used in peripheral nerve regeneration. For that reason, these two biomaterials were chosen to proceed for *in vivo* pre-clinical trials using the rat sciatic model. As a matter of fact, the microscopic exam performed to lung, heart, kidneys, liver and spleen collected after animal euthanasia, confirmed the absence of inflammation, cell degeneration, necrosis and fibrosis, and no signs of nanotubes, neither carbon deposits were detected in all organs, confirming the biocompatibility of these biomaterials loaded with CNTs. The evaluation of cytocompatibility was performed by measuring the $[Ca^{2+}]_i$ in Fura-2-loaded MSCs cells by using dual wavelength spectrofluorometry, sub-cultured over *PVA* discs, over PVA loaded with carbon nanotubes (PVA-CNTs) and PVA loaded with PPy (PVA-PPy) discs of 10 mm diameter, as previously described[3,25,27]. Results correspond to $[Ca^{2+}]_i$ from viable MSCs that did not begin the apoptosis

process, confirming the MSCs ability to expand and viability when associated to PVA, PVA-PPy and PVA-CNTs tube-guides.

The MSCs isolated from the WJ used as cell-based therapy for promoting nerve regeneration when associated to electric conductive tube-guides was previously *in vitro* validated concerning flow cytometry profile, RT-PCR, and cytogenetic analysis. MSCs were expanded to P5-P6 where the culture appeared homogeneous and cells presented their typical fusiform, fibroblast-like, morphology (Figure 1). Also, the flow cytometry analysis confirmed their profile according to ISCT[19] and the karyotype demonstrated that no structural alterations were present demonstrating absence of neoplastic characteristics in these cells, as well as chromosomal stability to the cell culture procedures. RT-PCR and qPCR targeting specific genes expressed by the MSCs *in vivo* applied was performed to certify that the MSCs used *in vivo* were not differentiated into neuro-glial cells. For the MSCs, the molecular analysis showed a very small amplification of *GFAP* gene, absence of amplification of the *NF-H* and *GAP-43* genes, and reasonable amplification of NeuN, β-actin, *GAPDH* and Nestin genes, confirming that MSCs used *in vivo* were undifferentiated and not neuro-glial differentiated. In fact, the small detection of the *GFAP* gene expression may be due to the high sensitivity of the molecular tests in comparison with immunocytochemistry tests previously performed using undifferentiated and neuro-glial type differentiated MSCs[3,18]. Moreover, the expression of the remaining genes, NeuN, β-actin, GAPDH and Nestin was also observed in undifferentiated MSCs. The expression of the housekeeping genes, β-actin and GAPDH, is expected to occur. As per the NeuN and Nestin gene, the observation of its expression in undifferentiated MSCs is not new; Bertani *et al*[50] showed that naïve MSCs express at a constitutive level NeuN gene, which increases when these cells are chemically induced to differentiate to pre-neuronal cells. Furthermore, compared gene expression profiles before and after MSCs induction for a number of germ layers, and observed that even before neuronal induction, MSCs population and clonal lines expressed a mixture of mesodermal, germinal, endodermal and ectodermal genes, including several whose expression was thought to be restricted to neuronal cells[51]. Molecular analysis previously performed[18] on these same genetic markers over the differentiated MSCs showed an increase in the expression of *GFAP*, *NF-H* and *GAP-43* genes. These genes were not expressed, or expressed at very low levels, in the undifferentiated MSCs transcriptome. Overall, these results support the fact that the MSCs used *in vivo* were not differentiated but presented a neuro-glial potential for differentiation confirming previous results where the same MSCs undifferentiated and *in vitro* differentiated into neuro-glial cells were tested in axonotmesis and neurotmesis injuries associated to other biomaterials namely poly(DL-lactide-ε-caprolactone), hybrid chitosan and collagen[3,25,31].

The rat sciatic nerve model has been widely used in experiments on peripheral nerve regeneration and it has been demonstrated that it is reliable and reproducible model, but research on peripheral nerve injury needs to include both functional and morphological analysis[52]. Since it is not generally agreed which type of evaluation tool is the most useful for evaluation of functional recovery; our research group like others has been using different methods for an overall assessment of nerve function, which has been widely recommended[53]. The sciatic nerve regeneration after neurotmesis studies described by the authors were followed during 20 wk after the surgical procedure based on the previous experimental work[17,29,54,55]. The morphological evaluation together with functional data has been used to assess neural regeneration after induced neurotmesis injuries, but some subjective evaluation, depending on the operator/research analysis is observed[9]. Some methods for evaluation of nerve recovery, like peroxidase and retrograde fluorescent labeling, histomorphometry, and retrograde transport of horseradish[47,56] fail in assessing the functional recovery, which is essential to evaluate the success of a scaffold application[57,58]. The present experimental work includes a variety of independent evaluation tools considering the morphologic and functional recovery, in order to understand and estimate the potential therapeutic benefit of a nerve repair strategy[9]. EPT, WRL, SSI and SFI, have been proven to be valid methods and to give some information to determine functional recovery following sciatic nerve injury, including motor and nociceptive evaluation[59]. The use of biomechanical techniques and rat's gait kinematic evaluation was a progress in documenting functional recovery, largely published by our research group[3,9,17,31,33,35]. Indeed, the use of biomechanical parameters allows an accurate analysis of the sciatic denervation/reinnervation process, permitting to understand the integration of the neural control acting on the ankle and foot muscles, and thus allowing to evaluate the nerve and muscle regeneration after neurogenic muscle atrophy associated to neurotmesis injuries[60,61]. At the end of the 20-wk healing period, it was performed kinematic gait analysis of rats from the groups where it was applied the biomaterial alone or associated to MSCs-based therapies (PVA, PVA-CNTs, PVA-PPy, and PVA-CNTs-MSCs groups) and measures of ankle joint angle at the four selected instants of the stance phase (IC, OT, HR and TO) were obtained (Table 3 and Figure 4). Considering the histological analysis, it was performed stereology of the regenerated sciatic nerves and morphometry analysis of the TA muscles, trying in this way, not only correlate the neurotmesis injury and the secondary neurogenic regional atrophy, but also consider and validate the morphometry of regional muscles (for instance, by biopsy of the injured muscle) as a method to assess functional recovery after peripheral nerve injuries[18,25]. The restoration of locomotor activity following damage of the PNS has emerged as one of the most important and critical clinical problem in

neuroscience and neurosurgery fields. Regional muscle weakness and impairment of joint control and mobility occurs in many patients with peripheral nerve or spinal cord injuries which results in gait disorders only evaluated with accuracy by kinematics analysis. During the past 10-15 years, experimental work has been carried out on rat gait analysis which may significantly contribute in the future for a more precise peripheral nerve research. Indeed, the use of biomechanical parameters permits an integration of the neural control acting on the ankle and foot muscles, relevant for the analysis of the sciatic denervation/reinnervation effects. The biomechanical analysis is very useful and accurate to evaluate different therapeutic approaches, describing high number of kinematic variables including positions, velocities, and accelerations, often using high speed digital cameras[35,40,62,63]. There is high variability between individual joint kinematics and between different animals from the same the same experimental group[64]. The high level of variability observed in normal quadruped walking, affects significantly the precision of joint kinematic measures of functional recovery after nerve injury. It is important to reduce this variability in kinematics analysis to assess functional recovery after neurogenic muscle atrophy and neurotmesis/axonotmesis injuries. One evident advantage is that using a treadmill the operator reduces step-by-step variability in joint kinematics[59] which has the disadvantage of being expensive equipment. Also the possibility of combining kinematic analysis with other data, such as ground reaction forces, should be consider for a more accurate evaluation of nerve regeneration[59,64,65]. Our research group has recently analyzed hip, knee and ankle joint kinematics during recovery of rat sciatic nerve axonotmesis injury, using reflective markers attached to the rat hind-limb to track the motion with infra-red capture cameras, to better assess the rat sciatic nerve model hind-limb joint kinematics during walking. Due to physiological constraints and muscle actions it was observed that different joints have different motion patterns within motion planes, more evident when a 3D segmental kinematic analysis using a 3D reconstruction of the rat hind-limb was performed[9]. This method allowed a more complete segmental kinematic analysis using both planar angles computation (2D) and a 3D reconstruction of the rat hind-limb but unfortunately, in the present experimental work it was only possible to perform a 2D gait analysis[9]. In the present work, 2D biomechanical analysis (sagittal plan) was carried out applying a two-segment model of the ankle joint, adopted from the model firstly developed by Varejão *et al*[40]. For that reason, ankle joint angle values were similar across the experimental groups at the times of IC, OT and HR. However, less acute ankle joint angles observed in PVA-CNTs-MSCs group, compared with PVA-PPy and PVA-CNTs groups might suggest improved ankle muscles function during the push off phase of the rat's gait cycle (Figure 4 and Table 3). It is well known and demonstrated by the scientific bibliography that neuromuscular pathologies are related to important clinical signs or motor deficits that should be observed, qualified, and quantified, only possible with a precise kinematic analysis[65,66]. In the field of peripheral nerve research using the rat sciatic nerve model, an improved walking analysis might include several methods combination like joint kinematics, ground reaction forces and electromyographical data of muscle activity. These methods refinements might be important to differentiate the regenerative potential of different scaffolds used, that are not evident when using the traditional standardized methods previously referred[9,66].

The recent published paper by di Summa *et al*[67] where collagen tube-guides (Neurogen®) were used *in vivo* to promote peripheral nerve regeneration, combined with schwann cells (SCs), it was possible to demonstrate an improved distal stump sprouting[68]. This sprouting was more pronounced in the experimental group where the SCs were derived from BM-MSCs when compared to SCs derived from adipose tissue MSCs (AT-MSCs). On the other hand, no significant differences were observed in proximal regeneration among all the experimental groups. BM-MSCs and AT-MSCs -loaded conduits induced a diffuse sprouting pattern of the axons. On the other hand, the tube-guides loaded with SCs induced an enhanced cone pattern and a typical sprouting along the collagen type Ⅰ conduits walls, showing improved regenerating results. This observation is important and should be related to results obtained from the innervated muscle morphometry analysis. It should be bear in mind that the sprouting is also evaluated and a constant observation in the histomorphometry analysis of the regenerated peripheral nerve after axonotmesis and neurotmesis lesions, where different reconstruction strategies were tested *in vivo* in the rat model by our research group for the past years[3,25,31,68].

The morphometry and histological analysis of TA muscles collected from rats where the neurotmesis injury was reconstructed with PVA-CNTs-MSCs tube-guides is in fact somehow surprising since in the treatment groups presented in a previous published study (Gärtner *et al*[3], 2014), no adverse effect was noticed when MSCs isolated from UC WJ were used. The TA muscles from PVA-CNTs-MSCs group presented the worst results in terms of muscular atrophy after denervation, results not correlated with functional analysis (considering mostly kinematics gait analysis and SSI) (Figure 5). The decreased fiber size observed in these TA muscles was coincident with the smaller sized muscles that were collected at 20 wk, macroscopically evaluated during the collection for histological evaluation. Histologically it was also possible to detect a considerable amount of necrosis with delayed muscle regeneration in this group's TA muscles (Figure 6). Some toxic metabolite resulting from the interaction between the vehicle where the MSCs are suspended (PBS) which has calcium and magnesium, and PVA-CNTs tube-guide, could explain the histological results. These results may occur, not because there is a deleterious effect of the cellular

system, but because the vehicle is not appropriate to the cells microenvironment. As a matter of fact these MSCs were previously tested associated to Floseal® and some local nerve necrosis could be observed by histological analysis. On the other hand, the myelin sheath of the MSCs-treated regenerated nerves was thicker, suggesting that MSCs might exert their positive effects on SCs, the key element in Wallerian degeneration and consequent axonal regeneration[3]. From the data obtained from the stereology analysis of PVA, PVA-CNTs, PVA-PPy, Graft, End-to-End and PVA-CNTs-MSCs groups, it was also demonstrated a synergistic positive effect on regenerated nerve fibers resulting from combined use of MSCs with the PVA-CNTs tube-guides, where PVA-CNTs-MSCs presented higher myelin thickness (M), ratio myelin thickness/axon diameter (M/d) and ratio axon diameter/fiber diameter (d/D; g-ratio) when compared to PVA, PVA-CNTs, PVA-PPy groups (Table 4). Also, these three stereologic parameters (M, M7d, and g-ratio) measured in PVA-CNTs-MSCs regenerated nerves, were not significantly different from the values obtained from End-to-End and Graft groups. In conclusion, as it was previously reported[3,25], in the MSCs-based cell therapy applied to neurotmesis nerve injuries, it is observed a significantly higher myelin thickness, and similar to Graft and End-to-End regenerated nerves, which are considered the Gold Standards in nerve neurosurgery. These results clearly are consisted with functional data, from SSI and kinematic gait analysis. The PVA-CNTs and PVA-PPy groups presented significantly higher axon diameters (d) and fiber diameters (D), suggesting also the positive effect of these electric conductive materials on axon regeneration and reestablishment of the neuro-muscular junction in agreement with the TA muscle morphometry analysis.

In conclusion, the results revealed that treatment with MSCs associated to PVA-CNTs tube-guides induced an increased number of regenerated fibers and thickening of the myelin sheet. Functional and kinematics analysis has revealed positive synergistic effects brought by MSCs and PVA-CNTs. The PVA-CNTs and PVA-PPy are promising scaffolds with electric conductive properties, bio and cytocompatible, that might prevent in some degree the secondary neurogenic muscular atrophy by improving the reestablishment of the neuro-muscular junction. Since the present studies were carried out in rats with human MSCs, it is important to continue these studies to evaluate the therapeutic potential of these MSCs in human nerve injuries. However, the results discussed herein show a promising effect of MSCs and PVA-CNTs tube-guides in in neurodegenerative diseases that are typified by demyelination since this scaffold induced myelin production in surgically reconstructed nerves after a neurotmesis injury.

COMMENTS

Background

The sought for effective new therapeutic strategies for improving peripheral nerve regeneration represents one of the hot topics in biomedicine because of the high number of lesions affecting peripheral nerves (much higher than lesions to the spinal cord).

Research frontiers

In this study, the authors have tested *in vitro* and *in vivo* mesenchymal stem cells (MSCs) derived from the umbilical cord matrix [Wharton's jelly (WJ)] associated to electric conductive tube-guides developed by their research group, focusing on its effect in promoting nerve regeneration in the rat neurotmesis model. In particular, *in vivo* assessment of nerve regeneration and functional recovery was carried out using a comprehensive battery of complementary methods of analysis that the authors have developed along their previous experience in the study of nerve repair and regeneration and which include behavioral analysis of motor and nociceptive function, kinematic analysis using high speed cameras and histological analysis of nerve fiber regeneration.

Innovations and breakthroughs

The results of this study open interesting perspectives for the clinical application of biodegradable membranes in peripheral nerve reconstruction associated to MSCs isolated from the umbilical cord matrix. Interestingly, these cells, which are major histocompatibility complex class Ⅱ negative, not only express both an immune-privileged and immune-modulatory phenotype, but their major histocompatibility complex class Ⅰ expression levels can also be manipulated, making them a potential cell source for MSC-based therapies. In addition, these cells represent a non controversial source of primitive mesenchymal progenitor cells that can be harvested after birth, cryogenically stored, thawed, and expanded for therapeutic uses.

Applications

The results revealed that polyvinyl alcohol (PVA)-carbon nanotubes (CNTs) and PVA-polypyrrole (PPy) are promising scaffolds with electric conductive properties, bio and cytocompatible, that might prevent in some degree the secondary neurogenic muscular atrophy by improving the reestablishment of the neuro-muscular junction. Also, a promising effect of MSCs and PVA-CNTs tube-guides in promoting myelin production in surgically reconstructed nerves after a neurotmesis injury was demonstrated. A new gateway it therefore opened for using these cells in neurodegenerative diseases that are typified by demyelination.

Terminology

Neurotmesis (in Greek tmesis signifies "to cut") is part of Seddon's classification used to classify nerve damage. It is the most serious nerve injury. In this type of injury, both the nerve and the nerve sheath are disrupted. Nowadays, when a nerve is damage and there is a neurotmesis injury with a gap, it can be repaired using a nerve tube-guide, whenever it is not possible to perform an end-to-end suture without tension or there isn't a graft available. This work focused on the development of electrical conductive nerve tube-guides, which was achieved by loading PVA with PPy or COOH-functionalized CNTs and their *in vivo* application in the rat sciatic nerve neurotmesis injury model. The inclusion of CNTs and PPy brought a significant increase of electrical conductivity of the simple PVA tube-guide. MSCs as defined by the international society for cellular therapy in 2006, are cells characterized by: (1) their capacity to adhere to plastic; and (2) expression of specific surface markers, namely, CD73, CD90, and CD105, and no expression of CD14, CD19, CD34, CD45 and human leukocyte antigen-DR. Additionally, MSCs are able to undergo tri-lineage differentiation into adipocytes, chondrocytes and osteoblasts.

Peer-review

The article is very interesting. The experimental part is very well designed.

REFERENCES

1 **Lundborg G**. Enhancing posttraumatic nerve regeneration. *J Peripher Nerv Syst* 2002; **7**: 139-140 [PMID: 12365560 DOI: 10.1046/j.1529-8027.2002.02019.x]

2 **Ribeiro J**, Gartner A, Pereira T, Gomes R, Lopes MA, Gonçalves

C, Varejão A, Luís AL, Maurício AC. Perspectives of employing mesenchymal stem cells from the Wharton's jelly of the umbilical cord for peripheral nerve repair. *Int Rev Neurobiol* 2013; **108**: 79-120 [PMID: 24083432 DOI: 10.1016/B978-0-12-410499-0.00004-6]

3 **Gärtner A**, Pereira T, Armada-da-Silva P, Amado S, Veloso A, Amorim I, Ribeiro J, Santos J, Bárcia R, Cruz P, Cruz H, Luís A, Santos J, Geuna S, Maurício A. Effects of umbilical cord tissue mesenchymal stem cells (UCX®) on rat sciatic nerve regeneration after neurotmesis injuries. *J Stem Cells Regen Med* 2014; **10**: 14-26 [PMID: 25075157]

4 **May M**. Trauma to the facial nerve. *Otolaryngol Clin North Am* 1983; **16**: 661-670 [PMID: 6634187]

5 **Fields RD**, Le Beau JM, Longo FM, Ellisman MH. Nerve regeneration through artificial tubular implants. *Prog Neurobiol* 1989; **33**: 87-134 [PMID: 2678271 DOI: 10.1016/0301-0082(89)90036-1]

6 **Meek MF**, Coert JH. Clinical use of nerve conduits in peripheral-nerve repair: review of the literature. *J Reconstr Microsurg* 2002; **18**: 97-109 [PMID: 11823940 DOI: 10.1055/s-2002-19889]

7 **Ghasemi-Mobarakeh L**, Prabhakaran MP, Morshed M, Nasr-Esfahani MH, Baharvand H, Kiani S, Al-Deyab SS, Ramakrishna S. Application of conductive polymers, scaffolds and electrical stimulation for nerve tissue engineering. *J Tissue Eng Regen Med* 2011; **5**: e17-e35 [PMID: 21413155 DOI: 10.1002/term.383]

8 **Jiang X**, Lim SH, Mao HQ, Chew SY. Current applications and future perspectives of artificial nerve conduits. *Exp Neurol* 2010; **223**: 86-101 [PMID: 19769967 DOI: 10.1016/j.expneurol.2009.09.009]

9 **Maurício AC**, Gärtner A, Armada-da-Silva P, Amado S, Pereira T, Veloso AP, Varejão A, Luís AL, Geuna S. Cellular Systems and Biomaterials for Nerve Regeneration in Neurotmesis Injuries. Pignatello R, editor. Biomaterials Applications for Nanomedicine, 2011: 978-979 [DOI: 10.5772/24247]

10 **Hudson TW**, Evans GR, Schmidt CE. Engineering strategies for peripheral nerve repair. *Orthop Clin North Am* 2000; **31**: 485-498 [PMID: 10882473 DOI: 10.1016/S0030-5898(05)70166-8]

11 **Schmidt CE**, Leach JB. Neural tissue engineering: strategies for repair and regeneration. *Annu Rev Biomed Eng* 2003; **5**: 293-347 [PMID: 14527315 DOI: 10.1146/annurev.bioeng.5.011303.120731]

12 **George PM**, Saigal R, Lawlor MW, Moore MJ, LaVan DA, Marini RP, Selig M, Makhni M, Burdick JA, Langer R, Kohane DS. Three-dimensional conductive constructs for nerve regeneration. *J Biomed Mater Res A* 2009; **91**: 519-527 [PMID: 18985787 DOI: 10.1002/jbm.a.32226]

13 **Chronakis IS**, Grapenson S, Jakob A. Conductive polypyrrole nanofibers via electrospinning: Electrical and morphological properties. *Polymer* 2006; **47**: 1597-1603 [DOI: 10.1016/j.polymer.2006.01.032]

14 **Baker MI**, Walsh SP, Schwartz Z, Boyan BD. A review of polyvinyl alcohol and its uses in cartilage and orthopedic applications. *J Biomed Mater Res B Appl Biomater* 2012; **100**: 1451-1457 [PMID: 22514196 DOI: 10.1002/jbm.b.32694]

15 **Harun MH**, Saion E, Kassim A, Ekramul Mahmud HNM, Hussain MY, Mustafa IS. Dielectric properties of poly (vinyl alcohol)/polypyrrole composite polymer films. *JASS* 2009; **1**: 9-16

16 **Ghasemi-Mobarakeh L**, Prabhakaran MP, Morshed M, Nasr-Esfahani MH, Ramakrishna S. Electrical stimulation of nerve cells using conductive nanofibrous scaffolds for nerve tissue engineering. *Tissue Eng Part A* 2009; **15**: 3605-3619 [PMID: 19496678 DOI: 10.1089/ten.tea.2008.0689]

17 **Luís AL**, Rodrigues JM, Geuna S, Amado S, Shirosaki Y, Lee JM, Fregnan F, Lopes MA, Veloso AP, Ferreira AJ, Santos JD, Armada-Da-silva PA, Varejão AS, Maurício AC. Use of PLGA 90: 10 scaffolds enriched with in vitro-differentiated neural cells for repairing rat sciatic nerve defects. *Tissue Eng Part A* 2008; **14**: 979-993 [PMID: 18447635 DOI: 10.1089/ten.tea.2007.0273]

18 **Pereira T**, Ivanova G, Caseiro AR, Barbosa P, Bártolo PJ, Santos JD, Luís AL, Maurício AC. MSCs conditioned media and umbilical cord blood plasma metabolomics and composition. *PLoS One* 2014; **9**: e113769 [PMID: 25423186 DOI: 10.1371/journal.pone.0113769]

19 **Dominici M**, Le Blanc K, Mueller I, Slaper-Cortenbach I, Marini F, Krause D, Deans R, Keating A, Prockop Dj, Horwitz E. Minimal criteria for defining multipotent mesenchymal stromal cells. The International Society for Cellular Therapy position statement. *Cytotherapy* 2006; **8**: 315-317 [PMID: 16923606 DOI: 10.1080/14653240600855905]

20 **Yang CC**, Shih YH, Ko MH, Hsu SY, Cheng H, Fu YS. Transplantation of human umbilical mesenchymal stem cells from Wharton's jelly after complete transection of the rat spinal cord. *PLoS One* 2008; **3**: e3336 [PMID: 18852872 DOI: 10.1371/journal.pone.0003336]

21 **Weiss ML**, Medicetty S, Bledsoe AR, Rachakatla RS, Choi M, Merchav S, Luo Y, Rao MS, Velagaleti G, Troyer D. Human umbilical cord matrix stem cells: preliminary characterization and effect of transplantation in a rodent model of Parkinson's disease. *Stem Cells* 2006; **24**: 781-792 [PMID: 16223852 DOI: 10.1634/stemcells.2005-0330]

22 **Fu YS**, Cheng YC, Lin MY, Cheng H, Chu PM, Chou SC, Shih YH, Ko MH, Sung MS. Conversion of human umbilical cord mesenchymal stem cells in Wharton's jelly to dopaminergic neurons in vitro: potential therapeutic application for Parkinsonism. *Stem Cells* 2006; **24**: 115-124 [PMID: 16099997 DOI: 10.1634/stemcells.2005-0053]

23 **Shin DH**, Lee E, Hyun JK, Lee SJ, Chang YP, Kim JW, Choi YS, Kwon BS. Growth-associated protein-43 is elevated in the injured rat sciatic nerve after low power laser irradiation. *Neurosci Lett* 2003; **344**: 71-74 [PMID: 12782330 DOI: 10.1016/S0304-3940(03)00354-9]

24 **Carvalho MM**, Teixeira FG, Reis RL, Sousa N, Salgado AJ. Mesenchymal stem cells in the umbilical cord: phenotypic characterization, secretome and applications in central nervous system regenerative medicine. *Curr Stem Cell Res Ther* 2011; **6**: 221-228 [PMID: 21476975 DOI: 10.2174/157488811796575332]

25 **Pereira T**, Gärtner A, Amorim I, Almeida A, Caseiro AR, Armada-da-Silva PA, Amado S, Fregnan F, Varejão AS, Santos JD, Bartolo PJ, Geuna S, Luís AL, Mauricio AC. Promoting nerve regeneration in a neurotmesis rat model using poly(DL-lactide-ε-caprolactone) membranes and mesenchymal stem cells from the Wharton's jelly: in vitro and in vivo analysis. *Biomed Res Int* 2014; **2014**: 302659 [PMID: 25121094]

26 **Yoo KH**, Jang IK, Lee MW, Kim HE, Yang MS, Eom Y, Lee JE, Kim YJ, Yang SK, Jung HL, Sung KW, Kim CW, Koo HH. Comparison of immunomodulatory properties of mesenchymal stem cells derived from adult human tissues. *Cell Immunol* 2009; **259**: 150-156 [PMID: 19608159 DOI: 10.1016/j.cellimm.2009.06.010]

27 **Rodrigues JM**, Luís AL, Lobato JV, Pinto MV, Lopes MA, Freitas M, Geuna S, Santos JD, Maurício AC. Determination of the intracellular Ca2+ concentration in the N1E-115 neuronal cell line in perspective of its use for peripheric nerve regeneration. *Biomed Mater Eng* 2005; **15**: 455-465 [PMID: 16308461]

28 **Thalhammer JG**, Vladimirova M, Bershadsky B, Strichartz GR. Neurologic evaluation of the rat during sciatic nerve block with lidocaine. *Anesthesiology* 1995; **82**: 1013-1025 [PMID: 7717536 DOI: 10.1097/00000542-199504000-00026]

29 **Amado S**, Rodrigues JM, Luís AL, Armada-da-Silva PA, Vieira M, Gartner A, Simões MJ, Veloso AP, Fornaro M, Raimondo S, Varejão AS, Geuna S, Maurício AC. Effects of collagen membranes enriched with in vitro-differentiated N1E-115 cells on rat sciatic nerve regeneration after end-to-end repair. *J Neuroeng Rehabil* 2010; **7**: 7 [PMID: 20149260 DOI: 10.1186/1743-0003-7-7]

30 **Koka R**, Hadlock TA. Quantification of functional recovery following rat sciatic nerve transection. *Exp Neurol* 2001; **168**: 192-195 [PMID: 11170734 DOI: 10.1006/exnr.2000.7600]

31 **Gärtner A**, Pereira T, Alves MG, Armada-da-Silva PA, Amorim I, Gomes R, Ribeiro J, França ML, Lopes C, Carvalho RA, Socorro S, Oliveira PF, Porto B, Sousa R, Bombaci A, Ronchi G, Fregnan F, Varejão AS, Luís AL, Geuna S, Maurício AC. Use of poly(DL-lactide-ε-caprolactone) membranes and mesenchymal stem cells from the Wharton's jelly of the umbilical cord for promoting nerve regeneration in axonotmesis: in vitro and in vivo analysis.

Differentiation 2012; **84**: 355-365 [PMID: 23142731 DOI: 10.1016/j.diff.2012.10.001]
32 **Masters DB**, Berde CB, Dutta SK, Griggs CT, Hu D, Kupsky W, Langer R. Prolonged regional nerve blockade by controlled release of local anesthetic from a biodegradable polymer matrix. *Anesthesiology* 1993; **79**: 340-346 [PMID: 8342843 DOI: 10.1097/00000542-199308000-00020]
33 **Amado S**, Simões MJ, Armada da Silva PA, Luís AL, Shirosaki Y, Lopes MA, Santos JD, Fregnan F, Gambarotta G, Raimondo S, Fornaro M, Veloso AP, Varejão AS, Maurício AC, Geuna S. Use of hybrid chitosan membranes and N1E-115 cells for promoting nerve regeneration in an axonotmesis rat model. *Biomaterials* 2008; **29**: 4409-4419 [PMID: 18723219 DOI: 10.1016/j.biomaterials.2008.07.043]
34 **Shir Y**, Zeltser R, Vatine JJ, Carmi G, Belfer I, Zangen A, Overstreet D, Raber P, Seltzer Z. Correlation of intact sensibility and neuropathic pain-related behaviors in eight inbred and outbred rat strains and selection lines. *Pain* 2001; **90**: 75-82 [PMID: 11166972 DOI: 10.1016/S0304-3959(00)00388-2]
35 **Varejão AS**, Cabrita AM, Meek MF, Bulas-Cruz J, Melo-Pinto P, Raimondo S, Geuna S, Giacobini-Robecchi MG. Functional and morphological assessment of a standardized rat sciatic nerve crush injury with a non-serrated clamp. *J Neurotrauma* 2004; **21**: 1652-1670 [PMID: 15684656]
36 **Varejão AS**, Melo-Pinto P, Meek MF, Filipe VM, Bulas-Cruz J. Methods for the experimental functional assessment of rat sciatic nerve regeneration. *Neurol Res* 2004; **26**: 186-194 [PMID: 15072638 DOI: 10.1179/016164104225013833]
37 **Dijkstra JR**, Meek MF, Robinson PH, Gramsbergen A. Methods to evaluate functional nerve recovery in adult rats: walking track analysis, video analysis and the withdrawal reflex. *J Neurosci Methods* 2000; **96**: 89-96 [PMID: 10720672 DOI: 10.1016/S0165-0270(99)00174-0]
38 **Bain JR**, Mackinnon SE, Hunter DA. Functional evaluation of complete sciatic, peroneal, and posterior tibial nerve lesions in the rat. *Plast Reconstr Surg* 1989; **83**: 129-138 [PMID: 2909054 DOI: 10.1097/00006534-198901000-00025]
39 **Bervar M**. Video analysis of standing--an alternative footprint analysis to assess functional loss following injury to the rat sciatic nerve. *J Neurosci Methods* 2000; **102**: 109-116 [PMID: 11040407 DOI: 10.1016/S0165-0270(00)00281-8]
40 **Varejão AS**, Cabrita AM, Meek MF, Bulas-Cruz J, Filipe VM, Gabriel RC, Ferreira AJ, Geuna S, Winter DA. Ankle kinematics to evaluate functional recovery in crushed rat sciatic nerve. *Muscle Nerve* 2003; **27**: 706-714 [PMID: 12766982 DOI: 10.1002/mus.10374]
41 **Geuna S**, Gigo-Benato D, Rodrigues Ade C. On sampling and sampling errors in histomorphometry of peripheral nerve fibers. *Microsurgery* 2004; **24**: 72-76 [PMID: 14748030 DOI: 10.1002/micr.10199]
42 **Raimondo S**, Fornaro M, Di Scipio F, Ronchi G, Giacobini-Robecchi MG, Geuna S. Chapter 5: Methods and protocols in peripheral nerve regeneration experimental research: part II-morphological techniques. *Int Rev Neurobiol* 2009; **87**: 81-103 [PMID: 19682634 DOI: 10.1016/S0074-7742(09)87005-0]
43 **Di Scipio F**, Raimondo S, Tos P, Geuna S. A simple protocol for paraffin-embedded myelin sheath staining with osmium tetroxide for light microscope observation. *Microsc Res Tech* 2008; **71**: 497-502 [PMID: 18320578 DOI: 10.1002/jemt.20577]
44 **Geuna S**, Tos P, Battiston B, Guglielmone R. Verification of the two-dimensional disector, a method for the unbiased estimation of density and number of myelinated nerve fibers in peripheral nerves. *Ann Anat* 2000; **182**: 23-34 [PMID: 10668555 DOI: 10.1016/S0940-9602(00)80117-X]
45 **Lacerda L**, Ali-Boucetta H, Herrero MA, Pastorin G, Bianco A, Prato M, Kostarelos K. Tissue histology and physiology following intravenous administration of different types of functionalized multiwalled carbon nanotubes. *Nanomedicine* (Lond) 2008; **3**: 149-161 [PMID: 18373422 DOI: 10.2217/17435889.3.2.149]
46 **He C**, Yang C, Li Y. Chemical synthesis of coral-like nanowires and nanowire networks of conducting polypyrrole. *Synthetic Metals* 2003; **139**: 539-545 [DOI: 10.1016/S0379-6779(03)00360-6]
47 **Mackinnon SE**, Hudson AR, Hunter DA. Histologic assessment of nerve regeneration in the rat. *Plast Reconstr Surg* 1985; **75**: 384-388 [PMID: 2579408 DOI: 10.1097/00006534-198503000-00014]
48 **Ronchi G**, Nicolino S, Raimondo S, Tos P, Battiston B, Papalia I, Varejão AS, Giacobini-Robecchi MG, Perroteau I, Geuna S. Functional and morphological assessment of a standardized crush injury of the rat median nerve. *J Neurosci Methods* 2009; **179**: 51-57 [PMID: 19428511 DOI: 10.1016/j.jneumeth.2009.01.011]
49 **Parekkadan B**, Milwid JM. Mesenchymal stem cells as therapeutics. *Annu Rev Biomed Eng* 2010; **12**: 87-117 [PMID: 20415588 DOI: 10.1146/annurev-bioeng-070909-105309]
50 **Bertani N**, Malatesta P, Volpi G, Sonego P, Perris R. Neurogenic potential of human mesenchymal stem cells revisited: analysis by immunostaining, time-lapse video and microarray. *J Cell Sci* 2005; **118**: 3925-3936 [PMID: 16091422 DOI: 10.1242/jcs.02511]
51 **Woodbury D**, Reynolds K, Black IB. Adult bone marrow stromal stem cells express germline, ectodermal, endodermal, and mesodermal genes prior to neurogenesis. *J Neurosci Res* 2002; **69**: 908-917 [PMID: 12205683 DOI: 10.1002/jnr.10365]
52 **Dellon AL**, Mackinnon SE. Selection of the appropriate parameter to measure neural regeneration. *Ann Plast Surg* 1989; **23**: 197-202 [PMID: 2782818 DOI: 10.1097/00000637-198909000-00002]
53 **Morris JH**, Hudson AR, Weddell G. A study of degeneration and regeneration in the divided rat sciatic nerve based on electron microscopy. IV. Changes in fascicular microtopography, perineurium and endoneurial fibroblasts. *Z Zellforsch Mikrosk Anat* 1972; **124**: 165-203 [PMID: 5012670 DOI: 10.1007/BF00335678]
54 **Luís AL**, Amado S, Geuna S, Rodrigues JM, Simões MJ, Santos JD, Fregnan F, Raimondo S, Veloso AP, Ferreira AJ, Armada-da-Silva PA, Varejão AS, Maurício AC. Long-term functional and morphological assessment of a standardized rat sciatic nerve crush injury with a non-serrated clamp. *J Neurosci Methods* 2007; **163**: 92-104 [PMID: 17397932 DOI: 10.1016/j.jneumeth.2007.02.017]
55 **Simões MJ**, Amado S, Gärtner A, Armada-Da-Silva PA, Raimondo S, Vieira M, Luís AL, Shirosaki Y, Veloso AP, Santos JD, Varejão AS, Geuna S, Maurício AC. Use of chitosan scaffolds for repairing rat sciatic nerve defects. *Ital J Anat Embryol* 2010; **115**: 190-210 [PMID: 21287974]
56 **Mackinnon SE**, Dellon AL. A comparison of nerve regeneration across a sural nerve graft and a vascularized pseudosheath. *J Hand Surg Am* 1988; **13**: 935-942 [PMID: 3225423 DOI: 10.1016/0363-5023(88)90275-4]
57 **de Medinaceli L**, Freed WJ, Wyatt RJ. An index of the functional condition of rat sciatic nerve based on measurements made from walking tracks. *Exp Neurol* 1982; **77**: 634-643 [PMID: 7117467 DOI: 10.1016/0014-4886(82)90234-5]
58 **Shen N**, Zhu J. Application of sciatic functional index in nerve functional assessment. *Microsurgery* 1995; **16**: 552-555 [PMID: 8538433 DOI: 10.1002/micr.1920160809]
59 **Gärtner A**, Pereira T, Gomes R, Luis AL, França ML, Geuna S, Armada-da-Silva P, Mauricio AC. Mesenchymal Stem Cells from Extra-Embryonic Tissues for Tissue Engineering-Regeneration of the Peripheral Nerve. 2013 [DOI: 10.5772/53336]
60 **Varejão AS**, Cabrita AM, Geuna S, Melo-Pinto P, Filipe VM, Gramsbergen A, Meek MF. Toe out angle: a functional index for the evaluation of sciatic nerve recovery in the rat model. *Exp Neurol* 2003; **183**: 695-699 [PMID: 14552911]
61 **Varejão AS**, Cabrita AM, Meek MF, Bulas-Cruz J, Gabriel RC, Filipe VM, Melo-Pinto P, Winter DA. Motion of the foot and ankle during the stance phase in rats. *Muscle Nerve* 2002; **26**: 630-635 [PMID: 12402284 DOI: 10.1002/mus.10242]
62 **Varejão AS**, Cabrita AM, Meek MF, Fornaro M, Geuna S, Giacobini-Robecchi MG. Morphology of nerve fiber regeneration along a biodegradable poly (DLLA-epsilon-CL) nerve guide filled with fresh skeletal muscle. *Microsurgery* 2003; **23**: 338-345 [PMID: 12942524 DOI: 10.1002/micr.10147]
63 **Costa LM**, Simões MJ, Maurício AC, Varejão AS. Chapter 7: Methods and protocols in peripheral nerve regeneration experi-

mental research: part IV-kinematic gait analysis to quantify peripheral nerve regeneration in the rat. *Int Rev Neurobiol* 2009; **87**: 127-139 [PMID: 19682636 DOI: 10.1016/S0074-7742(09)87007-4]

64 **Jacobson S**, Guth L. An electrophysiological study of the early stages of peripheral nerve regeneration. *Exp Neurol* 1965; **11**: 48-60 [PMID: 14272559 DOI: 10.1016/0014-4886(65)90022-1]

65 **Pereira T**, Gärtner A, Amorim I, Armada-da-Silva P, Gomes R, Pereira C, França ML, Morais DM, Rodrigues MA, Lopes MA, Santos JD, Luis AL, Maurício AC. Biomaterials and Stem Cell Therapies for Injuries Associated to Skeletal Muscular Tissues. 2013 [DOI: 10.5772/5335]

66 **Harley BA**, Hastings AZ, Yannas IV, Sannino A. Fabricating tubular scaffolds with a radial pore size gradient by a spinning technique. *Biomaterials* 2006; **27**: 866-874 [PMID: 16118016 DOI: 10.1016/j.biomaterials.2005.07.012]

67 **di Summa PG**, Kingham PJ, Campisi CC, Raffoul W, Kalbermatten DF. Collagen (NeuraGen®) nerve conduits and stem cells for peripheral nerve gap repair. *Neurosci Lett* 2014; **572**: 26-31 [PMID: 24792394 DOI: 10.1016/j.neulet.2014.04.029]

68 **Gärtner A**, Pereira T, Simões MJ, Armada-da-Silva PA, França ML, Sousa R, Bompasso S, Raimondo S, Shirosaki Y, Nakamura Y, Hayakawa S, Osakah A, Porto B, Luís AL, Varejão AS, Maurício AC. Use of hybrid chitosan membranes and human mesenchymal stem cells from the Wharton jelly of umbilical cord for promoting nerve regeneration in an axonotmesis rat model. *Neural Regen Res* 2012; **7**: 2247-2258 [PMID: 25538746]

P- Reviewer: Aramwit P, Romani A **S- Editor**: Ji FF
L- Editor: A **E- Editor**: Liu SQ

World Journal of Stem Cells

Submit a Manuscript: http://www.wjgnet.com/esps/
Help Desk: http://www.wjgnet.com/esps/helpdesk.aspx
DOI: 10.4252/wjsc.v7.i6.976

World J Stem Cells 2015 July 26; 7(6): 976-991
ISSN 1948-0210 (online)

Mesenchymal stem cells in maxillary sinus augmentation: A systematic review with meta-analysis

Francesco G Mangano, Marco Colombo, Giovanni Veronesi, Alberto Caprioglio, Carlo Mangano

Francesco G Mangano, Marco Colombo, Alberto Caprioglio, Carlo Mangano, Department of Surgical and Morphological Science, Dental School, University of Varese, 21100 Varese, Italy

Giovanni Veronesi, Department of Clinical and Experimental Medicine, University of Varese, 21100 Varese, Italy

Author contributions: Mangano FG, Colombo M, Veronesi G, Caprioglio A and Mangano C equally contributed to this paper.

Conflict-of-interest statement: The authors declare that they have no financial relationship with any commercial firm that may pose a conflict of interests regarding the publication of this study. No grants, equipment, or other sources of support were provided.

Data sharing statement: Technical appendix, statistical code, and dataset available from the corresponding author at Francesco Mangano (francescomangano1@mclink.net). Participants gave informed consent for data sharing even though are anonymized and the risk of identification is low.

Correspondence to: Francesco G Mangano, DDS, Department of Surgical and Morphological Science, Dental School, University of Varese, Piazza Trento 4, 21100 Varese, Italy. francescomangano1@mclink.net
Telephone: +39-344-85524
Fax: +39-344-530251

Received: November 25, 2014
Peer-review started: November 26, 2014
First decision: December 27, 2014
Revised: March 27, 2015
Accepted: May 5, 2015
Article in press: May 6, 2015
Published online: July 26, 2015

Abstract

AIM: To investigate the effectiveness of mesenchymal stem cells (MSCs) in maxillary sinus augmentation (MSA), with various scaffold materials.

METHODS: MEDLINE, EMBASE and SCOPUS were searched using keywords such as sinus graft, MSA, maxillary sinus lift, sinus floor elevation, MSC and cell-based, in different combinations. The searches included full text articles written in English, published over a 10-year period (2004-2014). Inclusion criteria were clinical/radiographic and histologic/ histomorphometric studies in humans and animals, on the use of MSCs in MSA. Meta-analysis was performed only for experimental studies (randomized controlled trials and controlled trials) involving MSA, with an outcome measurement of histologic evaluation with histomorphometric analysis reported. Mean and standard deviation values of newly formed bone from each study were used, and weighted mean values were assessed to account for the difference in the number of subjects among the different studies. To compare the results between the test and the control groups, the differences of regenerated bone in mean and 95% confidence intervals were calculated.

RESULTS: Thirty-nine studies (18 animal studies and 21 human studies) published over a 10-year period (between 2004 and 2014) were considered to be eligible for inclusion in the present literature review. These studies demonstrated considerable variation with respect to study type, study design, follow-up, and results. Meta-analysis was performed on 9 studies (7 animal studies and 2 human studies). The weighted mean difference estimate from a random-effect model was 9.5% (95%CI: 3.6%-15.4%), suggesting a positive effect of stem cells on bone regeneration. Heterogeneity was measured by the I^2 index. The formal test confirmed the presence of substantial heterogeneity (I^2 = 83%, P < 0.0001). In attempt to explain the substantial heterogeneity observed, we considered a meta-regression model with publication year, support type (animal *vs* humans) and

follow-up length (8 or 12 wk) as covariates. After adding publication year, support type and follow-up length to the meta-regression model, heterogeneity was no longer significant (I^2 = 33%, P = 0.25).

CONCLUSION: Several studies have demonstrated the potential for cell-based approaches in MSA; further clinical trials are needed to confirm these results.

Key words: Mesenchymal stem cells; Maxillary sinus; Sinus floor augmentation; Scaffolds; Bone regeneration

Core tip: Cell-based approaches, utilizing adult mesenchymal stem cells, may overcome the limitations of conventional bone augmentation procedures. The present review of the current literature aims to systematically review the available evidence on the characteristics and clinical effectiveness of cell-based maxillary sinus augmentation, compared to current evidence-based methods.

Mangano FG, Colombo M, Veronesi G, Caprioglio A, Mangano C. Mesenchymal stem cells in maxillary sinus augmentation: A systematic review with meta-analysis. *World J Stem Cells* 2015; 7(6): 976-991 Available from: URL: http://www.wjgnet.com/1948-0210/full/v7/i6/976.htm DOI: http://dx.doi.org/10.4252/wjsc.v7.i6.976

INTRODUCTION

Implant dentistry is a successful treatment procedure, as demonstrated by more than 20 years of clinical evidence[1-3].

However, the edentulous posterior maxilla is often characterized by a lack of bone because of severe post-extraction alveolar crest resorption coupled with age-linked sinus pneumatization[4,5]. This anatomic limitation often dictates the need for reconstructive osseous surgery to re-establish adequate bone volume for implant positioning[4,5].

Accordingly, different augmentation approaches have been introduced to obtain more maxillary bone volume, placing various grafting materials in the maxillary sinus[6-9]. Nowadays maxillary sinus augmentation (MSA) has become a reliable, commonly used procedure to increase bone volume in the posterior maxilla[4,5,9,10].

Autogenous bone (AB) is still the best grafting material in bone reconstructive surgery, and MSA has been originally carried out with it[10,11]. In fact, AB exhibits osteogenic and osteoconductive potential, since it contains living cells and growth factors[10-12]. However, additional surgical procedures are needed to harvest bone chips from other skeletal sites (intraorally or from the iliac crest); the available AB supply is limited, and morbidity at donor site is often a problem[11,12]. In addition, AB shows resorption patterns proportional to the quantity of harvested material, and this may results in a significant loss of grafted bone in large defect fillings over time[11,12].

To overcome these limitations, several osteoconductive materials have been used in MSA, such as autogenetic bone [allografts (AL)][13,14], xenografts [bovine bone mineral (BBM)][9,15,16], synthetic bone grafts [calcium phosphate ceramics (CPC)][4,17] or composite materials[18]. However, these bone grafting substitutes don't contain living cells, so their healing times are longer than AB[12,19].

Bone tissue engineering (BTE) procedures may help lo overcome these limits[20]. According to BTE, a bone substitute should have biological and morphological features as similar as possible to AB, and the fabrication of the ideal bone graft requires the manipulation of three essential components: osteogenic cells, growth factors and osteoconductive scaffolds[20,21]. In particular, BTE aims to achieve bone augmentation without surgical AB harvesting from other donor sites, through the use of specific scaffolds seeded with osteogenic cells[12,19,21].

The aim of the present review was to evaluate the effectiveness of cell-based approaches in MSA, associated with various scaffold materials, in animals and humans.

MATERIALS AND METHODS

Study design

The protocol of this review is in accordance with Preferred Reporting Items for Systematic Reviews and Meta-Analyses[22], the Cochrane Collaboration[23] and CheckReview[24] checklists. It was developed a priori, covering rationale, design of the study, focused question, inclusion/exclusion criteria, search strategy, data synthesis. The protocol was examined and refereed by researchers with experience in systematic reviews. The focused questions was: "What is the effectiveness of cell-based approaches in MSA, with different materials?".

Inclusion and exclusion criteria

Most important study designs to address the focused question were randomized controlled trials (RCTs) and controlled trials. Although this, both experimental and observational studies (RCTs, controlled trials, case series, case reports and prospective cohort trials) were included in this review. Inclusion criteria were studies of BTE methods in MSA using different scaffolds, in animals and humans, with analysis using either radiographic or histologic/histomorphometric approaches. Exclusion criteria were studies where there was no information about the surgical team or the location (private practice/hospital/university) where MSA was performed.

Search strategy

Systematic searches were performed in MEDLINE, EMBASE and SCOPUS databases including full text articles published in English between October 2004 and October 2014, presenting either radiographic or

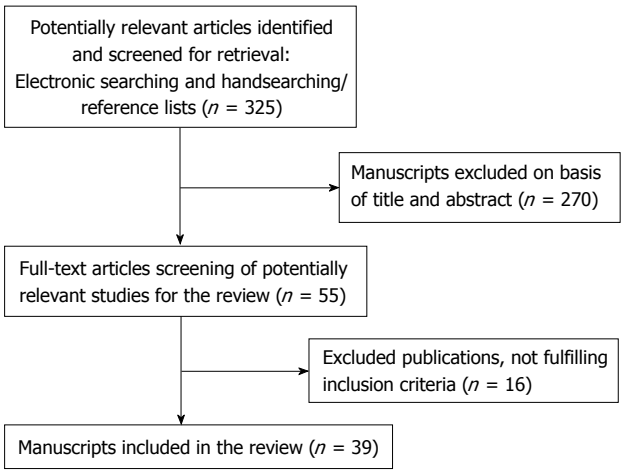

Figure 1 Flow chart of manuscripts screened trough the review process.

histologic/histomorphometric evaluations.

Keywords such as sinus graft, MSA, maxillary sinus lift, sinus floor elevation, mesenchymal stem cell (MSC) and cell-based, in different combinations, were used. Titles and abstracts were examined and then expert reviewers (Mangano FG and Colombo M) evaluated full text of publications extrapolating relevant information. Data extraction procedures affected title, authors, year of publication, type of study, cells and scaffold used, design, randomization/blinding if present, number of procedures performed, treatment phase, follow-up, radiographic and/ or histologic/histomorphometric outcomes, statistical findings, conclusions. In addition, the reference lists of included studies were hand searched.

Statistical analysis

Experimental studies (RCTs/CTs) on MSA with an outcome measurement of histologic/histomorphometric evaluation were subjected to meta-analysis. Mean and standard deviation values of new bone formation were used; to overcome the differences of sample size between studies weighted mean was calculated. Test and the control groups values were compared by calculating the differences of bone gain in mean, and 95%CIs. Software package R version 2.14 (Package Metafor; Wolfgang Viechtbauer, Maastricht, The Netherlands) was used to perform all statistical analyses.

RESULTS

Result of search and included studies

Of the 325 eligible articles initially identified, 270 were excluded following assessment of the title and/or abstract. In total, 39 studies (18 animal studies and 21 human studies) were eligible for inclusion in the present literature review (Figure 1). All these publications were issued between 2004 and 2014, and were variable with respect to study type, design, follow-up, and results.

MSCs

A stem cell is an undifferentiated cell with the capability to renew itself and to get a specific cell-phenotype if exposed to proper stimuli[25-28]. The more relevant stem cells types in clinical researches are embryonic stem cells (ESCs), typical of embryonic blastocyst, and adult stem cells, also defined as pluripotent MSCs[28-31].

ESCs have unlimited proliferation potential and are able, under appropriate inductive conditions, to produce all three germ layers cellular phonotypes[28-31]. ESCs can be cultured indefinitely *in vitro* for more than two years, with approximately 400 doubling cycles, without the loss of differentiation potential. They can be re-implanted into a host embryo giving rise to progenies that differentiate into all kind of tissues[29-31]. Although their clinical potentials several issues remain to be addressed with ESCs[30,31]. The use of these cells, in fact, presents the potential risks of immunorejection or teratomagenesis[30]. Moreover, despite the pluripotency of ESCs, moral and legal controversies concerning their use for therapeutic and clinical application have encouraged to find the reservoirs of progenitor cells in adult tissues[28,32,33].

Adult stem cells or pluripotent MSCs, derived from different adult tissues, have a wide self-renewal and proliferation capability, whereas if correctly stimulated have the ability to differentiate into specific cell-lines[25-31]. Although MSCs display a finite life span and get into senescence faster than ESCs, current *in vitro* techniques allow to expand them in sufficient number for clinical uses maintaining the undifferentiated phenotype[25-31]. MSCs lack immunogenic or tumorigenic features[26-28]; moreover, there is no ethical or legal concern for the clinical use of MSCs[32]. For all these reasons, these cells can be used in cell-based approaches in bone regeneration[25-31,33].

MSCs can be extracted from different tissues such as bone marrow [bone marrow stem cells (BMSCs)][25-31,34], periosteum (periosteal derived stem cells)[35], trabecular bone[36], adipose tissue [adipose stem cells (ADSCs)][37] or skeletal muscle[38], umbilical chord[39], amniotic fluid [amniotic fluid stem cells (AFSCs), and amniotic epithelial stem cells (AESCs)][40,41], skin [skin-derived stem cells (SDSCs)][42], dental pulp (dental pulp stem cells)[43,44], deciduous teeth [deciduous tooth stem cells (DTSCs)][45] and periodontal ligament [periodontal ligament stem cells (PDLSCs)][46].

The bone marrow aspirates (BMA), from the iliac crest of the pelvis, has always been considered the first source for MSCs[25-34]. The tibial and femoral marrow compartments are also available as alternative sources. Due to the morbidity and the operative difficulties of this procedure the possibility to harvest MSCs from other tissues, such as periosteum or maxillary tuberosity has become of interest[35,36]. At present, MSCs can be also achieved from adipose tissue by liposuction[37] or from the dental pulp[43,44]. The latter represents a very interesting option in the field of oral surgery[43,44].

As the number and the concentration of transplanted MSCs are critical to induce a significant clinical outcome, an adequate number of cells for cell culture/replication is

needed. BMA represent a heterogeneous cell population; the amount of MSC is very small compared to that of hematopoietic cells and averaging 0.001%-0.01% of the total nucleated cells[47], thus requiring extensive *in vitro* separation steps and expansion. Moreover, the number of MSCs that can be collected is inversely correlated to patient age and to his/her systemic health state. Younger donors tend to provide higher yield of stem cells in the aspirate, and the age of the donor seems to be directly associated with detrimental effects in term of proliferation and differentiation, such as senescence[47]. Cell density varies with different skeletal sites of the donor: on average, human BMA yield 400 to 500 cells/mL with an estimated total volume of 600 cc in the iliac crest[48].

At present, using standard cell culture techniques, MSCs can be isolated and expanded with great efficiency, inducing to grow into multiple lineages if exposed to the appropriate culture conditions[25]. For *in vitro* separation and expansion, cultured MSCs undergo successive passages. Cells are cultured in a medium supplemented with autogenous serum or fetal bovine serum and growth factors[49]. MSCs have fibroblastic morphological features in a monolayer culture and tend to adhere to the tissue culture substrate[49]; changing the medium, non-adherent hematopoietic cells are discharged[28,50]. MSCs are identified by their adhesion to plastic and their expression of peculiar membrane epitopes (CD73, CD90, CD105), with a lack of expression of human leucocyte antigen-DR and the hematopoietic markers (CD14, CD34, CD38, CD45)[49,50]. Unfortunately, MSCs display finite life spans. Recent studies have shown that extensive *in vitro* proliferation can affect MSCs replicative potential and differentiation capability: long-term culture and sequential passages affect the quality of MSCs in that their proliferation rate decreases and gradually lose their progenitor properties due to senescence and telomere shortening[51]. Since MSCs undergo limited mitotic divisions *in vitro*, the number of passages in *in vitro* expansion should not exceed five[51]. The addition of fibroblast growth factor-2 to the culture medium can stimulate the proliferation of MSCs maintaining their osteogenic potential, keeping the cells in a more immature state[52].

Usually, the osteogenic differentiation is initiated by supplementing the medium with dexamethasone, ascorbic acid and beta-glycerolphosphate[53]. In addition, soluble signals like bone morphogenetic proteins (BMPs) such as BMP-2, BMP-6 and BMP-9 can be used[53,54].

Scaffold

Cells are usually seeded onto a three dimensional (3D) scaffold that guides their growth and proliferation[55]. At present, there are at least 4 different strategies for the delivery of MSCs into the recipient site: MSCs can be replicated and differentiated in culture, then seeded on a 3D solid scaffold that can be implanted, after a stabilization time to obtain cell adhesion; MSCs can be replicated in culture and seeded into the 3D solid scaffold, then the cell-scaffold composite is placed in differentiation medium to stimulate the shift into the osteoblastic phenotype, ready to be implanted into the site; MSCs can be replicated and differentiated directly in the 3D scaffold *in vitro*, and the cell-scaffold composite can be implanted after a maturation time; finally MSCs can be replicated and differentiated *in vitro*, and the cell-scaffold composite can be incubated for a short time to prepare an injectable bone preparation.

In all these strategies, the scaffold has a key role providing a substrate into which bone cells migrate, proliferate, differentiate and make new bone[55,56]. The scaffold should be characterized by specific physical structure and chemical composition in order to mimic the hierarchical architecture and biological functions of native extracellular bone matrix[55,56]. Native extracellular matrix offers a physical substrate for cells, but also a biological environment for cell adhesion and chemotaxis through specific ligands. Providing specific growth factor, bone matrix regulates cellular proliferation and function[55,56]. First generation biomaterials were designed promoting mechanical resistance and stability over time, bioinertness or biocompatibility; nowadays new generation scaffold materials are developed with biologically-inspired approach; these new materials should incorporate signals into the scaffold, to modulate proliferation and differentiation[55-57]. Architectural characteristics define the ultimate shape of the new tissue. Highly porous structures with many interconnection and with large surface areas related to volumes, can aid cell ingrowth and their diffusion throughout the scaffold as well as the passage of nutrients and waste products[55,57].

Angiogenesis is a pre-requisite for osteogenesis[57]. Accordingly, pore sizes in the range of 200-800 μm have good results in these situations: in fact, they stimulate osteoprogenitor and endothelial cells to migrate into the matrix. Endothelial cells produce the vascular vessels for new bone nourishment[55-58]. Surface roughness, surface energy and the presence of cell attachment sites all influence specific proteins expression, quantity and structural conformation which adsorb onto materials surfaces, modulating cells behaviours[55,57]. Finally, substrate degradation by matrix enzymes[57] is critical. The ideal material should incorporate controlled resorption, and the regenerated tissue should assume function while the scaffold is slowly degraded[55,57].

Scaffolds and stem cells: Animal studies

In total, 18 animal studies evaluating the histologic/histomorphometric results obtained with MSCs combined with different scaffold materials were found in the literature[40-42,59-73]. Among these, one single study was on MSCs with allogeneic bone matrix (AL)[42], 6 studies were on MSCs with xenografts (BBM)[59-64], 10 studies were on MSCs with synthetic bone grafts (CPC)[40,41,65-71], and 2 studies were on MSCs with platelet-rich-plasma (PRP)[72,73].

AL (bone tissue from human cadavers), provides an osteoconductive scaffold which offers structural support

for vascular and perivascular tissues growth, and for osteoprogenitor cells migration from the adjacent environment[13,14,42]. In a study on minipigs, Kang *et al*[42] evaluated *in vivo* osteogenesis of SDSCs with scaffolds composed by allogeneic demineralized bone (AL) and fibrin glue. The animals were allocated in two groups: in one group, MSA was performed with SDSCs + AL/fibrin glue (test), while in the other group the scaffold without cells was used[42]. They observed better trabecular bone formation and osteocalcin expression with scaffolds seeded with SDSCs compared with controls[42]. The authors found that autogenous SDSC grafting with a AL and fibrin glue scaffold can provide an adequate alternative to bone grafting in MSA procedures[42].

BBM associated with bone marrow aspirate concentrate (BMAC) could provide a substitute for AB to stimulate new bone formation[9,15,16,59-64]. Sununliganon *et al*[59] investigated the bone regeneration capacity of autologous BMAC mixed with BBM in MSA. Twenty-four white New Zealand rabbits were randomly subdivided into groups and when subjected to maxillary sinus floor elevation and augmentation with four different materials: saline solution, AB, BBM and BMAC + BBM[59]. Four MSA procedures were performed per each material. The animals were sacrificed at 2, 4 and 8 wk, and rates of new bone apposition in augmented surgical sites were evaluated; bone histomorphometry was also examined. Significant increase in the quantity of nucleated cells and colony forming unit-fibroblasts were confirmed in BMAC. MSCs in BMAC retained their *in vitro* multi-differentiation capability. BMAC + BBM showed a similar benefit to AB in term of acceleration, since higher (though not significantly different) rates of mineral appositions in the early period were detected in BMAC + BBM and AB than BBM alone[59]. Furthermore, graft volume/tissue volumes in BBM and BMAC + BBM resulted to be higher than in AB and saline solution. The results of this study suggest benefit in early bone formation *in vivo* using immediate autologous BMAC transplantation[59]. In a similar study, Yu *et al*[60] compared the potential of tissue-engineered bone derived from different stem cell sources for canine MSA. Bilateral MSA were performed in six beagle dogs and were randomly repaired with three graft types: BBM granules alone (n = 4), a complex of osteoblasts derived from BMSCs + BBM (n = 4), and a complex of osteoblasts derived from PDLSCs and BBM (n = 4). After 12 wk, the animals were sacrificed and fluorescent labeling, maxillofacial computed tomography (CT), scanning electron microscopy, and histologic/histomorphometric analyses were used to evaluate new bone deposition, mineralization, and healing processes in the augmented area[60]. At the end of the study, the osteogenic capacity was greater with BMSCs + BBM and PDLSCs + BBM than with BBM alone[60]. The level tended to be higher with PDLSCs than with BMSCs; however, the difference was not statistically significant[60]. Oshima *et al*[61] investigated the *in vivo* osteogenic potential of a novel gabapentin-lactam (GBP-L) in MSA. Bilateral MSA in 10 adult sheep were conducted. BBM and MSCs combined with novel GBP-L were placed into the test sinus of each sheep; MSCs + BBM alone served as the control on the contralateral side[61]. The animals were sacrificed after 8 and 16 wk, and the amount of newly formed bone was analysed using histology/histomorphometry. The histologic evaluation showed newly formed bone connected with the original bone in the control and test groups; however, the amount of newly formed bone was not significantly different between the test and control sites[61]. The authors concluded that the application of GBP-L did not induce faster new bone formation. However, GBP-L did not alter the multipotency of the MSCs or impair bone formation[61]. Jhin *et al*[62] evaluated the potential of *BMP-2* gene-transduced BMSCs to facilitate osseous healing after MSA in rabbit. BMSCs derived from New Zealand white rabbits were cultured and some of these cells were transduced with BMP-2 (BMP-2/BMSCs) using an adenovirus vector. Then, BMSCs and BMP-2/BMSCs were seeded on a BBM scaffold. Twenty-seven animals were randomly allocated into three groups: MSA with BMSCs + BBM, MSA with BMP-2/BMSCs + BBM and MSA with BBM alone[62]. During all these procedures, a mini-implant was placed in the floor of each sinus[62]. Animals were sacrificed at 2, 4, and 8 wk after surgery, and new bone area and bone-to-implant contact (BIC) were evaluated histomorphometrically. The histomorphometric evaluation revealed that at 2 and 4 wk, the BMP-2/BMSC group showed more new bone and higher BIC than the other two groups; however, at 8 wk, there was no difference in new bone area or BIC among the three groups[62]. The authors concluded that BMP-2 delivery using BMSCs may result in earlier and increased bone formation in MSA; nevertheless, limitations in the stimulatory effect of BMP-2/BMSCs were evidenced in later healing stages[62]. Gutwald *et al*[63] compared the efficacy of mononuclear cells (MNCs, including MSCs) plus BBM with AB in MSA in sheep. Bilateral MSA were performed in 6 adult sheep. MNCs + BBM were mixed together and used into one sinus, AB in the other sinus[63]. After 8 and 16 wk, animals were sacrificed. Sites of augmentation were evaluated through radiographic and histological methods. After 8 wk, no difference in new bone formation was noticed between the two groups, but after 16 wk, sites grafted with MNCs + BBM showed 29% of newly formed bone *vs* 16% in sites grafted with AB[63]. The authors concluded that MNCs combined with BBM have the potential to stimulate new bone formation in MSA[63]. Finally, in a similar study, bilateral MSA were performed in 6 adult sheep by the same group of authors[64]. BBM and MSCs were used in test side and only BBM in the contra-lateral control side of each animal[64]. Animals were sacrificed after 8 and 16 wk. The regenerated areas were evaluated by CT, histology and histomorphometry. They observed that the newly formed bone was closely connected to BBM particles; furthermore its apposition was significantly faster in the test sides[64]. The authors concluded that mixture of BBM and MSCs could stimulate new bone

deposition in MSA[64].

Synthetic CPC such as porous hydroxyapatite (HA), beta-tricalcium phosphate (beta-TCP) and biphasic combinations of these two are excellent bone alternatives[40,41,65-71]. CPC are considered biocompatible, non-immunological, osteoconductive (they act as scaffolds witch allow internal growth of vessels from neighbouring bone tissue)[40,41,65-71]. Zhao *et al*[65] investigated the effect of MSA with engineered bone constructs from DTSCs and CPC in goats. Eighteen bilateral maxillary sinuses of nine goats were randomly assigned into three groups (6 sinuses per group). In the first group, MSA was performed with DTSCs + CPC, while in the second and in the third group MSA was performed with CPC alone and AB, respectively[65]. All augmentation sites were analysed using CT, histology and histomorphometry. After 12 wk of healing, CT analysis evidenced that the volume of new bone with DTSCs + CPC was greater than that in the other two groups[65]. In addition, the histological/histomorphometrical evaluation indicated that the DTSCs + CPC compound significantly stimulated new bone formation and mineralization, when compared with CPC and AB alone[65]. The authors concluded that DTSCs can stimulate new bone formation and maturation in the maxillary sinus of goats, and that the engineered mixture of DTSCs and CPC should represent a possible substitute for MSA procedures[65]. Zhang *et al*[66] compared the bone formation capacity of ADSCs and BMSCs in a canine MSA model. Bilateral MSA were performed in nine beagle dogs using randomly three graft material combinations: BMSCs + CPC (n = 9), ADSCs + CPC (n = 9) and CPC alone (n = 9)[66]. After 6 wk, the animals were sacrificed and the histological/histomorphometric evaluation suggested that BMSCs might be more advantageous than ADSCs for fast bone regeneration in MSA[66]. Barboni *et al*[41] evaluated the bone regenerative property of AESCs seeded on a CPC synthetic bone substitute (fabricated using rapid prototyping techniques) in MSA in sheep. Two blocks of CPC, engineered with ovine AESCs or alone, were grafted bilaterally into maxillary sinuses of six adult sheep[41]. The sheep were randomly divided into two groups and sacrificed at 45 and 90 d after surgery. Micro-CT, morphological, biochemical and morphometric analyses were performed to evaluate tissue regeneration in the sinus explants. AESCs seem to influence positively scaffold integration and new bone deposition[41]. Engineered scaffolds, derived from explanted sinuses grafted with AESCs, displayed an accelerated process of angiogenesis; moreover, AESCs significantly promoted osteogenesis[41]. These results confirmed those of a previous study by the same group of authors[40] in which bilateral MSA was performed on eight adult sheep, in order to evaluate the bone regeneration process at 6 and 12 wk after implantation of AFSCs combined with a magnesium-enriched HA/collagen-based scaffold (test) with the scaffold alone (control). In fact, the use of AFSCs increased bone apposition and promoted a faster angiogenesis[40]. The authors concluded that AFSCs may be a new, easily accessible source of MSCs to develop cell-based therapy for oral augmentation procedures: in fact, the osteoinduction of a biomimetic commercial scaffold may be significantly enhanced by these cells[40].

Zeng *et al*[67] evaluated the efficacy of BMSCs seeded on CPC, magnesium phosphate cement (MPC), and a calcium-MPC (CMPC), in MSA in rabbit. In test groups augmentation procedures were performed using BMSCs in addition to CPC, MPC, and CMPC; the same materials (CPC, MPC and CMPC), without cells, were used for surgical procedures as control[67]. In each group new bone formation was investigated histologically and by fluorochrome labeling at weeks 2 and 8 after MSA[67]. The authors found that CMPC cement could better help new bone formation and mineralization than CPC or MPC cements, and that the addition of BMSCs could further promote its osteogenic capacity significantly[67].

Zou *et al*[68] assessed the potential of BMSCs when combined with CPC in MSA in goats. They randomly allocated nine goats in three different groups: the first group received BMSCs + CPC, the second CPC alone and the third AB. Each animal underwent a bilateral MSA procedure. Implants were also placed in order to evaluate BIC[68]. After 12 wk, the histological/histomorphometric evaluations showed that the BMSCs + CPC composite could foster earlier bone formation and mineralization, and could preserve more volume and height after MSA[68]. In addition, BIC was significantly higher in the BMSCs + CPC group than in the other two groups. The authors concluded that BMSCs + CPC seems to be a good graft material for MSA, allowing faster healing in augmented sites and a better stability of implants[68]. In a study by Xia *et al*[69] 36 rabbits were randomly allocated in 4 groups, to test CPC scaffolds associated with recombinant BMP-2 and BMSCs, in different combinations. Although the authors found no significant difference among groups for augmented height, histomorphometric analysis showed significantly less residual graft material and more new bone formation and mineralization in BMP-2/BMSCs + CPC than in other groups[69]. Based on these outcomes, they suggested that combining BMP-2/BMSCs with CPC could enhance new bone formation and maturation as compared with BMP-2 + CPC or BMSCs + CPC[69]. In two different studies, Sun *et al*[70,71] evaluated the outcome of MSA with CPC and BMSCs in rabbits. In the first study[70] 16 MSA were performed bilaterally in 8 animals and randomly grafted by BMSCs + CPC, CPC alone, AB and blood clot (4 sites per group). The animals were sacrificed 2, 4 and 8 wk after the surgery and studied histologically and histomorphometrically[70]. After 8 wk, the authors observed a significantly higher amount of new bone in the test groups (BMSCs + scaffold and scaffold alone) than in control groups (AB and blood clot). An increase in bone height along time was found for the test groups, while control groups showed a constant decrease of augmented height[70]. Surgical sites augmented with BMSCs + CPC showed more bone than areas grafted with CPC alone, but this difference was not statistically significant. These results suggested that CPC could be used as a bone graft substitute in

bone augmentation procedures and that adding BMSCs to this material could successfully promote new bone formation in maxillary sinus elevation[70]. In a second, similar study[71] the same authors evaluated the effects of MSA by a tissue engineered bone composite with *BMP-2* and *EGFP* gene modified BMSCs and CPC. In this study, eight rabbits were allocated in two groups (four rabbits per group), and subjected to bilateral MSA with two different materials: BMP-2/BMSCs + CPC (test) and EGFP/BMSCs + CPC (control)[71]. Histological/histomorphometric evaluation was performed 2 and 4 wk after surgery. The vertical bone gain was maintained, over all the experimental period, for both groups, while new bone volume increased over time for test group[71]. Four weeks after surgery, bone area in test group was significantly more than that in control group[71]. The authors concluded that BMSCs modified with *BMP-2* gene can stimulate new bone formation in MSA in rabbit animal model, and that CPC scaffold can be a valid vector for gene improved BTE[71].

Finally, in a split-mouth controlled study on eight minipigs, Pieri *et al*[72] investigated whether BMSCs and PRP loaded on a HA substrate can influence bone formation and BIC in MSA, when compared to HA scaffold alone. Bilateral MSA procedures were performed in eight minipigs: each animal received BMSCs + PRP + HA in one sinus (test) and HA alone in the other (control)[72]. In addition, distal to the augmented site, one endosseous implant was placed per sinus, to evaluate BIC. The animals were sacrificed 12 wk after surgical procedures. Block sections of the implant sites were extracted and prepared for histologic/histomorphometric analysis. The histomorphometric observations revealed statistically significant increase both in bone quantity and in the BIC for the test sites[72]. This study showed that the use of BMSCs and PRP with a HA scaffold can significantly promote bone growth in MSA techniques, and can enhance the osseointegration of endosseous dental implants positioned in the augmented sites, in comparison with HA alone[72]. In another, similar study, Ohya *et al*[73] evaluated the outcomes of BMSCs associated with PRP *vs* particulate cancellous bone and marrow (PCBM) with PRP. Bilateral MSA procedures were performed in 18 adult Japanese white rabbits. Each rabbit received BMSCs + PRP in one sinus (test) and PCBM + PRP in the other (control)[73]. The animals were sacrificed at 2, 4, and 8 wk after surgery, and histological/histomorphometric evaluation was executed. Both test and control sites displayed newly formed bone and neovascularization at 2 and 4 wk in histological preparations; at 8 wk, authors observed large areas of fatty marrow inside lamellar bone in both sites. The analysis of bone volume and augmented height did not highlight any significant differences between BMSCs + PRP and PCBM + PRP groups. On the other hand, significant differences in bone volume and augmented height between 2 and 8 wk in PCBM + PRP or BMSCs + PRP groups were found, as well as in bone volume between 4 and 8 wk in the PCBM + PRP group[73]. The authors concluded that the use of a BMSCs + PRP compose could give good outcomes in osteogenesis and bone volume gain comparable to that achieved by particulate cancellous bone in MSA[73].

The histologic/histomorphometric results of all these animal studies are reported in Table 1.

Scaffolds and stem cells: Human studies

In total, 21 human studies evaluating the histologic/histomorphometric results obtained in MSA with MSCs combined with different scaffold materials were found in the literature[74-95]. Among these, 2 studies were on MSCs with allogeneic bone matrix (AL)[74,75], 9 studies were on MSCs with xenografts (BBM)[77-85], 2 were on MSCs with synthetic grafts (CPC)[86,87], 6 were on MSCs with synthetic polymers [polylactid-co-glycolic acid, (PLGA)][88-93], and 2 were on MSCs with PRP[94,95].

A commercially available AL containing native MSCs has been clinically used for MSA in 2 different studies[74,75]. McAllister *et al*[74] evaluated the bone formation following MSA using an AL containing native stem cells. After a healing period of 4 mo, biopsy and histologic evaluation were performed. The histologic and histomorphometric evaluation for the five cases reported revealed a high percentage of vital bone content, after a relatively short healing period[74]. A recent clinical study by Gonshor *et al*[75] evaluated bone formation in MSA sites using either an AL cellular bone matrix containing MSCs or a conventional AL. Statistically significant difference were found between the two groups, in terms of vital and residual bone content, using histomorphometric comparison[75]. In AL, cryopreservation is used to maintain cell viability and multipotential characteristics[75]. This might help the healing process stimulating bone formation directly from within the graft material, allowing earlier and larger quantity of available vital bone[74,75]. However, there is a high level of uncertainty around the possibility of iatrogenic transmission of prion or viral infections with AL, due to a lack of evidence-based research on this problem[76].

BBM has excellent osteoconductive properties[9,15,16] and the encouraging results emerged from pre-clinical studies[59-64] have led to the clinical use of this material in MSA, with the cell-based approach[77-85]. Unfortunately, however, human studies[77-85] on MSCs + BBM have not confirmed the excellent outcomes originally emerged from animal studies. In a recent clinical study on implant survival after MSA, Duttenhoefer *et al*[77] concentrated MSCs with either Ficoll (control group, n = 6 sinus) or BMAC (test group, n = 12 sinus) and transplanted in combination with BBM. 50 dental endosseous implants were positioned with other surgical procedures (17 Ficoll/33 BMAC) and loaded after 4 mo. At the end of the study, implant survival of the Ficoll group was 100% compared with 93.4% survival of the BMAC group; however, both cell isolation methods were found to be efficient because the difference between the groups was not statistically significant[77]. In a randomized, controlled, split-mouth design study by Rickert *et al*[78], a

Table 1 Histomorphometric results of the animal studies included in the review

Ref.	Animal model	Study design	Histomorphometry (% of newly formed bone)
Kang *et al*[42]	Minipig	SDSCs + AL	NR
		AL alone	NR
Sununliganon *et al*[59]	Rabbit	BMSCs + BBM	59.2 ± 2.1 (4 wk)
			55.9 ± 3.6 (8 wk)
		BBM alone	54.3 ± 2.8 (4 wk)
			51.5 ± 2.6 (8 wk)
		AB	NR
		Saline solution	NR
Yu *et al*[60]	Dog	BMSCs + BBM	NR
		PDLSCs + BBM	NR
		BBM alone	NR
Oshima *et al*[61]	Sheep	BMSCs + GBP-L + BBM	17.0 ± NR (8 wk)
			23.0 ± NR (16 wk)
		BMSCs + BBM	18.0 ± NR (8 wk)
			23.0 ± NR (16 wk)
Jhin *et al*[62]	Rabbit	BMP-2/BMSCs + BBM	12.6 ± 2.8 (2 wk)
			29.3 ± 4.6 (4 wk)
			25.7 ± 3.8 (8 wk)
		BMSCs + BBM	6.2 ± 2.6 (2 wk)
			25.7 ± 2.8 (4 wk)
			27.7 ± 8.2 (8 wk)
		BBM alone	4.2 ± 2.0 (2 wk)
			15.1 ± 2.9 (4 wk)
			22.7 ± 3.3 (8 wk)
Gutwald *et al*[63]	Sheep	MNCs + BBM	19.0 ± 11 (8 wk)
			29.0 ± 12 (16 wk)
		AB	20.0 ± 13 (8 wk)
			16.0 ± 6 (16 wk)
Sauerbier *et al*[64]	Sheep	MSCs + BBM	NR
		BBM alone	NR
Zhao *et al*[65]	Goat	DTSCs + CPC	41.8 ± 6.2 (12 wk)
		CPC alone	30.1 ± 8.0 (12 wk)
		AB	23.0 ± 10.2 (12 wk)
Zhang *et al*[66]	Dog	BMSCs + CPC	NR
		ADSCs + CPC	NR
		CPC alone	NR
Barboni *et al*[41]	Sheep	AESCs + CPC	NR
		CPC alone	NR
Berardinelli *et al*[40]	Sheep	AFSCs + MgHA/collagen	NR
		MgHA/collagen alone	NR
Zeng *et al*[67]	Rabbit	BMSCs + CPC	11.7 ± 1.8 (2 wk)
			25.4 ± 3.4 (8 wk)
		CPC alone	5.9 ± 1.4 (2 wk)
			20.5 ± 3.6 (8 wk)
		BMSCs + MPC	5.1 ± 1.7 (2 wk)
			13.5 ± 3.5 (8 wk)
		MPC alone	4.0 ± 1.2 (2 wk)
			6.5 ± 2.0 (8 wk)
		BMSCs + CMPC	12.7 ± 1.9 (2 wk)
			30.9 ± 3.1 (8 wk)
		CMPC alone	6.8 ± 1.3 (2 wk)
			25.5 ± 4.1 (8 wk)
Zou *et al*[68]	Goat	BMSCs + CPC	35.6 ± 9.4 (12 wk)
		CPC alone	22.4 ± 4.2 (12 wk)
		AB	28.2 ± 8.0 (12 wk)
Xia *et al*[69]	Rabbit	BMSCs + rhBMP-2/CPC	17.9 ± 4.3 (2 wk)
			30.5 ± 5.7 (4 wk)
			42.2 ± 4.0 (8 wk)
		BMSCs + CPC	13.9 ± 2.5 (2 wk)
			21.8 ± 4.4 (4 wk)
			28.7 ± 3.7 (8 wk)
		rhBMP-2/CPC	12.8 ± 3.0 (2 wk)
			18.9 ± 2.6 (4 wk)
			31.1 ± 4.5 (8 wk)
		CPC alone	8.0 ± 2.0 (2 wk)
			12.2 ± 3.1 (4 wk)
			22.7 ± 5.7 (8 wk)
Sun *et al*[70]	Rabbit	BMSCs + CPC	21.0 ± 2.6 (2 wk)

			23.4 ± 3.0 (4 wk)
			35.3 ± 10.5 (8 wk)
		CPC alone	19.2 ± 2.2 (2 wk)
			22.9 ± 2.1 (4 wk)
			19.5 ± 2.4 (8 wk)
		AB	34.7 ± 7.1 (2 wk)
			28.7 ± 5.8 (4 wk)
			NR (8 wk)
		Blood clot	NR (2 wk)
			17.5 ± 3.3 (4 wk)
			13.8 ± 4.0 (8 wk)
Sun *et al*[71]	Rabbit	BMP-2/BMSCs + CPC	21.2 ± 2.1 (2 wk)
			31.9 ± 2.2 (4 wk)
		EGFP/BMSCs + CPC	18.9 ± 1.9 (2 wk)
			23.19 ± 1.9 (4 wk)
Pieri *et al*[72]	Minipig	BMSCs + PRP + HA	42.5 ± 7.0 (12 wk)
		HA alone	18.9 ± 0.9 (12 wk)
Ohya *et al*[73]	Rabbit	BMSCs + PRP	29.1 ± 4.4 (2 wk)
			24.1 ± 3.6 (4 wk)
			20.9 ± 4.1 (8 wk)
		PCBM + PRP	35.0 ± 5.2 (2 wk)
			28.6 ± 3.4 (4 wk)
			20.6 ± 4.0 (8 wk)

SDSCs: Skin-derived stem cells; AL: Allograft; NR: Not reported; BMSCs: Bone marrow stem cells; BBM: Bovine bone mineral; AB: Autogenous bone; PDLSCs: Periodontal ligament stem cells; GBP-L: Gabapentin-lactam; MNCs: Mononuclear cells; DTSCs: Deciduos tooth stem cells; CPC: Calcium phosphate ceramics; AESCs: Amniotic epithelial stem cells; AFSCs: Amniotic fluid stem cells; Mg/HA: Magnesium/hydroxyapatite; MPC: Magnesium phosphate cement; CMPC: Calcium-magnesium phosphate cement; Rh-BMP-2: Recombinant human bone morphogenetic protein 2; PRP: Platelet rich in plasma; HA: Hydroxyapatite; PCBM: Particulate cancellous bone and marrow; ADSC: Adipose stem cell.

bilateral MSA procedure was executed in 12 edentulous patients. At random, one side was treated with BMSCs + BBM (test side) and the other with BBM mixed with AB (control side)[78]. Three to four months after MSA, 66 implants were placed. Implant survival, plaque, gingival, and bleeding indices, probing depth, and peri-implant radiographic bone levels were assessed at baseline and 1 year after functional loading. During osseointegration, 3 implants failed on the test side and no implants failed on the control side, resulting in 3-mo survival rates of 91% and 100%, respectively. No other implants were lost after 1 year of functional loading[78]. Even if the two reconstructive techniques were reliable in providing new bone for implant placement in the posterior maxilla, a higher implant failure rate was reported in MSA procedures with BMSCs + BBM[78]. In a radiographic study, Kühl *et al*[79] investigated BMA and BMAC influence on graft materials stability when added to BBM within the first 6 mo after MSA. Using a 3D reconstruction software, CT data of 13 patients undergoing bilateral MSA in a split-mouth study, were processed to evaluate graft volumes 2 wk after the sinus lift procedure and 6 mo later[79]. The comparison between volumes at 2 wk and 6 mo showed a statistically significant decrease in all single groups between 15% and 21%. However, changes in volumes between the different groups were not statistically significant[79]. Since an evident decrease in graft volume over the first 6 mo of healing has to be expected, over-augmentation of the sinus is recommended with this cell-based approach[79]. In an interesting split-mouth design study, Wildburger *et al*[80] evaluated early bone formation in BBM sinus grafts using also BMSCs in test group, after 3 and 6 mo. Seven patients, with a posterior maxilla characterized by atrophic bone, were included in this study[80]. In test side, augmentation procedures were performed with BMSCs mixed to BBM; control sides were grafted using pure BBM. At 3 and 6 mo, biopsies of augmented sites were taken[80]. The histologic/histomorphometric evaluation found no significant difference in new bone formation between the test and control group[80]. These results confirmed those of a previous multicentric, controlled study by Sauerbier *et al*[81]; they found that BMAC + BBM or a mixture of AB + BBM, used in sinus augmentation, give similar new bone formation values, after 3-4 mo of healing. However, these outcomes are partially in contrast with those of a previous histologic/histomorphometric study[82], where adding MSCs to BBM leaded to more new bone formation compared with BBM combined with AB. In this study, Rickert *et al*[82], in fact, described how BMSCs seeded on BBM particles could bring sufficient volume of new bone to allow clinicians to place endosseous implants with a comparable timing regarding to the use of AB or a mixture of AB + BBM. The slow resorption rate of BBM permits an adequate bone integration before scaffold resorption[81-83]; however, the rate of non-mineralized material is generally high, even 6 mo after augmentation procedure[81-83]. Finally, Fuerst *et al*[84] examined the 12-mo histologic/histomorphometric and radiologic outcomes after MSA with autogenous culture-expanded bone cells and BBM. In total, 22 sinuses of 12 patients were grafted with AB cells seeded on BBM. Six months after MSA, during endosseous implants (n = 82) placement procedures, a

biopsy was taken from each sinus[84]. The percent newly formed bone was determined on undecalcified histologic preparations. Graft stability was estimated using dental CT scans after MSA (CT 1), after implant insertion (CT 2) and after implant uncover (CT 3)[84]. Despite a considerable reduction of the graft volume along time, AB cells and BBM provided an adequate bone volume, which permitted implant placement and tolerated functional loading[84].

Synthetic porous CPC ceramics can support new bone apposition by MSCs *in vivo*[86,87]. Osteoconductive scaffolds such as HA and beta-TCP have the ability to attract fibronectin and vitronectin, which are ligands for the integrin family of cell adhesion receptors; these proteins mediates adhesion of MSCs and osteoblast precursors[20,21,86,87]. In addition, HA/beta-TCP degradation products may favour an alkaline microenvironment and provide calcium and phosphate ions requested for the mineralization of extracellular matrix phases during ossification process[20,21,86,87]. Finally, microporosity of synthetic CPC (given by pores with a controlled size, communicating through interconnections) supports angiogenesis[20,21,86,87]. Blood vessels carry cells and soluble signals that promote new bone apposition[86,87]. In a recent study by Shayesteh *et al*[86], CPC has been used in combination with BMSCs in MSA. Six patients underwent MSA with BMSCs + HA/beta-TCP. Three and twelve months after MSA, a radiographic evaluation was performed[86]. In total, 30 fixtures were inserted and a biopsy was taken from each implant site. Prosthetic rehabilitation were delivered after 4 mo. Clinical successful implant rate was 93% (28 implants over 30)[86]. Histologic evaluation showed several areas of osteoid and bone formation without any inflammatory cell infiltration. Mean bone regenerate was 41.34%. No complications were clinically observed. Mean bone height was 12.0 mm, 10.0 mm, 3 and 12 mo after MSA, respectively[86]. The authors concluded that sinus grafting with HA/beta-TCP seeded with BMSCs can offer reliable results[86]. A previous study by Smiler *et al*[87] evaluated the effect of bone marrow aspirate added to xenografts or alloplast graft matrix scaffold (beta-TCP) to enhance bone formation in MSA. Clinical procedures involved harvesting four cc of bone marrow aspirate from the anterior iliac crest; these materials were seeded on matrix scaffold before sinus augmentation operations. Seven graft sites were evaluated in five patients; various MSA techniques were performed such as particulate onlay graft of the maxilla *via* a tunneling procedure, and particulate onlay graft of the maxilla stabilized with titanium mesh. Biopsies at 4 mo showed, in beta-TCP scaffolds, 40% a newly formed bone completely vital[87]; there was 57% of interstitial material and 3% of residual graft scaffold[87]. With these histological preparations, the authors presented evidence that stem cells aspirated from bone marrow and seeded onto beta-TCP scaffolds can be a useful method to obtain new bone in augmentation procedures[87].

Synthetic polymeric materials are an interesting category of materials. PLGA copolymer and its homopolymer derivatives have been considered for potential use in bone reconstruction procedures. MSCs have been associated to PLGA in MSA[88-93]. MSCs were isolated from periosteum, re-suspended and cultured; the suspension was soaked in polymer fleeces and the cell-polymer association were used in MSA[88-93]. Under specific conditions, periosteum-derived, tissue engineered bone grafts showed typical osteogenic differentiation characteristics such as: expression of alkaline phosphatase activity, bone gene expression and mineralization[93]. Trautvetter *et al*[88] performed MSA with simultaneous dental implant placement; they used an autologous tissue-engineered periosteal bone grafts based on bioresorbable PLGA scaffolds. Ten patients were radiologically assessed 5 years after MSA; in addition, histologic evaluation was performed[88]. The authors reported excellent outcomes after only 4 mo from surgical procedure; they observed significantly greater bone height over the 5-years follow-up observation period. Furthermore histological preparation from bone biopsies of two patients six months after surgery showed trabecular bone with osteocytes and active osteoblasts[88]. Accordingly, the authors concluded that the use of autologous periosteal bone grafts with simultaneous dental endosseous implants placement is a valid procedure, with excellent clinical, radiographic and histologic outcomes[88]. Although this clinical study[88] and those of previous researches[89,93] have reported that the newly formed bone provided by augmentation procedures, using tissue engineered bone grafts, allowed proper initial stability for dental implant placement[89,90], the degradation rate of the PLGA scaffold may be too fast to maintain an optimal substrate to support bone formation[90-92]. This was evidenced by a recent MSA study, where AB transplants from the iliac crest were compared with tissue engineered grafts (BMSCs loaded on PLGA scaffolds): this research showed considerable graft resorption (approximately 90%, in a 3 mo observation period) and less mineralization density in the sites augmented with tissue engineered bone[92]. Two other comparative studies revealed that coral-derived HA[90] and AB[91] show greater volume maintenance than PLGA scaffolds cultured with MSCs. These studies showed that the significant resorption of the PLGA grafts may be an important problem in the clinical scenario, with potential failure of augmentation particularly in large areas[90,91]. The fast resorption rate of the PLGA, in fact, represents an unfavourable factor for bone regeneration, making it impossible to provide mechanical stability to MSCs transplanted in the augmentation site. Osteoblasts must adhere to a stable structure to produce a new bone matrix that will be interested by consequent mineralization and maturation processes. In this way, a too fast and extended degradation of the supporting scaffold determines an instability of augmented area and then the probably failure of bone regeneration because of the collapse of newly formed, immature bone matrix[90,91]. Supply of oxygen and nutrients is essential

Table 2 Histomorphometric results of the human studies included in the review

Ref.	Patients	Study design	Histomorphometry (% of newly formed bone)
McAllister *et al*[74]	5	5 MSA: MSCs + AL	33.0 ± NR (16 wk)
Gonshor *et al*[75]	18	18 MSA: MSCs + AL	32.5 ± 6.8 (12 wk)
		8 MSA: AL	18.3 ± 10.6 (12 wk)
Duttenhoefer *et al*[77]	11	12 MSA: BMAC + BBM	NR
		6 MSA: Ficoll + BBM	
Rickert *et al*[78]	12	12 MSA: BMSCs + BBM	NR
		12 MSA: AB + BBM	
Kühl *et al*[79]	13	13 MSA: BMA + BBM	NR
		13 MSA: BMAC + BBM	
Wildburger *et al*[80]	7	7 MSA: BMSCs + BBM	7.4 ± 4.1 (12 wk)
			13.5 ± 5.4 (24 wk)
		7 MSA: BBM	11.8 ± 6.2 (12 wk)
			13.9 ± 8.5 (24 wk)
Sauerbier *et al*[81]	26	34 MSA: BMAC + BBM	12.6 ± 1.7 (12 wk)
		11 MSA: AB + BBM	14.3 ± 1.8 (12 wk)
Rickert *et al*[82]	12	12 MSA: BMSCs + BBM	17.7 ± 7.3 (14 wk)
		12 MSA: AB + BBM	12.0 ± 6.6 (14 wk)
Schmelzeisen *et al*[83]	1	2 MSA: BMAC + BBM	26.9 ± NR (12 wk)
Fuerst *et al*[84]	12	22 MSA: BMSCs + BBM	17.9 ± 4.6 (24 wk)
Beaumont *et al*[85]	3	6 MSA: PDSCs + BBM	NR
Shayesteh *et al*[86]	6	6 MSA: BMSCs + HA/β-TCP	41.3 ± NR (24 wk)
Smiler *et al*[87]	4	2 MSA: BMSCs + β-TCP	40.0 ± NR (16 wk)
		1 MSA: BMSCs + BBM	13.0 ± NR (16 wk)
		1 MSA: BMSCs + HA	31.0 ± NR (16 wk)
Trautvetter *et al*[88]	10	10 MSA: PDSCs + PLGA	NR
Mangano *et al*[89]	1	1 MSA: PDSCs + PLGA	28.8 ± NR
Voss *et al*[91]	35	50 MSA: PDSCs + PLGA	NR
		63 MSA: AB	
Mangano *et al*[90]	5	5 MSA: PDSCs + PLGA	37.3 ± 19.5 (24 wk)
		5 MSA: HA	54.6 ± 21.1 (24 wk)
Zizelmann *et al*[92]	20	14 MSA: PDSCs + PLGA	NR
		17 MSA: AB	
Schimming *et al*[93]	27	27 MSA: PDSCs + PLGA	NR
Yamada *et al*[94]	23	23 MSA: BMSCs + PRP	NR
Ueda *et al*[95]	6	6 MSA: BMSCs + PRP	NR

MSA: Maxillary sinus augmentation; MSCs: Mesenchymal stem cells; AL: Allograft; NR: Not reported; BMAC: Autologous bone marrow aspirate concentrate; BBM: Bovine bone mineral; BMSCs: Bone marrow stem cells; AB: Autogenous bone; BMA: Bone marrow aspirate; PDSCs: Periosteal derived stem cells; HA/β-TCP: Hydroxyapatite/beta-tricalcium phosphate; PLGA: Polylactid-co-glycolic acid; PRP: Platelet rich in plasma.

to cells embedded within large cell-polymer constructs, in order to sustain their survival and proliferation[89-92]. In addition, PLGA resorption generates a low pH that is detrimental to osteoblasts[89-92].

Finally, two different clinical studies used an injectable tissue engineered bone, composed by BMSCs and PRP, to conduct MSA[94,95]. In a recent study, Yamada *et al*[94] evaluated the effects of an injectable tissue engineered bone on osteotome technique with simultaneous implant placement. Injectable bone, composed of BMSCs and PRP, was used as bone graft in 23 cases of MSA[94]. The osteotome technique was used[7]: after dental implant sites were pre-prepared with pilot drills and/or using the osteotomes, the injectable bone was inserted and then endosseous implants were placed. The bone regeneration technique was effective, as the lift-up bone height by injectable bone using BMSCs showed an increase of 6.1 ± 1.5 mm; the authors concluded that the application of injectable bone using osteotome technique can stably predict the success of bone formation and dental implants, providing also minimally invasive cell therapy[94]. These results confirmed those of a previous study by Ueda *et al*[95] in which the height of mineralized tissue after 2 years showed a mean gain of 8.8 mm compared to pre-operative values. However, more studies are needed to understand the efficacy of injectable bone as a graft for MSA: this material has poor compressive and tensile strength[94].

The histologic/histomorphometric results of all these human studies are reported in Table 2.

In vivo experiment meta-analysis

A meta-analysis of 9 studies (7 animal and 2 human studies) was performed to give a quantitative estimate of the mean difference of the newly formed bone between the two groups (stem cells + scaffold *vs* scaffold alone). We considered the mean difference in % newly formed bone at 12 wk as it was the most frequently reported time period; the latest examination period was at 8 wk in 4 studies, all of them on animals. All the analyses were conducted using Package Metafor (R version 2.14). The weighted mean difference estimate from a

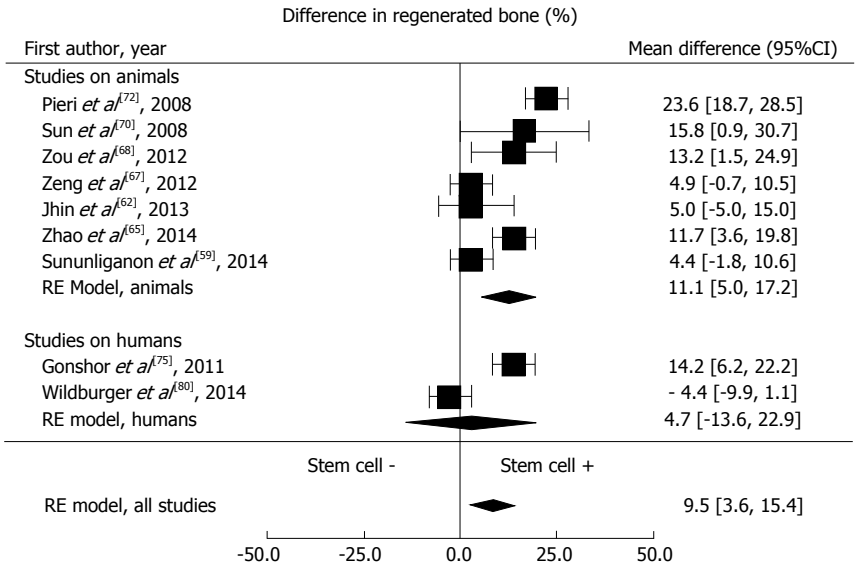

Figure 2 Differences in regenerated bone between test and control groups from meta-analysis. RE: Reference.

random-effect model was 9.5% (95%CI: 3.6%-15.4%), suggesting a positive effect of stem cells on the bone re-growth (Figure 2). Heterogeneity was measured by the I^2 index. The formal test confirmed the presence of substantial heterogeneity (I^2 = 83%, P < 0.0001). In an attempt to explain the substantial heterogeneity observed, we considered a meta-regression model with publication year, support type (animals *vs* humans) and follow-up length (8 or 12 wk) as covariates. After adding publication year, support type and follow-up length to the meta-regression model, heterogeneity was no longer significant (I^2 = 33%, P = 0.25).

DISCUSSION

The finding that adult MSCs can be manipulated *in vitro* and subsequently form bone *in vivo* provides new therapeutic strategies for bone regeneration in dentistry.

Several researches have demonstrated that MSCs can be used in MSA: controlled experimental and clinical studies showed higher bone regeneration applying MSCs compared with controls. However, further clinical trials, which clearly demonstrate benefits of cell-based approach compared to conventional treatments are still needed: these studies should evaluate patient-based outcomes, including the time and cost-effectiveness of cell-based approaches.

In the future, the use of stem cells seeded on appropriated scaffold materials will dictates advances in bone regeneration: as a consequence, improvements upon current therapeutic strategies will depend on innovations in material science. It will be mandatory to search for appropriate scaffolds for MSCs, with adequate resorption rate and osteoconductive surface, over which new bone formation can occur.

The merger between these two disciplines - stem cell research and scaffold engineering - will draw the future of regenerative medicine.

ACKNOWLEDGMENTS

Dr. Francesco Mangano is a fellow of the PHD program in Biotechnology Biosciences and Surgical Technologies at the School in Biological/Medical Science, University of Insubria, Varese, Italy.

COMMENTS

Background

Adult mesenchymal stem cells (MSCs) that can be obtained from several tissues represents the new frontier for bone regeneration, due to their proven ability to differentiate into functional osteoblast, capable to produce new bone. Maxillary sinus augmentation (MSA) enables rehabilitation with oral implants in the posterior maxilla. Fresh autogenous bone (AB) has been always considered the gold-standard for MSA, but limited availability and donor-site morbidity reduce its application. Several osteoconductive scaffolds, such as allografts, bovine bone mineral and synthetic bone grafts (calcium phosphate ceramics) have been used in MSA with clinically successful results, but these materials do not have cells and require more time for healing. The science of bone tissue engineering (BTE) aims to overcome this problem, as it promises to obtain bone regeneration through the use of scaffolds seeded with osteogenic cells, without harvesting AB from other anatomical sites.

Research frontiers

According to BTE, a bone substitute should possess the same biological and structural properties as native bone, and the fabrication of the ideal bone graft requires the manipulation of three essential elements: scaffold, growth factors and osteogenic cells. BTE is a multidisciplinary science, based on harvesting of living cells that are expanded and differentiated in laboratory, then seeded on an appropriate scaffold, capable to mimic the structures and physiological behaviour of natural tissues. Ultimately, these "engineered scaffold" are implanted in patients. In this context, cells are the basic unit for the regeneration strategy. Several cell types have been investigated for their application in bone regeneration: MSCs can be a suitable for this aim. The authors' present review aimed to investigate the effectiveness of MSCs in MSA, with differents scaffold materials, in animals and humans.

Innovations and breakthroughs

In total, 39 studies (18 animal studies, 21 human studies) published over a 10-year period (between 2004 and 2014) were included in our present review; these studies were variables with respect to type, study design, follow-up, and results. Meta-analysis was performed on 9 studies (7 animal studies and 2

human studies): the weighted mean difference estimate from a random-effect model was 9.5% (95%CI: 3.6%-15.4%), suggesting a positive effect of MSCs on bone regeneration. These results are similar to those of previous reviews of the literature on the same topic, where a positive influence of MSCs on bone regeneration was evidenced.

Applications

The use of scaffolds seeded with MSCs seems to represent a safe and successful treatment procedure to achieve bone regeneration in MSA. In the coming years there will be a further, huge flood of new studies on MSA with MSCs. Accordingly, dental professionals/surgeons need to change the way they think and work, to adapt to a new challenging scenario that is increasingly driven by the fascinating concepts of BTE. BTE will change the world of dentistry, changing patients' expectations towards dental treatments: waiting to adopt or integrate these new techniques would leave oral surgeons decades behind.

Terminology

MSA is a surgical procedure to increase the amount of bone in the posterior maxilla by sacrificing some of the volume of the maxillary sinus. In case of tooth/teeth loss (due to caries, periodontal disease or traumatic injury) the alveolar process undergoes remodelling, usually losing both height and width; in addition, the floor of the sinus gradually becomes lower. This represents a problem for the correct placement of dental implants, which rely on osseointegration. The aim of MSA is to graft extra bone into the maxillary sinus, in order to support dental implant. BTE is a new science that combines cells, materials and growth factors, with the aim to obtain bone regeneration in the clinical field. While most definitions of tissue engineering cover a broad range of applications, in practice the term is closely associated with applications that repair or replace portions of or whole tissues (*i.e.*, bone, BTE: science that aims to achieve bone regeneration, without harvesting AB from other anatomical sites, through the use in combination of scaffolds, osteogenic cells and soluble signals).

Peer-review

Several studies have reported the potential for cell-based approaches in MSA; however, most of these are animal studies. Accordingly, further clinical studies, which clearly demonstrate benefits of cell-based approach compared to conventional treatments are still needed.

REFERENCES

1 **Mangano C**, Iaculli F, Piattelli A, Mangano F. Fixed restorations supported by Morse-taper connection implants: a retrospective clinical study with 10-20 years of follow-up. *Clin Oral Implants Res* 2014; Epub ahead of print [PMID: 24954285 DOI: 10.1111/clr.12439]

2 **Chappuis V**, Buser R, Brägger U, Bornstein MM, Salvi GE, Buser D. Long-term outcomes of dental implants with a titanium plasma-sprayed surface: a 20-year prospective case series study in partially edentulous patients. *Clin Implant Dent Relat Res* 2013; **15**: 780-790 [PMID: 23506385 DOI: 10.1111/cid.12056]

3 **Mangano F**, Macchi A, Caprioglio A, Sammons RL, Piattelli A, Mangano C. Survival and complication rates of fixed restorations supported by locking-taper implants: a prospective study with 1 to 10 years of follow-up. *J Prosthodont* 2014; **23**: 434-444 [PMID: 24750435 DOI: 10.1111/jopr.12152]

4 **Mangano C**, Sinjari B, Shibli JA, Mangano F, Hamisch S, Piattelli A, Perrotti V, Iezzi G. A Human Clinical, Histological, Histomorphometrical, and Radiographical Study on Biphasic HA-Beta-TCP 30/70 in Maxillary Sinus Augmentation. *Clin Implant Dent Relat Res* 2015; **17**: 610-618 [PMID: 24004190 DOI: 10.1111/cid.12145]

5 **Mangano C**, Iaculli F, Piattelli A, Mangano F, Shibli JA, Perrotti V, Iezzi G. Clinical and histologic evaluation of calcium carbonate in sinus augmentation: a case series. *Int J Periodontics Restorative Dent* 2014; **34**: e43-e49 [PMID: 24600666 DOI: 10.11607/prd.1832]

6 **Tatum H**. Maxillary and sinus implant reconstructions. *Dent Clin North Am* 1986; **30**: 207-229 [PMID: 3516738]

7 **Summers RB**. A new concept in maxillary implant surgery: the osteotome technique. *Compendium* 1994; **15**: 152, 154-156, 158 passim; quiz 162 [PMID: 8055503]

8 **Kfir E**, Kfir V, Goldstein M, Mazor Z, Kaluski E. Minimally invasive subnasal elevation and antral membrane balloon elevation along with bone augmentation and implants placement. *J Oral Implantol* 2012; **38**: 365-376 [PMID: 21668352 DOI: 10.1563/AAID-JOI-D-10-00129]

9 **Mangano F**, Zecca P, Pozzi-Taubert S, Macchi A, Ricci M, Luongo G, Mangano C. Maxillary sinus augmentation using computer-aided design/computer-aided manufacturing (CAD/CAM) technology. *Int J Med Robot* 2013; **9**: 331-338 [PMID: 22961733 DOI: 10.1002/rcs.1460]

10 **Duttenhoefer F**, Souren C, Menne D, Emmerich D, Schön R, Sauerbier S. Long-term survival of dental implants placed in the grafted maxillary sinus: systematic review and meta-analysis of treatment modalities. *PLoS One* 2013; **8**: e75357 [PMID: 24058679 DOI: 10.1371/journal.pone.0075357]

11 **Rickert D**, Slater JJ, Meijer HJ, Vissink A, Raghoebar GM. Maxillary sinus lift with solely autogenous bone compared to a combination of autogenous bone and growth factors or (solely) bone substitutes. A systematic review. *Int J Oral Maxillofac Surg* 2012; **41**: 160-167 [PMID: 22099314 DOI: 10.1016/j.ijom.2011.10.001]

12 **Mangano FG**, Tettamanti L, Sammons RL, Azzi L, Caprioglio A, Macchi A, Mangano C. Maxillary sinus augmentation with adult mesenchymal stem cells: a review of the current literature. *Oral Surg Oral Med Oral Pathol Oral Radiol* 2013; **115**: 717-723 [PMID: 23313230 DOI: 10.1016/j.oooo.2012.09.087]

13 **Xavier SP**, Dias RR, Sehn FP, Kahn A, Chaushu L, Chaushu G. Maxillary sinus grafting with autograft vs. fresh frozen allograft: a split-mouth histomorphometric study. *Clin Oral Implants Res* 2014; Epub ahead of print [PMID: 24734909 DOI: 10.1111/clr.12404]

14 **Sbordone C**, Toti P, Guidetti F, Califano L, Pannone G, Sbordone L. Volumetric changes after sinus augmentation using blocks of autogenous iliac bone or freeze-dried allogeneic bone. A non-randomized study. *J Craniomaxillofac Surg* 2014; **42**: 113-118 [PMID: 23726762 DOI: 10.1016/j.jcms.2013.03.004]

15 **Schmitt CM**, Moest T, Lutz R, Neukam FW, Schlegel KA. Anorganic bovine bone (ABB) vs. autologous bone (AB) plus ABB in maxillary sinus grafting. A prospective non-randomized clinical and histomorphometrical trial. *Clin Oral Implants Res* 2014; Epub ahead of print [PMID: 24730602 DOI: 10.1111/clr.12396]

16 **Mangano C**, Scarano A, Perrotti V, Iezzi G, Piattelli A. Maxillary sinus augmentation with a porous synthetic hydroxyapatite and bovine-derived hydroxyapatite: a comparative clinical and histologic study. *Int J Oral Maxillofac Implants* 2007; **22**: 980-986 [PMID: 18271380]

17 **Mangano C**, Scarano A, Iezzi G, Orsini G, Perrotti V, Mangano F, Montini S, Piccirilli M, Piattelli A. Maxillary sinus augmentation using an engineered porous hydroxyapatite: a clinical, histological, and transmission electron microscopy study in man. *J Oral Implantol* 2006; **32**: 122-131 [PMID: 16836176 DOI: 10.1563/796.1]

18 **Mendonça-Caridad JJ**, Nunez M, Juiz-Lopez P, Pita-Fernandez S, Seoane J. Sinus floor elevation using a composite graft: clinical outcome of immediate implant placement. *Int J Oral Maxillofac Implants* 2013; **28**: 252-260 [PMID: 23377072 DOI: 10.11607/jomi.2379]

19 **Park JB**. Use of cell-based approaches in maxillary sinus augmentation procedures. *J Craniofac Surg* 2010; **21**: 557-560 [PMID: 20216438 DOI: 10.1097/SCS.0b013e3181d02577]

20 **Tevlin R**, McArdle A, Atashroo D, Walmsley GG, Senarath-Yapa K, Zielins ER, Paik KJ, Longaker MT, Wan DC. Biomaterials for craniofacial bone engineering. *J Dent Res* 2014; **93**: 1187-1195 [PMID: 25139365 DOI: 10.1177/0022034514547271]

21 **Ferretti C**, Ripamonti U, Tsiridis E, Kerawala CJ, Mantalaris A, Heliotis M. Osteoinduction: translating preclinical promise into clinical reality. *Br J Oral Maxillofac Surg* 2010; **48**: 536-539 [PMID: 20430492 DOI: 10.1016/j.bjoms.2010.07.020]

22 **Moher D**, Liberati A, Tetzlaff J, Altman DG; PRISMA Group. Preferred reporting items for systematic reviews and meta-analyses: the PRISMA statement. *J Clin Epidemiol* 2009; **62**: 1006-1012 [PMID: 19631508 DOI: 10.1016/j.jclinepi.2009.06.005]

23 **Higgins JPT**, Green S. Cochrane handbook for systematic reviews of interventions version 5.1.0. [Updated 2011 March]. The Cochrane Collaboration. Available from: URL: http://www.cochrane-handbook.org

24 **Chambrone L**, Faggion CM, Pannuti CM, Chambrone LA. Evidence-based periodontal plastic surgery: an assessment of quality of systematic reviews in the treatment of recession-type defects. *J Clin Periodontol* 2010; **37**: 1110-1118 [PMID: 21070325 DOI: 10.1111/j.1600-051X.2010.01634.x]

25 **Ramirez JM**, Bai Q, Dijon-Grinand M, Assou S, Gerbal-Chaloin S, Hamamah S, De Vos J. Human pluripotent stem cells: from biology to cell therapy. *World J Stem Cells* 2010; **2**: 24-33 [PMID: 21607113 DOI: 10.4252/wjsc.v2.i2.24]

26 **Ripamonti U**. Soluble and insoluble signals sculpt osteogenesis in angiogenesis. *World J Biol Chem* 2010; **1**: 109-132 [PMID: 21540997 DOI: 10.4331/wjbc.v1.i5.109]

27 **Rosso F**, Marino G, Giordano A, Barbarisi M, Parmeggiani D, Barbarisi A. Smart materials as scaffolds for tissue engineering. *J Cell Physiol* 2005; **203**: 465-470 [PMID: 15744740 DOI: 10.1002/jcp.20270]

28 **Marolt D**, Knezevic M, Novakovic GV. Bone tissue engineering with human stem cells. *Stem Cell Res Ther* 2010; **1**: 10 [PMID: 20637059 DOI: 10.1186/scrt10]

29 **Handschel J**, Wiesmann HP, Depprich R, Kübler NR, Meyer U. Cell-based bone reconstruction therapies--cell sources. *Int J Oral Maxillofac Implants* 2006; **21**: 890-898 [PMID: 17190298]

30 **Bifari F**, Pacelli L, Krampera M. Immunological properties of embryonic and adult stem cells. *World J Stem Cells* 2010; **2**: 50-60 [PMID: 21607122 DOI: 10.4252/wjsc.v2.i3.50]

31 **Razzouk S**, Schoor R. Mesenchymal stem cells and their challenges for bone regeneration and osseointegration. *J Periodontol* 2012; **83**: 547-550 [PMID: 21942789 DOI: 10.1902/jop.2011.110384]

32 **Daar AS**, Sheremeta L. The science of stem cells: ethical, legal and social issues. *Exp Clin Transplant* 2003; **1**: 139-146 [PMID: 15859920]

33 **Mahalakshmi S**. Potentials of stem cell research and the implications of legislation. *J Stem Cells Regen Med* 2006; **1**: 37-39 [PMID: 24692860]

34 **Liao HT**, Chen CT. Osteogenic potential: Comparison between bone marrow and adipose-derived mesenchymal stem cells. *World J Stem Cells* 2014; **6**: 288-295 [PMID: 25126378 DOI: 10.4252/wjsc.v6.i3.288]

35 **Ferretti C**, Mattioli-Belmonte M. Periosteum derived stem cells for regenerative medicine proposals: Boosting current knowledge. *World J Stem Cells* 2014; **6**: 266-277 [PMID: 25126377 DOI: 10.4252/wjsc.v6.i3.266]

36 **Cicconetti A**, Sacchetti B, Bartoli A, Michienzi S, Corsi A, Funari A, Robey PG, Bianco P, Riminucci M. Human maxillary tuberosity and jaw periosteum as sources of osteoprogenitor cells for tissue engineering. *Oral Surg Oral Med Oral Pathol Oral Radiol Endod* 2007; **104**: 618.e1-618.12 [PMID: 17613258 DOI: 10.1016/j.tripleo.2007.02.022]

37 **Tsuji W**, Rubin JP, Marra KG. Adipose-derived stem cells: Implications in tissue regeneration. *World J Stem Cells* 2014; **6**: 312-321 [PMID: 25126381 DOI: 10.4252/wjsc.v6.i3.312]

38 **Bosch P**, Musgrave DS, Lee JY, Cummins J, Shuler T, Ghivizzani TC, Evans T, Robbins TD. Osteoprogenitor cells within skeletal muscle. *J Orthop Res* 2000; **18**: 933-944 [PMID: 11192254 DOI: 10.1002/jor.1100180613]

39 **Zeddou M**, Relic B, Malaise MG. Umbilical cord fibroblasts: Could they be considered as mesenchymal stem cells? *World J Stem Cells* 2014; **6**: 367-370 [PMID: 25126385 DOI: 10.4252/wjsc.v6.i3.367]

40 **Berardinelli P**, Valbonetti L, Muttini A, Martelli A, Peli R, Zizzari V, Nardinocchi D, Vulpiani MP, Tetè S, Barboni B, Piattelli A, Mattioli M. Role of amniotic fluid mesenchymal cells engineered on MgHA/collagen-based scaffold allotransplanted on an experimental animal study of sinus augmentation. *Clin Oral Investig* 2013; **17**: 1661-1675 [PMID: 23064983 DOI: 10.1007/s00784-012-0857-3]

41 **Barboni B**, Mangano C, Valbonetti L, Marruchella G, Berardinelli P, Martelli A, Muttini A, Mauro A, Bedini R, Turriani M, Pecci R, Nardinocchi D, Zizzari VL, Tetè S, Piattelli A, Mattioli M. Synthetic bone substitute engineered with amniotic epithelial cells enhances bone regeneration after maxillary sinus augmentation. *PLoS One* 2013; **8**: e63256 [PMID: 23696804 DOI: 10.1371/journal.pone.0063256]

42 **Kang EJ**, Byun JH, Choi YJ, Maeng GH, Lee SL, Kang DH, Lee JS, Rho GJ, Park BW. In vitro and in vivo osteogenesis of porcine skin-derived mesenchymal stem cell-like cells with a demineralized bone and fibrin glue scaffold. *Tissue Eng Part A* 2010; **16**: 815-827 [PMID: 19778183 DOI: 10.1089/ten.TEA.2009.0439]

43 **Mangano C**, Paino F, d'Aquino R, De Rosa A, Iezzi G, Piattelli A, Laino L, Mitsiadis T, Desiderio V, Mangano F, Papaccio G, Tirino V. Human dental pulp stem cells hook into biocoral scaffold forming an engineered biocomplex. *PLoS One* 2011; **6**: e18721 [PMID: 21494568 DOI: 10.1371/journal.pone.0018721]

44 **Rodríguez Lozano FJ**, Moraleda JM. Mesenchymal dental pulp stem cells: a new tool in sinus lift. *J Craniofac Surg* 2011; **22**: 774-775 [PMID: 21415669 DOI: 10.1097/SCS.0b013e318208ba61]

45 **Behnia A**, Haghighat A, Talebi A, Nourbakhsh N, Heidari F. Transplantation of stem cells from human exfoliated deciduous teeth for bone regeneration in the dog mandibular defect. *World J Stem Cells* 2014; **6**: 505-510 [PMID: 25258673 DOI: 10.4252/wjsc.v6.i4.505]

46 **Ohta S**, Yamada S, Matuzaka K, Inoue T. The behavior of stem cells and progenitor cells in the periodontal ligament during wound healing as observed using immunohistochemical methods. *J Periodontal Res* 2008; **43**: 595-603 [PMID: 18705651 DOI: 10.1111/j.1600-0765.2007.01002.x]

47 **Stenderup K**, Justesen J, Clausen C, Kassem M. Aging is associated with decreased maximal life span and accelerated senescence of bone marrow stromal cells. *Bone* 2003; **33**: 919-926 [PMID: 14678851 DOI: 10.1016/j.bone.2003.07.005]

48 **McLain RF**, Fleming JE, Boehm CA, Muschler GF. Aspiration of osteoprogenitor cells for augmenting spinal fusion: comparison of progenitor cell concentrations from the vertebral body and iliac crest. *J Bone Joint Surg Am* 2005; **87**: 2655-2661 [PMID: 16322615 DOI: 10.2106/JBJS.E.00230]

49 **Tuan RS**, Boland G, Tuli R. Adult mesenchymal stem cells and cell-based tissue engineering. *Arthritis Res Ther* 2003; **5**: 32-45 [PMID: 12716446 DOI: 10.1186/ar614]

50 **Ueda M**, Tohnai I, Nakai H. Tissue engineering research in oral implant surgery. *Artif Organs* 2001; **25**: 164-171 [PMID: 11284882 DOI: 10.1046/j.1525-1594.2001.025003164.x]

51 **Ly H**. Telomere dynamics in induced pluripotent stem cells: Potentials for human disease modeling. *World J Stem Cells* 2011; **3**: 89-95 [PMID: 22110834 DOI: 10.4252/wjsc.v3.i10.89]

52 **Banfi A**, Muraglia A, Dozin B, Mastrogiacomo M, Cancedda R, Quarto R. Proliferation kinetics and differentiation potential of ex vivo expanded human bone marrow stromal cells: Implications for their use in cell therapy. *Exp Hematol* 2000; **28**: 707-715 [PMID: 10880757 DOI: 10.1016/S0301-472X(00)00160-0]

53 **Park BW**, Hah YS, Kim DR, Kim JR, Byun JH. Vascular endothelial growth factor expression in cultured periosteal-derived cells. *Oral Surg Oral Med Oral Pathol Oral Radiol Endod* 2008; **105**: 554-560 [PMID: 18296084 DOI: 10.1016/j.tripleo.2007.08.018]

54 **Fakhry M**, Hamade E, Badran B, Buchet R, Magne D. Molecular mechanisms of mesenchymal stem cell differentiation towards osteoblasts. *World J Stem Cells* 2013; **5**: 136-148 [PMID: 24179602 DOI: 10.4252/wjsc.v5.i4.136]

55 **Kuboki Y**, Jin Q, Kikuchi M, Mamood J, Takita H. Geometry of artificial ECM: sizes of pores controlling phenotype expression in BMP-induced osteogenesis and chondrogenesis. *Connect Tissue Res* 2002; **43**: 529-534 [PMID: 12489210 DOI: 10.1080/713713489]

56 **Kuboki Y**, Takita H, Kobayashi D, Tsuruga E, Inoue M, Murata

M, Nagai N, Dohi Y, Ohgushi H. BMP-induced osteogenesis on the surface of hydroxyapatite with geometrically feasible and nonfeasible structures: topology of osteogenesis. *J Biomed Mater Res* 1998; **39**: 190-199 [PMID: 9457547]

57 **Murphy CM**, O'Brien FJ, Little DG, Schindeler A. Cell-scaffold interactions in the bone tissue engineering triad. *Eur Cell Mater* 2013; **26**: 120-132 [PMID: 24052425]

58 **Logeart-Avramoglou D**, Anagnostou F, Bizios R, Petite H. Engineering bone: challenges and obstacles. *J Cell Mol Med* 2005; **9**: 72-84 [PMID: 15784166 DOI: 10.1111/j.1582-4934.2005.tb00338.x]

59 **Sununliganon L**, Peng L, Singhatanadgit W, Cheung LK. Osteogenic efficacy of bone marrow concentrate in rabbit maxillary sinus grafting. *J Craniomaxillofac Surg* 2014; **42**: 1753-1765 [PMID: 25052732 DOI: 10.1016/j.jcms.2014.06.011]

60 **Yu BH**, Zhou Q, Wang ZL. Comparison of tissue-engineered bone from different stem cell sources for maxillary sinus floor augmentation: a study in a canine model. *J Oral Maxillofac Surg* 2014; **72**: 1084-1092 [PMID: 24576438 DOI: 10.1016/j.joms.2013.12.024]

61 **Oshima T**, Duttenhoefer F, Xavier S, Nelson K, Sauerbier S. Can mesenchymal stem cells and novel gabapentin-lactam enhance maxillary bone formation? *J Oral Maxillofac Surg* 2014; **72**: 485-495 [PMID: 24528562 DOI: 10.1016/j.joms.2013.10.026]

62 **Jhin MJ**, Kim KH, Kim SH, Kim YS, Kim ST, Koo KT, Kim TI, Seol YJ, Ku Y, Rhyu IC, Lee YM. Ex vivo bone morphogenetic protein-2 gene delivery using bone marrow stem cells in rabbit maxillary sinus augmentation in conjunction with implant placement. *J Periodontol* 2013; **84**: 985-994 [PMID: 22897653 DOI: 10.1902/jop.2012.120221]

63 **Gutwald R**, Haberstroh J, Kuschnierz J, Kister C, Lysek DA, Maglione M, Xavier SP, Oshima T, Schmelzeisen R, Sauerbier S. Mesenchymal stem cells and inorganic bovine bone mineral in sinus augmentation: comparison with augmentation by autologous bone in adult sheep. *Br J Oral Maxillofac Surg* 2010; **48**: 285-290 [PMID: 19665265 DOI: 10.1016/j.bjoms.2009.06.226]

64 **Sauerbier S**, Stubbe K, Maglione M, Haberstroh J, Kuschnierz J, Oshima T, Xavier SP, Brunnberg L, Schmelzeisen R, Gutwald R. Mesenchymal stem cells and bovine bone mineral in sinus lift procedures--an experimental study in sheep. *Tissue Eng Part C Methods* 2010; **16**: 1033-1039 [PMID: 20050809 DOI: 10.1089/ten.TEC.2009.0734]

65 **Zhao W**, Lu JY, Hao YM, Cao CH, Zou DR. Maxillary sinus floor elevation with a tissue-engineered bone composite of deciduous tooth stem cells and calcium phosphate cement in goats. *J Tissue Eng Regen Med* 2014; Epub ahead of print [PMID: 24616333 DOI: 10.1002/term.1867]

66 **Zhang W**, Zhang X, Wang S, Xu L, Zhang M, Wang G, Jin Y, Zhang X, Jiang X. Comparison of the use of adipose tissue-derived and bone marrow-derived stem cells for rapid bone regeneration. *J Dent Res* 2013; **92**: 1136-1141 [PMID: 24097853 DOI: 10.1177/0022034513507581]

67 **Zeng D**, Xia L, Zhang W, Huang H, Wei B, Huang Q, Wei J, Liu C, Jiang X. Maxillary sinus floor elevation using a tissue-engineered bone with calcium-magnesium phosphate cement and bone marrow stromal cells in rabbits. *Tissue Eng Part A* 2012; **18**: 870-881 [PMID: 22066969 DOI: 10.1089/ten.TEA.2011.0379]

68 **Zou D**, Guo L, Lu J, Zhang X, Wei J, Liu C, Zhang Z, Jiang X. Engineering of bone using porous calcium phosphate cement and bone marrow stromal cells for maxillary sinus augmentation with simultaneous implant placement in goats. *Tissue Eng Part A* 2012; **18**: 1464-1478 [PMID: 22452368 DOI: 10.1089/ten.TEA.2011.0501]

69 **Xia L**, Xu Y, Chang Q, Sun X, Zeng D, Zhang W, Zhang X, Zhang Z, Jiang X. Maxillary sinus floor elevation using BMP-2 and Nell-1 gene-modified bone marrow stromal cells and TCP in rabbits. *Calcif Tissue Int* 2011; **89**: 53-64 [PMID: 21584647 DOI: 10.1007/s00223-011-9493-1]

70 **Sun XJ**, Zhang ZY, Wang SY, Gittens SA, Jiang XQ, Chou LL. Maxillary sinus floor elevation using a tissue-engineered bone complex with OsteoBone and bMSCs in rabbits. *Clin Oral Implants Res* 2008; **19**: 804-813 [PMID: 18705812 DOI: 10.1111/j.1600-0501.2008.01577.x]

71 **Sun XJ**, Xia LG, Chou LL, Zhong W, Zhang XL, Wang SY, Zhao J, Jiang XQ, Zhang ZY. Maxillary sinus floor elevation using a tissue engineered bone complex with BMP-2 gene modified bMSCs and a novel porous ceramic scaffold in rabbits. *Arch Oral Biol* 2010; **55**: 195-202 [PMID: 20144455 DOI: 10.1016/j.archoralbio.2010.01.006]

72 **Pieri F**, Lucarelli E, Corinaldesi G, Iezzi G, Piattelli A, Giardino R, Bassi M, Donati D, Marchetti C. Mesenchymal stem cells and platelet-rich plasma enhance bone formation in sinus grafting: a histomorphometric study in minipigs. *J Clin Periodontol* 2008; **35**: 539-546 [PMID: 18422697 DOI: 10.1111/j.1600-051X.2008.01220.x]

73 **Ohya M**, Yamada Y, Ozawa R, Ito K, Takahashi M, Ueda M. Sinus floor elevation applied tissue-engineered bone. Comparative study between mesenchymal stem cells/platelet-rich plasma (PRP) and autogenous bone with PRP complexes in rabbits. *Clin Oral Implants Res* 2005; **16**: 622-629 [PMID: 16164471 DOI: 10.1111/j.1600-0501.2005.01136.x]

74 **McAllister BS**, Haghighat K, Gonshor A. Histologic evaluation of a stem cell-based sinus-augmentation procedure. *J Periodontol* 2009; **80**: 679-686 [PMID: 19335089 DOI: 10.1902/jop.2009.080345]

75 **Gonshor A**, McAllister BS, Wallace SS, Prasad H. Histologic and histomorphometric evaluation of an allograft stem cell-based matrix sinus augmentation procedure. *Int J Oral Maxillofac Implants* 2011; **26**: 123-131 [PMID: 21365047]

76 **Tyshenko MG**, ElSaadany S, Oraby T, Darshan S, Aspinall W, Cooke R, Catford A, Krewski D. Expert elicitation for the judgment of prion disease risk uncertainties. *J Toxicol Environ Health A* 2011; **74**: 261-285 [PMID: 21218351 DOI: 10.1080/15287394.2011.529783]

77 **Duttenhoefer F**, Hieber SF, Stricker A, Schmelzeisen R, Gutwald R, Sauerbier S. Follow-up of implant survival comparing ficoll and bone marrow aspirate concentrate methods for hard tissue regeneration with mesenchymal stem cells in humans. *Biores Open Access* 2014; **3**: 75-76 [PMID: 24804168 DOI: 10.1089/biores.2014.0003]

78 **Rickert D**, Vissink A, Slot WJ, Sauerbier S, Meijer HJ, Raghoebar GM. Maxillary sinus floor elevation surgery with BioOss® mixed with a bone marrow concentrate or autogenous bone: test of principle on implant survival and clinical performance. *Int J Oral Maxillofac Surg* 2014; **43**: 243-247 [PMID: 24183511 DOI: 10.1016/j.ijom.2013.09.006]

79 **Kühl S**, Payer M, Kirmeier R, Wildburger A, Wegscheider W, Jakse N. The influence of bone marrow aspirates and concentrates on the early volume stability of maxillary sinus grafts with deproteinized bovine bone mineral - first results of a RCT. *Clin Oral Implants Res* 2014; **25**: 221-225 [PMID: 23294470 DOI: 10.1111/clr.12101]

80 **Wildburger A**, Payer M, Jakse N, Strunk D, Etchard-Liechtenstein N, Sauerbier S. Impact of autogenous concentrated bone marrow aspirate on bone regeneration after sinus floor augmentation with a bovine bone substitute--a split-mouth pilot study. *Clin Oral Implants Res* 2014; **25**: 1175-1181 [PMID: 23875876 DOI: 10.1111/clr.12228]

81 **Sauerbier S**, Rickert D, Gutwald R, Nagursky H, Oshima T, Xavier SP, Christmann J, Kurz P, Menne D, Vissink A, Raghoebar G, Schmelzeisen R, Wagner W, Koch FP. Bone marrow concentrate and bovine bone mineral for sinus floor augmentation: a controlled, randomized, single-blinded clinical and histological trial--per-protocol analysis. *Tissue Eng Part A* 2011; **17**: 2187-2197 [PMID: 21529247 DOI: 10.1089/ten.TEA.2010.0516]

82 **Rickert D**, Sauerbier S, Nagursky H, Menne D, Vissink A, Raghoebar GM. Maxillary sinus floor elevation with bovine bone mineral combined with either autogenous bone or autogenous stem cells: a prospective randomized clinical trial. *Clin Oral Implants Res* 2011; **22**: 251-258 [PMID: 20831758 DOI: 10.1111/j.1600-05

01.2010.01981.x]
83 **Schmelzeisen R**, Gutwald R, Oshima T, Nagursky H, Vogeler M, Sauerbier S. Making bone II: maxillary sinus augmentation with mononuclear cells--case report with a new clinical method. *Br J Oral Maxillofac Surg* 2011; **49**: 480-482 [PMID: 20678831 DOI: 10.1016/j.bjoms.2010.06.020]
84 **Fuerst G**, Strbac GD, Vasak C, Tangl S, Leber J, Gahleitner A, Gruber R, Watzek G. Are culture-expanded autogenous bone cells a clinically reliable option for sinus grafting? *Clin Oral Implants Res* 2009; **20**: 135-139 [PMID: 19077153 DOI: 10.1111/j.1600-0501.2008.01624.x]
85 **Beaumont C**, Schmidt RJ, Tatakis DN, Zafiropoulos GG. Use of engineered bone for sinus augmentation. *J Periodontol* 2008; **79**: 541-548 [PMID: 18315438 DOI: 10.1902/jop.2008.070255]
86 **Shayesteh YS**, Khojasteh A, Soleimani M, Alikhasi M, Khoshzaban A, Ahmadbeigi N. Sinus augmentation using human mesenchymal stem cells loaded into a beta-tricalcium phosphate/hydroxyapatite scaffold. *Oral Surg Oral Med Oral Pathol Oral Radiol Endod* 2008; **106**: 203-209 [PMID: 18424115 DOI: 10.1016/j.tripleo.2007.12.001]
87 **Smiler D**, Soltan M, Lee JW. A histomorphogenic analysis of bone grafts augmented with adult stem cells. *Implant Dent* 2007; **16**: 42-53 [PMID: 17356371 DOI: 10.1097/ID.0b013e3180335934]
88 **Trautvetter W**, Kaps C, Schmelzeisen R, Sauerbier S, Sittinger M. Tissue-engineered polymer-based periosteal bone grafts for maxillary sinus augmentation: five-year clinical results. *J Oral Maxillofac Surg* 2011; **69**: 2753-2762 [PMID: 21680073 DOI: 10.1016/j.joms.2011.02.096]
89 **Mangano C**, Piattelli A, Tettamanti L, Mangano F, Mangano A, Borges F, Iezzi G, d'Avila S, Shibli JA. Engineered bone by autologous osteoblasts on polymeric scaffolds in maxillary sinus augmentation: histologic report. *J Oral Implantol* 2010; **36**: 491-496 [PMID: 20545540 DOI: 10.1563/AAID-JOI-D-09-00028]
90 **Mangano C**, Piattelli A, Mangano A, Mangano F, Mangano A, Iezzi G, Borges FL, d'Avila S, Shibli JA. Combining scaffolds and osteogenic cells in regenerative bone surgery: a preliminary histological report in human maxillary sinus augmentation. *Clin Implant Dent Relat Res* 2009; **11** Suppl 1: e92-102 [PMID: 19673958 DOI: 10.1111/j.1708-8208.2009.00227.x]
91 **Voss P**, Sauerbier S, Wiedmann-Al-Ahmad M, Zizelmann C, Stricker A, Schmelzeisen R, Gutwald R. Bone regeneration in sinus lifts: comparing tissue-engineered bone and iliac bone. *Br J Oral Maxillofac Surg* 2010; **48**: 121-126 [PMID: 19487059 DOI: 10.1016/j.bjoms.2009.04.032]
92 **Zizelmann C**, Schoen R, Metzger MC, Schmelzeisen R, Schramm A, Dott B, Bormann KH, Gellrich NC. Bone formation after sinus augmentation with engineered bone. *Clin Oral Implants Res* 2007; **18**: 69-73 [PMID: 17224026 DOI: 10.1111/j.1600-0501.2006.01295.x]
93 **Schimming R**, Schmelzeisen R. Tissue-engineered bone for maxillary sinus augmentation. *J Oral Maxillofac Surg* 2004; **62**: 724-729 [PMID: 15170286 DOI: 10.1016/j.joms.2004.01.009]
94 **Yamada Y**, Nakamura S, Ueda M, Ito K. Osteotome technique with injectable tissue-engineered bone and simultaneous implant placement by cell therapy. *Clin Oral Implants Res* 2013; **24**: 468-474 [PMID: 22150696 DOI: 10.1111/j.1600-0501.2011.02353.x]
95 **Ueda M**, Yamada Y, Kagami H, Hibi H. Injectable bone applied for ridge augmentation and dental implant placement: human progress study. *Implant Dent* 2008; **17**: 82-90 [PMID: 18332761 DOI: 10.1097/ID.0b013e31815cd591]

P- Reviewer: Guo ZK, Minana MD, Wang LS
S- Editor: Tian YL **L- Editor**: A **E- Editor**: Liu SQ

Published by **Baishideng Publishing Group Inc**
8226 Regency Drive, Pleasanton, CA 94588, USA
Telephone: +1-925-223-8242
Fax: +1-925-223-8243
E-mail: bpgoffice@wjgnet.com
Help Desk: http://www.wjgnet.com/esps/helpdesk.aspx
http://www.wjgnet.com